

UNIVERSITÉ PARIS XIII - SORBONNE PARIS NORD  
École Doctorale Sciences, Technologies, Santé Galilée

---

# Plans discrets substitutifs

Substitution discrete planes

---

THÈSE DE DOCTORAT

présentée par

**Victor Hubert LUTFALLA**

Laboratoire d'Informatique de Paris Nord

pour l'obtention du grade de  
DOCTEUR EN INFORMATIQUE

soutenue le 7 juillet 2021 devant le jury composé de :

**ARNOUX Pierre** ..... Rapporteur  
**BODINI Olivier** ..... Examineur  
**FERNIQUE Thomas** ..... Directeur de thèse  
**KARI Jarkko** ..... Examineur  
**MASÁKOVÁ Zuzana** ..... Examinatrice  
**POURNIN Lionel** ..... Examineur  
**THUSWALDNER Jörg** ..... Rapporteur

# Abstract

A tiling is a covering of the plane by tiles which do not overlap. We are mostly interested in edge-to-edge rhombus tilings, this means that the tiles are unit rhombuses and any two tiles either do not intersect at all, intersect on a single common vertex or along a full common edge.

Substitutions are applications that to each tile associate a patch of tiles (which usually has the same shape as the original tile but bigger), a substitution can be extended to tilings by applying it to each tile and gluing the obtained patches together. Substitutions are a way to grow and define tilings with a strong hierarchical structure.

Discrete planes are edge-to-edge rhombus tilings with finitely many edge directions that can be lifted in  $\mathbb{R}^n$  and which approximate a plane in  $\mathbb{R}^n$ , such a tiling is also called planar. Note that discrete planes are a relaxed version of cut-and-project tilings.

In this thesis we mostly study edge-to-edge substitution rhombus tilings lifted in  $\mathbb{R}^n$ . We prove that the Sub Rosa tilings are not discrete planes, the Sub Rosa tilings are edge-to-edge substitution rhombus tilings with  $n$ -fold rotational symmetry that were defined by Jarkko Kari and Markus Rissanen [KR16] and which were good candidates for being discrete planes. We define a new family of tilings which we call the Planar Rosa tilings which are substitution discrete planes with  $n$ -fold rotational symmetry.

We also study the multigrid method which is a construction for cut-and-project tiling and we give an explicit construction for cut-and-project rhombus tilings with global  $n$ -fold rotational symmetry.

## Résumé

Un pavage est un recouvrement du plan par des tuiles qui ne se chevauchent pas. Nous nous intéressons principalement aux pavages dont les tuiles sont des losanges unitaires et qui sont exacts c'est à dire que si on prend deux tuiles dans le pavage soit elles ne se touchent pas, soit elles ont un unique sommet en commun, soit elles ont une arête entière en commun.

Les substitutions sont des applications qui à chaque tuile associent un ensemble de tuiles appelé motif (dont la forme est habituellement la même que celle de la tuile initiale mais en plus grand), une substitution peut être étendue aux pavages en l'appliquant à chaque tuile séparément et en recollant les motifs obtenus. Les substitutions permettent de construire des pavages avec une forte structure hiérarchique.

Les plans discrets sont des pavages exacts par losanges unitaires avec un nombre fini de directions d'arêtes  $n$  que l'on peut relever dans  $\mathbb{R}^n$  et qui lorsqu'on les relève approximent un plan. On dit aussi pavages planaires pour plans discrets. Notons que les plans discrets sont une version relâchée des pavages coupe-et-projections.

Dans cette thèse nous étudions principalement les pavages substitutifs par losange relevés dans  $\mathbb{R}^n$ . Nous prouvons que les pavages Sub Rosa ne sont pas des plans discrets, les pavages Sub Rosa sont des pavages substitutifs par losange avec symétrie rotationnelle d'ordre  $n$  qui ont été définis par Jarkko Kari et Markus Rissanen [KR16] et qui étaient de bons candidats pour être des plans discrets. Nous définissons une nouvelle famille de pavages que l'on appelle les pavages Planar Rosa qui sont des plans discrets substitutifs avec symétrie rotationnelle d'ordre  $n$ .

Nous étudions aussi la méthode de la multigrille qui permet de construire des pavages coupe-et-projection. On utilise cette méthode pour donner une construction explicite pour des pavages coupe-et-projection par losanges avec symétrie rotationnelle globale d'ordre  $n$ .

## Remerciements / Acknowledgements

En premier ma gratitude va à mon directeur de thèse, Thomas Fernique, pour son accompagnement et son soutien pendant la période de crise sanitaire.

I thank Jörg Thuswaldner for accepting to review this thesis, and also Jarkko Kari and Zuzana Masáková for accepting to be a part of my jury and for their interest in my work.

Je remercie Pierre Arnoux pour ses encouragements et pour avoir accepté la charge de rapporteur ainsi que Olivier Bodini et Lionel Pournin pour leur soutien tout au long de ma thèse et pour avoir accepté de faire partie de mon jury.

Je suis très reconnaissant à tous les collègues avec qui j'ai fait de la recherche en stage ou pendant ma thèse, en particulier Laurent Vuillon, Jarkko Kari, Uwe Grimm et Michael Rao.

Je remercie tou-te-s les collègues du Laboratoire d'Informatique de Paris Nord, de l'équipe CALIN et du GT SDA2 qui m'ont fait me sentir bienvenu dans la communauté scientifique.

Merci aussi à tou-te-s les enseignant·e·s d'informatique et de mathématiques que j'ai eu au cours de ma vie d'étudiant.

Pour terminer je remercie mes proches: ma famille (en particulier mon frère et presque-coloc Adrien), mes ami·e·s (en particulier Arthur et Nicolas sans qui la crise sanitaire aurait été insupportable) et Marine.



# Contents

<b>1</b>	<b>Introduction</b>	<b>7</b>
<b>2</b>	<b>Tilings</b>	<b>14</b>
2.1	Geometrical tilings of the plane . . . . .	14
2.2	Local rules . . . . .	20
2.3	Order . . . . .	23
2.4	Substitutions . . . . .	28
2.5	Planarity . . . . .	39
2.6	The multigrid method . . . . .	43
2.7	Penrose rhombus tilings . . . . .	46
2.8	Ammann-Beenker tilings . . . . .	52
2.9	Canonical substitution tilings . . . . .	55
2.10	Generalized substitutions . . . . .	57
2.11	Expansions of self-similar tilings and cut-and-project sets . . .	64
2.12	Tileability of finite domains . . . . .	66
<b>3</b>	<b>Sub Rosa substitution tilings</b>	<b>67</b>
3.1	Definition and construction . . . . .	67
3.2	Main result . . . . .	73
3.3	Lifted substitutions and expansions . . . . .	73
3.4	Proof for odd $n$ . . . . .	80
	3.4.1 Lifting . . . . .	80
	3.4.2 Expansion matrix . . . . .	81
	3.4.3 Eigenvalues of the Sub Rosa expansion matrices . . . .	84
	3.4.4 Conclusion . . . . .	90
3.5	Proof for even $n$ . . . . .	91
	3.5.1 Lifting . . . . .	91
	3.5.2 Expansion matrix . . . . .	92

3.5.3	Eigenvalues of the Sub Rosa expansion matrices . . . .	95
3.5.4	Conclusion . . . . .	99
<b>4</b>	<b>Planar Rosa : substitution <math>n</math>-fold discrete planes</b>	<b>101</b>
4.1	Introduction . . . . .	101
4.2	Strategy . . . . .	102
4.2.1	Adapting Sub Rosa . . . . .	102
4.2.2	Adapting $P_n(\frac{1}{2})$ . . . . .	103
4.3	Tileability of Sub Rosa-like metatiles . . . . .	103
4.4	Construction for odd $n$ . . . . .	118
4.4.1	Lifting and eigenvalues . . . . .	118
4.4.2	Choosing the edge word . . . . .	119
4.4.3	Proof of Lemma 4.4.3 (planarity) . . . . .	122
4.4.4	Proof of Lemma 4.4.4 (tileability) . . . . .	124
4.4.5	Proof of Lemma 4.4.5 (primitivity) . . . . .	128
4.4.6	Regular fixpoint tiling . . . . .	129
4.5	Construction for even $n$ . . . . .	130
4.5.1	Lifting and eigenvalues . . . . .	130
4.5.2	Choosing the edge word . . . . .	132
4.5.3	Proof of Lemma 4.5.3 (planarity) . . . . .	134
4.5.4	Proof of Lemma 4.5.4 (tileability) . . . . .	135
4.5.5	Proof of Lemma 4.5.5 (primitivity) . . . . .	141
4.5.6	Regular fixpoint tiling . . . . .	142
<b>5</b>	<b>Regular <math>n</math>-fold multigrids and their dual tilings</b>	<b>144</b>
5.1	Main result . . . . .	144
5.2	From regular $n$ -fold multigrids to tilings with global $n$ -fold symmetry . . . . .	145
5.3	Regularity of $n$ -fold multigrids and trigonometric equations . .	147
5.4	Trigonometric diophantine equations . . . . .	149
5.5	Proof of Theorem 16 . . . . .	151
5.5.1	For odd $n$ . . . . .	151
5.5.2	For even $n$ . . . . .	153
<b>6</b>	<b>Examples of tilings</b>	<b>157</b>
6.1	4-fold tilings . . . . .	159
6.1.1	Ammann-Beenker . . . . .	159
6.1.2	Sub Rosa 4 . . . . .	161

6.1.3	Planar Rosa 4 . . . . .	163
6.1.4	Diffraction patterns of 4-fold tiling . . . . .	165
6.2	5-fold tilings . . . . .	166
6.2.1	Penrose . . . . .	166
6.2.2	Anti-Penrose . . . . .	167
6.2.3	Sub Rosa 5 . . . . .	168
6.2.4	Planar Rosa 5 . . . . .	170
6.2.5	Diffraction patterns of 5-fold tilings . . . . .	171
6.3	6-fold tilings . . . . .	173
6.3.1	$P_6(\frac{1}{2})$ . . . . .	173
6.3.2	Sub Rosa 6 . . . . .	174
6.3.3	Planar Rosa 6 . . . . .	175
6.3.4	Diffraction patterns of 6-fold tilings . . . . .	177
6.4	7-fold tilings . . . . .	179
6.4.1	$P_7(\frac{1}{7})$ and $P_7(\frac{1}{2})$ . . . . .	179
6.4.2	Sub Rosa 7 . . . . .	182
6.4.3	Planar Rosa 7 . . . . .	183
6.4.4	A smaller planar 7-fold Sub Rosa-like substitution . . .	187
6.4.5	Diffraction pattern of 7-fold tilings . . . . .	190
6.5	Other examples of multigrid dual tilings . . . . .	192
<b>7</b>	<b>Conjectures and future work</b>	<b>194</b>
7.1	Planar Rosa substitution tilings . . . . .	194
7.2	General substitution discrete planes . . . . .	196

# Chapter 1

## Introduction

**Tilings.** Tilings are coverings of the Euclidean plane by tiles without overlap. They are studied in many branches of Mathematics and Computer Science such as decidability [Ber66], dynamical systems [Rob04], topology [Sad08] and mathematical crystallography [BG13].

Aperiodic tilesets, which are sets of tiles that can tile the whole plane but only in a non-periodic way, are at the center of the study of tilings: they are linked to decidability problems such as the Domino Problem, they can induce minimal infinite dynamical systems and specific aperiodic tilesets are used to model quasicrystals.

The first aperiodic tileset was discovered by Robert Berger [Ber66]. This tileset consisted of 20426 Wang tiles which are square tiles with a color on each edge and with the condition that two adjacent tiles must have the same color on their common edge.

In the decade that followed aperiodic tilesets with simple geometric tiles were discovered by Roger Penrose [Pen74]. The Penrose rhombus tiles are two rhombus tiles with decorations (cuts and notches) on the edges, these decorations (local rules) enforce the aperiodicity of any tiling with these tiles.

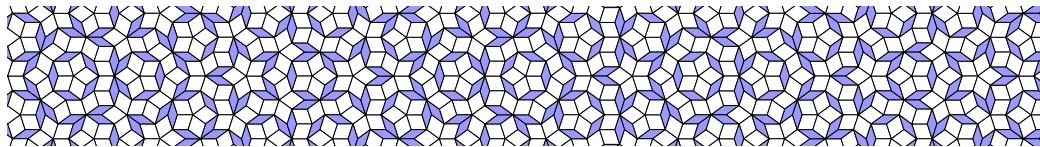


Figure 1.1: A small fragment of the Penrose rhombus tilings without decorations.

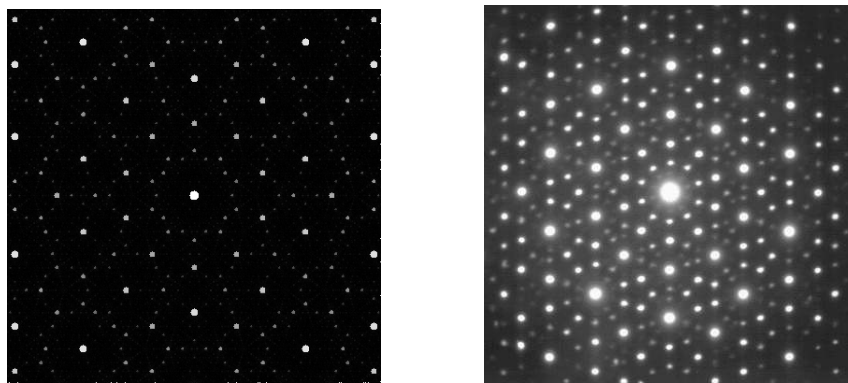
**Long-range order.** In the 1980s Dan Shechtman discovered quasicrystals [SBGC84] which are materials that have long-range order shown by a sharp X-ray diffraction pattern (see Figure 1.2) but no translational symmetry (periodicity).

This discovery contradicted the belief, which was held as an axiom in the crystallographic community, that only crystals (periodic materials) had sharp X-ray diffraction patterns. Together with the crystallographic restriction, which states that a lattice can only have 2,3,4 or 6 fold rotational symmetry, this “axiom” implied in particular that a sharp diffraction pattern with 10-fold symmetry was impossible.

However the Al-Mn quasicrystal alloy observed by Dan Shechtman [SBGC84] had a sharp X-ray diffraction pattern with 10-fold symmetry, for more details on this discovery and its repercussions see the preface and introduction of [Sen96]. Note that since the rotational symmetries of materials translate to their diffraction pattern, high-order rotational symmetries in quasicrystals are of particular interest to physicists.

Shortly after the discovery of quasicrystals the similarities between the properties of the Al-Mn alloy and Penrose’s fivefold tilings [Pen74] were observed [AG86] and quasiperiodic tilings quickly became one of the commonly used mathematical models to study quasicrystals, see [Sen96].

However quasiperiodicity is not sufficient for long-range order so a new



(a) The diffraction pattern of a fragment of Penrose rhombus tiling. (b) The diffraction pattern of a quasicrystal from [Wik].

Figure 1.2: Long-range order shown by diffraction patterns on tilings and quasicrystals .

class of tilings was defined: the cut-and-project tilings. The idea of cut-and-project is to see tilings of the plane as the projection onto an irrational plane of a discrete surface in higher dimension, for more details on cut-and-project tilings see for example [Sen96] or [BG13]. The generic cut-and-project tilings have pure point diffraction pattern which makes them a strong model for quasicrystals.

In this thesis we also consider quasiperiodic discrete planes which are a relaxed version of cut-and-project tilings. Quasiperiodic discrete planes also have long-range order and their diffraction pattern is usually essentially discrete which makes them a sufficient model for quasicrystals.

**Substitutions.** Substitutions are applications that to each tile associate a patch of tiles that usually has the same shape, they are generalized to application on tilings by applying the substitution rule separately to each tile and then merging the results. Numerous examples of substitutions and substitution tilings can be found online in the Tilings Encyclopedia [FGH].

Substitution tilings have a strong hierarchical structure and this was used to produce many aperiodic tilings. The original proof of aperiodicity of Berger [Ber66], Robinson [Rob71] and Penrose use the hierarchical structure induced by substitution even though the tilings and tilesets in question were defined by local rules, the idea in these three cases is that the local rules force the tile to be arranged in such a way that we can group them in so-called *metatiles* which have the same shape and same local rules as the original *prototiles*. See for example Figure 1.3b where we show how tiles from a

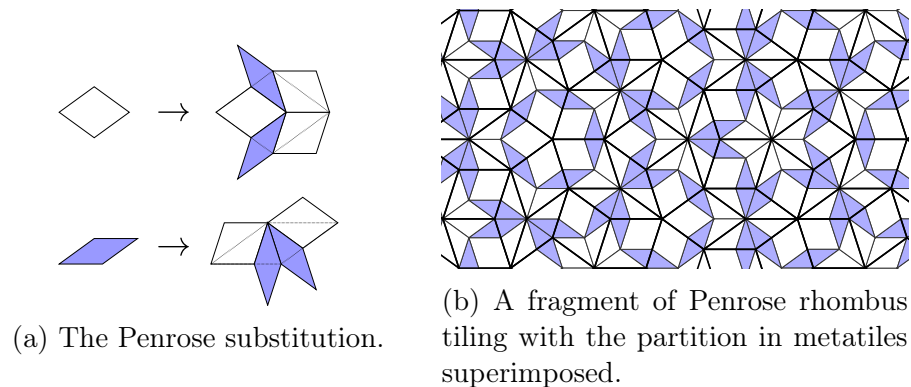


Figure 1.3: The hierarchical structure in the Penrose rhombus tiling.

Penrose rhombus tiling can be grouped in metatiles which are drawn in bold lines, remark that for the Penrose tilings some tiles overlap on two metatiles.

Note that under reasonable assumptions on the substitution, substitution tilings can also be defined by local rules [Moz89, GS98, FO10].

Substitution are also particularly useful to compute tiling invariants. It is sometimes quite easy to show that tilings are conjugate (also called mutually locally derivable or MLD for short) for example the three tilings defined by Penrose called the Penrose pentagonal tiling, the Penrose kite-and-dart tiling and the Penrose rhombus tiling are conjugate and it is simply a matter of describing the way a Penrose rhombus tiling can be locally derived from a Penrose pentagonal or kite-and-dart tiling and vice-versa [Pen74]. The conjugacy problem is undecidable and in practice proving non-conjugacy requires to compute tiling invariants such as cohomology groups and prove that the invariants are different. There exist methods to compute the cohomology group of different classes of tilings [Kal05, GHK13, BGL21] but the most developed and most used technique is for substitution tilings [AP98].

**Main results.** As we just explained, tilings with long-range order and especially with high-order rotational symmetry are of particular interest to physicists and crystallographists and substitutions give us a tool to study the tilings in an intricate way.

In this thesis we study tilings that have long-range order (cut-and-project tilings or quasiperiodic discrete planes) and can be defined by substitution with an emphasis on high-order rotational symmetry.

Our first result concerns the Sub Rosa substitution tilings defined by Jarkko Kari and Markus Rissanen in [KR16]. These tilings have  $2n$ -fold rotational symmetry but they unfortunately are not discrete planes.

**Theorem 1** (Fernique, Kari, L.2020). *For any  $n \geq 3$  the canonical Sub Rosa tiling  $\mathcal{T}_n$  can be lifted to a discrete surface of  $\mathbb{R}^n$  and:*

1. *The canonical Sub Rosa tilings  $\mathcal{T}_3$  and  $\mathcal{T}_5$  are discrete planes.*
2. *For  $n = 4$  and for any  $n \geq 6$  the canonical Sub Rosa tiling  $\mathcal{T}_n$  is not a discrete plane.*

*The same holds when replacing the canonical Sub Rosa tiling  $\mathcal{T}_n$  by the set of Sub Rosa substitution tilings  $X_{\sigma_n}$ .*

The natural followup question was: does there exist a similar family of substitution discrete planes with  $2n$ -fold rotational symmetry.

Our second result is the existence of substitution discrete planes with  $n$ -fold rotational symmetry. For this we define a new family of substitution tilings which we call Planar Rosa substitution tilings or Planar Rosa substitution discrete planes.

**Theorem 2** (Kari, L. 2020). *For any  $n \geq 3$  the canonical Planar Rosa tiling  $\mathcal{T}'_n$  is a substitution discrete plane with global  $2n$ -fold rotational symmetry. For any  $n \geq 3$  the Planar Rosa tilings i.e. tilings in  $X_{\sigma'_n}$ , are substitution discrete planes with local  $2n$ -fold rotational symmetry.*

Theorems 1 and 2 (restricted to the case of odd  $n$ ) were submitted in [KL20].

For the proof of Theorem 2 we use the  $n$ -fold multigrid dual tilings  $P_n(\frac{1}{2})$ . The fact that the tilings  $P_n(\frac{1}{2})$  are rhombus tilings may be considered as “folk” but we were unable to find it in the literature and this result is interesting in itself so we decided to prove it in Theorem 3.

This result is an effective construction for rhombus quasiperiodic cut-and-project tilings with global  $n$ -fold rotational symmetry. A SageMath program which generates these tilings and outputs their svg files is publicly available in [Lut21b].

**Theorem 3** ([Lut21a]).

1. *For any  $n \geq 4$  the  $n$ -fold multigrid dual tiling  $P_n(\frac{1}{2})$  is a quasiperiodic rhombus cut-and-project tiling with global  $2n$ -fold rotational symmetry.*
2. *For any **odd**  $n \geq 5$  the  $n$ -fold multigrid dual tiling  $P_n(\frac{1}{n})$  is a quasiperiodic rhombus cut-and-project tiling with global  $n$ -fold rotational symmetry.*



**Overview of the thesis.** In Chapter 2 we give all the classical definitions for the study of tilings, substitution tilings, discrete planes and multigrid dual tilings. We also present the Penrose rhombus tilings, the Ammann-Beenker tilings and a few known results related to this thesis. Sections 2.1 to 2.8 can be considered as an introduction to tilings with an emphasis on substitution tilings and discrete planes with all necessary definitions and examples. Sections 2.9 to 2.12 are a quick overview on more advanced related results.

In Chapter 3 we study the Sub Rosa substitution tilings and prove Theorem 1. In Section 3.3 we give general considerations on how substitutions and expansions are lifted in  $\mathbb{R}^n$  which gives us a sufficient condition for the planarity of substitution tilings and a sufficient condition for the non-planarity of substitution tilings. In Section 3.4 we prove Theorem 1 for odd  $n$  and in Section 3.5 we prove it for even  $n$ . The first key point is the fact that the Sub Rosa expansions are lifted to circulant integral linear applications in  $\mathbb{R}^n$ , the second key point is a link between the sequence of rhombuses on the edges of the Sub Rosa metatiles and the eigenvalues of the lifted expansion and the last key point is just trigonometric considerations that give us an exact value for the eigenvalues of Sub Rosa expansions. From this we conclude using the sufficient conditions of Section 3.3

In Chapter 4 we present the construction for Planar Rosa substitution discrete planes and prove Theorem 2. The Planar Rosa substitution are defined similarly to Sub Rosa substitution by a sequence of rhombuses along the edges of the metatiles *i.e.* by the boundary of the metatiles. The two key points are to prove that the boundary of the metatiles ensures the fact that the Planar Rosa substitutions are planar *i.e.* they generate discrete planes, and that the interior of the metatiles are tileable with unit rhombuses. For the planarity we re-use the work of Chapter 3, for the tileability we use the Kenyon criterion [Ken93] and some regions of multigrid dual tilings. Actually for a given  $n$  what we define is an infinite sequence of candidate substitutions and we prove that infinitely many of them are both planar and tileable as primitive substitutions. The Planar Rosa substitution is defined as the smallest of these candidate substitutions which is both planar and tileable as a primitive substitution.

In Chapter 5 we study  $n$ -fold multigrids and their dual tilings to prove Theorem 3. This theorem is actually a consequence of the more technical Theorem 16 on the regularity of  $n$ -fold multigrids. We prove that the regularity or singularity of  $n$ -fold multigrids is equivalent to some diophantine

trigonometric equations, we then use a known result on trigonometric diophantine equations [CJ76] to prove the theorem.

In Chapter 6 we present several examples of multigrid dual tilings, Sub Rosa tilings and Planar Rosa tilings. We use these examples to illustrate some remarks on Planar Rosa tilings and multigrid dual tilings. The Planar Rosa tilings presented here have long-range order and are substitution tilings, they would be nice objects to study tiling invariants and in particular we could study their cohomology group with the techniques developed in [AP98].

In Chapter 7 we present a few unanswered questions and conjectures in relation with the work presented here.

# Chapter 2

## Tilings

In this chapter we will present the general definitions for tilings of the Euclidean plane  $\mathbb{R}^2$ , then more specific definitions for the notion of order on tilings, substitution tilings, tilings lifted in  $\mathbb{R}^n$  and planarity. Readers familiar with these notion can skip these sections. We will then present known classes of tilings and known tilings such as the Penrose rhombus tilings and the Ammann-Beenker tilings. Other examples of tilings are presented in Chapter 6. In Sections 2.10 and 2.11 we present more advanced results which are related to the work presented in this thesis.

### 2.1 Geometrical tilings of the plane

Tilings are coverings of the space (here the Euclidean plane  $\mathbb{R}^2$ ) without overlap by a set of tiles. In this section we will give the basic definitions for tilings and tiling subshifts.

**Definition 2.1.1** (Tile, rhombus tiles, edges and vertices). *A (geometrical) tile is a compact set  $t$  of  $\mathbb{R}^2$  which is the closure of its interior.*

*A unit rhombus tile  $t$  can be described as*

$$t = (p, \vec{u} \wedge \vec{v}) = \{p + \lambda\vec{u} + \mu\vec{v}, 0 \leq \lambda, \mu \leq 1\}$$

*with  $p$  a point of  $\mathbb{R}^2$  and  $\vec{u}, \vec{v}$  two non-collinear unit vectors of  $\mathbb{R}^2$ .*

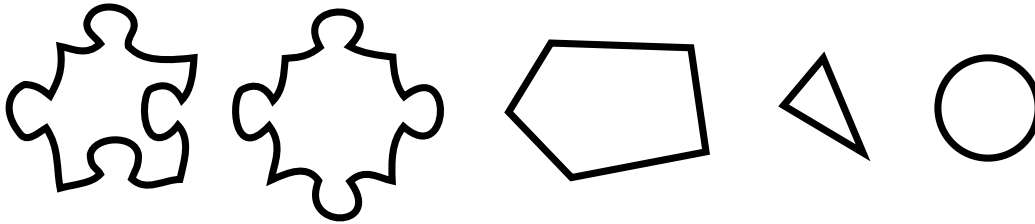


Figure 2.1: Examples of tiles : classical jigsaw tiles, polygons and circles are tiles.

The set of edges of a unit rhombus  $t$  denoted  $E(t)$  is

$$E(t) := \left\{ \begin{aligned} &\{p + \lambda \vec{u}, 0 \leq \lambda \leq 1\}, \\ &\{p + \lambda \vec{v}, 0 \leq \lambda \leq 1\}, \\ &\{p + \vec{v} + \lambda \vec{u}, 0 \leq \lambda \leq 1\}, \\ &\{p + \vec{u} + \lambda \vec{v}, 0 \leq \lambda \leq 1\} \end{aligned} \right\}$$

The set of vertices of a unit rhombus  $t$  denoted  $V(t)$  is

$$V(t) = \{p, p + \vec{u}, p + \vec{v}, p + \vec{u} + \vec{v}\}$$

The notions of edges and vertices of a tile can be generalized to all polygon tiles, but no formal definition will be given as non-rhombus tiles will only be used in basic examples.

**Definition 2.1.2** (Tiling). A tiling noted  $\mathcal{T}$  is a countable set of non-overlapping tiles which covers  $\mathbb{R}^2$ , i.e. a set  $\{t_i, i \in \mathbb{N}\}$  of tiles such that

- $\bigcup_{i \in \mathbb{N}} t_i = \mathbb{R}^2$
- $\forall i, j \in \mathbb{N}, i \neq j \Rightarrow \overset{\circ}{t}_i \cap \overset{\circ}{t}_j = \emptyset$

When the tiles are polygons we define the set of edges and of vertices of the tiling by

$$E(\mathcal{T}) := \bigcup_{i \in \mathbb{N}} E(t_i) \quad V(\mathcal{T}) := \bigcup_{i \in \mathbb{N}} V(t_i).$$

In this work we are interested not only in tilings but on set of tilings, however we are not interested in any sets of tilings but on sets that are consistent with the definition and the structure of tilings. In this context the “nice” sets are called Subshifts.

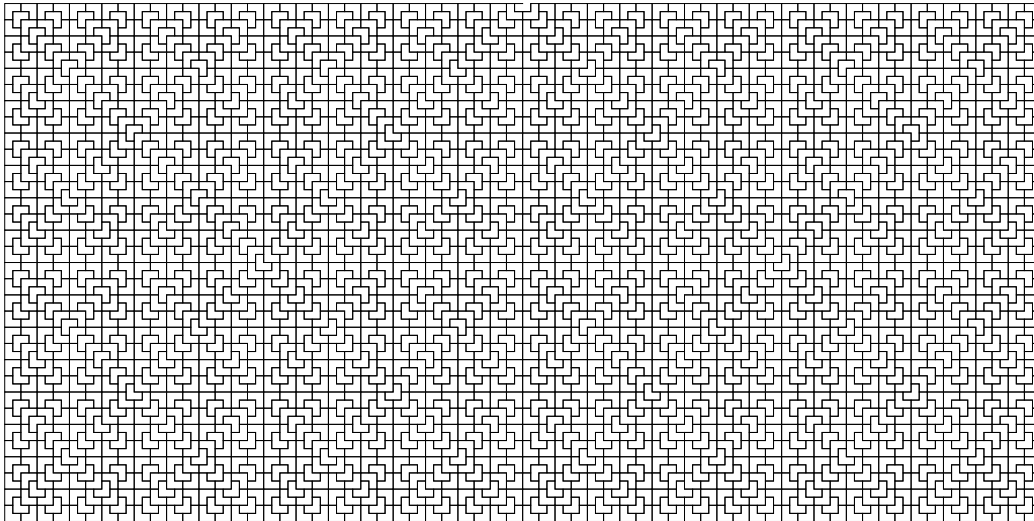


Figure 2.2: The Chair tiling.

**Definition 2.1.3** (Subshift). *There are two equivalent definitions for tiling subshifts:*

- *a subshift is a set of tilings which is closed for the cylinder topology [Rob04] and invariant by translation*
- *given a set of patterns called forbidden patterns and denoted by  $F$ , the subshift  $X_F$  is the set of all tilings that contain none of the forbidden patterns.*

We will not go into details on the cylinder topology on tilings since it is not the main topic of this work, see [Rob04] for more details. Remark that the set of patterns  $F$  is not necessarily finite, when it is finite the subshift  $X_F$  is called Subshift of Finite Type.

In this work we only consider tilings where the set of the tiles are copies on a finite set of *prototiles* *i.e.* the set of tiles is finite up-to translation. In all generality the “up-to translation” relation can be replaced by any congruence.

**Definition 2.1.4** (Prototiles and Congruence). *We call prototiles (or sometimes tile shapes) the canonical representants of the set of geometrical tiles (possibly with labels) quotiented by a congruence relation which we denote  $\equiv$ . By default we consider the up-to translation congruence, we sometimes*

use up-to translation and rotation congruence or the up-to isometry congruence. For example unit rhombus prototiles can be described only by their two vectors and we write them as  $\mathbf{t} = \vec{u} \wedge \vec{v}$ .

A finite set of prototiles is called a tiling set and is denoted by  $\mathbf{T}$ .

The Chair tiling in Figure 2.2 has four prototiles up-to translation but only one up to translation and rotation. The Pinwheel tiling in Figure 2.3 has infinitely many prototiles up to translation but only two up to translation and rotation and only one up to isometry (see Section 2.4 for precise definition of these two tilings).

**Definition 2.1.5** (Edge-to-edge tiling). *A polygon tiling is called edge-to-edge when any two tiles that intersect, either intersect on a full common edge or on a single common vertex i.e. a tiling  $\{t_i, i \in \mathbb{N}\}$  is edge-to-edge when*

$$\begin{aligned} \forall i, j \in \mathbb{N}, i \neq j \Rightarrow t_i \cap t_j = \emptyset \\ \text{or } \exists e \in E(t_i) \cap E(t_j), t_i \cap t_j = e \\ \text{or } \exists v \in V(t_i) \cap V(t_j), t_i \cap t_j = \{v\} \end{aligned}$$

Remark that the Chair tiling of Figure 2.2 and the Pinwheel tiling of Figure 2.3 are not edge-to-edge, though if we allow to add vertices in to split edges in two they are edge-to-edge.

**Definition 2.1.6** (Patch and Pattern). *A patch is a simply-connected set of non-overlapping tiles, i.e. a connected set of non-overlapping tiles with no holes.*

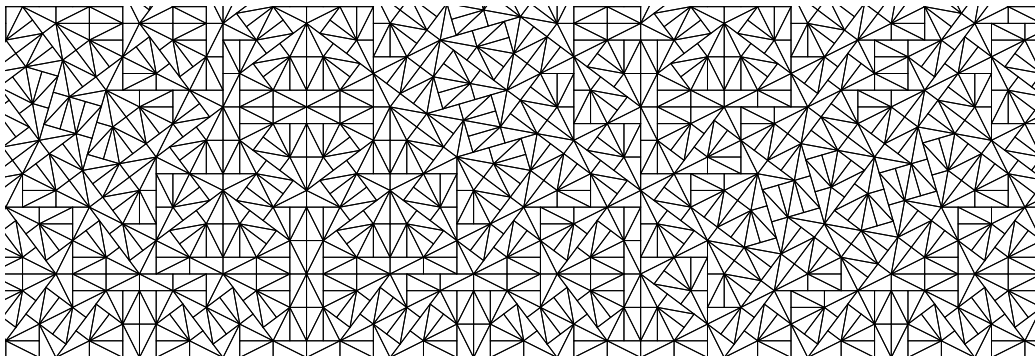


Figure 2.3: The Pinwheel tiling.

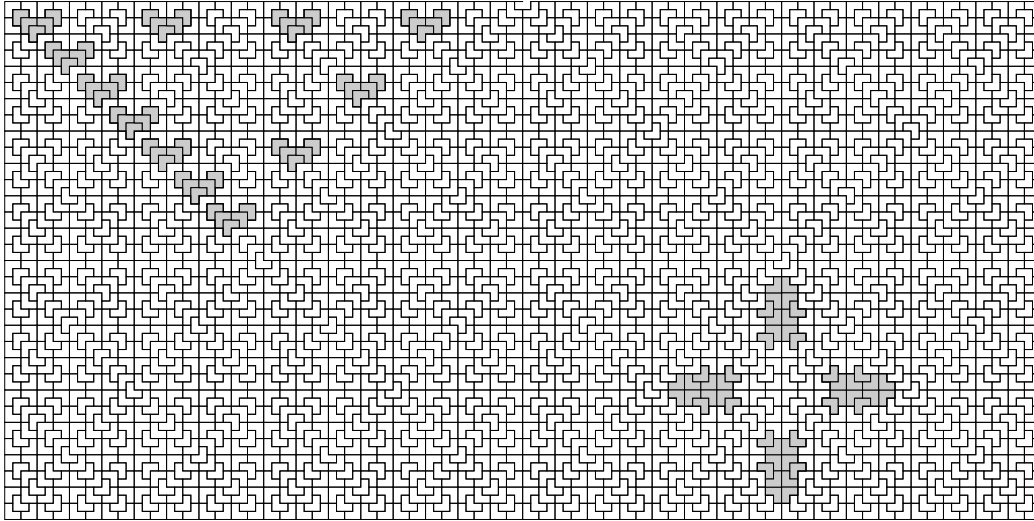


Figure 2.4: Patches and patterns of the Chair tiling.

*A pattern is a patch up to translation, or in general up to the congruence relation we consider on the tiles.*

*We say that  $P$  is a patch of a tiling  $\mathcal{T}$  (resp. of another patch  $P'$ ) if it is a subset of the tiling (resp. of the other patch) i.e.  $P \subseteq \mathcal{T}$  (resp.  $P \subseteq P'$ ).*

*We say that a pattern  $P$  appears in  $\mathcal{T}$  denoted by  $P \triangleleft \mathcal{T}$  (resp. in a patch  $P'$ ) if there is a patch  $P''$  of the tiling (resp. of the patch  $P'$ ) which is congruent to  $P$ , recall that when it is not otherwise mentioned we consider the up-to translation congruence.*

For example in Figure 2.4 in the upper-left corner are 12 highlighted patches which are all equal up to translation so they are the same pattern up to translation, in the bottom right corner are 4 highlighted patches which are equal up to translation and rotation so they are not the same pattern up to translation but they are the same pattern up to translation and rotation.

Remark that in this definition a patch or a pattern does not necessarily need to appear in an infinite valid tiling.

**Definition 2.1.7** (Deceptions and Fragments). *A patch or pattern is called a fragment of tiling when it appears in some infinite valid tiling. A patch or pattern is called a deception when there is no infinite valid tiling which contains it.*

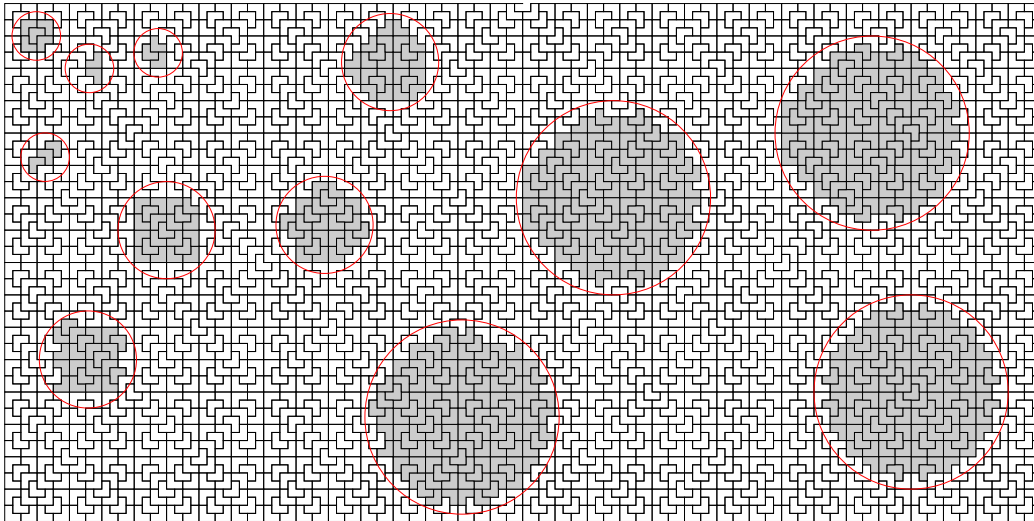


Figure 2.5: Balls of the Chair tiling.

For some definitions and some properties we are interested in a specific kind of patches: the balls of the tiling.

**Definition 2.1.8** (Balls and local complexity). *Let  $D(r, p)$  be the disk of centre  $p$  and radius  $r$  of  $\mathbb{R}^2$  and let  $\mathcal{T}$  be a tiling of  $\mathbb{R}^2$ .*

*We call ball of centre  $p$  and radius  $r$  of  $\mathcal{T}$  the patch*

$$B_{\mathcal{T}}(p, r) := \{t \in \mathcal{T} \mid t \subseteq D(r, p)\}.$$

*The tiling  $\mathcal{T}$  is said to have finite local complexity if for any a radius  $r$  the set  $\{B_{\mathcal{T}}(p, r), p \in \mathbb{R}^2\}$  is finite up to translation.*

*Otherwise the tiling is said to have infinite local complexity.*

For example in Figure 2.5 are highlighted 12 balls of various radiuses, remark that balls of the same radius can vary in shape and in number of tiles.

The Pinwheel tiling of Figure 2.3 is an example of tiling with infinite local complexity and this is due to the fact that the tile appears in infinitely many orientations [Rad94, Rad97]. Other than this specific example we will only consider tilings with finite local complexity.



## 2.2 Local rules

Local rules are in all generality a set of condition that can be checked locally and that in addition to the usual tiling condition, restrict the possible *valid* tilings of a given tileset. The edge-to-edge condition of Definition 2.1.5 for example can be seen as a local rule. Local rules can also be seen as a way to impose conditions on the validity of a tiling without using tiles of complex shapes for example the cut-and-notch Penrose rhombus tiles that were used to define the Penrose rhombus tiling [Pen74] and their coloured rhombus equivalent shown in Figure 2.29 page 48, or even to simplify tiles that are not connex such as in the case of the Socolar-Taylor tile that can either be realized as a non-connex tile or a labelled hexagon tile [ST11]

There are three ways to define local rules either by forbidden pattern, by an atlas of allowed local configurations or by a colouring or labelling of the tiles. We will first quickly present the forbidden patterns definition and the atlas definition without going in much details, and then give a more detailed presentation of colouring of tiles.

Let us consider a tileset  $\mathbf{T}$  of finitely many polygon prototiles.

Let  $F$  called set of forbidden patterns be a set of edge-to-edge patterns from tileset  $\mathbf{T}$ . A tiling  $\mathcal{T}$  is admissible for  $F$  when no pattern of the set  $F$  is a pattern of  $\mathcal{T}$ . We denote  $X_F$  called subshift of  $F$  the set of valid tilings for  $F$ . When  $F$  is finite then  $X_F$  is called Subshift of Finite Type or SFT, see [Rob04] for more details.

Given an integer  $r$ , a  $r$ -pattern of centre  $x$  is an edge-to-edge pattern of tiles  $P$  such that  $x$  is a vertex of  $P$  and any tile of  $P$  is linked to  $x$  by a path of at most  $r$  edges.

A  $r$ -atlas or  $r$ -vertex-atlas is a set of  $r$ -patterns and is usually denoted by  $\mathbf{A}_r$ . Given a tiling  $\mathcal{T}$  we denote by  $\mathbf{P}_r(\mathcal{T})$  the set of all  $r$ -patterns that appear in  $\mathcal{T}$ . A tiling  $\mathcal{T}$  is called valid for the atlas  $\mathbf{A}_r$  when  $\mathbf{P}_r(\mathcal{T}) \subseteq \mathbf{A}_r$ , and we denote by  $X_{\mathbf{A}_r}$  the set of tilings valid for  $\mathbf{A}_r$  called subshift of  $\mathbf{A}_r$ . In Figure 2.6 is shown the 0-atlas of the Penrose rhombus tiling (for more details see Section 2.7).

Let us remark that when the tileset  $\mathbf{T}$  allows only edge-to-edge tilings of finite local complexity, SFT (subshifts defined by a finite set of forbidden patterns) and  $r$ -atlas subshifts (subshifts defined by some  $r$ -atlas) are equivalent.

Let us now present local rules through labelling or colouring, though the definition can be given for any shape of geometrical tiles we will restrict to

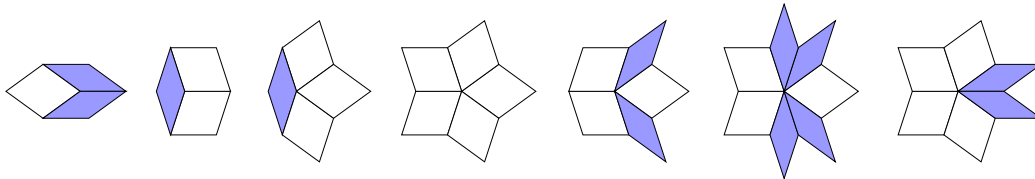


Figure 2.6: The 0-atlas for Penrose rhombus tiling up to translation and rotation.

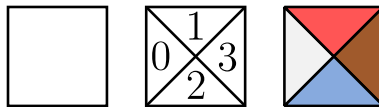


Figure 2.7: Example of a square tile and the graphical representation of a Wang tile with integer labels or with colours.

polygon tiles and edge-to-edge tilings.

**Definition 2.2.1** (Labelled or coloured tile). *A labelled or coloured tile is a couple  $(t, l)$  where  $t$  is a polygon tile and  $l$  is a function from  $t$  to a finite set of labels or colours.*

*A labelled prototile is a labelled tile up to translation (or up to a congruence). Two labelled tiles that have the same geometrical tile but not the same labelling function are not equivalent up-to translation.*

*A finite set of labelled prototiles is called a labelled tileset and is denoted by  $\mathbf{T}$ .*

The Wang tiles which are unit square tiles with colours on the edges (see Figure 2.7) are the most simple and classical example of coloured tiles.

**Definition 2.2.2** (Tiling valid for local rules). *A valid tiling (resp. patch) for labelled tileset  $\mathbf{T}$  is a countable set of labelled tiles  $\mathcal{T} := \{(t_i, l_i), i \in \mathbb{N}\}$  (resp. a finite set of labelled tiles) such that:*

- *each tile  $(t_i, l_i)$  is equal up-to translation to some prototile  $(\mathbf{t}, \mathbf{l}) \in \mathbf{T}$*
- *the set  $\{t_i, i \in \mathbb{N}\}$  is an edge-to-edge tiling of  $\mathbb{R}^2$ , see Definition 2.1.5 (resp. an edge-to-edge patch)*
- *for any two tiles  $(t_0, l_0)$  and  $(t_1, l_1)$  that share an edge  $e$  then the labellings of the two tiles agree on their common edge i.e.  $l_0(e) = l_1(e)$*

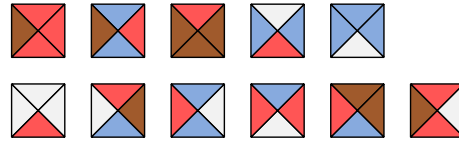


Figure 2.8: The Jeandel-Rao Wang tileset [JR21].

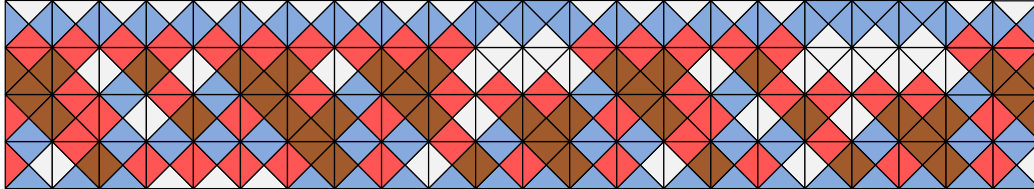


Figure 2.9: A fragment of Jeandel-Rao tiling.

*Valid patterns are up-to the translation valid patches.*

*The set (subshift) of valid tilings for a labelled tileset  $\mathbf{T}$  is denoted by  $X_{\mathbf{T}}$ .*

See Figure 2.8 for an example of labelled tileset and Figure 2.9 for a fragment of valid tiling.

**Definition 2.2.3** (Label simplification and sofic tilings). *Given two finite sets of labels  $\mathbf{L}' \subset \mathbf{L}$  and a projection  $\pi : \mathbf{L} \rightarrow \mathbf{L}'$ , we define the operator of label simplification on labelled tiles by  $\pi$  by  $\pi((t, l)) = (t, \pi \circ l)$ , the operator is generalized to patches and tilings by applying it separately on each tile.*

*A set of labelled tilings  $X$  is called sofic when there exists a labelled tileset  $\mathbf{T}$  such that  $X$  is the projection of the set of valid tilings for  $\mathbf{T}$  by some label simplification i.e.  $X = \pi(X_{\mathbf{T}})$ .*

*A set of geometrical tilings  $X$  is called sofic when there exists a labelled tileset  $\mathbf{T}$  such that  $X = \pi(X_{\mathbf{T}})$  with the trivial projection  $\pi$ .*

The label simplification operator is very similar to *factor maps* and *sliding block codes* [LM21]. In the definition of sofic geometrical tilings, it is considered that a geometrical tile  $t$  is a labelled tile  $(t, 0)$  with the null label function.

The set of Penrose rhombus tilings presented in Section 2.7 and the set of Ammann-Beenker tilings presented in Section 2.8 are both sofic.

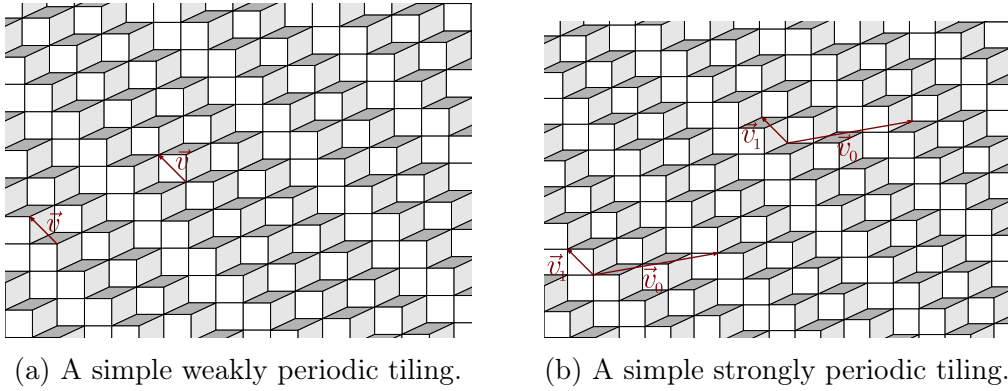


Figure 2.10: Weak and strong periodicity.

### 2.3 Order

The notions of order are central in the study of tilings. We will first define periodicity which is the most basic notion of order and we will then move on to notions of order for aperiodic tilings.

**Definition 2.3.1** (Periodicity). *A geometrical or labelled tiling  $\mathcal{T}$  is periodic of period  $\vec{v} \neq \vec{0}$  when it is invariant under the translation of vector  $\vec{v}$  i.e. any ball of centre  $p$  of the tiling is equal to the ball of centre  $p + \vec{v}$  up to translation i.e.*

$$\forall r \in \mathbb{R}^+, p \in \mathbb{R}^2, B_{\mathcal{T}}(p, r) \equiv B_{\mathcal{T}}(p + \vec{v}, r).$$

*A tiling that admits two non-collinear periods is called strongly-periodic or fully-periodic. A tiling which is periodic but not strongly-periodic is called weakly-periodic. A tiling that admits no periods is called non-periodic.*

Remark that for tilings of  $\mathbb{R}^d$  with  $d \geq 2$ , a tiling is strongly periodic when it admits a base of  $\mathbb{R}^d$  for periods and it is weakly periodic when it admits at least 1 period but is not strongly periodic.

**Definition 2.3.2** (Aperiodic subshifts and tilesets). *A subshift  $X$  is called aperiodic when it is not empty and it contains no periodic tiling. A geometrical or labelled tileset  $\mathbf{T}$  is called aperiodic when its induced subshift  $X_{\mathbf{T}}$  is aperiodic.*

Remark that a tiling that admits no period is called non-periodic and not aperiodic, only a subshift is called aperiodic when it contains no periodic

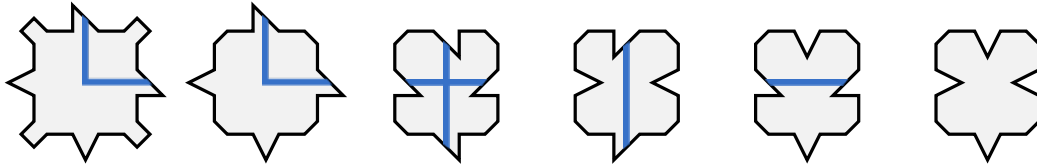


Figure 2.11: Robinson tileset, classical version with square tiles cut and notches.

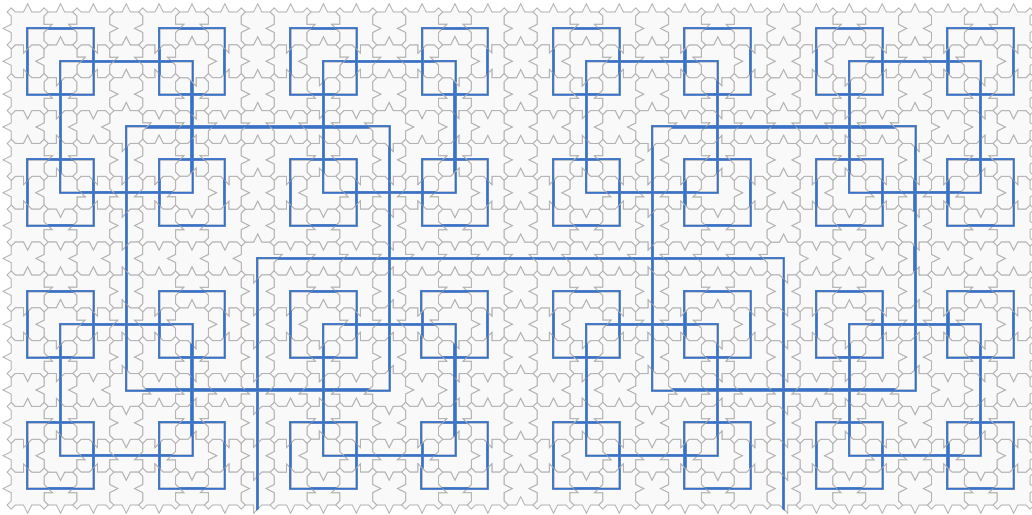


Figure 2.12: The hierarchical structure of Robinson tilings.

tiling. Sometimes a tiling that belong to an aperiodic subshift (*i.e.* its orbit closure is aperiodic) is called aperiodic.

**Theorem 4** ([Ber66]). *There exist aperiodic tilesets.*

This theorem was first formulated and proved on Wang tiles with a tileset of 20426 tiles up-to translation but it was quickly reduced to 56 tiles by Robinson in [Rob71] which are represented in Figure 2.11 up-to isometry, the hierarchical structures of Robinson tilings are shown in Figure 2.12. The minimal number of tiles up-to translation in an aperiodic Wang tileset is 11 [JR21], the Jeandel-Rao tileset in Figure 2.8 is aperiodic and minimal for the number of tiles up to translation among aperiodic Wang tilesets.

Though it is not strongly related to our topic let us mention that the existence of aperiodic tilings is closely related to the Domino Problem.

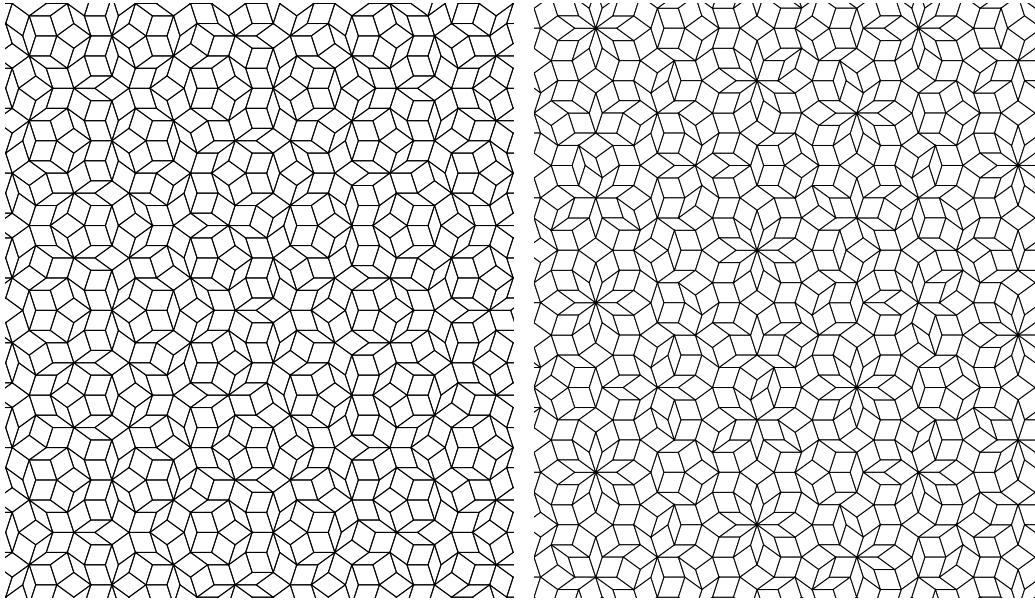


Figure 2.13: Examples of tilings with local 10-fold rotational symmetry.

**Problem 2.3.1** (Domino problem). *Given a geometrical or labelled tileset  $\mathbf{T}$ , does there exist a valid tiling for  $\mathbf{T}$ .*

**Theorem 5** ([Ber66]). *The domino problem is undecidable.*

The proof is based on the embedding of Turing machine computation in a specific aperiodic tiling, a nice introduction to this topic can be found in [JV17] which has been published in [AA17].

Now that we have defined periodicity we will define other notions of order.

**Definition 2.3.3** (Global and local  $n$ -fold rotational symmetry). *A tiling is said to have global  $n$ -fold rotational symmetry when there exists a point  $p$  such that the tiling is invariant under the rotation of centre  $p$  and angle  $\frac{2\pi}{n}$ .*

*A tiling  $\mathcal{T}$  is said to have local  $n$ -fold rotational symmetry when for every pattern  $P$  that appears in  $\mathcal{T}$ , the pattern  $P'$  obtained by rotating  $P$  by  $\frac{2\pi}{n}$  is also a pattern of  $\mathcal{T}$ . Alternatively we can define local  $n$ -fold rotational symmetry as the tiling and the tiling rotated by  $\frac{2\pi}{n}$  having the same patterns up to translation.*

The best known result regarding periodicity and rotational symmetries for tilings is the crystallographic restriction which can be formulated as follows.

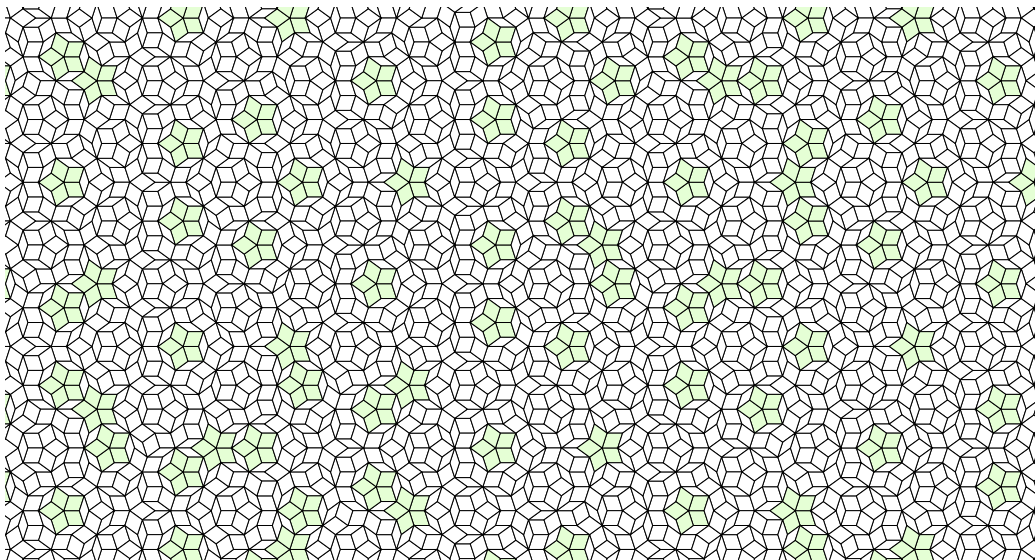


Figure 2.14: The Penrose tilings are uniformly recurrent, here we picked a pattern and highlighted all its occurrences (up to translation). Remark that this pattern also appears in another orientation but we did not highlight these occurrences.

**Theorem 6** (Crystallographic restriction). *If a periodic tiling has global or local  $n$ -fold rotational symmetry then  $n \in \{1, 2, 3, 4, 6\}$ , conversely if a tiling has global or local  $n$ -fold rotational symmetry with  $n \notin \{1, 2, 3, 4, 6\}$  then the tiling is non-periodic.*

**Definition 2.3.4** (Uniform recurrence). *A tiling  $\mathcal{T}$  is called uniformly recurrent when for any pattern  $P$  that appears in  $\mathcal{T}$  there exists a radius  $r$  such that  $P$  appears in every ball of radius  $r$  in  $\mathcal{T}$  i.e.*

$$\forall P \triangleleft \mathcal{T}, \exists r \in \mathbb{R}^+, \forall p \in \mathbb{R}^2, P \triangleleft B_{\mathcal{T}}(p, r).$$

One can easily remark that every strongly-periodic tiling is uniformly-recurrent, however it is not necessarily the case for weakly-periodic and non-periodic tilings. See Figure 2.14 for an illustration of uniform recurrence.

**Definition 2.3.5** (Quasiperiodic). *A tiling which is non-periodic and uniformly-recurrent is called quasiperiodic.*

Remark that a tiling which is non-periodic and uniformly-reccurent is aperiodic in the sense that its induced subshift is aperiodic.

In this work we are mostly interested in rhombus edge-to-edge quasiperiodic tilings with  $n$ -fold rotational symmetry, see Sections 2.7 and 2.8 for classical examples of such tilings.

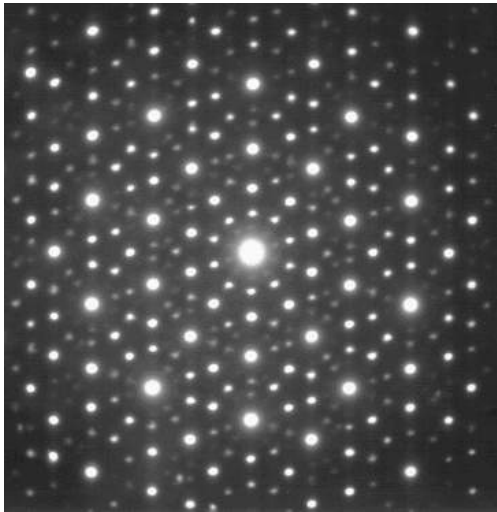
Another way of describing the order of tilings is through their diffraction patterns. We will not give precise definitions here but we will give the general ideas, see the article [BDDG16] for an introduction and the book [BG13] for full definitions and discussions on this topic.

The idea of studying tilings through their diffraction patterns comes from physics and more precisely crystallography which is the study of arrangement of atoms (or molecules) in a homogeneous solid. Crystallographists use X-ray diffraction of thin slices of material to study its atomic structure, the idea being that each atom diffracts the incoming X-ray and all the diffracted waves superpose to form a diffraction pattern. If the material has a strongly ordered structure the diffraction pattern is a collection of bright points called *pure-point diffraction pattern* (see Figure 2.15), on the contrary if the material has no ordered structure the diffraction pattern is uniform.

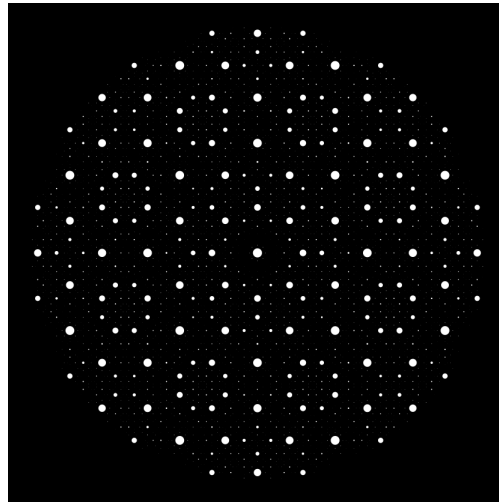
It was originally believed that pure point diffraction patterns were equivalent with crystals (periodic arrangement), however in the 80s new materials were discovered that had no periodic arrangement but had pure-point diffraction pattern [SBGC84]. Such materials are now called *quasi-crystals*.

Pure-point diffraction, or essentially discrete diffraction which is a weaker property, can be used as a definition of long-range order for tilings. In the context of tilings the X-ray diffraction is replaced with a Fourier transform on the vertex set. We will see in Section 2.5 the classes of discrete planes and cut-and-project tilings which have respectively essentially discrete diffraction patterns and pure-point diffraction patterns.





(a) An experimental diffraction pattern with 10-fold rotational symmetry [Wik].



(b) The diffraction pattern of the canonical Ammann-Beenker tiling with 8-fold rotational symmetry [BDDG16].

Figure 2.15: Diffraction patterns.

## 2.4 Substitutions

Substitutions were first introduced in the study of words so let us first define them in this context.

Let  $\Sigma$  be a finite set called alphabet. Let  $\Sigma^*$  be the set of finite words,  $\varepsilon$  be the empty word and  $\Sigma^+$  be the set of non-empty finite words and  $\cdot$  be the concatenation.

**Definition 2.4.1** (Substitution on words). *A substitution  $\sigma$  is a non-erasing morphism of  $\Sigma^*$  i.e. for any letter  $a \in \Sigma$ ,  $\sigma(a) \neq \varepsilon$  and for any two words  $u, v$ ,  $\sigma(u \cdot v) = \sigma(u) \cdot \sigma(v)$ .*

We usually define a substitution by the image of the letters.

For example the Fibonacci substitution  $\sigma_f : 0 \rightarrow 01, 1 \rightarrow 0$  and the tribonacci substitution  $\sigma_t : 0 \rightarrow 01, 1 \rightarrow 02, 2 \rightarrow 0$

Let  $\Sigma^{\mathbb{Z}}$  be the set of bi-infinite words on alphabet  $\Sigma$ .

**Definition 2.4.2** (Factors). *Let  $u$  be a finite word and  $v$  be a possibly-infinite word on the same alphabet  $\Sigma$ . We say that  $u$  is a factor of  $v$  denoted by  $u \triangleleft v$  when there exists two possibly empty and possibly infinite words  $w_p$  and  $w_s$  such that  $w = w_p \cdot u \cdot w_s$ .*

**Definition 2.4.3** (Infinite words and substitution). *A bi-infinite word  $w \in \Sigma^{\mathbb{Z}}$  is called regular for  $\sigma$  when for any finite factor  $u$  of  $w$  there exists a letter  $a \in \Sigma$  and an integer  $k$  such that  $u \triangleleft \sigma^k(a)$ .*

*A bi-infinite word  $w$  is called fixpoint of  $\sigma$  when  $w = \sigma(w)$ .*

The study of substitution on words is linked to the study of dynamical systems, Sturmian words, Rauzy fractal, S-adic systems and many other domains, see for example [Fog02].

Let us first remark that a bi-infinite word  $w \in \Sigma^{\mathbb{Z}}$  can be seen as a tiling of the line  $\mathbb{R}$  by segments as shown in Figure 2.16.

Now we can define substitutions on tilings.

Let  $\mathbf{T}$  be a finite set of polygon prototiles called tileset, remark we are only interested in edge-to-edge tilings so we chose a formalism adapted to that case which we borrowed from [FO10].

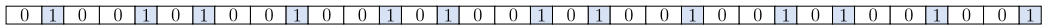
**Definition 2.4.4** (Substitution on tiles, combinatorial substitution). *A substitution on tileset  $\mathbf{T}$  is an application  $\sigma$  that to each prototile associates a patch of tiles paired to an application  $\partial\sigma$  that to each edge  $e$  of a prototile  $t$  associates a subset of external edges of  $\sigma(t)$ .*

*The images  $\sigma(t)$  of the prototiles by the substitution are called metatiles. The substitution is extended to an application on patches of tiles or tilings by applying the substitution separately on each tile and gluing the obtained metatiles together in such a way that it conserves the combinatorial structure i.e. if a patch  $P$  comprises two tiles  $t_0$  and  $t_1$  adjacent along edge  $e$  then the patch  $\sigma(P)$  is obtained from gluing the two patches of  $\sigma(t_0)$  and  $\sigma(t_1)$  along the set of edges  $\partial\sigma(t_0, e)$  and  $\partial\sigma(t_1, e)$  which have to be equal.*

We actually relax the definition of the boundary application  $\partial\sigma$  by allowing  $\partial\sigma(t, e)$  to contain boundary edges and boundary tiles, under the

$$\sigma_f : \begin{array}{l} \boxed{0} \rightarrow \boxed{0} \boxed{1} \\ \boxed{1} \rightarrow \boxed{0} \end{array}$$

(a) The Fibonacci substitution  $\sigma_f$  on segments.



(b) A factor of the Fibonacci word as a tiling of the real line.

Figure 2.16: Words as tilings of the line by segments.

condition that when a tile is in  $\partial\sigma(t_0, e)$  and  $t_0$  is adjacent to  $t_1$  by edge  $e$  then  $\partial\sigma(t_1, e)$  contains the same tile and the two copies overlap exactly.

In Figure 2.17a we represent up to rotation a substitution on two prototiles called the Penrose substitution. On the left of the figure are the two rhombus tiles and on the right are the images of the two tiles by the substitution, in the images the dashed lines represent the expanded shape of the original tile. On each tile one edge  $e$  and its image by the substitution  $\partial\sigma(e)$  have been highlighted.

In Figure 2.17b we represent how to apply the substitution on a patch of three tiles: first apply the substitution separately on each tile and then glue it back together in a way that if two tiles  $t_0$  and  $t_1$  share an edge  $e$  then the images  $\sigma(t_0)$  and  $\sigma(t_1)$  share the meta-edge  $\partial\sigma(e)$ . In the figure the internal edges and their images are highlighted.

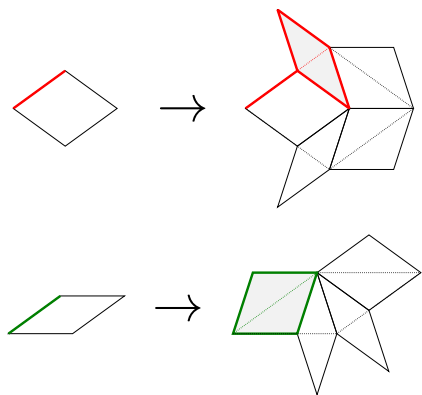
Let us remark that under this definition there is no reason that the substitution can be applied to any edge-to-edge patch (connected and with no holes) to obtain a valid patch *i.e.* also edge-to-edge connected, with no holes and which respects the combinatorial structure. For example the canonical Penrose substitution represented in Figure 2.17b cannot be applied to the star pattern (10 narrow rhombus tiles around a vertex).

**Definition 2.4.5** (Metatiles). *For each prototile  $t$  in the tilename, the sequence  $(\sigma^k(t))_{k \in \mathbb{N}}$  is called the sequence of metatiles for  $t$ .*

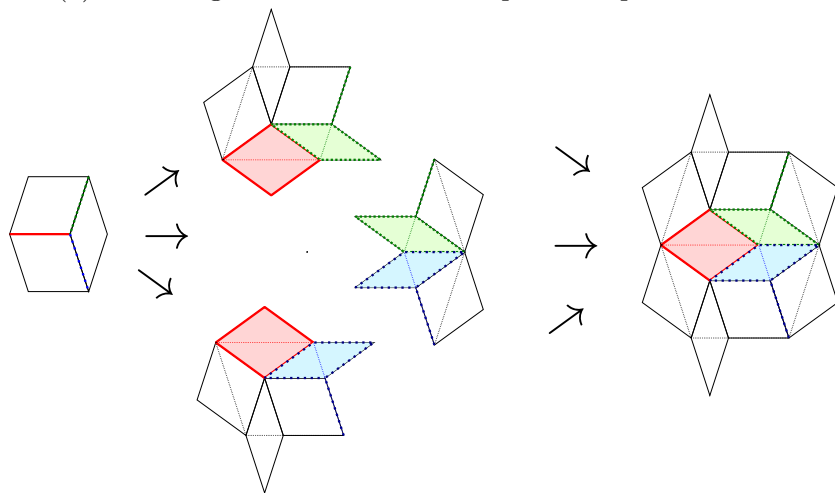
Figure 2.18 is an example of sequence of metatiles for the wide rhombus in the Penrose substitution. Narrow rhombus have been coloured in blue for easier readability of the patterns in the tiling, they are not labels used for local rules.

This definition assumes that the substitution can be applied on any  $\sigma^k(t)$  to obtain a valid patch of tiles *i.e.* an edge-to-edge connected patch with no holes. Also we want that for each prototile  $t$  the sequence  $(r_{\text{in}}(\sigma^k(t)))_k$  of the radius of the inscribed circle of the metatile  $\sigma^k(t)$  tends to infinity.

**Definition 2.4.6** (Degenerate and non-degenerate substitution). *A substitution  $\sigma$  such that there is a tile  $t$  and an integer  $k$  such that the substitution cannot be applied to  $\sigma^k(t)$  to obtain a edge-to-edge connected patch with no holes, is called degenerate. A substitution  $\sigma$  such that there is a tile  $t$  such that the sequence  $(r_{\text{in}}(\sigma^k(t)))_k$ , of the radius of the inscribed circle of the metatiles of  $t$  does not tend to infinity (for example if it is bounded) is also called degenerate. Otherwise it is called non-degenerate.*



(a) The image of the two rhombus protiles up to rotation.



(b) The substitution applied on a patch.

Figure 2.17: The Penrose substitution as a combinatorial substitution.

We will only consider non-degenerate substitutions. So in the rest “substitution” will mean “non-degenerate substitution”. There are classes of substitution that ensure non-degeneracy. Note that we imposed the edge-to-edge condition on high-order metatiles for the definition, this is due to the fact that we are interested in edge-to-edge tilings, but in general non-degeneracy is not necessarily defined with the edge-to-edge condition.

**Definition 2.4.7** (Edge-hierarchic substitution). *A substitution  $\sigma$  is called edge-hierarchic when there exists a linear application of  $\mathbb{R}^2$  called expansion*

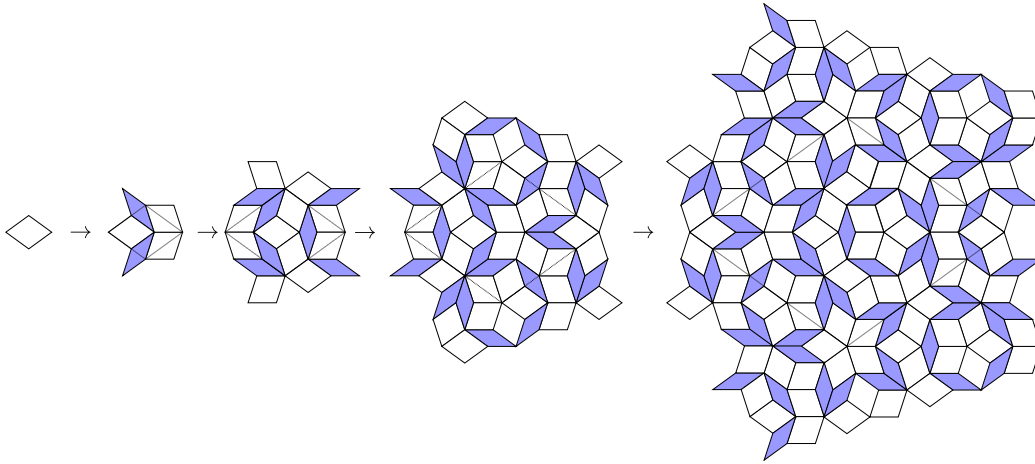


Figure 2.18: Metatiles of the wide rhombus for the Penrose substitution.

and denoted by  $\varphi$  such that for any prototile  $t$ , the metatile  $\sigma(t)$  has exactly the shape of  $\varphi(t)$  i.e.

$$\forall t \in \mathbf{T}, \bigcup_{t' \in \sigma(t)} t' = \varphi(t)$$

Examples of edge-hierarchical substitutions are shown in Figure 2.19 and the corresponding tilings are in Figures 2.2 and 2.3. However edge-hierarchy is very restrictive and most of the well-known cases are not edge-hierarchical, for example the Penrose substitution on rhombus tiles in Figure 2.18 is not edge-hierarchical though it is possible to split the rhombuses in two triangles to obtain an edge-hierarchical substitution. Note that the fact that first-order metatiles are edge-to-edge for an edge-hierarchical substitution does not imply that second order metatiles will be edge-to-edge.

Another class of (less restrictive) substitution are the vertex-hierarchical substitution.

**Definition 2.4.8** (Vertex-hierarchical substitution). *A substitution  $\sigma$  is called vertex-hierarchical when there exists a linear application of  $\mathbb{R}^2$  called expansion and denoted by  $\varphi$  such that for any prototile  $t$ , the vertices of the expanded tile  $\varphi(t)$  are vertices of the metatile  $\sigma(t)$  and also the areas of  $\varphi(t)$  and of  $\sigma(t)$  are the same i.e.*

$$\forall t \in \mathbf{T}, V(\varphi(t)) \subset V(\sigma(t)) \text{ and } \text{Area}(\varphi(t)) = \text{Area}(\sigma(t))$$

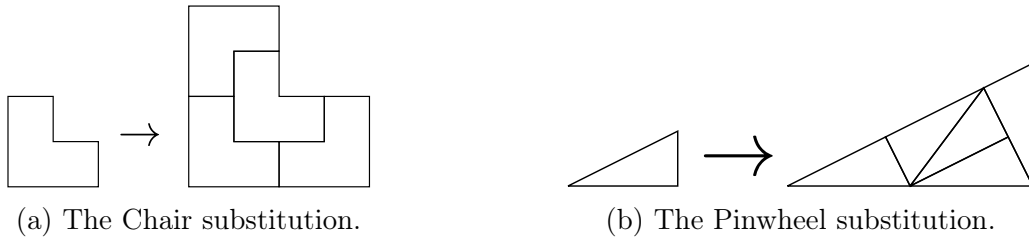


Figure 2.19: Edge hierarchic substitution.

The condition that the areas of the expanded tile and of the metatiles are the same is to be understood as a way to force the expansion to actually be the shape of the substitution. In some cases we can play around with this area condition, for example for the Penrose substitution in Figure 2.18 the tiles that overlap the expanded tile (in dotted lines) are actually cut by the edge of the expanding tile along one of their diagonals with one half of the tile inside the expanded tile and one half outside. When applying the substitution on two adjacent tiles such overlapping tiles will superpose exactly as in Figure 2.17b, when counting the Area ( $\varphi(t)$ ) these overlapping tiles are only counted as half. With this consideration the Penrose substitution is vertex-hierarchical.

Now that we have defined substitutions their metatiles and some classes of substitution that are easier to work with let us define the tiling space defined by a substitution.

**Definition 2.4.9** (Tilings regular for a substitution). *A pattern of tiles  $P$  is said to be admissible for a substitution  $\sigma$  when there exists a prototile  $t$  and an integer  $k$  such that  $P$  appears in  $\sigma^k(t)$ .*

*A tiling  $\mathcal{T}$  is said to be regular for a substitution  $\sigma$  when all the patterns that appear in  $\mathcal{T}$  are admissible for  $\sigma$  i.e.*

$$\forall P \triangleleft \mathcal{T}, \exists t \in \mathbf{T}, \exists k \in \mathbb{N}, P \triangleleft \sigma^k(t)$$

*The set of regular tilings for a substitution  $\sigma$  is called the tiling space of  $\sigma$ , or subshift of  $\sigma$  and is denoted by  $X_\sigma$ .*

Up to translation and rotation the Chair tiling has only one prototile, so we represent only one sequence of metatiles in Figure 2.20, but up to translation it has 4 sequences of metatiles. The Chair tilings are defined by the fact that their patterns all appear in a sequence of metatiles shown in Figure 2.20.

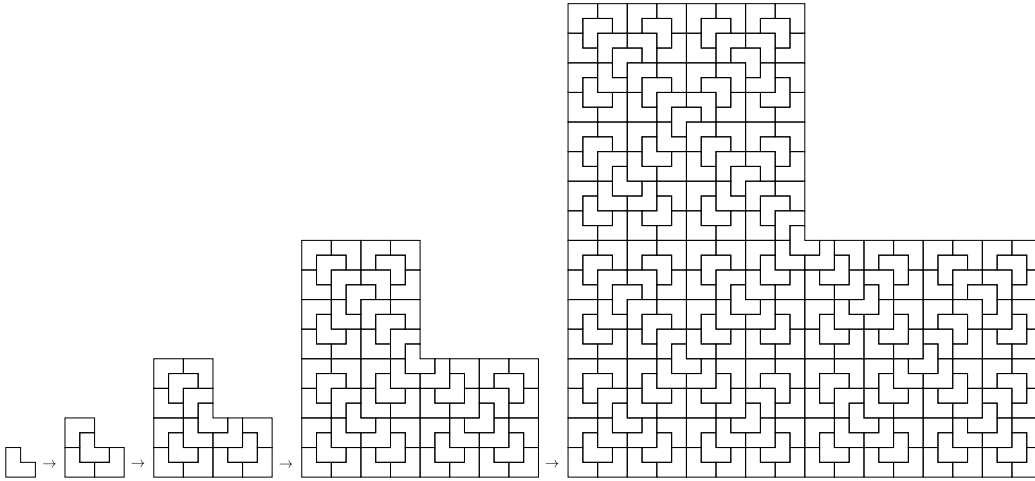


Figure 2.20: The sequences of metatiles for the Chair substitution.

**Definition 2.4.10** (Primitivity). *A substitution  $\sigma$  is called primitive of order  $k$  when for any two prototiles  $t$  and  $t'$ ,  $t'$  appears in  $\sigma^k(t)$ . A substitution is called primitive when there exists an integer  $k$  such that it is primitive of order  $k$ .*

In this definition the appearance of  $t'$  in  $\sigma^k(t)$  is understood to be only up to translation and not up to rotation. In the case where the prototiles are defined up to translation and rotation one must understand that every tile  $t'$  in every orientation must appear in  $\sigma(t)$ .

For example the Penrose rhombus substitution is primitive of order 4, the Chair substitution is primitive of order 2 and the Pinwheel substitution is not primitive.

**Proposition 2.4.1** (Primitivity and uniform recurrence). *Let  $\sigma$  be a primitive substitution. Every tiling regular for  $\sigma$  is uniformly recurrent.*

*Proof.* This is a classical result but we will give a proof nonetheless to familiarize the reader with substitution. Let  $\sigma$  be a primitive substitution of order  $k$ ,  $\mathcal{T}$  be a tiling regular for  $\sigma$  and  $P$  be a pattern that appears in  $\mathcal{T}$ . Let us prove that there exists a radius  $r$  such that for all  $p \in \mathbb{R}^2$ ,  $P \triangleleft B_{\mathcal{T}}(p, r)$ .

Since  $\mathcal{T}$  is regular for  $\sigma$  there exists a prototile  $t_0$  and an integer  $k_0$  such that  $P \triangleleft \sigma^{k_0}(t_0)$ .

Since  $\sigma$  is primitive of order  $k$ , for any prototile  $t$ ,  $t_0$  appears in  $\sigma^k(t)$ .

So  $P$  appears in  $\sigma^{k+k_0}(t)$  for any tile  $t$ .

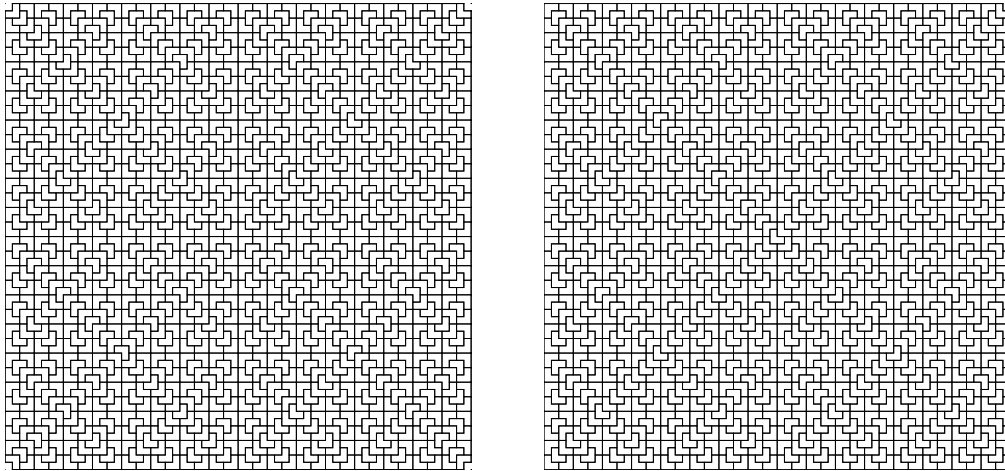


Figure 2.21: Two slightly different fragments of regular tilings for the Chair substitution.

Let  $r$  be twice the maximum radius of the circumscribed circle of all metatiles  $\sigma^{k+k_0}(t)$ , since the tileset is finite this maximum exists and is finite.

By definition of  $r$ , in any ball of radius  $r$  there is at least one metatile of order  $k + k_0$ , and since  $P$  appears in every metatile of order  $k + k_0$  then  $P$  appears in every ball of radius  $r$ .

□

The other good thing about primitive substitution is that no metatile can be absent of a regular tiling.

**Proposition 2.4.2** (Primitivity and metatiles). *Let  $\sigma$  be a (non-degenerate) primitive substitution. Every metatile  $\sigma^k(t)$  appears in every tiling regular for  $\sigma$ .*

*Proof.* Let  $\sigma$  be a non-degenerate primitive (of order  $k_0$ ) substitution, let  $\sigma^k(t)$  be a metatile of this substitution and let  $\mathcal{T}$  be a tiling regular for the substitution.

For any prototile  $t'$ , for any  $k' \geq k + k_0$ ,  $\sigma^k(t) \triangleleft \sigma^{k'}(t')$  by primitivity of order  $k_0$ . By regularity of the tiling, there exists at least one prototile of order  $k' \geq k + k_0$  that appears in the tiling, so  $\sigma^k(t)$  appears in the tiling.

The fact that a prototile of order at least  $k + k_0$  necessarily appears in the tiling derives from the fact that the diameter of the circumscribed circle



to metatiles of order less than  $k + k_0$  is bounded by finiteness of the tiling and of the possible  $k_1 < k + k_0$  i.e.

$$\exists B \in \mathbb{R}^+, \forall t_1 \in \mathbf{T}, \forall k_1 < k + k_0, r_{\text{ext}}(\sigma^{k_1}(t_1)) \leq B$$

But every finite patch of the tiling, including those of inscribed circle bigger than this bound  $B$  must appear in the sequence of metatiles. So metatiles of arbitrarily large order appear in the tiling. □

Another way to define a tiling set from a substitution is as follows.

**Definition 2.4.11** (Limit set of a substitution). *The limit set of a substitution  $\sigma$  is the set of tilings  $\mathcal{T}$  that have an infinite sequence of pre-images by  $\sigma$  i.e.*

$$\exists (\mathcal{T}_k)_{k \in \mathbb{N}}, \mathcal{T}_0 = \mathcal{T} \text{ and } \forall k, \sigma(\mathcal{T}_{k+1}) = \mathcal{T}_k$$

And the limit set of a substitution may contain fixpoint tilings.

**Definition 2.4.12** (Fixpoints). *A fixpoint of substitution  $\sigma$  is a tiling  $\mathcal{T}$  such that  $\sigma(\mathcal{T}) = \mathcal{T}$ . A fixpoint is called regular when it is regular for the substitution, and singular otherwise.*

*We sometimes say that  $\mathcal{T}$  is a fixpoint of  $\sigma$  when in fact there exists some integer  $k \geq 1$  such that  $\mathcal{T}$  is a fixpoint of  $\sigma^k$  i.e.  $\sigma^k(\mathcal{T}) = \mathcal{T}$ .*

The usual way to create a fixpoint is to start from a patch called seed and to iterate the substitution on it.

**Definition 2.4.13** (Seed). *Given a substitution  $\sigma$  a seed is a patch of tiles  $P_0$  such that  $P_0 \subset \sigma(P_0)$ , in this definition  $P_0$  is a patch and not a pattern and when we say  $P_0 \subset \sigma(P_0)$  it is to be understood that the seed  $P_0$  is not moved by the substitution (see Figure 2.22).*

*A seed is called regular when it is admissible for the substitution i.e. it appears in some metatile  $\sigma^k(t)$ , and singular otherwise.*

**Proposition 2.4.3** (Fixpoint from a seed). *Given a substitution  $\sigma$  and a seed  $P_0$ , the tiling  $\mathcal{T}_\infty = \lim_{k \rightarrow \infty} \sigma^k(P_0)$  exists, has the patches  $\sigma^k(P_0)$  as central patterns and is a fixpoint of the substitution.*

*If the seed is regular then so is the tiling.*

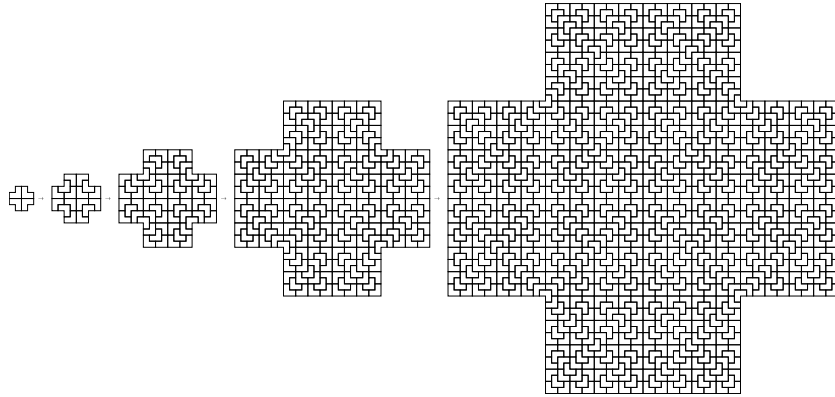


Figure 2.22: A regular seed for the chair substitution and its images.

*Proof.* Since the work presented here is little concerned with topology of tiling spaces we will not go at length on how we define in all generality the convergence of sequences of tilings. Here we consider the classical cylinder topology on tilings [Rob04].

This result is based on two things, the fact that  $P_0$  is a seed so if we define  $P_k = \sigma^k(P_0)$  we have

$$P_0 \subset P_1 \subset P_2 \subset P_3 \cdots \subset P_k \subset P_{k+1} \dots$$

with the  $\subset$  relation meaning that the patch appears at precisely its own position and not up-to translation. Moreover since the substitution is non-degenerate for each prototile the sequence of the radius of the inscribed circles of metatiles tends to infinity. So the sequence of the inscribed circles of the patches  $P_k$  tends to infinity. So the limit tiling exists and is a fixpoint.

Moreover if the seed is regular there exists a prototile  $t_0$  and an integer  $k_0$  such that  $P_0$  appears in  $\sigma^{k_0}(t_0)$ , so each  $P_k$  appears in  $\sigma^{k_0+k}(t_0)$ . So every finite patch that appears in  $\mathcal{T}$  appears in some  $P_k$  so it appears in some  $\sigma^{k_0+k}(t_0)$ . So when the seed is regular the tiling is also regular.  $\square$

Let us remark however that a singular seed does not necessarily induce a singular tiling, it may so happen that the singularity disappears at some step  $k_i$  of the substitution. In that case  $\sigma^{k_i}(P_0)$  is a regular seed for the same tiling.

A family of singular fixpoint tilings with rotational symmetries is presented in [Har05], and a family of regular fixpoint tilings with rotational

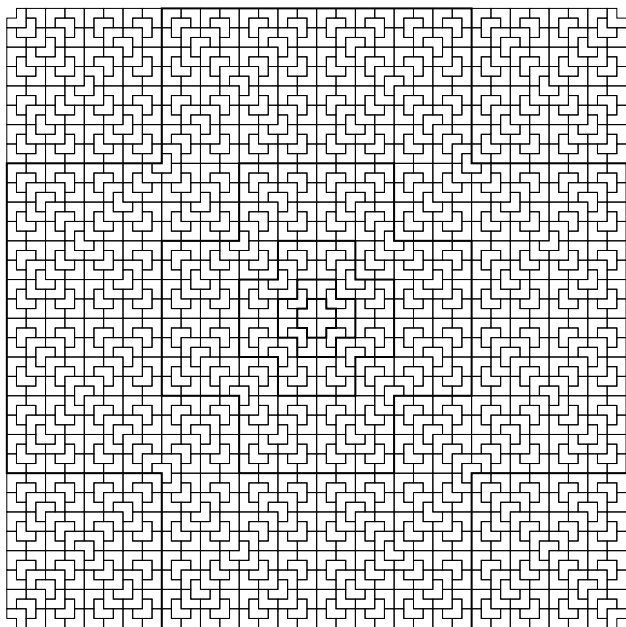


Figure 2.23: A Chair fixpoint tiling.

symmetries is presented in [KR16] and will be presented in details in Chapter 3.

If we combine Propositions 2.4.1 and 2.4.3 we get the following corollary which will be used throughout this work.

**Corollary 2.4.1** (Uniformly recurrent fixpoint tilings). *Let  $\mathbf{T}$  be a set of unit rhombus prototiles and let  $\sigma$  be a non-degenerate primitive edge-to-edge substitution on  $\mathbf{T}$ .*

*Let  $P_0$  be a regular seed for  $\sigma$ .*

*The tiling  $\mathcal{T} := \lim_{k \rightarrow \infty} \sigma^k(P_0)$  exists and is a uniformly-recurrent edge-to-edge rhombus tiling which is a regular fixpoint of the substitution.*

Though it is not worded identically it is this result which is used in [KR16] to prove the existence of regular substitution tilings with  $n$ -fold rotational symmetry for any  $n$ , it is also one of the results used in Chapter 4 to prove Theorem 2.

As illustrated in this section substitutions on tilings can be used to define tiling spaces and to study the topology, the dynamics, or the combinatorics of tiling spaces. But substitution can also be used to define specific tilings

through the fixpoint construction presented above and it is this last aspect that this work is primarily interested.

Let us also remark that most of the classical tilings can be defined by substitution such as the Penrose tiling [Pen74], the Amman-Beenker tiling [Bee82], the Robinson tiling [Rob71] and many other that can be found for example in the Tilings encyclopedia [FGH].

The hierarchical structures provided by the metatiles in a substitution tiling are often use to prove such results as aperiodicity [Ber66, Rob71], however some proofs of aperiodicity are done without substitution nor hierarchical structures such as the 14-tiles aperiodic Wang tileset defined by Jarkko Kari in [Kar96] and then refined to 13 tiles in [Cul96] which has been proven to not be substitutive by the cylindricity argument of Thierry Monteil which was orally presented in [Mon], another example is the 11-tiles aperiodic Wang tileset in [JR21] though it can be derived from a substitution tiling [Lab19].

## 2.5 Planarity

A rhombus tiling with finitely many edge directions can be lifted to a discrete surface of  $\mathbb{R}^n$  where  $n$  is the number of edge directions. Before defining the lifting let us define discrete surfaces.

Let  $n$  be a positive integer and let  $(\vec{e}_0, \vec{e}_1, \dots, \vec{e}_{n-1})$  be the canonical basis of  $\mathbb{R}^n$ .

**Definition 2.5.1** (Discrete squares and segments). *A discrete square is defined by:*

- its position  $x \in \mathbb{Z}^n$
- its two directions  $i_1$  and  $i_2$  with  $0 \leq i_1, i_2 < n$  and  $i_1 \neq i_2$

as the set

$$(x, i_1 \wedge i_2) := \{x + \lambda \vec{e}_{i_1} + \mu \vec{e}_{i_2}, 0 \leq \lambda, \mu \leq 1\}.$$

We similarly define discrete segments as  $(x, i) := \{x + \lambda \vec{e}_i, 0 \leq \lambda \leq 1\}$  with  $x \in \mathbb{Z}^n$  and  $0 \leq i < n$ .

**Definition 2.5.2** (Discrete surface). *A discrete surface  $\mathcal{S}$  is a collection of discrete squares  $\mathcal{S} := \{s_i, i \in I \subseteq \mathbb{N}\}$  such that:*

- $\mathcal{S}$  is simply-connected

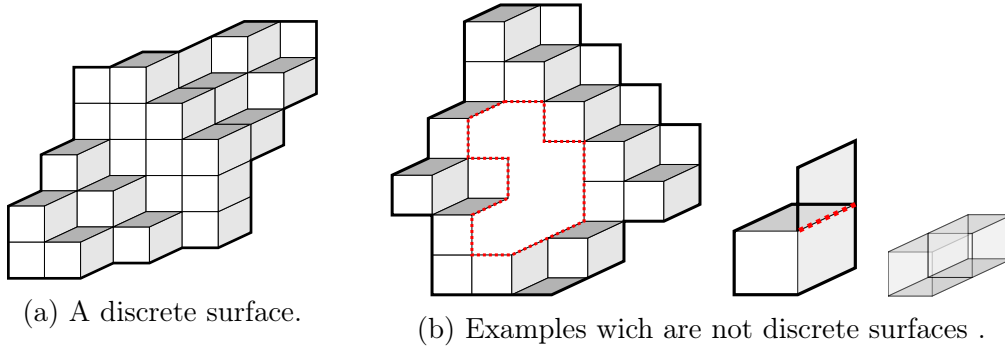


Figure 2.24: Discrete surfaces and collections of squares that are not discrete surfaces in  $\mathbb{R}^3$ .

- for any discrete segment  $(x, i)$  there are at most two squares in  $\mathcal{S}$  that have  $(x, i)$  as an edge
- in the boundary of  $\mathcal{S}$  which is the set of discrete segments that are the edge of exactly one square of  $\mathcal{S}$ , there are either only unbounded connected components or the boundary is exactly a cycle.

**Definition 2.5.3** (Lift). Any edge-to-edge rhombus patch or tiling with  $n$  edge directions  $\{\vec{v}_0, \vec{v}_1, \dots, \vec{v}_{n-1}\}$  can be lifted to a discrete surface of  $\mathbb{R}^n$  by

- picking a vertex that is mapped to the origin of  $\mathbb{R}^n$
- mapping each edge direction  $\vec{v}_i$  to  $i$ th vector of the canonical basis the  $\vec{e}_i$

This lift is unique up to choice of the origin vertex and the lift operator is denoted by  $\hat{\cdot}$ .

**Definition 2.5.4** (Discrete plane or planar tiling). A rhombus tiling  $\mathcal{T}$  with  $n$  edge directions is called planar or a discrete plane when its lifted version  $\hat{\mathcal{T}}$  approximates a 2D real plane  $\mathcal{E}$  of  $\mathbb{R}^n$  in the sense that it stays within bounded distance of  $\mathcal{E}$  i.e.

$$\exists \mathcal{E} \text{ plane of } \mathbb{R}^n, \exists d \in \mathbb{R}^+, \forall s \in \hat{\mathcal{T}}, d(s, \mathcal{E}) < d$$

The approximated plane  $\mathcal{E}$  is called slope of the tiling.

We can also define discrete planes in terms of  $\mathcal{E}^\perp$ -diameter.

**Definition 2.5.5** ( $\mathcal{V}$ -diameter, orthogonal subspace and alternate definition for discrete planes). *Given a subspace  $\mathcal{V}$  and a set  $X$  we define  $\mathcal{V}$ -diameter of  $X$  as*

$$\mathcal{V}\text{-diameter}(X) := \sup_{x_0, x_1 \in X} \|\Pi_{\mathcal{V}}(x_0 - x_1)\|$$

with  $\Pi_{\mathcal{V}}$  the orthogonal projection onto  $\mathcal{V}$ .

Given a subspace  $\mathcal{V}$  we denote by  $\mathcal{V}^\perp$  the orthogonal subspace or orthogonal supplement to  $\mathcal{V}$ .

A rhombus tiling  $\mathcal{T}$  with  $n$  edge directions is called planar or a discrete plane when its lifted version  $\widehat{\mathcal{T}}$  approximates a 2D real plane  $\mathcal{E}$  of  $\mathbb{R}^n$  in the sense that the  $\mathcal{E}^\perp$ -diameter of  $\mathcal{T}$  is finite.

A more restrictive version of planarity is cut-and-project. There are many equivalent definitions for cut-and-project tilings which can be found in [BG13] but we will present a simple definition based on the lifting of tilings.

**Definition 2.5.6** (Cut-and-project tiling and window). *A rhombus tiling  $\mathcal{T}$  with  $n$  edge directions is called cut-and-project when there exist a 2D plane  $\mathcal{E}$  of  $\mathbb{R}^n$  called slope and a compact  $W$  of  $\mathbb{R}^n$  called thickness such that*

- $\mathcal{T}$  is planar of slope  $\mathcal{E}$
- the vertex set of the lifted tiling  $V(\widehat{\mathcal{T}})$  is exactly equal to the intersection of the cone  $\mathcal{E} + W$  with  $\mathbb{Z}^n$  i.e.

$$V(\widehat{\mathcal{T}}) = (\mathcal{E} + W) \cap \mathbb{Z}^n$$

- $W$  is the closure of its interior i.e.

$$W = \overline{W^\circ}$$

The orthogonal projection of  $W$  onto the orthogonal space  $\mathcal{E}^\perp$  is called window of the tiling and is denoted by  $\Omega$ .

**Definition 2.5.7** (Canonical cut-and-project tiling). *A cut-and-project tiling  $\mathcal{T}$  is called canonical when the thickness is a translate of the unit hypercube which we denote  $\mathcal{H}$ .*

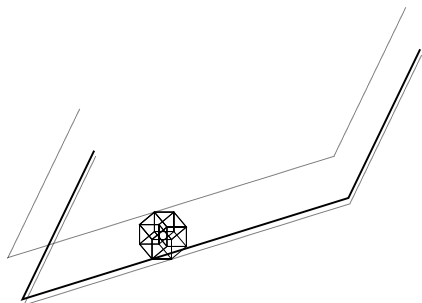


Figure 2.25: A sketch of what  $\mathcal{E} + \mathcal{H}$  looks like in dimension 4.

The idea behind this refinement of planarity is that it is not only planar but also very regular. A consequence of the fact that the vertices of a cut-and-project tiling are exactly  $(\mathcal{E} + \mathcal{W}) \cap \mathbb{Z}^n$  is that we can define a cut-and-project tiling just by its slope and thickness, this gives us the vertex set of the tiling, then we get the edges by linking vertices that are neighbour in  $\mathbb{Z}^n$  and we can project the obtained discrete surface onto  $\mathcal{E}$  to get a rhombus tiling of the plane.

In all generality any lattice  $\mathcal{L}$  of  $\mathbb{R}^n$  could be used in place of  $\mathbb{Z}^n$  but we will only consider this case here. Note that the pair  $(\mathbb{Z}^n, \mathcal{E})$  is called a *cut-and-project scheme*.

Examples of canonical cut-and-project tilings are the Penrose tiling (see Section 2.7) and the Ammann-Beenker tiling (see Section 2.8).

Now that we have presented the formalism of tilings, of substitutions and of planarity, let us recall the Theorems 1 and 2.

**Theorem 1** (Fernique, Kari, L.2020). *For any  $n \geq 3$  the canonical Sub Rosa tiling  $\mathcal{T}_n$  can be lifted to a discrete surface of  $\mathbb{R}^n$  and:*

1. *The canonical Sub Rosa tilings  $\mathcal{T}_3$  and  $\mathcal{T}_5$  are discrete planes.*
2. *For  $n = 4$  and for any  $n \geq 6$  the canonical Sub Rosa tiling  $\mathcal{T}_n$  is not a discrete plane.*

*The same holds when replacing the canonical Sub Rosa tiling  $\mathcal{T}_n$  by the set of Sub Rosa substitution tilings  $X_{\sigma_n}$ .*

**Theorem 2** (Kari, L. 2020). *For any  $n \geq 3$  the canonical Planar Rosa tiling  $\mathcal{T}'_n$  is a substitution discrete plane with global  $2n$ -fold rotational symmetry. For any  $n \geq 3$  the Planar Rosa tilings i.e. tilings in  $X_{\sigma'_n}$ , are substitution discrete planes with local  $2n$ -fold rotational symmetry.*

In the remaining sections of this chapter I will present related results, constructions and I will present in details two notable tiling subshifts: the Penrose rhombus tilings and the Ammann-Beenker tilings.

## 2.6 The multigrid method

In the 80s Nicolaas Govert de Bruijn introduced a new algebraic construction to study tilings which he called the Pentagrid and which was designed at first to study the Penrose tilings [DB81]. This construction was later generalized to multigrids to produce tilings with  $n$ -fold rotational symmetry for any  $n$ , and a generalized version of this construction was proved to be equivalent to the projection method in [GR86]. So the multigrid is a way of describing cut-and-project tilings with  $n$ -fold rotational symmetry for arbitrary  $n$ .

**Definition 2.6.1** (Grid and multigrid). *Let  $\xi$  be a unit complex number and  $\gamma$  be a real number. The grid of direction  $\xi$  and offset  $\gamma$  is defined as*

$$H(\xi, \gamma) := \{z \in \mathbb{C} \mid \operatorname{Re}(z \cdot \bar{\xi}) - \gamma \in \mathbb{Z}\}$$

*Let  $(\xi_i)_{0 \leq i < n}$  be pairwise non-collinear unit complex numbers and  $(\gamma_i)_{0 \leq i < n}$  be real numbers. The multigrid of directions  $\xi$  and offsets  $\gamma$  is*

$$G_\xi(\gamma) := \bigcup_{0 \leq i < n} H(\xi_i, \gamma_i)$$

**Definition 2.6.2** ( $n$ -fold multigrid). *Let  $n \geq 3$  be an integer. Let us define  $\zeta$  as*

$$\zeta = \begin{cases} e^{i\frac{2\pi}{n}} & \text{if } n \text{ is odd} \\ e^{i\frac{\pi}{n}} & \text{if } n \text{ is even} \end{cases}$$

*and let us define  $\gamma = (\gamma_i)_{0 \leq i < n} \in [0, 1)^n$ . The  $n$ -fold multigrid of offset  $\gamma$  is defined as*

$$G_n(\gamma) := \bigcup_{0 \leq i < n} H(\zeta^i, \gamma_i)$$

*by extension we write  $G_n(x)$  for  $G_n(x, x, \dots, x)$  with  $x \in [0, 1)$ .*

A grid  $H(\zeta^k, \gamma_k)$  is a set of equidistant lines orthogonal to  $\zeta^k$  and with offset  $\gamma_k$  from the origin. Examples of multigrid of order 4 and 5 are shown in Figure 2.26 with the vectors orthogonal to the grid also shown.



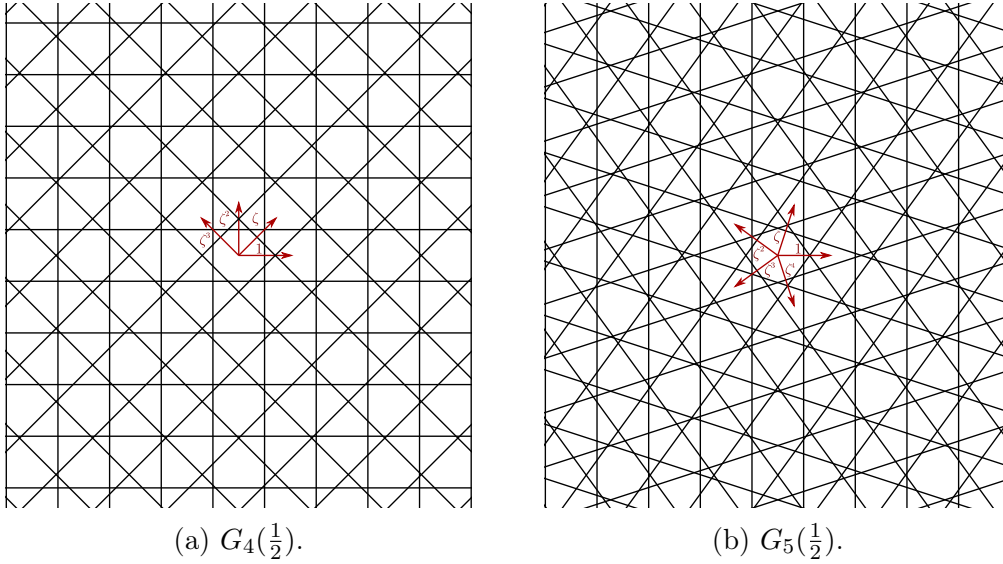


Figure 2.26: Examples of multigrids.

From a multigrid  $G_\xi(\gamma)$  we can define a tiling  $P_\xi(\gamma)$  by a duality process. This tiling is dual to the multigrid in the sense that the multigrid, seen as a graph, is the adjacency graph of the tiling, see Figure 2.28 for an example. We will define this tiling only in the  $n$ -fold case, but one can easily adapt it to the general case by replacing the directions  $\zeta_n^i$  by  $\xi_i$ .

**Definition 2.6.3** ( Grid function and dual tiling). *To define the dualization we first define two functions:  $K$  from  $\mathbb{C}$  to  $\mathbb{Z}^n$  and  $f$  from  $\mathbb{C}$  to  $\mathbb{C}$  defined by*

$$K(z) := ([\operatorname{Re}(z \cdot \bar{\zeta}^i) - \gamma_i])_{0 \leq i < n} \quad \text{and} \quad f(z) := \sum_{i=0}^{n-1} [\operatorname{Re}(z \cdot \bar{\zeta}^i) - \gamma_i] \zeta^i.$$

*Let us now define the dual tiling  $P_n(\gamma)$  by its set of vertices  $V(P_n(\gamma))$  and of edges  $E(P_n(\gamma))$  with*

$$V(P_n(\gamma)) := f(\mathbb{C})$$

$$E(P_n(\gamma)) := \{(x, y), x, y \in V(P_n(\gamma)) \mid \exists i, y = x + \zeta^i\}.$$

Lets remark that the function  $f$  is constant on every cell of the multigrid, this means that we have one vertex of the dual tiling for each cell of the multigrid, for example see the red and yellow cells and their dual vertices in Figure 2.28. Moreover if vertices  $x$  and  $y$  are dual to two cell which are

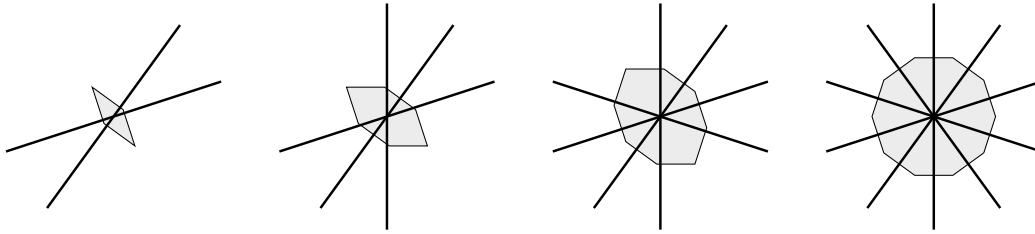


Figure 2.27: Some possible intersection points in  $G_5(\gamma)$  and their dual tiles .

adjacent along an edge of  $H(\zeta^k, \gamma^k)$  then  $y = x \pm \zeta^k$  so  $y$  and  $x$  are linked by an edge of direction  $\zeta^k$ .

Now let us take an intersection point of the multigrid  $G_n(\gamma)$  where  $k$  lines intersect. This intersection point is surrounded by  $2k$  cells which are each adjacent to their 2 neighbours. So this intersection point is dualized to a  $2k$ -gon tile with unit sides as shown in Figure 2.27, in particular if  $k = 2$  then it is dualized to a rhombus. Remark that the dual of a line of the multigrid is a chain or ribbon of tiles that share an edge, see for example the green and blue lines and their duals in Figure 2.28.

**Definition 2.6.4** (Regular multigrid). *A multigrid  $G_n(\gamma)$  is called singular when there is at least one intersection point where at least 3 lines intersect, it is otherwise called regular.*

**Proposition 2.6.1** (Dual of a regular grid). *The dual of a regular grid is a rhombus edge-to-edge tiling.*

Now that we have presented the formalism of regular multigrids in detail let us recall the Theorem 3.

**Theorem 3** ([Lut21a]). *1. For any  $n \geq 4$  the  $n$ -fold multigrid dual tiling  $P_n(\frac{1}{2})$  is a quasiperiodic rhombus cut-and-project tiling with global  $2n$ -fold rotational symmetry.*

*2. For any **odd**  $n \geq 5$  the  $n$ -fold multigrid dual tiling  $P_n(\frac{1}{n})$  is a quasiperiodic rhombus cut-and-project tiling with global  $n$ -fold rotational symmetry.*

As the  $n$ -fold multigrid dual tilings have an explicit and easily computable construction, this result gives an explicit and effective construction for cut-and-project rhombus tilings with global  $n$ -fold rotational symmetry and local

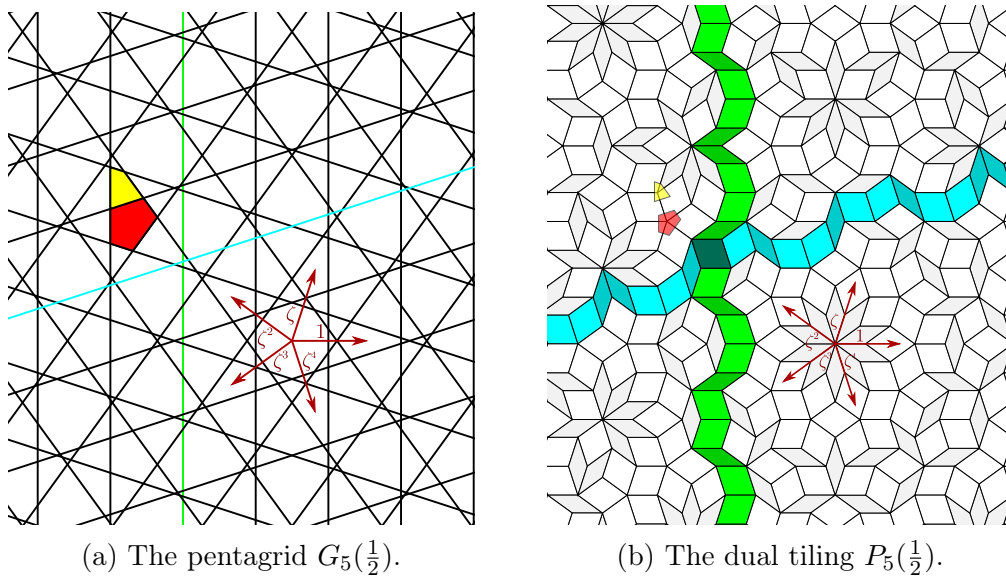


Figure 2.28: Example of a regular multigrid and its dual tiling.

$2n$ -fold rotational symmetry for the  $P_n(\frac{1}{n})$  tilings and global and local  $2n$ -fold rotational symmetry for the  $P_n(\frac{1}{2})$  tilings.

As seen in Sections 2.7 and 2.8 the canonical Penrose tiling can be defined as  $P_n(\frac{1}{n})$  with  $n = 5$ , and the canonical Ammann-Beenker tiling can be defined as  $P_n(\frac{1}{2})$  for  $n = 4$ .

## 2.7 Penrose rhombus tilings

The Penrose rhombus tilings are a family of rhombus tilings defined by Roger Penrose in [Pen74, Pen79] which are non-periodic and have local 10-fold rotational symmetry. Originally Penrose was primarily interested in tilings by pentagons (with some additional tiles to join the pentagons) and then he proved the equivalence with tilings with kite and darts tiles and then with tilings with rhombus tiles. The two rhombus tiles in the Penrose rhombus tilings are the unit rhombus with angles  $\frac{\pi}{5}$  and  $\frac{4\pi}{5}$ , and the unit rhombus with angles  $\frac{2\pi}{5}$  and  $\frac{3\pi}{5}$  depicted in Figure 2.29d.

In the set of Penrose rhombus tilings there is a specific tiling which we call canonical Penrose rhombus tiling and which we denote by  $\mathcal{T}_{Pen}$  and which has global 5-fold rotational symmetry.

**Definition 2.7.1** (Penrose tilings). *The set  $X_{Pen}$  of Penrose rhombus tilings can be defined or characterized in many ways:*

1.  $X_{Pen}$  is a sofic subshift

$$X_{Pen} = \pi(X_{\mathbf{T}_0}) = \pi(X_{\mathbf{T}_1}) = \pi(X_{\mathbf{T}_2})$$

*with labelled tilesets  $\mathbf{T}_0$ ,  $\mathbf{T}_1$  and  $\mathbf{T}_2$  defined in Figure 2.29*

2.  $X_{Pen}$  is the substitutive subshift

$$X_{Pen} = X_{\sigma_{Pen}}$$

*with substitution  $\sigma_{Pen}$  defined in Figure 2.31*

3.  $X_{Pen}$  is the set of cut-and-project tilings with slope  $(\mathcal{E}_5 + t)$  and thickness  $\mathcal{H}$  with

$$\mathcal{E}_5 = \left\langle (e^{i\frac{2k\pi}{5}})_{0 \leq k < 5} \right\rangle$$

*and  $\mathcal{H}$  is the unit hypercube and offset  $t \in \mathbb{R}^5$  such that  $(\mathcal{E}_5 + t) \cap \mathbb{Z}^5 = \emptyset$  and such that there exists a point  $p \in (\mathcal{E}_5 + t)$  such that the sum of its coordinates is in  $\mathbb{Z}$ .*

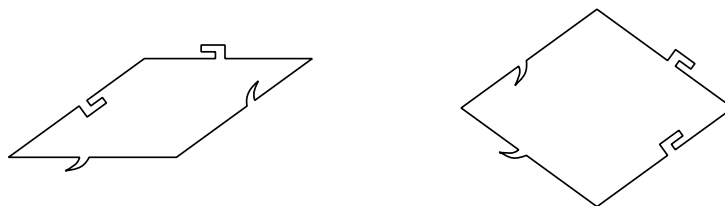
4.  $X_{Pen}$  is the closure of the set of 5-fold multigrid dual tilings  $P_5(\gamma)$  with  $\gamma \in [0, 1]^5$  such that  $\sum_{0 \leq k < 5} \gamma_k = 0 \pmod{1}$  and such that the grid  $G_5(\gamma)$  is regular

The first definition [Pen79] was with two rhombus tiles with cut-and-notches up to isometry as pictured in Figure 2.29a with two pairs of cut-notch the “shark-tooth” and the “bent-arm”, it is equivalent to rhombus tiles with arrow-labels [DB81] or coloured arcs as pictured in Figure 2.29 with the equivalence “shark-tooth” equals single-arrow equals bold red line and “bent-arm” equals double-arrow equals thin blue line.

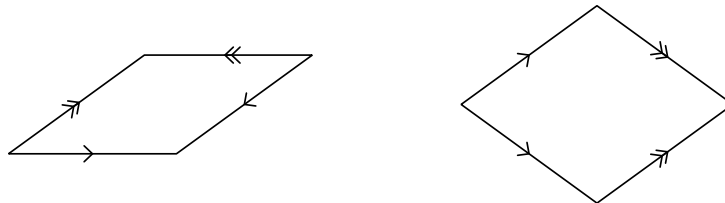
The second definition of Penrose tilings is as a substitutive subshift with the substitution of Figure 2.31a, in this figure the narrow rhombus is coloured in blue this colour is just here to help differentiate the narrow and the wide rhombus in big fragments of tilings and to help recognize patterns in a big fragment of tiling. For an easier use of the substitution we can define the substitution on the labelled tiles as shown in Figure 2.31b, these two definitions give the same metatiles up-to-labelling but when using the unlabelled substitution it can be quite tedious to compute the metatiles.

Remark also that there exists an equivalent edge-hierarchic substitution (also called stone substitution) with labels shown in Figure 2.32, the idea is to bisect the two rhombus tiles and labels are needed to force each half-tile to pair with a tile to form a rhombus.

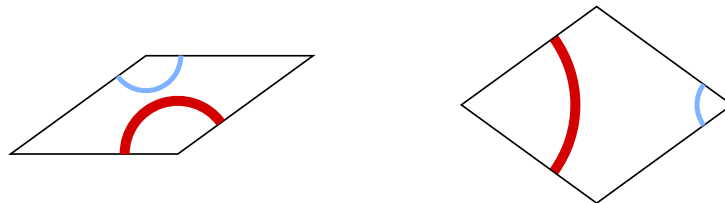
The equivalence between the sofic definition (from cut-and-notches or labels) and the substitution definition is hinted at in the original paper [Pen79], though for a complete proof see [Sen96] or [BG13].



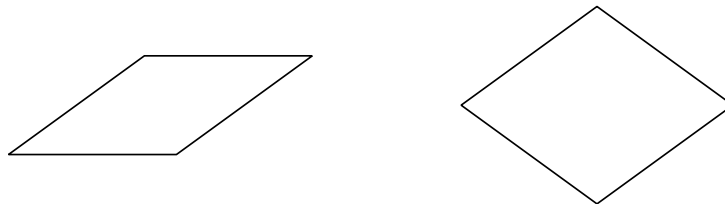
(a) Original tileset  $\mathbf{T}_0$  with cuts and notches.



(b) Tileset  $\mathbf{T}_1$  with arrow labels.



(c) Tileset  $\mathbf{T}_2$  with coloured arcs.



(d) Tileset  $\mathbf{T}_{Pen}$  with no labels.

Figure 2.29: Penrose rhombus tiles.

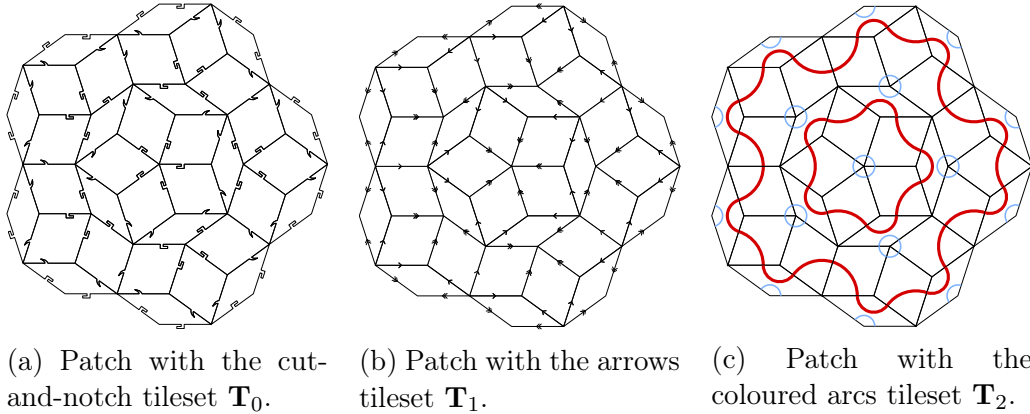


Figure 2.30: A patch with tilesets  $\mathbf{T}_0$ ,  $\mathbf{T}_1$  and  $\mathbf{T}_2$ .

The third definition by the projection method is also thoroughly discussed in [Sen96] but we will not go into details of the projection method because we can look at it from the point of view of multigrids which I prefer.

The fourth definition is due to Nicolas Govert De Bruijn in [DB81] and this paper contains the proof of equivalence with the sofic definition. The condition that  $\sum_{0 \leq k < 5} \gamma_k = 0 \pmod{1}$  is quite easy to check but the second condition is not easy to check, in [DB81] there is an exact characterization of pentagrid that are regular among those that respect the first condition, however that condition is hard to check and does not generalize easily when the first condition is not satisfied. Remark that the dual of regular pentagrids with  $\sum_{0 \leq k < 5} \gamma_k \neq 0 \pmod{1}$  are rhombus tilings that do not belong to the set of Penrose tilings, for example see the tilings in Figure 2.13 page 25 which are multigrind dual tilings but the one on the right has pattern that do not exist in Penrose tilings.

Remark that the Penrose rhombus tilings can be defined by local rules without labels, either by a finite set of forbidden patterns or by a finite set of allowed patterns. We were unable to find a reference for this result though it is mentioned in [Bee82] and cited as “De Bruijn, oral communication”.

**Definition 2.7.2** (Canonical Penrose rhombus tiling). *The canonical Penrose rhombus tiling  $\mathcal{T}_{Pen}$  is a rhombus tiling with global 5-fold rotational symmetry and 10-fold local rotational symmetry that can be defined in three ways:*

1.  $\mathcal{T}_{Pen}$  is the regular fixpoint tiling of substitution  $\sigma_{Pen}^2$  from the seed of

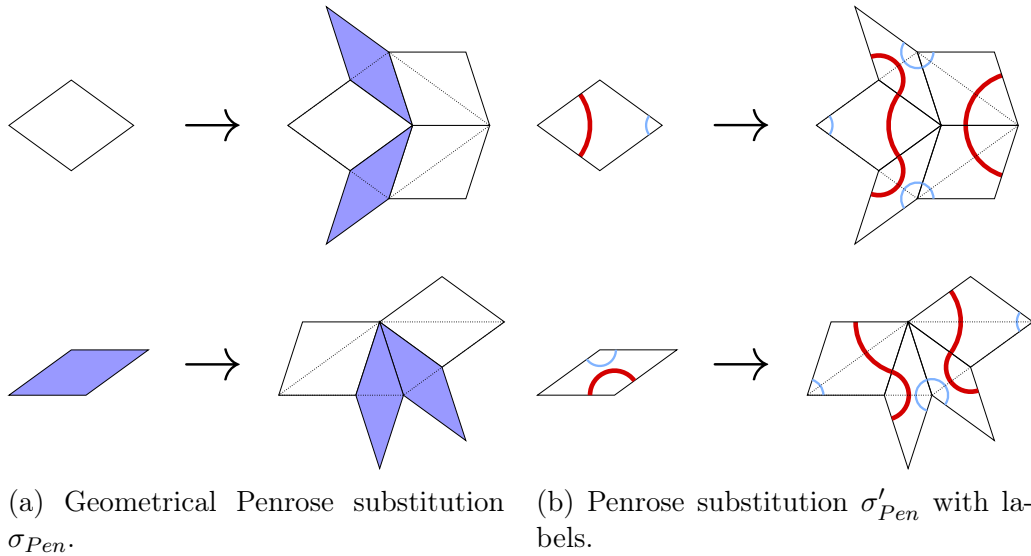


Figure 2.31: Penrose substitutions.

Figure 2.33

2.  $\mathcal{T}_{Pen}$  is the multigrid dual tiling  $P_5(\frac{1}{5})$  (or  $P_5(\frac{4}{5})$  up to rotation)
3.  $\mathcal{T}_{Pen}$  is the canonical cut-and-project tiling of slope  $\mathcal{E}_5 + (\frac{1}{5}, \frac{1}{5}, \frac{1}{5}, \frac{1}{5}, \frac{1}{5})$

Let us first remark that there is no definition of the canonical Penrose rhombus tiling with local rules. Remark also that up to translation and rota-

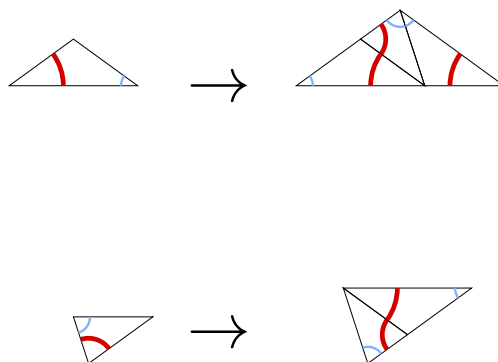


Figure 2.32: Penrose substitution  $\sigma''_{Pen}$  with rhombus tiles split in triangles.

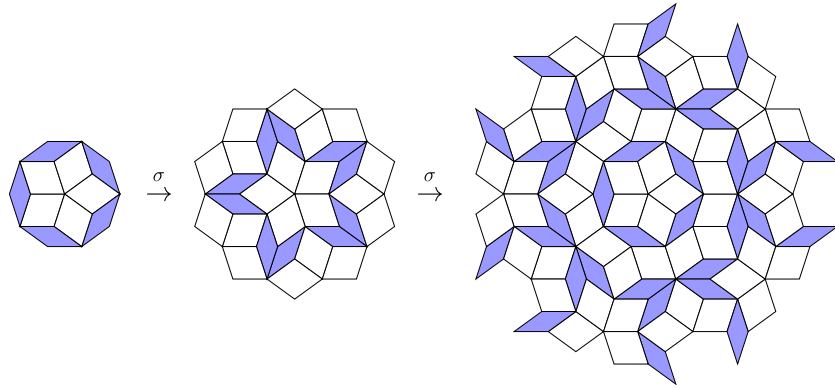


Figure 2.33: The seed for  $\mathcal{T}_{Pen}$  and its images by  $\sigma_{Pen}$ , see that the seed appears at the center of its image by  $\sigma_{Pen}^2$ .

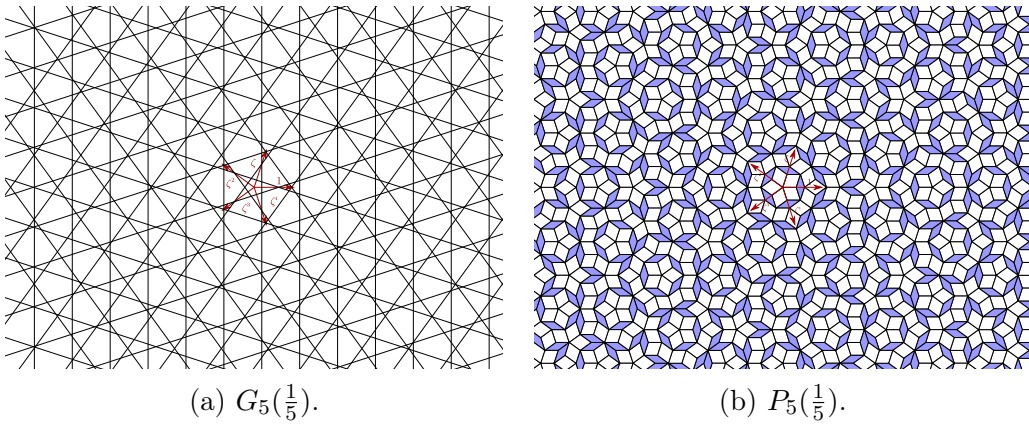


Figure 2.34: The canonical Penrose rhombus tiling as a multigrid dual.

tion there are two tilings in  $X_{Pen}$  that have global 5-fold rotational symmetry which are  $\mathcal{T}_{Pen} = P_5(\frac{1}{5}) \equiv P_5(\frac{4}{5})$  and  $\sigma_{Pen}(\mathcal{T}_{Pen}) = P_5(\frac{3}{5}) \equiv P_5(\frac{2}{5})$ .

The first definition is as the fixpoint of  $\sigma_{Pen}^2$  from the seed shown in 2.33, as shown in the figure we have indeed that the seed is at the centre of its image by  $\sigma_{Pen}^2$ . And the seed is a regular pattern for  $\sigma_{Pen}$  and  $\sigma_{Pen}^2$  because it appears in  $\sigma_{Pen}^4$  of both prototiles.

The second definition as multigrid dual tiling and the third as a cut-and-project tiling are essentially the same definition due to the correspondance between multigrid dual tilings and cut-and-project tilings [GR86].

For the cut-and-project definition we can study the window  $\Omega$  of the tiling



which is the projection of the set of vertices of the tiling  $V(\mathcal{T}_{Pen})$  on the orthogonal subspace  $\mathcal{E}_5^\perp$ , for a detailed description of the window see [Sen96].

## 2.8 Ammann-Beenker tilings

Another famous family of rhombus tilings are the Ammann-Beenker tilings defined independently by Ammann in the 70s and by Beenker in [Bee82]. The Ammann-Beenker tiles are a unit square and a unit rhombus with angles  $\frac{\pi}{4}$  and  $\frac{3\pi}{4}$ .

**Definition 2.8.1** (Ammann-Beenker tilings). *The set of Ammann-Beenker denoted by  $X_{AB}$  can be characterized in many ways:*

1.  $X_{AB}$  is a sofic subshift

$$X_{AB} = \pi(X_{\mathbf{T}})$$

*with labelled tileset  $\mathbf{T}$  in Figure 2.35a and with the condition that the green corner shapes form little houses*

2.  $X_{AB}$  is the closure of the set of 4-fold multigrid dual tilings  $P_4(\gamma)$  such that the grid  $G_4(\gamma)$  is regular

3.  $X_{AB}$  is a substitutive subshift

$$X_{AB} = X_{\sigma_{AB}}$$

*with the substitution  $\sigma_{AB}$  from Figure 2.37*

4.  $X_{AB}$  is the set of canonical cut-and-project tilings with slope  $(\mathcal{E}_4 + t)$  with  $t$  such that  $(\mathcal{E}_4 + t)$  has no point with integer coordinates.

The first definition, due to Ammann dates from the 70s even if it was only published in [GS87, AGS92], is with 2 decorated tiles up to isometry represented in Figure 2.35a and with the condition that the green corner shapes form house shapes as in Figure 2.36b this condition forbids patterns such as the one in Figure 2.36a. Note that by changing the decorations we can have equivalent tilings without the additional house condition, but

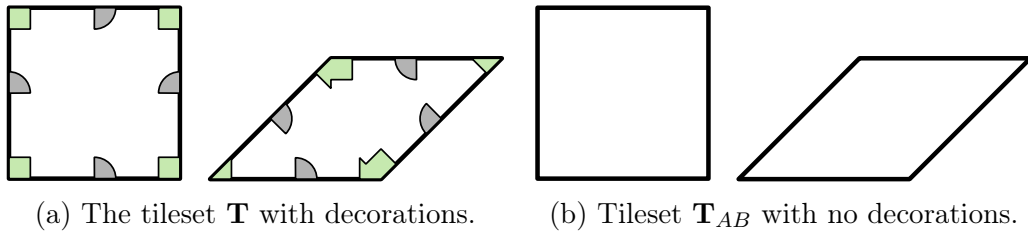


Figure 2.35: The Ammann-Beenker tiles.

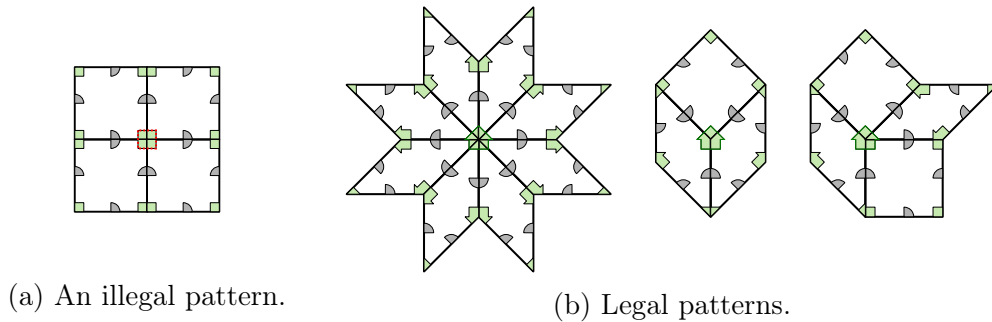


Figure 2.36: The house condition on Ammann-Beenker tiles.

in that case we have more tiles up to isometry (both the rhombus and the square will have copies with different decorations).

The second definition, due to Beenker in [Bee82], was inspired by the pentagrid approach of the Penrose tilings by De Bruijn in [DB81] and uses a 4-fold multigrad or tetragrid.

The third definition as a substitutive subshift is present in [GS87, AGS92] remark that just as in the case of Penrose tilings we have an equivalent edge-hierarchic substitution with labels by bisecting the square tile in two. Remark also that we can use either the labelled or unlabelled substitution in this definition, however the labelled one is easier to manipulate because the substitution can be applied to any valid pattern. Whereas if we use the unlabelled substitution it can be quite tricky to determine whether the substitution can be applied to a given patch, determining if the substitution can be applied is as hard as determining if the patch is valid and as mentioned above this can not be done locally.

The fourth definition can be seen as a corollary of the tetragrid definition.

Remark that there is no definition of Ammann-Beenker tilings by vertex-atlas or by a finite set of forbidden patterns. The labelling of the tiles is

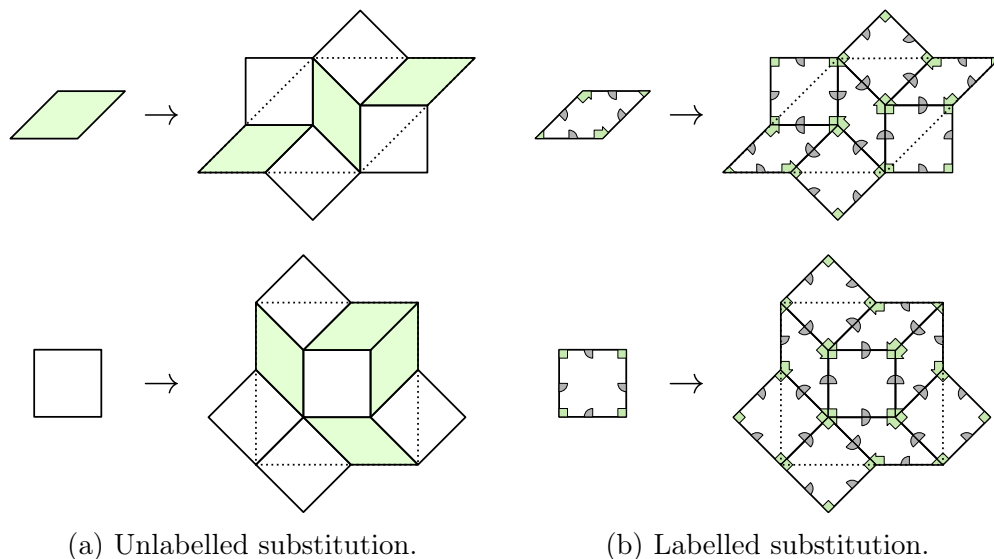


Figure 2.37: Ammann-Beenker substitution  $\sigma_{AB}$ .

necessary to define it by local rules only, and this labelling can not be decided locally from an unlabelled tiling. It means that there is no local algorithm that from input a tiling with squares and rhombuses either outputs a correct Ammann labelling of the tiling when there exists one, for more details on this see [Sen96, BG13].

**Definition 2.8.2** (Canonical Ammann-Beenker tiling). *The canonical Ammann-Beenker tiling  $\mathcal{T}_{AB}$  has three equivalent definitions:*

1.  $\mathcal{T}_{AB}$  is the regular fixpoint tiling of substitution  $\sigma_{AB}$  from seed  $S_4$  shown in Figure 2.38
2.  $\mathcal{T}_{AB}$  is the multigrad dual tiling  $P_4(\frac{1}{2})$
3.  $\mathcal{T}_{AB}$  is the canonical cut-and-project tiling of slope  $\mathcal{E}_4 + (\frac{1}{2}, \frac{1}{2}, \frac{1}{2}, \frac{1}{2})$

Remark that as in the case of the canonical Penrose rhombus tiling there is no definition of the Canonical Ammann-Beenker tiling with local rules.

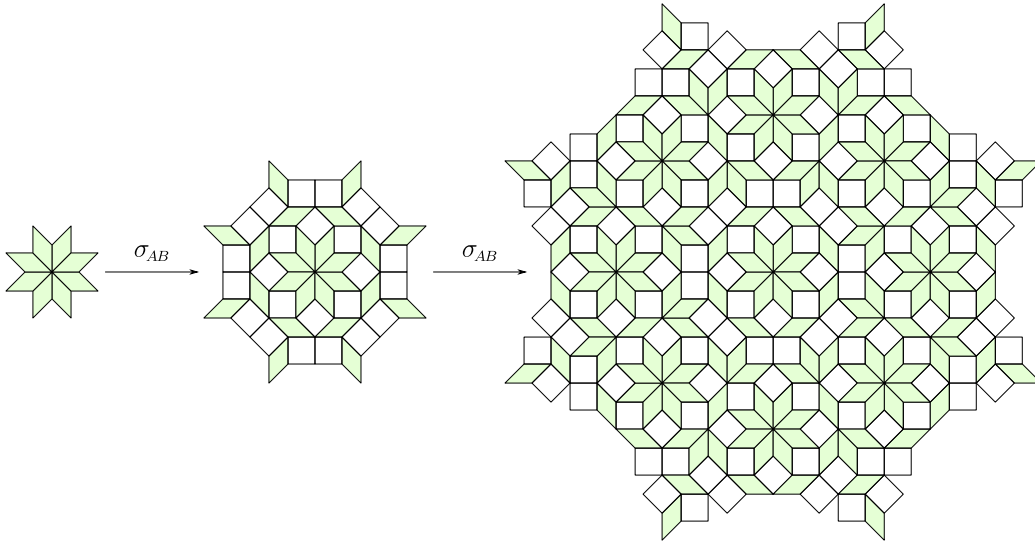


Figure 2.38: The seed for the Ammann-Beenker substitution  $\sigma_{AB}$ , remark that it is at the centre of its image by  $\sigma_{AB}$ .

## 2.9 Canonical substitution tilings

Canonical substitution tilings were defined and studied by Edmund Harriss [Har04].

**Definition 2.9.1** (Canonical substitution tilings). *A canonical substitution tiling is a tiling  $\mathcal{T}$  such that:*

1.  $\mathcal{T}$  is regular for some vertex hierarchic substitution (with condition on the expansion  $\varphi(t) = \lambda t$ )
2.  $\mathcal{T}$  is a canonical cut-and-project tiling

As seen in Sections 2.7 and 2.8 the Penrose tilings and Ammann-Beenker tilings are canonical substitution tilings. The most classic examples for substitution cut-and-project tilings that are not canonical (which means that the thickness of the cut-and-project tiling is not the unit hypercube) is actually for tilings of the line where the thickness is a Rauzy fractal [AI<sup>+</sup>01], an example of non-canonical substitution cut-and-project tiling in dimension 2 is given in Section 2.10.

To state Harriss' theorem we need a refinement on the definition of canonical cut-and-project tilings. Given a tiling  $\mathcal{T}$  which is cut and project of slope

$\mathcal{E}$  we decompose the orthogonal subspace  $\mathcal{E}^\perp$  as an orthogonal direct sum

$$\mathcal{E}^\perp = \mathcal{W} \oplus \mathcal{R}$$

where  $\mathcal{R}$  is a rational subspace which means that it is generated by vectors with integer coordinates, and  $\mathcal{W}$  is a totally irrational subspace (contains no point of  $\mathbb{Z}^n$  except the origin).

Remark that the rationality of  $\mathcal{R}$  together with the fact the window  $\Omega$  (projection of  $\mathcal{T}$  on  $\mathcal{E}^\perp$ ) is bounded implies that  $\Pi_{\mathcal{R}}(V(\mathcal{T}))$  is finite. We denote

$$\Pi_{\mathcal{R}}(V(\mathcal{T})) := \{r_i, 0 \leq i < m\}$$

and we can partition the window as

$$\Omega := \bigsqcup_{0 \leq i < m} \Omega_i \times \{r_i\}$$

with  $\Omega_i \subset \mathcal{W}$ .

**Theorem 7** (Harriss2004). *A canonical projection tiling  $\mathcal{T}$  with decomposition  $\mathcal{E}$ ,  $\mathcal{W}$ ,  $\mathcal{R}$  and offset  $t + r$  with  $t \in \mathcal{W}$  and  $r \in \mathcal{R}$  is a canonical substitution tiling if and only if*

1.  $\mathcal{E}$ ,  $\mathcal{W}$ ,  $\mathcal{R}$  are eigenspace of a quadratic expansion matrix  $M$  i.e.
  - $M$  is a square integer matrix
  - $\dim(\mathcal{E}) = \dim(\mathcal{W})$
  - $M$  has eigenvalue  $\lambda$  on  $\mathcal{E}$  and  $\pm\lambda^{-1}$  on  $\mathcal{W}$  for some quadratic unit  $\lambda$
  - $\Pi_{\mathcal{E} \oplus \mathcal{W}}(M\mathbb{Z}^n) = \Pi_{\mathcal{E} \oplus \mathcal{W}}(\mathbb{Z}^n)$
  - $\Pi_{\mathcal{E} \oplus \mathcal{W}}(\mathbb{Z}^n)$  and  $\Pi_{\mathcal{R}}(\mathbb{Z}^n)$  are lattices
2.  $M$  has the vertex hierarchic property
3. the rational offset of the projection tiling  $r$  is in  $\Pi_{\mathcal{R}}(\mathbb{Z}^n \otimes \mathbb{Q}(\lambda))$  where  $\lambda$  is the expanding eigenvalue of  $M$

This characterization is quite complex but we will only consider the first three conditions on the quadratic expansion matrix. The spaces  $\mathcal{E}$  and  $\mathcal{W}$  must be of the same dimension and must be quadratic. These conditions are very restrictive and mean that there are no canonical substitution tilings with arbitrarily high rotational symmetry.

## 2.10 Generalized substitutions

Generalized substitutions are a framework introduced by Pierre Arnoux and Shunji Ito for the study of Rauzy fractals and their dynamics in [AI<sup>+</sup>01] and generalized in [SAI01, AFHI11].

The idea of this framework is to start from a generalized substitution on words with  $n$  letters and from this to define a substitution on discrete lines of  $\mathbb{R}^n$ , a substitution on discrete surfaces of  $\mathbb{R}^n$  and actually substitutions on discrete  $k$ -surfaces of  $\mathbb{R}^n$  for any  $0 \leq k < n$ .

This framework is very powerful but also quite complicated to use. It is well understood for  $n = 3$  [AI<sup>+</sup>01, Fer07, Jol13] but only one case has been extensively studied for  $n = 4$  in [AFHI11].

**Definition 2.10.1** (Generalized substitution). *A generalized substitution  $\sigma$  on alphabet  $\mathcal{A} = \{0, 1, 2, \dots, (n-1)\}$  is a substitution where we accept inverted letters noted  $a^{-1}$  in the image of letters. It can also be defined as non-erasing morphisms on the free group on  $n$  elements.*

We give as example to illustrate this framework the substitution studied in [AFHI11]

$$\sigma : \begin{array}{l} 0 \rightarrow 1 \\ 1 \rightarrow 2 \\ 2 \rightarrow 3 \\ 3 \rightarrow 30^{-1} \end{array}$$

Now let us define the generalized  $k$ -surfaces on which we will define the geometrical realizations of  $\sigma$ .

**Definition 2.10.2** (Generalized  $k$ -surfaces). *For  $0 \leq k < n$  the set of generalized discrete  $k$ -surfaces denoted  $\mathcal{G}_k$  is the set of formal sums of discrete  $k$ -facets where :*

- *The set of discrete vertices or discrete 0-facets is  $\mathbb{Z}^n$ , we denote its elements either  $(x)$  or  $(x, \bullet)$*
- *For  $1 \leq k < n$  a discrete  $k$ -facet is a couple  $(x, i_0 \wedge i_1 \wedge \dots \wedge i_{k-1})$  with  $x \in \mathbb{Z}^n$  and  $0 \leq i_0 < i_1 < \dots < i_{k-1} < n$ , the geometrical realization of  $(x, i_0 \wedge i_1 \wedge \dots \wedge i_{k-1})$  is*

$$\left\{ x + \sum_{0 \leq j < k} \lambda_j \vec{e}_{i_j}, 0 \leq \lambda_j \leq 1 \right\}$$

where  $(\vec{e}_i)_{0 \leq i < n}$  is the canonical basis of  $\mathbb{R}^n$

On generalized  $k$ -surface for  $k \geq 1$  we define the boundary operator  $\partial_k : \mathcal{G}_k \rightarrow \mathcal{G}_{k-1}$ . The boundary operator is defined on the facets (and extended by linearity) by

$$\begin{aligned} \partial_k(x, i_0 \wedge i_1 \wedge \cdots \wedge i_{k-1}) &= \sum_{0 \leq j < k} (-1)^j ((x, i_0 \wedge \cdots \wedge i_{j-1} \wedge i_{j+1} \wedge \cdots \wedge i_{k-1}) \\ &\quad - (x + \vec{e}_{i_j}, i_0 \wedge \cdots \wedge i_{j-1} \wedge i_{j+1} \wedge \cdots \wedge i_{k-1})) \end{aligned}$$

Note that we take the convention that  $(x, i^{-1}) := -(x - e_i, i)$ ,  $(x, i \wedge j) := -(x, j \wedge i)$  and  $(x, i \wedge i) = 0$ .

On these generalized  $k$ -surfaces we can define the geometrical realizations  $E_k(\sigma)$  which have the nice property of commuting with the boundary operator.

**Definition 2.10.3** (Geometrical realizations of  $\sigma$ ).

- We define the 0-geometrical realization  $E_0(\sigma)$  on the 0-facets which are  $\mathbb{Z}^n$  and we extend it by linearity. On  $\mathbb{Z}^n$ ,  $E_0(\sigma)$  is the linear application obtained by abelianization of  $\sigma$  usually called incidence matrix.
- For  $1 \leq k < n$  define the  $k$ -geometrical realization  $E_k(\sigma)$  on the  $k$ -facets and we extend it by linearity.

$$\begin{aligned} E_k(\sigma)(x, i_0 \wedge \cdots \wedge i_{k-1}) &:= \\ &\sum_{0 \leq l_0 < |\sigma(i_0)|} \cdots \sum_{0 \leq l_{k-1} < |\sigma(i_{k-1})|} (E_0(\sigma)(x) + \sum_{0 \leq j < k} \text{abel}(\text{pref}_{l_j-1}(\sigma(i_j))), \\ &\quad \sigma(i_0)_{l_0} \wedge \sigma(i_1)_{l_1} \wedge \cdots \wedge \sigma(i_{k-1})_{l_{k-1}}) \end{aligned}$$

where  $\sigma(i)_l$  is the  $l^{\text{th}}$  letter of  $\sigma(i)$ ,  $\text{pref}_l(\sigma(i))$  is the prefix of length  $l$  of  $\sigma(i)$ ,  $|\sigma(i)|$  is the length of  $\sigma(i)$  and  $\text{abel}(u)$  is the vector of  $\mathbb{Z}^n$  of which the  $j^{\text{th}}$  coordinate is the number of occurrences of the letter  $j$  in  $\sigma(i)$ .

When all goes well the image of “good” surface by  $E_k(\sigma)$  is a “good” surface, where “good” means that it can be lifted from a simply connected patch of rhombus tiles.

Let us go back to the example. The 0-geometrical realization of  $\sigma$  is

$$E_0(\sigma) := \begin{pmatrix} 0 & 0 & 0 & -1 \\ 1 & 0 & 0 & 0 \\ 0 & 1 & 0 & 0 \\ 0 & 0 & 1 & 1 \end{pmatrix}.$$

The 1-geometrical realization of  $\sigma$  is

$$E_1(\sigma) : \begin{array}{l} (0, 0) \rightarrow (0, 1) \\ (0, 1) \rightarrow (0, 2) \\ (0, 2) \rightarrow (0, 3) \\ (0, 3) \rightarrow (0, 3) - (e_3 - e_0, 0) \end{array} .$$

Note that  $E_1(\sigma)(0, 3) = (0, 3) + (e_3, 0^{-1})$  by definition of  $E_1$  and we get  $E_1(\sigma)(0, 3) = (0, 3) - (e_3 - e_0, 0)$  with  $(x, i^{-1}) = -(x - e_i, i)$ .

The 2-geometrical realization of  $\sigma$  is

$$E_2(\sigma) : \begin{array}{l} (0, 0 \wedge 1) \rightarrow (0, 1 \wedge 2) \\ (0, 0 \wedge 2) \rightarrow (0, 1 \wedge 3) \\ (0, 0 \wedge 3) \rightarrow (0, 1 \wedge 3) + (e_3 - e_0, 0 \wedge 1) \\ (0, 1 \wedge 2) \rightarrow (0, 2 \wedge 3) \\ (0, 1 \wedge 3) \rightarrow (0, 2 \wedge 3) + (e_3 - e_0, 0 \wedge 2) \\ (0, 2 \wedge 3) \rightarrow (e_3 - e_0, 0 \wedge 3) \end{array} .$$

Let us detail the computations of two special cases:

$$\begin{aligned} E_2(\sigma)(0, 0 \wedge 3) &= (0, 1 \wedge 3) - (e_3 - e_0, 1 \wedge 0) = (0, 1 \wedge 3) + (e_3 - e_0, 0 \wedge 1) \\ E_2(\sigma)(0, 2 \wedge 3) &= (0, 3 \wedge 3) - (e_3 - e_0, 3 \wedge 0) = 0 + (e_3 - e_0, 0 \wedge 3). \end{aligned}$$

Let us define two planes  $P_e$  and  $P_c$  in  $\mathbb{R}^4$  where  $P_e$  is the expanding eigenspace and  $P_c$  the contracting subspace of  $E_0(\sigma)$ , we define  $\pi_e$  the projection on  $P_e$  along  $P_c$  and  $\pi_c$  the projection on  $P_c$  along  $P_e$ . For a formal definition of  $P_e$  and  $P_c$  we define  $\lambda, \bar{\lambda}, \mu, \bar{\mu}$  the eigenvalues of  $X^4 - X^3 + 1$  which is the characteristic polynomial of  $E_0(\sigma)$  with  $|\lambda| > 1 > |\mu|$ . By convention  $Im(\lambda), Im(\mu) > 0$ . We have

$$P_e = \left\langle \left\langle \begin{pmatrix} 1 \\ \lambda \\ \lambda^2 \\ \lambda^3 \end{pmatrix} \right\rangle \right\rangle \quad P_c = \left\langle \left\langle \begin{pmatrix} 1 \\ \mu \\ \mu^2 \\ \mu^3 \end{pmatrix} \right\rangle \right\rangle .$$

**Lemma 2.10.1** ([AFHI11]).

- $E_2(\sigma)$  induces a geometrical substitution on the tiles  $\pi_e(i \wedge j)$  which is represented in Figure 2.41



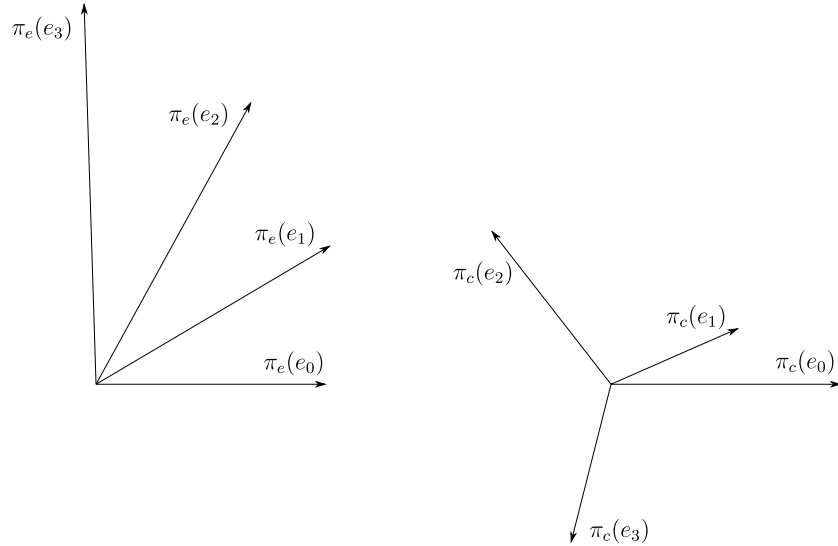


Figure 2.39: On the left the projection of the canonical basis of  $\mathbb{R}^4$  onto  $P_e$ , and on the right onto  $P_c$ .

- The tile  $(-e_2, 2 \wedge 3)$  is a seed for  $E_2(\sigma)$ , more precisely

$$(-e_2, 2 \wedge 3) \in E_2(\sigma)^3(-e_2, 2 \wedge 3),$$

as shown in Figure 2.42

Let us denote by  $\mathcal{T}_e$  the fixpoint tiling obtained by  $E_2(\sigma)$  from the seed  $(-e_2, 2 \wedge 3)$ .

**Theorem 8** ([AFHI11]).  $\mathcal{T}_e$  is a substitution cut-and-project tiling of slope  $P_e$  and with a fractal window.

Generalized substitutions  $\sigma$  and their geometrical realizations  $E_k(\sigma)$  allow us to generate cut-and-project substitution tilings with rhombus tiles of which the slope is determined by the abelianization of  $\sigma$  which we also call the 0-geometrical realization  $E_0(\sigma)$ .

Under the condition that  $\sigma$  is an automorphism of the free group we can also define the geometrical dual realizations of  $\sigma$ .

For simplicity we use a Poincaré map to associate the dual of a  $k$ -facet to a  $n - k$  facet.

**Definition 2.10.4** (Poincaré map, dual geometric realization).

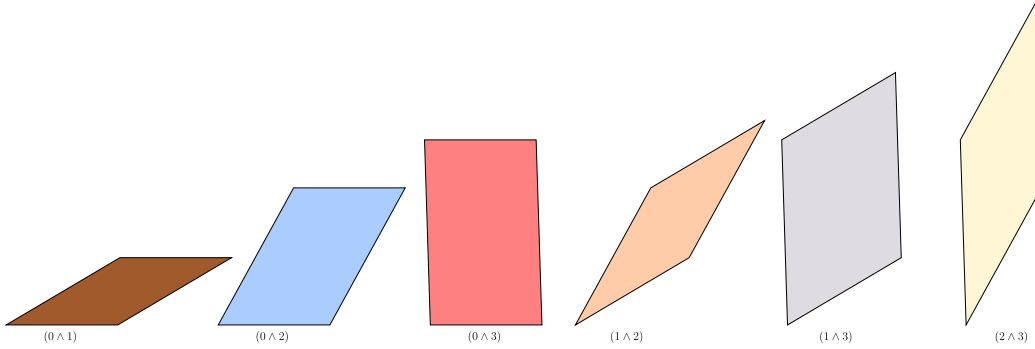


Figure 2.40: Tiles on  $P_e$ .

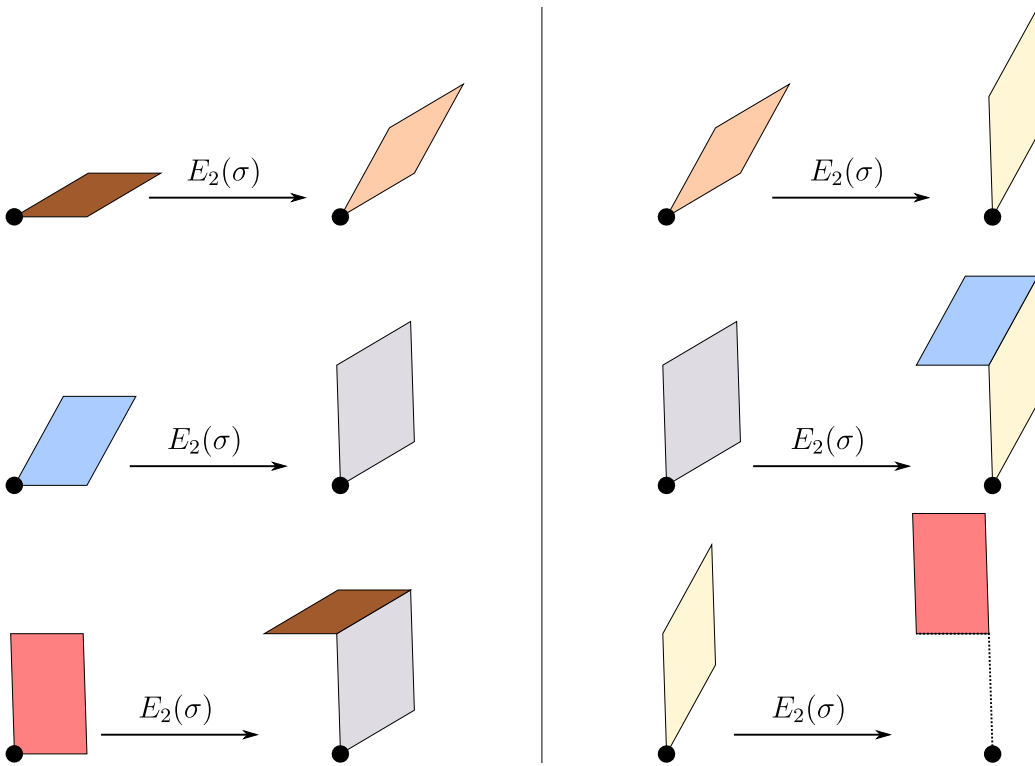
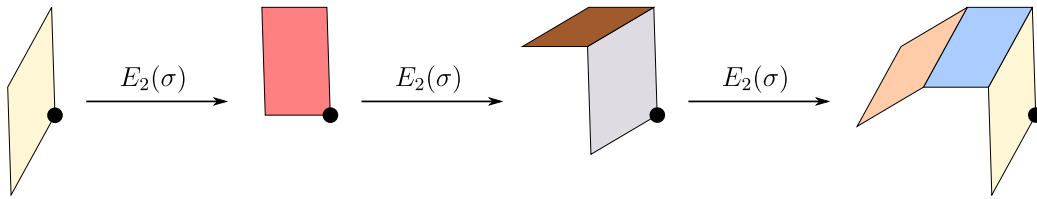
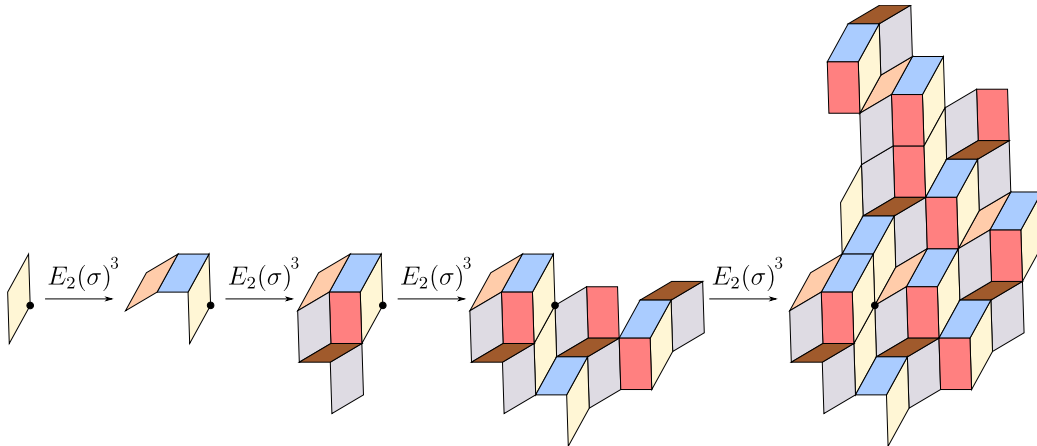


Figure 2.41: The geometrical realization  $E_2(\sigma)$  on  $P_e$ , the bold point represents the origin and in  $E_2(\sigma)(0, 2 \wedge 3)$  the dashed line represents the path from the origin to the tile.



(a) The first 3 iterations, remark that  $(-e_2, 2 \wedge 3)$  is in  $E_2(\sigma)^3 e(-e_2, 2 \wedge 3)$ .



(b) The first 4 iterations of  $E_2(\sigma)^3$ , remark that the patch grows in every direction.

Figure 2.42: Iterating  $E_2(\sigma)$  from  $(-e_2, 2 \wedge 3)$ , the bold point represents the origin.

- the Poincaré map  $\varphi_k$  is defined as

$$\varphi_k((i_0 \wedge i_1 \wedge \dots \wedge i_{k-1})^*) = (-1)^{i_0+i_1+\dots+i_{k-1}}(j_0 \wedge j_1 \wedge \dots \wedge j_{n-k-1}),$$

where  $\{i_0, i_1, \dots, i_{k-1}\}$  and  $\{j_0, j_1, \dots, j_{n-k-1}\}$  are a partition of  $\{0, 1, \dots, n-1\}$  with  $i_0 < i_1 < \dots < i_{k-1}$  and  $j_0 < j_1 < \dots < j_{n-k-1}$ .

- the geometric dual realization of dimension  $k$  denoted by  $E^k(\sigma)$  is defined as

$$E^k(\sigma) := \varphi_{n-k} \circ E_{n-k}^*(\sigma) \circ \varphi_{n-k}^{-1},$$

where  $E_{n-k}^*(\sigma)$  is the dual application of  $E_{n-k}(\sigma)$ .

The geometrical realizations and the geometrical dual realizations commute with the boundary operator *i.e.*

$$\partial_k E_k(\sigma)(f) = E_{k-1}(\sigma)(\partial_k f) \quad \partial_k E^k(\sigma)(f) = E^{k-1}(\sigma)(\partial_k f),$$

where  $\partial_k f$  is the boundary of the generalized  $k$ -surface  $f$ .

**Theorem 9** ([Ei03]). *Let  $\sigma$  be an automorphism of the free group on  $n$  elements, let  $\tilde{\sigma} := \sigma^{-1}$  be the mirror image of the inverse automorphism  $\sigma^{-1}$ . We have*

$$E^k(\sigma) = E_k(\tilde{\sigma}).$$

In our example  $E^2(\sigma)$  also induces a geometrical substitution on the tiles projected on  $P_c$ ,  $(0, 0 \wedge 1)$  is a seed for  $E^2(\sigma)$  which generates a cut-and-project fixpoint substitution tiling of slope  $P_c$  with a fractal window.

As we have illustrated in this Section, the formalism of generalized substitution is very powerful and can be used to generate substitution cut-and-project tilings (that are not necessarily canonical) but the formalism is quite heavy and cumbersome which is why, though it has been widely used to study tilings in codimension 1 [AI<sup>+</sup>01, Fer07, Jol13], it has little been used for cut-and-project tilings in codimension more than 1. The only case fully studied in the literature is in [AFHI11] which is the example we presented above.

## 2.11 Expansions of self-similar tilings and cut-and-project sets

In this Section our goal is to quickly present the results of [Kwa16] on the expansions of substitution tilings and the results of [MMP20] on the expansions of self-similar cut-and-project sets.

The main topic of this thesis being substitution discrete planes and substitution cut-and-project tilings, the question of expansions and their eigenspaces and eigenvalues will arise constantly. It is therefore important to discuss known results on these expansions.

Though the following results apply to tilings of  $\mathbb{R}^d$  or to  $n \rightarrow d$  cut-and-project sets for arbitrary  $d$ , we are interested only on tilings of the plane and  $n \rightarrow 2$  cut-and-project sets so we will state these results only in this specific case.

**Theorem 10** ([Kwa16]). *If  $\varphi : \mathbb{R}^2 \rightarrow \mathbb{R}^2$  is the expansion of an edge-hierarchic substitution fixpoint tiling with finite local complexity, then:*

1.  *$\varphi$  is Integral Algebraic: every eigenvalue of  $\varphi$  is an algebraic integer, equivalently there exists a real vector space  $\mathcal{V}$  with a lattice  $\mathcal{L} \subset \mathcal{V}$  and an integral linear transformation  $M : \mathcal{V} \rightarrow \mathcal{V}$  for which there exists a  $M$ -invariant splitting  $\mathcal{V} = \mathcal{E} \oplus \mathcal{K}$  so that the restriction  $M|_{\mathcal{E}}$  is linearly conjugate to  $\varphi$ .*
2.  *$\varphi$  is Perron : for every eigenvalue  $\lambda$  of  $\varphi$  with multiplicity  $\text{mul}(\lambda)$  and any  $\mu$  algebraic conjugate of  $\lambda$  then either  $|\lambda| > |\mu|$  or  $\mu$  is also an eigenvalue with eigenvalue  $\text{mul}(\mu) \geq \text{mul}(\lambda)$ .*

Let us introduce a little terminology on cut-and-project sets before stating the next theorem. A pair  $(\mathcal{L}, \mathcal{E})$  where  $\mathcal{L}$  is a lattice of  $\mathbb{R}^n$  (in our case  $\mathbb{Z}^n$ ) and  $\mathcal{E}$  is a subspace of  $\mathbb{R}^n$  (in our case  $\mathcal{E}$  is a 2-dimensional subspace) is called a *cut-and-project scheme* and it is called:

1. *non-degenerate* when the orthogonal projection onto  $\mathcal{E}$ ,  $\pi$  restricted to  $\mathbb{Z}^n$  is injective
2. *aperiodic* when the orthogonal projection onto  $\mathcal{E}^\perp$ ,  $\pi_\perp$  restricted to  $\mathbb{Z}^n$  is injective
3. *irreducible* when  $\pi_\perp(\mathbb{Z}^n)$  is dense in  $\mathcal{E}^\perp$

4. *generic* when it is non-degenerate, aperiodic and irreducible

Given a generic cut-and-project scheme we can define cut-and-project sets by their window  $\Omega$ . The cut-and-project set of window  $\Omega$  is denoted by  $\Sigma(\Omega)$  and is defined by

$$\Sigma(\Omega) := \pi \circ \pi_{\perp}^{-1}(\Omega),$$

where  $\pi$  is the orthogonal projection onto  $\mathcal{E}$  and  $\pi_{\perp}$  the orthogonal projection onto the orthogonal subspace  $\mathcal{E}^{\perp}$ . Remark that here  $\Sigma(\Omega)$  is a set of points and not necessarily a tiling.

**Theorem 11** ([MMP20]). *Let  $\varphi \in \mathcal{M}_2(\mathbb{R})$  be a non-singular matrix diagonalizable over  $\mathbb{C}$ . Then there exists a generic cut-and-project scheme  $(\mathcal{L}, \mathcal{E})$  and a cut-and-project set  $\Sigma(\Omega)$  satisfying  $\varphi\Sigma(\Omega) \subset \Sigma(\Omega)$  if and only if the spectrum of  $\varphi$  has the following properties:*

1.  *$\varphi$  is Integral Algebraic: every eigenvalue of  $\varphi$  is an algebraic integer*
2. *every complex number  $\mu$  of modulus  $|\mu| > 1$  algebraically conjugate to an eigenvalue  $\lambda$  of  $\varphi$  is also an eigenvalue of  $\varphi$ .*
3. *for every eigenvalue  $\lambda$  of  $\varphi$  of modulus  $|\lambda| > 1$  and for every  $\mu$  algebraically conjugate to  $\lambda$  we have  $\text{mul}_{\varphi}(\lambda) \geq \text{mul}_{\varphi}(\mu)$  and the inequality is strict for at least one  $\mu$ .*

Remark that both Theorems are conditions on the eigenvalues of  $\varphi$  but Theorem 11 is a necessary and sufficient condition for  $\varphi$  to be the expansion of a self-affine cut-and-project set whereas Theorem 10 is only a necessary condition for  $\varphi$  to be the expansion of a self-affine tiling.

Remark also that the cut-and-project scheme usually used to describe Penrose tilings is not generic, indeed it is  $(\mathbb{Z}^5, \mathcal{E}_5)$  with  $\mathcal{E}_5$  called 5-fold slope defined by:

$$\mathcal{E}_5 := \langle (\cos(\frac{2i\pi}{5}))_{0 \leq i < 5}, (\sin(\frac{2i\pi}{5}))_{0 \leq i < 5} \rangle,$$

and the projection  $\pi_{\perp}(\mathbb{Z}^5)$  is not dense in  $\mathcal{E}_5^{\perp}$  because  $\mathcal{E}_5^{\perp}$  contains the line  $\Delta = \langle (1, 1, 1, 1, 1) \rangle$  on which the projection of  $\mathbb{Z}^5$  is  $\mathbb{Z}$ . However as detailed in [Har04] we can decompose  $\mathcal{E}_5^{\perp}$  in a rational subspace and a totally irrational subspace. Once we have decomposed between a rational subspace and a totally irrational subspace we give a new definition of *generic* which is suitable. We will not give all the details here since it is not the core subject of this work.

## 2.12 Tileability of finite domains

In this section we give a quick overview of the question of tileability of a finite domains with a given set of tiles. As explained in Section 2.3 the tileability of the full plane with a given set of tiles is undecidable [Ber66] and in all generality the tileability of finite domains with a set of tiles is a very complex problem [Thu90,BNRR95] which (when we can formalize it in a suitable way) is NP-complete, in particular the tileability of simply connected finite domain with Wang Tiles is NP-complete [Lev86,PY13]. However there are special cases of tilesets and/or of domains for which the tileability becomes polynomial.

In our study of substitution discrete planes we initially define substitution from the boundary of the metatiles and we then are faced with the problem of the tileability of the interior of these metatiles. See [KR16] and Chapter 3 for the case of Sub Rosa substitutions and see Chapter 4 and in particular Section 4.3 for the case of Planar Rosa substitutions.

In this specific case the tiles are unit rhombuses and the finite domain is a polygon with edges of unit length, for this case the problem of tileability is quadratic and we can use the Kenyon criterion and algorithm for tileability [Ken93]. The Kenyon criterion and the way we use it for the construction of Planar Rosa substitutions is detailed in Section 4.3 page 103.

# Chapter 3

## Sub Rosa substitution tilings

### 3.1 Definition and construction

The Sub Rosa tilings is a family of substitution rhombus tilings with  $2n$ -fold rotational symmetry defined by Jarkko Kari and Markus Rissanen in [KR16]. For the definition of  $n$ -fold rotational symmetry see Definition 2.3.3 page 25.

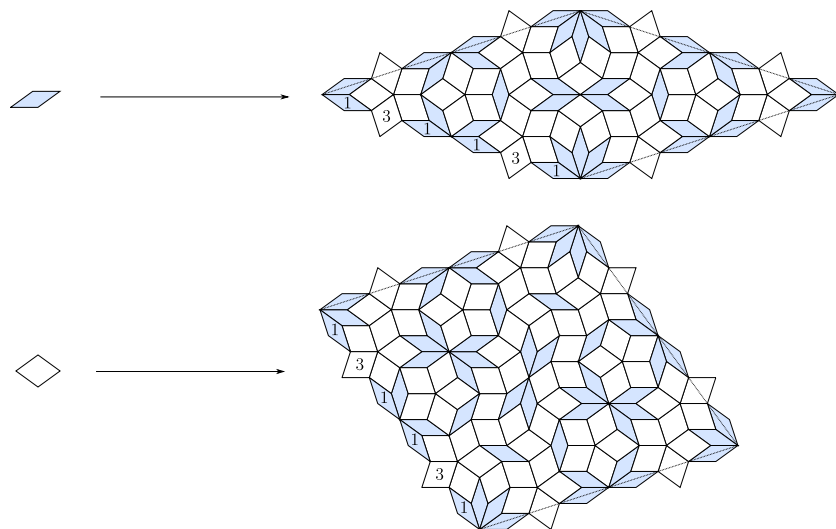


Figure 3.1: The Sub Rosa substitution of order 5 represented up to rotation, remark that there is the same sequence of rhombi on each side of each metatile.



In the Sub Rosa construction the substitution rule is mostly given by the sequence of edges and rhombuses called edge word which appears along all the edges of the substitution as in Figure 3.1 where on each edge of each metatile we have the same sequence of rhombuses which we code by 131131 on all the edges of the metatiles. Note that the Sub Rosa substitution are vertex-hierarchic and that the induced expansion is a homothety.

Let us first define the Rosa patterns, denoted by  $R_2^1$  in [KR16], from which the name Sub Rosa is derived.

**Definition 3.1.1** (Rosa pattern  $R(n)$ ). *For an integer  $n \geq 3$  the Rosa pattern which we denote by  $R(n)$  is the pattern formed of a star of  $2n$  copies of the  $(\frac{\pi}{n}, \frac{(n-1)\pi}{n})$  rhombuses around a vertex with their narrow angle to the centre vertex, surrounded by a ring of  $2n$  copies of the  $(\frac{2\pi}{n}, \frac{(n-2)\pi}{n})$  rhombuses with angle  $\frac{2\pi}{n}$  towards the centre, surrounded again by a ring of  $2n$  copies of  $(\frac{3\pi}{n}, \frac{(n-3)\pi}{n})$  rhombuses and so forth until a ring of  $(\frac{(n-2)\pi}{n}, \frac{2\pi}{n})$  with angle  $\frac{(n-2)\pi}{n}$  toward the centre.*

For  $n = 5$  it means that the Rosa  $R(5)$  has 3 layers: a star of narrow  $(\frac{\pi}{5}, \frac{4\pi}{5})$  rhombuses, then a ring of wide  $(\frac{2\pi}{5}, \frac{3\pi}{5})$  rhombuses with narrow angle towards the centre and then a second ring of wide rhombus but with wide angle towards the centre as depicted with other examples in Figure 3.2.

The Sub Rosa tilings are actually regular fixpoint tilings from the seed  $R(n)$  with a suitable substitution. We denote by  $\sigma_n$  the Sub Rosa substitution, which we decompose in an expansion  $\varphi_n$  and a subdivision  $\rho_n$  as in Figure 3.3. The Sub Rosa substitutions are such that there is the same sequence of rhombuses on each side of the metatiles and which we denote by  $\Sigma(n)$  and which we write as words with letters in the alphabet  $\{0, 1, \dots, n-1\}$  where 0 denotes a unit edge, and  $i$  denotes the rhombus of angles  $\frac{i\pi}{n}$  and  $\frac{(n-i)\pi}{n}$

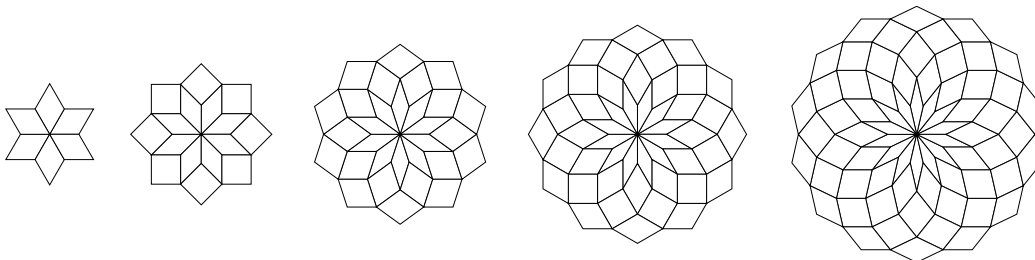


Figure 3.2: Rosa patterns  $R_2^1$  or  $R(n)$  for  $n \in \{3, 4, 5, 6, 7\}$ .

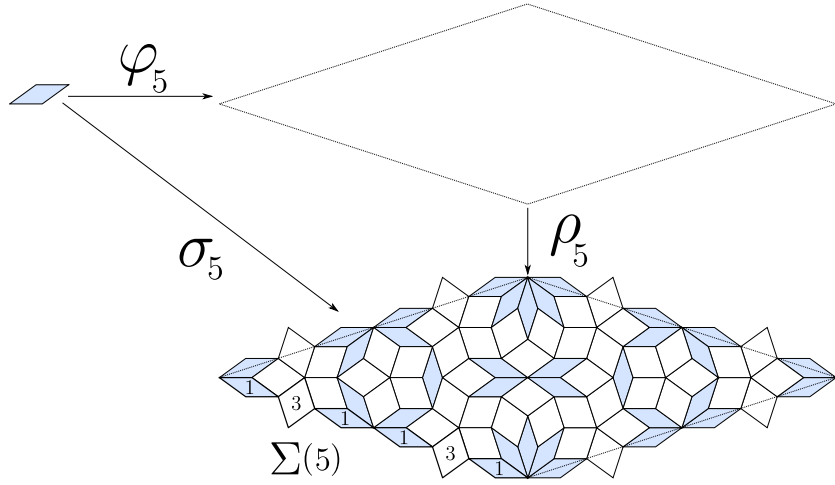


Figure 3.3: The decomposition  $\sigma_5 = \rho_5 \circ \varphi_5$  and the edge word  $\Sigma(5)$ .

bisected through the  $\frac{i\pi}{n}$  angle. When manipulating words we denote by  $\cdot$  the concatenation, by  $\bar{u}$  the mirror image of word  $u$ , and sometimes we denote by  $|$  the middle of a word when we want to emphasize it. For example as shown in Figures 3.1 and 3.3 the edge word for Sub Rosa 5 is  $\Sigma(5) = 131|131$ .

Let us now give the construction of the edge words  $\Sigma(n)$ , note that there are two distinct constructions, one for odd  $n$  and one for even  $n$ .

**Definition 3.1.2** (Edge word for odd  $n$ ). *Given  $k$  odd, let us define  $s_o(k) := 135 \dots (k-2)$  the word of odd integers from 1 to  $k-2$ . Given  $n$  odd, let us define the edge word  $\Sigma(n)$  by*

$$\Sigma(n) := s_o(n) \cdot \overline{s_o(3)} \cdot \overline{s_o(5)} \dots \overline{s_o(n-2)} | s_o(n-2) \cdot s_o(n-4) \dots s_o(3) \cdot \overline{s_o(n)}.$$

Recall that here the  $|$  symbol only represents the middle of the word.

$\Sigma(1)$	
$\Sigma(3)$	1 1
$\Sigma(5)$	131 131
$\Sigma(7)$	135131 131531
$\Sigma(9)$	1357131531 1351317531
$\Sigma(11)$	135791315317531 135713513197531

Table 3.1: The first values of the edge word  $\Sigma(n)$  for odd  $n$ .

**Definition 3.1.3** (Edge word for even  $n$ ). *Given  $k$  even, let us define  $s_e(k) := 024 \dots (k - 2)$  the word of even integers from 0 to  $k - 2$ . Given  $n$  even, let us define the edge word  $\Sigma(n)$  by*

$$\Sigma(n) := s_e(n) \cdot \overline{s_e(2)} \cdot \overline{s_e(4)} \dots \overline{s_e(n-2)} | s_e(n-2) \cdot s_e(n-4) \dots s_e(2) \cdot \overline{s_e(n)}.$$

For examples of  $\Sigma(n)$  see the Tables 3.1 and 3.2.

$\Sigma(0)$	
$\Sigma(2)$	0 0
$\Sigma(4)$	020 020
$\Sigma(6)$	024020 020420
$\Sigma(8)$	0246020420 0240206420
$\Sigma(10)$	024680204206420 024602402086420

Table 3.2: The first values of the edge word  $\Sigma(n)$  for even  $n$ .

**Definition 3.1.4** (Substitution  $\sigma_n$ ). *The substitution  $\sigma_n$  is defined as having the edge word  $\Sigma(n)$  on each side of each metatile and a portion of the rosa  $R(n)$  centred on each corner of each metatile as shown in Figure 3.4.*

This definition gives us the boundary of the metatiles of the substitution but not the interior of the metatiles as shown in Figure 3.4. It is not straightforward from this definition that the shapes defined are tileable.

**Proposition 3.1.1** (KR16). *For any  $n \geq 3$  the interior of the metatiles of  $\sigma_n$  are tileable.*

The proof of this proposition can be found in [KR16] and relies on the Kenyon criterion [Ken93] for tileability of a polygon by parallelograms which we mentioned in Section 2.12 and which we present and use in Chapter 4.

We now consider the interior of the substitution  $\sigma_n$  to be tiled, this means that we consider the substitution to be well-defined. The substitution  $\sigma_n$  defines a set of edge-to-edge rhombus tilings with local  $2n$ -fold rotational symmetry  $X_{\sigma_n}$ . Let us now define a canonical Sub Rosa tiling  $\mathcal{T}_n$  with global  $2n$ -fold rotational symmetry.

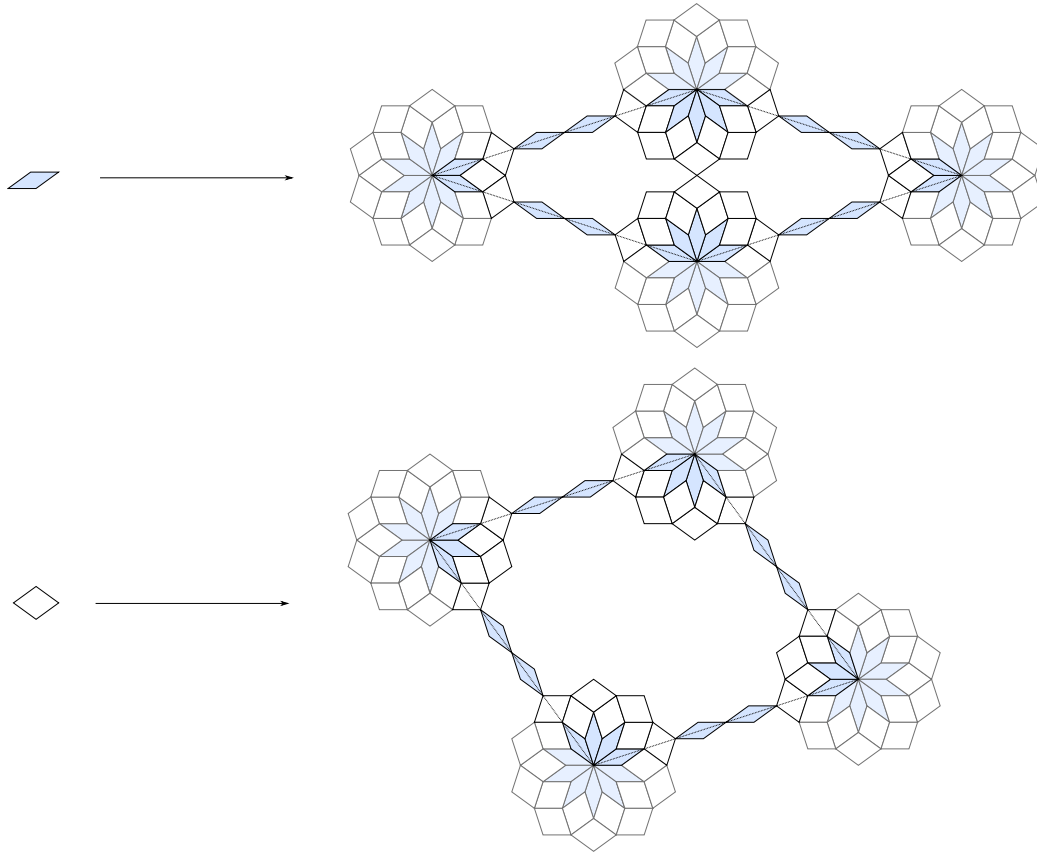


Figure 3.4: The definition of  $\sigma_5$  with the edge word  $\Sigma(5)$  on each edge and a portion of  $R(5)$  in each corner of the metatiles.

**Proposition 3.1.2** (KR16). *For any  $n \geq 3$*

1. *the substitution  $\sigma_n$  is primitive*
2. *the rosa  $R(n)$  is a regular seed for  $\sigma_n$*

*Proof.* The proof of this proposition is based on the definition of  $\sigma_n$  as having a portion of the rosa  $R(n)$  pattern in each corner of each metatiles. Indeed this implies that:

1. if we take a tile  $t$ , if we combine the four corners of  $\sigma_n(t)$  then we get a full rosa  $R(n)$  and the rosa contains every tile in every orientation. So for any tile  $t$ ,  $\sigma_n(t)$  contains every tile in every orientation which is the definition of  $\sigma_n$  being primitive

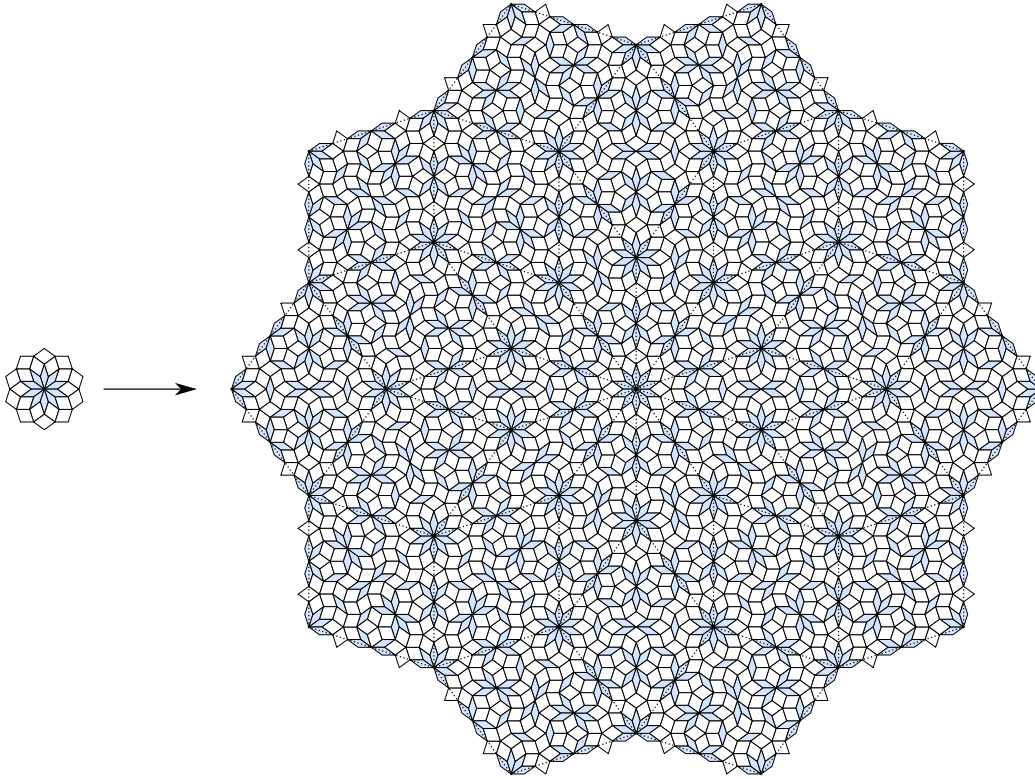


Figure 3.5: The substitution  $\sigma_5$  applied to the rosa  $R(5)$ , remark that  $R(5)$  appears at the centre of  $\sigma_5(R(5))$ .

2. at the centre of  $\sigma_n(R(n))$  we have a star of  $2n$  narrow metatiles  $\sigma_n(t)$  with  $t$  the rhombus with  $\frac{\pi}{n}$  and  $\frac{\pi-1}{n}$ . Recall that on each corner of these  $\sigma_n(t)$  we have a portion of  $R(n)$ , so overall at the centre of  $\sigma_n(R(n))$  we have  $R(n)$  which means that  $R(n)$  is a seed for  $\sigma_n$ , see Figure 3.5 for the case of  $\sigma_5(R(5))$ .

□

**Definition 3.1.5** (Canonical Sub Rosa tiling  $\mathcal{T}_n$ ). *The Sub Rosa tiling is the limit tiling  $\mathcal{T}_n := \lim_{k \rightarrow \infty} \sigma_n^k(R(n))$ .*

**Theorem 12** (KR16). *For every  $n \geq 3$ , there exists a quasiperiodic rhombic substitution tiling with global  $2n$ -fold rotational symmetry.*

*Proof.* A suitable tiling is  $\mathcal{T}_n$ . From Proposition 2.4.3  $\mathcal{T}_n$  is quasiperiodic and a regular fixpoint for  $\sigma_n$ .  $\mathcal{T}_n$  has  $2n$ -fold rotational symmetry because  $R(n)$  has  $2n$ -fold rotational symmetry.  $\square$

## 3.2 Main result

Sub Rosa tilings are edge-to-edge rhombus tilings with finitely many edge directions so we can lift these tilings to discrete surfaces of  $\mathbb{R}^n$ . The question that follows is whether these lifted tilings are discrete planes, recall that it means that the lifted discrete surface approximates a plane.

**Theorem 1** (Fernique, Kari, L.2020). *For any  $n \geq 3$  the canonical Sub Rosa tiling  $\mathcal{T}_n$  can be lifted to a discrete surface of  $\mathbb{R}^n$  and:*

1. *The canonical Sub Rosa tilings  $\mathcal{T}_3$  and  $\mathcal{T}_5$  are discrete planes.*
2. *For  $n = 4$  and for any  $n \geq 6$  the canonical Sub Rosa tiling  $\mathcal{T}_n$  is not a discrete plane.*

*The same holds when replacing the canonical Sub Rosa tiling  $\mathcal{T}_n$  by the set of Sub Rosa substitution tilings  $X_{\sigma_n}$ .*

In Section 3.3 we will show that under reasonable assumptions on a substitution  $\sigma$ , the planarity of the tilings  $X_\sigma$  is determined by the expansion  $\varphi$  induced by  $\sigma$ . We will also show that in the case of Sub Rosa substitution the induced expansion  $\varphi_n$  is lifted in  $\mathbb{R}^n$  to a linear application and the planarity of the tilings in  $X_{\sigma_n}$  is linked to the eigenspaces and eigenvalues of  $\varphi_n$ .

Since the construction of Sub Rosa substitution is separated between odd and even integer we will study the lifted version separately. In Section 3.4 we will study the eigenspaces and eigenvalues of  $\varphi_n$  and provide a proof of the Theorem for odd  $n$ . In Section 3.5 we will study do the same for even  $n$ .

## 3.3 Lifted substitutions and expansions

In this section we will consider the planarity or non-planarity of substitutions. Let fix some  $n \geq 3$ .

Let us first consider (non-degenerate) primitive substitutions  $\sigma$  of edge-to-edge rhombus tilings with  $n$  edge directions. Recall that non-degeneracy

means that for any prototile  $t$  the sequence of the radius of inscribed circle of the metatiles  $(r_{\text{in}}(\sigma^k(t)))_{k \in \mathbb{N}}$  is unbounded, which means that from any prototile the metatiles grow to span the full plane.

**Proposition 3.3.1** (Planarity of primitive substitutions). *Let  $\sigma$  be a (non-degenerate) primitive substitution.*

1. *if there exists a tiling  $\mathcal{T}$  regular for  $\sigma$  and a 2D plane  $\mathcal{E}$  of  $\mathbb{R}^n$  such that  $\mathcal{T}$  is a discrete plane of slope  $\mathcal{E}$ , then every tiling  $\mathcal{T}'$  regular for  $\sigma$  is a discrete plane of slope  $\mathcal{E}$ .*
2. *if there exists a tiling  $\mathcal{T}$  regular for  $\sigma$  which is not planar (there exist no slope of planarity), then every tiling  $\mathcal{T}'$  regular for  $\sigma$  is not planar.*

*Proof.* The proof is based on the fact that tilings regular for a primitive substitution have the same set of patterns: the metatiles of the substitution (see Proposition 2.4.2).

1. if there exists a tiling  $\mathcal{T}$  regular for  $\sigma$  and a 2D plane  $\mathcal{E}$  such that  $\mathcal{T}$  is planar with bound  $d$  along  $\mathcal{E}$ , then by Proposition 2.4.2 every metatile  $\sigma^k(t)$  appears in  $\mathcal{T}$ , there exists a translation vector  $\vec{v}$  such that  $\sigma^k(t) + \vec{v} \in \mathcal{T}$  which means that  $d(\sigma^k(t) + \vec{v}, \mathcal{E}) \leq d$ . We can reformulate it as the fact that the diameter of the projection of  $\sigma^k(t)$  on the orthogonal subspace  $\mathcal{E}^\perp$ , which we call  $\mathcal{E}^\perp$ -diameter, is bounded by  $2d$ .

Let us take a tiling  $\mathcal{T}'$  regular for  $\sigma$ , any finite patch is included in a metatile and so any finite patch has  $\mathcal{E}^\perp$ -diameter bounded by  $2d$ , which means that the full tiling  $\mathcal{T}'$  has  $\mathcal{E}^\perp$ -diameter bounded by  $2d$ . We can conclude two things: there exists a plane  $\mathcal{E}'$  parallel to  $\mathcal{E}$  such that  $\mathcal{T}'$  is planar with slope  $\mathcal{E}'$  and with the same bound  $d$ , or simply that there exists a bound  $d'$  such that  $\mathcal{T}'$  is planar of slope  $\mathcal{E}$  with bound  $d'$ , here  $d' = d(\mathcal{E}, \mathcal{E}') + d$ .

2. similarly if there exist a non-planar tiling  $\mathcal{T}$  regular for  $\sigma$  then for any plane  $\mathcal{E}$  there exists a sequence of metatiles of unbounded  $\mathcal{E}^\perp$ -diameter. This sequence of metatiles appears in any tiling  $\mathcal{T}'$  regular for  $\sigma$ . So no tiling admissible for  $\sigma$  is planar.

□

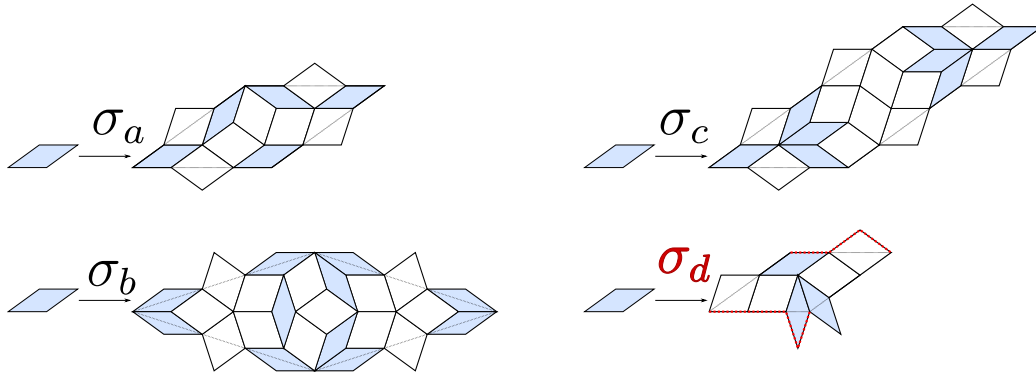


Figure 3.6: In these examples  $\sigma_a$ ,  $\sigma_b$  and  $\sigma_c$  are such that the image of two parallel edges are congruent, but  $\sigma_d$  is not.

This means that for primitive substitutions, the substitution itself (and its metatiles) determines the planarity of regular tilings.

**Definition 3.3.1** (Planar substitution). *A substitution  $\sigma$  is called planar of slope  $\mathcal{E}$  when its regular tilings are planar of slope  $\mathcal{E}$ .*

Remark that here  $\mathcal{E}$  is considered to be a vector subspace and not an affine subspace because the slope of a substitution is defined up-to-translation. We will now characterize the planarity of specific substitutions.

Let us consider substitutions  $\sigma$  of edge-to-edge rhombus tilings with  $n$  edge directions such that the image of two parallel edges by the substitution is the same up to translation *i.e.* for any two tiles  $t, t'$  and any two edges  $e \in t$  and  $e' \in t'$  such that  $e \equiv e'$  we have  $\partial\sigma(e) \equiv \partial\sigma(e')$ , see Figure 3.6 for examples and counter examples. Note that we can relax this condition to the fact that the image of two parallel edges by the substitution is the same up to reordering as in the case of the Ammann-Beenker substitution.

**Lemma 3.3.1** (Expansions). *Let  $\varphi$  be the expansion associated to a substitution of edge-to-edge rhombus tilings with  $n$  edge directions such that the image of two parallel edges by the substitution is the same up to translation (and possibly reordering).*

*The expansion  $\varphi$  is lifted in  $\mathbb{R}^n$  to a linear application of  $\mathbb{Z}^n$ .*

*Proof.* The condition means that when lifting a tiling  $\mathcal{T}$  and its image  $\sigma(\mathcal{T})$  in  $\mathbb{R}^n$ , for every vector of the canonical basis  $\vec{e}_i$  there exists a sequence of vectors of the canonical basis denoted  $\sigma(\vec{e}_i)$  such that for any two vertices



of  $\mathcal{T}$  linked by  $\vec{e}_i$ , their image by the substitution are linked by  $\sigma(\vec{e}_i)$ . This means that the expansion  $\varphi$  induced by the substitution is a linear application of  $\mathbb{Z}^n$ .  $\square$

The nice thing about this linear application  $\varphi$  is that it is closely linked to the planarity of  $\sigma$  and that we can use the tools of linear algebra to study  $\varphi$  and its properties.

**Proposition 3.3.2** (Necessary condition for planarity). *If a primitive  $\sigma$  is planar of slope  $\mathcal{E}$  and its induced expansion is a linear application of  $\mathbb{Z}^n$  then:*

- $\mathcal{E}$  is an (not necessarily strictly) expanding stable subspace for  $\varphi$
- any stable subspace  $\mathcal{V}$  included in the orthogonal  $\mathcal{E}^\perp$  subspace, is a (not necessarily strictly) contracting subspace for  $\varphi$

Here we say that  $\mathcal{E}$  is a (not necessarily strictly) expanding stable subspace for  $\varphi$  when  $\forall x \in \mathcal{E}$ ,  $\varphi(x) \in \mathcal{E}$  and  $\|\varphi(x)\| \geq \|x\|$ .

*Proof.* These necessary conditions for planarity are quite straightforward by contradiction:

- if the  $\varphi$  is not expanding along  $\mathcal{E}$  then the substitution is degenerate (the metatiles do not span the full plane, the radius of the inscribed circle of the metatiles will be bounded)
- if there is a stable expanding subspace  $\mathcal{V}$  for  $\varphi$  included in  $\mathcal{E}^\perp$ , then it means that the metatiles will have unbounded  $\mathcal{V}$ -diameter which implies unbounded  $\mathcal{E}^\perp$ -diameter so the substitution  $\sigma$  is not planar of slope  $\mathcal{E}$ . Here we use the fact that since all  $n$  edge directions appear in the metatiles (recall that the substitution is primitive) then there are vertices of the metatiles that have non-zero  $\mathcal{V}$ -component.

$\square$

From this necessary condition for planarity we can deduce a sufficient condition for non-planarity and a sufficient condition for planarity which we will use in Sections 3.4, 3.5, 4.4 and 4.5.

**Proposition 3.3.3** (Sufficient condition for non-planarity). *If  $\sigma$  is a primitive substitution and its induced expansion  $\varphi$  is a linear application of  $\mathbb{Z}^n$  such that there exists a strictly expanding stable subspace  $\mathcal{V}$  of  $\mathbb{R}^n$  for  $\varphi$  of dimension  $\dim(\mathcal{V}) \geq 3$  then  $\sigma$  is not a planar substitution.*

*Proof.* By contradiction assume that there is a planar substitution  $\sigma$  of slope  $\mathcal{E}$  with its induced expansion  $\varphi$  being a linear application such that  $\mathcal{V}$  is a stable strictly expanding subspace of dimension at least 3. By Proposition 3.3.2  $\mathcal{E}$  is a strictly expanding stable subspace for  $\varphi$ . So we can decompose  $\mathcal{V} = \mathcal{V}_0 \oplus \mathcal{V}_1$  with  $\mathcal{V}_0 \subset \mathcal{E}$  and  $\mathcal{V}_1 \subset \mathcal{E}^\perp$  and with both  $\mathcal{V}_0$  and  $\mathcal{V}_1$  stable subspaces, remark that  $\mathcal{V}_0$  is possibly the trivial subspace but since  $\dim(\mathcal{V}) = 3$  and  $\dim(\mathcal{E}) = 2$  we have  $\dim(\mathcal{V}_1) \geq 1$  so it is a strictly expanding stable subspace of  $\varphi$  which is a subspace of  $\mathcal{E}^\perp$  this contradicts Proposition 3.3.2.  $\square$

**Proposition 3.3.4** (Sufficient condition for planarity). *If  $\sigma$  is a primitive substitution and its induced expansion  $\varphi$  is a linear application of  $\mathbb{Z}^n$  such that there exists a plane  $\mathcal{E}$  with :*

1.  $\mathcal{E}$  is a strictly expanding stable subspace for  $\varphi$
2.  $\mathcal{E}^\perp$  is a strictly contracting stable subspace for  $\varphi$

then  $\sigma$  is planar of slope  $\mathcal{E}$ .

*Proof.* Let  $\sigma$  be such a substitution,  $\varphi$  be its induced expansion and  $\mathcal{E}$  a plane such that its orthogonal  $\mathcal{E}^\perp$  is a strictly contracting subspace for  $\varphi$ . As seen in Proposition 3.3.1 the important thing for the planarity of  $\sigma$  is the  $\mathcal{E}^\perp$ -diameter of the metatiles. We will show that the sequence  $(D_k^+)_{k \in \mathbb{N}}$  is bounded where  $D_k^+$  is the maximum  $\mathcal{E}^\perp$ -diameter of the metatiles of order  $k$  of the substitution *i.e.*

$$D_k^+ := \max_{t \in \mathbf{T}} \mathcal{E}^\perp\text{-diameter}(\sigma^k(t)).$$

We denote by  $\Pi$  the orthogonal projection on  $\mathcal{E}^\perp$ , recall that for a set  $X$  the  $\mathcal{E}^\perp$ -diameter of  $X$  is  $\sup_{x_0, x_1 \in X} \|\Pi(x_0 - x_1)\| = \sup_{x_0, x_1 \in X} \|\Pi(x_0) - \Pi(x_1)\|$ .

Actually we will prove that

$$\exists \lambda < 1, \exists C \in \mathbb{R}^+, \forall k \in \mathbb{N}, D_{k+1}^+ \leq \lambda D_k^+ + C. \quad (3.1)$$

Once we prove this inequation, we get that the sequence  $(D_k^+)_{k \in \mathbb{N}}$  is bounded and from that we get that the substitution  $\varphi$  is planar of slope  $\mathcal{E}$ .

Let us now prove Inequation 3.1. Our hypothesis is that  $\varphi$  is strictly contracting on  $\mathcal{E}^\perp$  *i.e.*

$$\forall x \in \mathcal{E}^\perp, \|\varphi(x)\| < \|x\|.$$

Since  $\mathcal{E}^\perp$  is of finite dimension we get that there is a contracting factor strictly smaller than 1 *i.e.*

$$\exists \lambda < 1, \forall x \in \mathcal{E}^\perp, \|\varphi(x)\| \leq \lambda \|x\|.$$

This comes from the compactness of the unit sphere in  $\mathcal{E}^\perp$  and continuity of the function  $x \rightarrow \|\varphi(x)\|$ .

Let us prove Inequation 3.1 with  $\lambda$  the contracting factor of  $\varphi$  and  $C = 2D_1^+$ .

Let us take an integer  $k \in \mathbb{N}$  and a tile  $t \in \mathbf{T}$ . Let us show that

$$\mathcal{E}^\perp\text{-diameter}(\sigma^{k+1}(t)) \leq \lambda D_k^+ + 2D_1^+.$$

The first step to get this inequation is to decompose  $\sigma^{k+1}(t) = \sigma \circ \sigma^k(t) = \sigma(\sigma^k(t))$  which means that  $\sigma^{k+1}(t)$  can be decomposed in first order metatile, which are arranged in a  $\sigma^k(t)$  patterns. In other words  $\sigma^{k+1}(t)$  is the same as if we replace the tiles  $t'$  of  $\sigma^k(t)$  by their metatiles  $\sigma(t')$  as illustrated in Figure 3.7 with a very simple substitution.

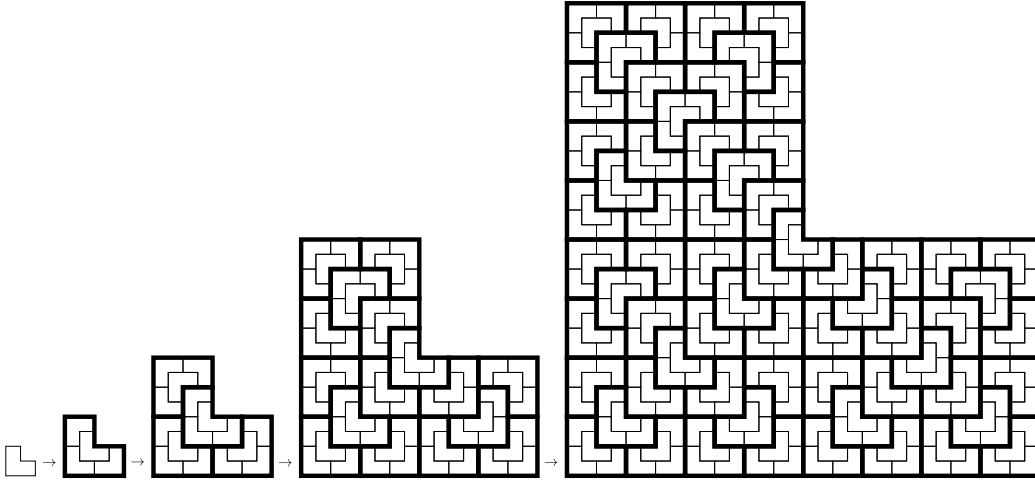


Figure 3.7: The metatiles of the Chair substitution decomposed as  $\sigma^k(t) = \sigma \circ \sigma^{k-1}(t)$  for  $k \in \{2, 3, 4\}$ .

Remark that in Figure 3.7 the substitution used is the chair substitution and is not a rhombus substitution, this choice is due to the fact that the point we want to illustrate is a very broad property of substitution tilings,

so we chose the simplest possible substitution on which it is true for clearer figures. For more details on the Chair substitution see Sections 2.1 and 2.4.

Let us take two vertices  $p_0, p_1$  in  $\sigma^{k+1}(t)$ , there exists  $p'_0, p'_1$  corners of first-order metatiles in the decomposition  $\sigma \circ \sigma^k(t)$  such that  $p_0$  belongs to a first-order metatile of corner  $p'_0$  and  $p_1$  to a first-order metatile of corner  $p'_1$ , see Figure 3.8 for an example with the Chair substitution. We have

$$\|\Pi(p_0 - p_1)\| \leq \|\Pi(p_0 - p'_0)\| + \|\Pi(p'_0 - p'_1)\| + \|\Pi(p'_1 - p_1)\|.$$

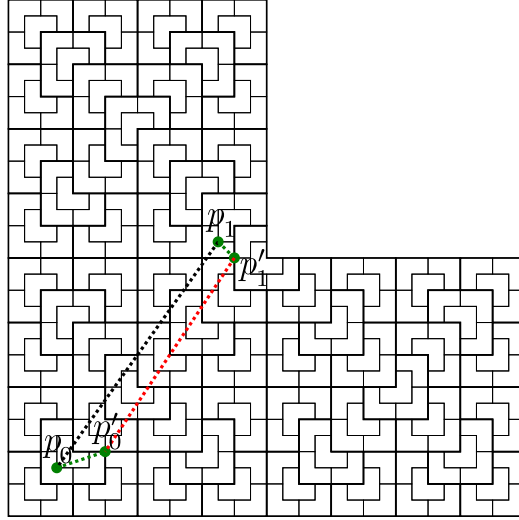


Figure 3.8: Decomposition of the path  $p_0 \rightarrow p_1$  as  $p_0 \rightarrow p'_0 \rightarrow p'_1 \rightarrow p_1$  in  $\sigma^4(t)$  with  $p'_0$  and  $p'_1$  being corners of the metatiles in the decomposition  $\sigma^4(t) = \sigma \circ \sigma^3(t)$ .

Since  $p_0$  and  $p'_0$  belong to the same metatile we have  $\|\Pi(p_0 - p'_0)\| \leq D_1^+$  and for the same reason  $\|\Pi(p_1 - p'_1)\| \leq D_1^+$ . Since  $p'_0$  and  $p'_1$  are corners of first order metatiles in the decomposition  $\sigma \circ \sigma^k(t)$  they actually belong to  $\varphi \circ \sigma^k(t)$ , so there exists  $p''_0$  and  $p''_1$  in  $\sigma^k(t)$  such that  $\varphi(p''_0) = p'_0$  and  $\varphi(p''_1) = p'_1$ . This means that  $\|\Pi(p'_0 - p'_1)\| \leq \lambda \|\Pi(p''_0 - p''_1)\|$  and since  $p''_0$  and

$p_1''$  belong to a metatile of order  $k$  we have  $\|\Pi(p_0'' - p_1'')\| \leq D_k^+$ . So overall

$$\begin{aligned} \|\Pi(p_0 - p_1)\| &\leq \|\Pi(p_0 - p_0')\| + \|\Pi(p_0' - p_1')\| + \|\Pi(p_1' - p_1)\| \\ &\leq \|\Pi(p_0' - p_1')\| + 2D_1^+ \\ &\leq \lambda \|\Pi(p_0'' - p_1'')\| + 2D_1^+ \\ &\leq \lambda D_k^+ + 2D_1^+. \end{aligned}$$

And with

$$D_{k+1}^+ = \max_{t \in \mathbf{T}} \sup_{p_0, p_1 \in \sigma^{k+1}(t)} \|\Pi(p_0 - p_1)\|.$$

We can conclude that

$$D_{k+1}^+ \leq \lambda D_k^+ + 2D_1^+.$$

□

Remark that we did not use the first condition in the proof, however this condition is related to the scaling factor and to the fact that a substitution is non-degenerate.

## 3.4 Proof for odd $n$

In this section  $n$  is an odd integer and  $n \geq 3$ .

### 3.4.1 Lifting

The Sub Rosa substitution  $\sigma_n$  and the canonical Sub Rosa tiling  $\mathcal{T}_n$  have  $n$  edge directions denoted  $\{\vec{v}_k, 0 \leq k < n\}$  which are exactly the  $n$ -th root of unit *i.e.*  $\vec{v}_k = e^{i\frac{2k\pi}{n}}$ .

As shown in Figures 3.9 and 3.10 we lift the tilings of  $X_{\sigma_n}$  with

$$\widehat{\vec{v}}_k = e^{i\frac{2k\pi}{n}} := \vec{e}_k.$$

Remark that this means that in the set  $\{\pm\vec{v}_k, 0 \leq k < n\}$  in the rotation ordering, the neighbours of  $\vec{v}_k$  are  $-\vec{v}_{k+\lceil\frac{n}{2}\rceil}$  and  $-\vec{v}_{k-\lceil\frac{n}{2}\rceil}$  where indices are modulo  $n$ , and in the positive orientation rotation ordering we have

$$-\vec{v}_{k-\lceil\frac{n}{2}\rceil} \prec \vec{v}_k \prec -\vec{v}_{k+\lceil\frac{n}{2}\rceil}.$$

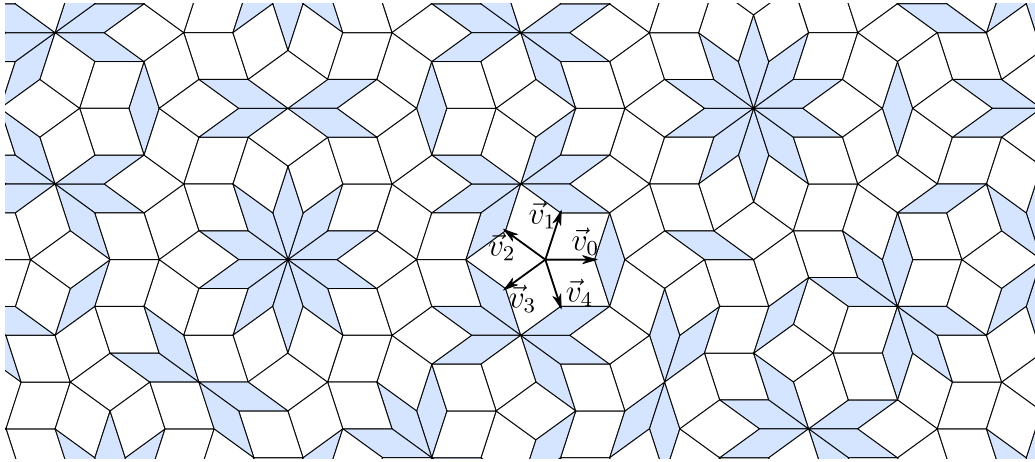


Figure 3.9: Edge directions for Sub Rosa  $n$  with  $n = 5$ .

Remark that  $2 \lceil \frac{n}{2} \rceil = n + 1$  which means that we have that the neighbours of  $-\vec{v}_{k+\lceil \frac{n}{2} \rceil}$  are as expected :

$$\vec{v}_k \prec -\vec{v}_{k+\lceil \frac{n}{2} \rceil} \prec \vec{v}_{k+1}.$$

So overall, as seen shown in Figures 3.9 an 3.11, we have

$$\vec{v}_0 \prec -\vec{v}_{\lceil \frac{n}{2} \rceil} \prec \vec{v}_1 \prec -\vec{v}_{1+\lceil \frac{n}{2} \rceil} \prec \vec{v}_2 \prec \dots \prec \vec{v}_{n-1} \prec -\vec{v}_{-\lceil \frac{n}{2} \rceil} \prec \vec{v}_0$$

### 3.4.2 Expansion matrix

As detailed in Section 3.1 the Sub Rosa substitution  $\sigma_n$  is defined as having the same sequence of rhombuses and edges on the edges of the metatiles (up to translation and rotation). In particular this means as seen in Section 3.3 that the Sub Rosa expansion  $\varphi_n$  is lifted to a linear application of  $\mathbb{Z}^n$ .

**Definition 3.4.1** (Decomposition of  $\mathbb{R}^n$  for odd  $n$ ). *We decompose  $\mathbb{R}^n$  as the orthogonal direct sum*

$$\mathbb{R}^n = \Delta \oplus \bigoplus_{0 \leq k < \lceil \frac{n}{2} \rceil} \mathcal{E}_n^k,$$

with  $\Delta := \langle (1)_{0 \leq i < n} \rangle$  and

$$\mathcal{E}_n^k := \left\langle \left( \cos\left(\frac{2i(2k+1)\pi}{n}\right) \right)_{0 \leq i < n}, \left( \sin\left(\frac{2i(2k+1)\pi}{n}\right) \right)_{0 \leq i < n} \right\rangle = \left\langle \left( e^{i\frac{2i(2k+1)\pi}{n}} \right)_{0 \leq i < n} \right\rangle.$$

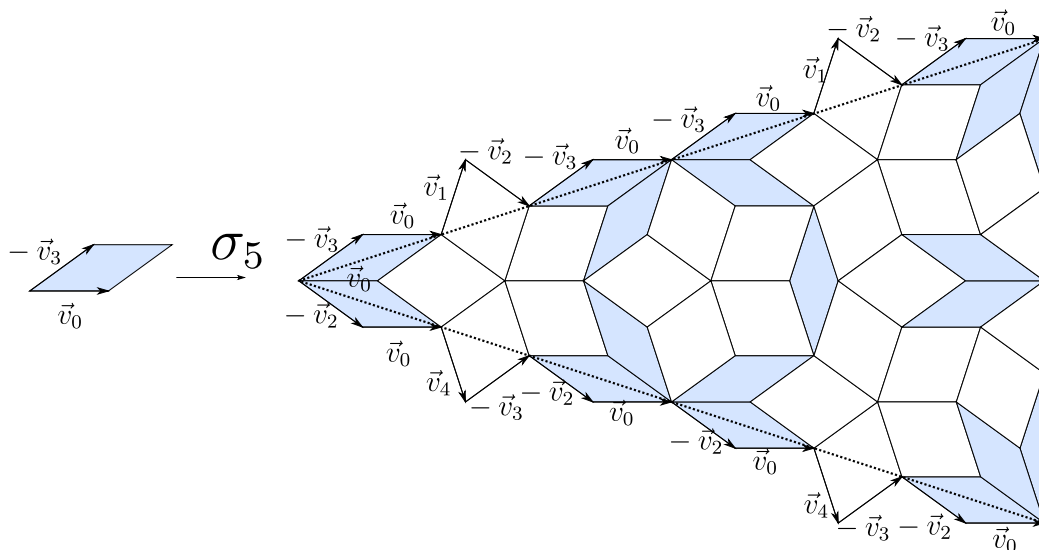


Figure 3.10: To lift  $\sigma_5$  in  $\mathbb{R}^5$  one only has to lift each edge direction  $\vec{v}_i$  to the corresponding vector of the canonical basis  $\vec{e}_i$ .

**Proposition 3.4.1** (Eigenspaces of  $\varphi_n$  for odd  $n$ ). *For odd  $n$ ,  $\varphi_n$  is a circulant or cyclic linear application and its eigenspaces are  $\Delta$  and  $\mathcal{E}_n^k$  for  $0 \leq k < \lfloor \frac{n}{2} \rfloor$ .*

The fact that  $\varphi_n$  is a circulant linear application is just a rewriting of the fact that the image of all edges  $\vec{v}_i$  is the same up to rotation, and all circulant application have  $\Delta$  and  $\mathcal{E}_n^k$  for eigenspaces. We will not go in details now on that since we will actually prove stronger results later.

Remark that what determines  $\varphi_n$  is the edges of the metatiles, and in the Sub Rosa case these edges are all the same sequence of rhombuses called the edge word  $\Sigma(n)$ . Actually what determines  $\varphi_n$  is the edge word up to reordering so we define the abelianized edge word.

**Definition 3.4.2** (Abelianized edge word). *The abelianized edge word denoted by  $[\Sigma(n)]$  is a vector on  $m$  coordinates where  $m$  is the number of different letters in the word/alphabet, where  $[\Sigma(n)]_i$  is the number of occurrences of the  $i^{\text{th}}$  letter of the alphabet in  $\Sigma(n)$ .*

*For odd  $n$ , the letters that appear in  $\Sigma(n)$  are the odd  $k$  from 1 to  $n - 2$ . So there are  $\lfloor \frac{n}{2} \rfloor$  letters in  $\Sigma(n)$ , and  $[\Sigma(n)] = ([\Sigma(n)]_i)_{0 \leq i < \lfloor \frac{n}{2} \rfloor}$  with  $[\Sigma(n)]_i$  the number of rhombuses of angle  $2i + 1$  in  $\Sigma(n)$ .*

From the definition of Sub Rosa edge words we can get an exact formula for the abelianized  $[\Sigma(n)]$ .

**Lemma 3.4.1** (Exact formula for the abelianized edge word). *For odd  $n$  we have*

$$[\Sigma(n)] = (n - (2i + 1))_{0 \leq i < \lfloor \frac{n}{2} \rfloor} = 2 \left( \lfloor \frac{n}{2} \rfloor - i \right)_{0 \leq i < \lfloor \frac{n}{2} \rfloor}.$$

*Proof.* Recall that  $\Sigma(n)$  is defined as  $\Sigma(n) = s_o(n) \cdot s_o(3) \cdot s_o(5) \dots s_o(n-2) | s_o(n-2) \cdot s_o(n-4) \dots s_o(3) \cdot \overline{s_o(n)}$  with  $s_o(k) = 135 \dots (k-2)$  which has abelianized word  $[s_o(k)] = (1)_{0 \leq i < \lfloor \frac{k}{2} \rfloor}$ . From this we immediately get that  $\Sigma(n)$  has  $n - 1$  occurrences of the rhombus of angle 1,  $n - 3$  occurrences of the rhombus of angle 3, etc until 2 occurrences of the rhombus of angle  $n - 2$ . Which we can write  $[\Sigma(n)] = (n - (2i + 1))_{0 \leq i < \lfloor \frac{n}{2} \rfloor}$ .  $\square$

We will use this exact formula later but for now let us focus on the link between the abelianized edge word  $[\Sigma(n)]$  and the expansion  $\varphi_n$ .

**Proposition 3.4.2** (Expansion matrix of  $\varphi_n$  for odd  $n$ ). *For odd  $n$ ,  $\varphi_n$  is a circulant linear application of the form*

$$\varphi_n = \begin{pmatrix} m_0 & m_{n-1} & \dots & m_1 \\ m_1 & m_0 & \dots & m_2 \\ \vdots & \ddots & \ddots & \vdots \\ m_{n-1} & m_{n-2} & \dots & m_0 \end{pmatrix}$$

$$\text{with } \forall i \in \{0, 1, \dots, \lfloor \frac{n}{2} \rfloor - 1\}, m_{i \lfloor \frac{n}{2} \rfloor} = (-1)^i [\Sigma(n)]_i \\ \text{and } m_{-(i+1) \lfloor \frac{n}{2} \rfloor} = (-1)^{i+1} [\Sigma(n)]_i.$$

*Proof.* In the Sub Rosa substitution for odd  $n$  the edge of the metatiles bisects the rhombus tiles along their odd angle (see Figure 3.1) so it means the metatiles are rotated by an angle  $\frac{-\pi}{14}$  compared to the tiles. So the if we take the edge  $\vec{v}_0$  (or in  $\mathbb{R}^n$ , the edge  $\vec{e}_0$ ), its image  $\partial\sigma(\vec{v}_0)$  is a succession of rhombuses where the rhombus of angle  $\frac{\pi}{n}$  has edges  $\vec{v}_0$  and its successor in the negative rotation ordering which is  $-\vec{v}_{-\lfloor \frac{n}{2} \rfloor}$ , and the rhombus of angle  $\frac{(2i+1)\pi}{n}$  has edges  $(-1)^i \vec{v}_{i \lfloor \frac{n}{2} \rfloor}$  which is the  $i^{\text{th}}$  successor of  $\vec{v}_0$  in the positive



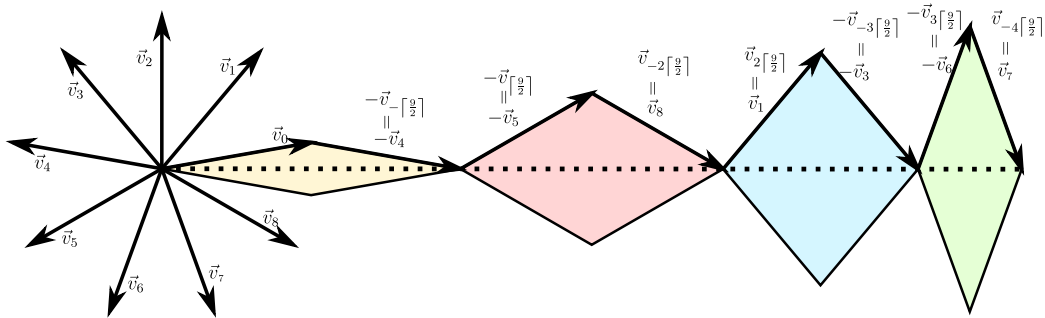


Figure 3.11: Edges of rhombuses along the edge of the metatiles for  $n = 9$ .

rotation ordering, and  $(-1)^{i+1}\vec{v}_{(i+1)\lceil\frac{n}{2}\rceil}$  which is the  $i^{\text{th}}$  successor of  $-\vec{v}_{-\lceil\frac{n}{2}\rceil}$  in the negative rotation ordering as shown in Figure 3.11. So each rhombus of angle  $\frac{(2i+1)\pi}{n}$  contributes as  $(-1)^i$  to  $m_{i\lceil\frac{n}{2}\rceil}$  and as  $(-1)^{i+1}$  to  $m_{(i+1)\lceil\frac{n}{2}\rceil}$ .  $\square$

### 3.4.3 Eigenvalues of the Sub Rosa expansion matrices

From this characterization of the expansion  $\varphi_n$  as a circulant matrix with coefficients determined by the abelianized edge word  $[\Sigma(n)]$  we can compute the eigenvalues of  $\varphi_n$ .

**Definition 3.4.3** (The eigenvalue matrix for odd  $n$ ). *Let us define the matrix*

$$N_n := \left( 2 \cos\left(\frac{(2i+1)(2j+1)\pi}{2n}\right) \right)_{0 \leq i, j < \lceil\frac{n}{2}\rceil}.$$

**Proposition 3.4.3** (Eigenvalues of the Sub Rosa expansion for odd  $n$ ). *For odd  $n$ , the SubRosa expansion  $\varphi_n$  admits the spaces  $\mathcal{E}_n^j$  for  $0 \leq j < \lceil\frac{n}{2}\rceil$  and  $\Delta$  as eigenspaces. We denote by  $\lambda_j(n)$  the eigenvalue of the SubRosa substitution of order  $n$  on eigenspace  $\mathcal{E}_n^j$  and  $\lambda_\Delta(n)$  on  $\Delta$ . We note  $|\lambda(n)|$  the vector of modules of the eigenvalues  $\lambda_j(n)$ . We have  $\lambda_\Delta(n) = 0$  and*

$$|[\Sigma(n)] \cdot N_n| = |\lambda(n)|.$$

More precisely we have

$$\begin{aligned}
\lambda_j(n) &= \left( \sum_{i=0}^{\lfloor \frac{n}{2} \rfloor - 1} [\Sigma(n)]_i 2 \cos \left( \frac{(2j+1)(2i+1)\pi}{2n} \right) \right) e^{-i \frac{(2j+1)\pi}{2n}} \\
&= \left( \sum_{i=0}^{\lfloor \frac{n}{2} \rfloor - 1} (n - (2i+1)) 2 \cos \left( \frac{(2j+1)(2i+1)\pi}{2n} \right) \right) e^{-i \frac{(2j+1)\pi}{2n}} \\
&= \left( \sum_{i=0}^{\lfloor \frac{n}{2} \rfloor - 1} 4 \left( \lfloor \frac{n}{2} \rfloor - i \right) \cos \left( \frac{(2j+1)(2i+1)\pi}{2n} \right) \right) e^{-i \frac{(2j+1)\pi}{2n}}.
\end{aligned}$$

*Proof.* Before giving a formal proof let us point out that  $2 \cos(\frac{(2i+1)(2j+1)\pi}{2n})$  is the diagonal of a rhombus of angle  $\frac{(2i+1)(2j+1)\pi}{n}$ , and that the rhombus of type  $i$  is lifted to some square that has angle  $\frac{(2i+1)\pi}{n}$  when projected in  $\mathcal{E}_n^0$  but angle  $\frac{(2i+1)(2j+1)\pi}{n}$  when projected on  $\mathcal{E}_n^j$ . So if we look at the eigenvalues as the scaling factors of the expansion projected on the planes  $\mathcal{E}_n^j$  then each rhombus contributes by the length of its diagonal which is  $2 \cos(\frac{(2i+1)(2j+1)\pi}{2n})$ . Let us now give a formal proof.

The main idea of the proof is to decompose the matrix of the expansion in a sum of elementary matrices  $M_i(n)$  which each correspond to one type of rhombus on the diagonal:

$$\varphi_n = \sum_{i=0}^{\lfloor \frac{n}{2} \rfloor - 1} [\Sigma(n)]_i \cdot M_i(n).$$

For example with the Sub Rosa 5 expansion (shown in Figure 3.1) we have

$$\varphi_5 = 4M_0(5) + 2M_1(5).$$

The matrix  $M_i(n)$  is a circulant matrix with one diagonal with value one and a diagonal of value  $-1$  which represent an expansion with one rhombus of index  $i$  (angle  $2i+1$ ) on the edge of the metatile. Let us denote  $I(i)$  and  $J(i)$  the indices of these non-zero diagonals where  $I(i) := i \lfloor \frac{n}{2} \rfloor = i \frac{n+1}{2}$  and the diagonal  $I(i)$  has value  $(-1)^i$ , and where  $J(i) := -(i+1) \lfloor \frac{n}{2} \rfloor = -(i+1) \frac{n+1}{2}$  and the diagonal  $J(i)$  has value  $(-1)^{i+1}$ .

Let  $z$  be a complex number such that  $z^n = 1$  and  $Z$  be the vector  $(z^k)_{0 \leq k < n}$ . We have

$$Z \cdot M_i(n) = (-1)^i (z^{I(i)} - z^{J(i)}) \cdot Z.$$

With  $z = (e^{i\frac{2(2j+1)\pi}{n}})$  we get that  $\mathcal{E}_n^j$  is eigenspace of  $M_i(n)$  with eigenvalue

$$\begin{aligned} \lambda_{i,j}(n) &= (-1)^i \left( e^{i\frac{2(2j+1)I(i)\pi}{n}} - e^{i\frac{2(2j+1)J(i)\pi}{n}} \right) \\ &= (-1)^i e^{i\frac{2(2j+1)i\frac{n+1}{2}\pi}{n}} + (-1)^{i+1} e^{-i\frac{2(2j+1)(i+1)\frac{n+1}{2}\pi}{n}} \\ &= (-1)^i e^{i\frac{(2j+1)i(n+1)\pi}{n}} + (-1)^{i+1} e^{-i\frac{(2j+1)(i+1)(n+1)\pi}{n}} \\ &= (-1)^i e^{i(2j+1)i\pi} e^{i\frac{(2j+1)i\pi}{n}} + (-1)^{i+1} e^{-i(2j+1)(i+1)\pi} e^{-i\frac{(2j+1)(i+1)\pi}{n}} \\ &= (-1)^i (-1)^i e^{i\frac{(2j+1)i\pi}{n}} + (-1)^{i+1} (-1)^{i+1} e^{-i\frac{(2j+1)(i+1)\pi}{n}} \\ &= e^{i\frac{(2j+1)i\pi}{n}} + e^{-i\frac{(2j+1)(i+1)\pi}{n}} \\ &= \left( 2 \cos \left( \frac{(2j+1)(2i+1)\pi}{2n} \right) \right) e^{-i\frac{(2j+1)\pi}{2n}}. \end{aligned}$$

Let us remark that the argument of  $\lambda_{i,j}(n)$  is  $\frac{-(2j+1)\pi}{2n}$  and it does not depend on  $i$ .

For  $z = 1$  we get  $\lambda_{i,\Delta}(n) = 0$ .

From these two results on the elementary matrices we have that the spaces  $\mathcal{E}_n^j$  and  $\Delta$  are eigenspaces of  $\varphi_n$  with  $\lambda_\Delta = 0$  and

$$\begin{aligned} \lambda_j(n) &= \sum_{i=0}^{\lfloor \frac{n}{2} \rfloor} [\Sigma(n)]_i \lambda_{i,j}(n) \\ &= \left( \sum_{i=0}^{\lfloor \frac{n}{2} \rfloor - 1} (n - (2i+1)) 2 \cos \left( \frac{(2j+1)(2i+1)\pi}{2n} \right) \right) e^{-i\frac{(2j+1)\pi}{2n}} \\ &= \left( \sum_{i=0}^{\lfloor \frac{n}{2} \rfloor - 1} 4(\lfloor \frac{n}{2} \rfloor - i) \cos \left( \frac{(2j+1)(2i+1)\pi}{2n} \right) \right) e^{-i\frac{(2j+1)\pi}{2n}}. \end{aligned}$$

□

Recall that the eigenvalues of the expansion  $\varphi_n$  is linked to the planarity of the substitution  $\sigma_n$ . Indeed from Proposition 3.3.3,  $|\lambda_0(n)|, |\lambda_1(n)| > 1$  is a sufficient condition for the non-planarity of  $\sigma_n$  and from Proposition 3.3.4,  $|\lambda_i(n)| < 1$  for all  $i > 0$  is a sufficient condition for planarity of slope  $\mathcal{E}_n^0$ .

We will now compute the actual values of the eigenvalues  $|\lambda_j(n)|$ .

**Proposition 3.4.4** (Value of the eigenvalues  $\lambda_j(n)$  for odd  $n$ ).

1. For any integers  $j$  and  $n$  such that  $0 \leq j < \lfloor \frac{n}{2} \rfloor$

$$|\lambda_j(n)| = \frac{\cos\left(\frac{(2j+1)\pi}{2n}\right)}{\sin^2\left(\frac{(2j+1)\pi}{2n}\right)}.$$

2. For fixed  $j$ , the sequence  $(|\lambda_j(n)|)_{n \text{ odd and } n > 2j+1}$  is increasing.

*Proof.* We define  $C_{j,k} := |\lambda_j(2k+1)|$  we will now study  $C_{j,k}$  for  $0 \leq j < k$ , we also define  $\theta_{j,k} := \frac{(2j+1)\pi}{2(2k+1)}$ . We will first prove the formula and then we will use it to prove the fact that the sequence  $(C_{j,k})_{k \in \mathbb{N}, k > j}$  is increasing at  $j$  fixed.

1. Let us take  $j, k$  such that  $0 \leq j < k$ . We have

$$\begin{aligned} C_{j,k} = |\lambda_j(2k+1)| &= \sum_{i=0}^{k-1} 4(k-i) \cos\left(\frac{(2j+1)(2i+1)\pi}{2(2k+1)}\right) \\ &= \sum_{i=0}^{k-1} 4(k-i) \cos((2i+1)\theta_{j,k}). \end{aligned}$$

We will now prove that

$$C_{j,k} \cdot \sin^2(\theta_{j,k}) = \cos(\theta_{j,k}).$$

With  $\theta_{j,k} \in (0, \frac{\pi}{2})$  for  $j < k$ , we have  $\sin \theta_{j,k} > 0$ , we get

$$C_{j,k} = \frac{\cos \theta_{j,k}}{\sin^2 \theta_{j,k}}.$$

We will write  $\theta$  for  $\theta_{j,k}$  for the sake of simplicity.

The sketch proof is as follows:

$$C_{j,k} \sin^2(\theta) = \sum_{i=0}^{k-1} 4(k-i) \cos((2i+1)\theta_{j,k}) \sin^2(\theta) \quad (3.2)$$

$$= \sum_{i=0}^{k-1} (k-i) (2 \cos((2i+1)\theta) - \cos((2i+3)\theta) - \cos((2i-1)\theta)) \quad (3.3)$$

$$= \cos \theta. \quad (3.4)$$

From line (3.2) to (3.3) we rewrite cosines and sines as sum of exponential, then we expand the product and pair the exponential terms by argument and find three cosine terms. From line (3.3) to (3.4) we split the sum in three, reindex to have  $\cos((2i+1)\theta)$  terms in each sum, then we merge back and the terms of the sum cancel out, we end out only with boundary terms which sum up to  $\cos \theta$ . Now the same proof but with all details:

$$\begin{aligned} & C_{j,k} \sin^2(\theta) \\ &= \sum_{i=0}^{k-1} 4(k-i) \cos\left(\frac{(2j+1)(2i+1)\pi}{2(2k+1)}\right) \sin^2(\theta) \\ &= \sum_{i=0}^{k-1} 4(k-i) \frac{e^{i(2i+1)\theta} + e^{-i(2i+1)\theta}}{2} \left(\frac{e^{i\theta} - e^{-i\theta}}{2i}\right)^2 \\ &= \sum_{i=0}^{k-1} \frac{k-i}{2} (e^{i(2i+1)\theta} + e^{-i(2i+1)\theta}) (2 - e^{i2\theta} - e^{-i2\theta}) \\ &= \sum_{i=0}^{k-1} \frac{k-i}{2} \left(2e^{i(2i+1)\theta} + 2e^{-i(2i+1)\theta} - e^{i(2i+3)\theta} \right. \\ &\quad \left. - e^{-i(2i-1)\theta} - e^{i(2i-1)\theta} - e^{-i(2i+3)\theta}\right) \\ &= \sum_{i=0}^{k-1} (k-i) (2 \cos((2i+1)\theta) - \cos((2i+3)\theta) - \cos((2i-1)\theta)) \\ &= \sum_{i=0}^{k-1} (k-i) 2 \cos((2i+1)\theta) - \sum_{i=0}^{k-1} (k-i) \cos((2i+3)\theta) \end{aligned}$$

$$\begin{aligned}
& - \sum_{i=0}^{k-1} (k-i) \cos((2i-1)\theta) \\
= & \sum_{i=0}^{k-1} (k-i) 2 \cos((2i+1)\theta) - \sum_{i=1}^k (k+1-i) \cos((2i+1)\theta) \\
& - \sum_{i=-1}^{k-2} (k-1-i) \cos((2i+1)\theta) \\
= & \sum_{i=0}^{k-1} (k-i) 2 \cos((2i+1)\theta) \\
& - \sum_{i=0}^{k-1} (k+1-i) \cos((2i+1)\theta) + (k+1) \cos \theta - \cos \frac{(2j+1)\pi}{2} \\
& - \sum_{i=0}^{k-1} (k-1-i) \cos((2i+1)\theta) + 0 \cos((2k-1)\theta) - k \cos \theta \\
= & \sum_{i=0}^{k-1} (2(k-i) - (k+1-i) - (k-1-i)) \cos((2i+1)\theta) \\
& + (k+1-k) \cos \theta \\
= & \cos \theta.
\end{aligned}$$

2. Let us fix  $j \in \mathbb{N}$ . Let us consider the function

$$f : k \rightarrow \frac{\cos \theta_{j,k}}{\sin^2 \theta_{j,k}} \quad \text{with } k > j.$$

For simplicity consider instead

$$h : x \rightarrow \frac{\cos \frac{1}{x}}{\sin^2 \frac{1}{x}} \quad \text{with } x > \frac{2}{\pi}.$$

We have

$$h'(x) = \frac{\frac{1}{\tan^2 \frac{1}{x}} + \frac{1}{\sin^2 \frac{1}{x}}}{x^2 \sin \frac{1}{x}}.$$

For  $x > \frac{2}{\pi}$  we have  $h(x) > 0$  and  $h'(x) > 0$ . We also have  $h(\frac{2}{\pi}) = 0$  and  $h \xrightarrow{x \rightarrow \infty} \infty$  so there exists a  $x_1 := h^{-1}(1)$  such that  $x > x_1 \Leftrightarrow h(x) > 1$ .

Now we can translate these results on  $h$  to results on  $f$ , we have  $f(k) > 0$  for  $k > j$  and  $f$  is an increasing function, moreover there exists  $a$  and  $b$  such that  $f(k) > 1$  for all  $k > a \cdot j + b$ , with  $a \approx 1.74$  and  $b \approx 0.37$ . For the eigenvalues for small  $n$  see Table 3.3.

□

### 3.4.4 Conclusion

When we compile the previous results we get the Theorem restricted to odd  $n$  as stated below.

**Proposition 3.4.5** (Planarity of Sub Rosa substitutions  $\sigma_n$  for odd  $n$ ).

1.  $\sigma_3$  and  $\sigma_5$  are planar, their regular tilings are discrete planes of slope  $\mathcal{E}_3$  and  $\mathcal{E}_5$ .
2. for all odd  $n \geq 7$ , the Sub Rosa substitution  $\sigma_n$  is not planar and its regular tilings are not discrete planes

*Proof.* The first step of the proof is to compute the eigenvalues of the Sub Rosa expansion  $\varphi_n$  for small  $n$ . Recall that  $\varphi_n$  has eigenspaces  $\mathcal{E}_n^k$  for  $0 \leq k < \lfloor \frac{n}{2} \rfloor$  with eigenvalues  $\lambda_k(n)$  and  $\Delta$  with eigenvalue  $\lambda_\Delta = 0$  as detailed in Proposition 3.4.4. In Table 3.3 you can find the modules of the eigenvalues of  $\varphi_n$  for  $n \in \{3, 5, 7, 9, 11\}$ , these modules can be computed using the formula provided by Proposition 3.4.4 or by usual tools of linear algebra applied on the matrices  $\varphi_n$  for which we have explicit descriptions.

Table 3.3: Approximate module of the eigenvalues of Sub Rosa expansions for small  $n$ .

n	$ \lambda_0(n) $	$ \lambda_1(n) $	$ \lambda_2(n) $	$ \lambda_3(n) $	$ \lambda_4(n) $
3	3.46	-	-	-	-
5	9.96	0.90	-	-	-
7	19.69	2.01	0.53	-	-
9	32.66	3.46	1.09	0.39	-
11	48.87	5.27	1.76	0.76	0.30

Now let us give the proof of the Proposition:

1. we apply Proposition 3.3.4.

- $\varphi_3$  has eigenvalues  $\lambda_0(3) = 4 \cos(\frac{\pi}{6})e^{-i\frac{\pi}{6}} \approx 3.46e^{-i\frac{\pi}{6}}$  and  $\lambda_\Delta = 0$ , so it is strictly expanding along  $\mathcal{E}_3^0$  and strictly contracting along  $\mathcal{E}_3^{0\perp} = \Delta$ . So  $\sigma_3$  is planar of slope  $\mathcal{E}_3 = \mathcal{E}_3^0$ .

- $\varphi_5$  has eigenvalues

$$\lambda_0(5) = (8 \cos(\frac{\pi}{10}) + 4 \cos(\frac{3\pi}{10}))e^{-i\frac{\pi}{10}} \approx 9.96e^{-i\frac{\pi}{10}}.$$

$$\lambda_1(5) = (8 \cos(\frac{3\pi}{10}) - 4 \cos(\frac{\pi}{10}))e^{-i\frac{3\pi}{10}} \approx 0.90e^{-i\frac{3\pi}{10}}.$$

$$\lambda_\Delta = 0.$$

So  $\varphi_5$  is strictly expanding along  $\mathcal{E}_5^0$  and strictly contracting along  $\mathcal{E}_5^{0\perp} = \mathcal{E}_5^1 \oplus \Delta$ , and the substitution  $\sigma_5$  is planar of slope  $\mathcal{E}_5 = \mathcal{E}_5^0$ .

2. we apply Propositions 3.3.3 and 3.4.4.

From Proposition 3.4.4 we get that for any odd  $n \geq 7$ ,

$$|\lambda_0(n)| \geq |\lambda_0(7)| \approx 19.69 > 1 \text{ and } |\lambda_1(n)| \geq |\lambda_1(7)| \approx 2.01 > 1.$$

So the expansion  $\varphi_n$  is strictly expanding on the stable subspace  $\mathcal{E}_n^0 \oplus \mathcal{E}_n^1$  which is of dimension 4. This implies by Proposition 3.3.3 that  $\sigma_n$  is not planar.

□

## 3.5 Proof for even $n$

The proof is very similar to the proof for odd  $n$  presented in Section 3.4, however we will give all the details so that this Section is independent from the previous Section. This means that there will be some redundancy. The main differences are the way we lift to  $\mathbb{R}^n$ , the coefficients of the expansion matrix and the formula for the eigenvalues of the expansion matrix.

### 3.5.1 Lifting

For even  $n$  we have  $n$  edge directions which we write as  $\{\pm \vec{v}_k, 0 \leq k < n\} = \{\pm e^{i\frac{k\pi}{n}}, 0 \leq k < n\}$ . So we lift Sub Rosa tilings to  $\mathbb{R}^n$  with  $\widehat{\vec{v}}_k = e^{i\frac{k\pi}{n}} := \vec{e}_k$ . With this choice, in the positive rotation ordering we have

$$\vec{v}_0 \prec \vec{v}_1 \prec \vec{v}_2 \cdots \prec \vec{v}_{n-1} \prec -\vec{v}_0 \prec -\vec{v}_1 \cdots \prec -\vec{v}_{n-1} \prec \vec{v}_0.$$



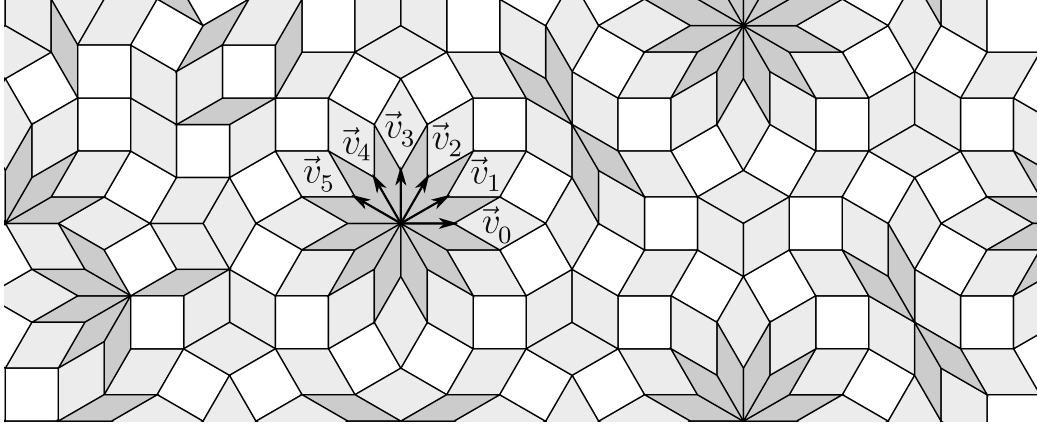


Figure 3.12: Edge directions in Sub Rosa for even  $n = 6$ .

### 3.5.2 Expansion matrix

As detailed in Section 3.1 the Sub Rosa substitution  $\sigma_n$  is defined as having the same sequence of rhombuses and edges on the edges of the metatiles (up to translation and rotation). In particular this means as seen in Section 3.3 that the Sub Rosa expansion  $\varphi_n$  is lifted to a linear application of  $\mathbb{Z}^n$ .

**Definition 3.5.1** (Decomposition of  $\mathbb{R}^n$  for even  $n$ ). *We decompose  $\mathbb{R}^n$  as the orthogonal direct sum*

$$\mathbb{R}^n = \bigoplus_{0 \leq k < \frac{n}{2}} \mathcal{E}_n^k.$$

$$\mathcal{E}_n^k := \left\langle \left( \cos\left(\frac{i(2k+1)\pi}{n}\right) \right)_{0 \leq i < n}, \left( \sin\left(\frac{i(2k+1)\pi}{n}\right) \right)_{0 \leq i < n} \right\rangle = \left\langle \left( e^{i \frac{i(2k+1)\pi}{n}} \right)_{0 \leq i < n} \right\rangle.$$

**Proposition 3.5.1** (Eigenspaces of  $\varphi_n$  for even  $n$ ). *For even  $n$ ,  $\varphi_n$  is a pseudo-circulant linear application and its eigenspaces are  $\mathcal{E}_n^k$  for  $0 \leq k < \frac{n}{2}$ .*

Here pseudo-circulant linear application means that if we write  $\varphi_n$  as a matrix  $(m_{i,j})_{0 \leq i,j < n}$  then  $|m_{i,j}| = |m_{i',j'}|$  whenever  $i - j \equiv i' - j' \pmod{n}$  with  $m_{i,j} = m_{i',j'}$  when  $i - j = i' - j'$  and  $m_{i,j} = -m_{i',j'}$  when  $i - j = i' - j' \pm n$ , for example see the matrices  $\varphi_4$  and  $\varphi_6$  below.

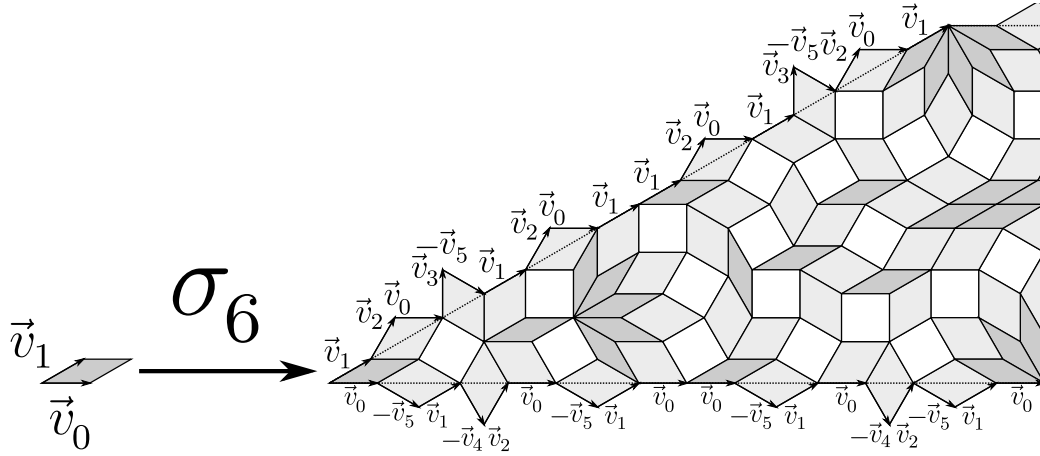


Figure 3.13: Lifting  $\sigma_6$ .

$$\varphi_4 = \begin{pmatrix} 4 & 2 & 0 & -2 \\ 2 & 4 & 2 & 0 \\ 0 & 2 & 4 & 2 \\ -2 & 0 & 2 & 4 \end{pmatrix} \quad \varphi_6 = \begin{pmatrix} 6 & 4 & 2 & 0 & -2 & -4 \\ 4 & 6 & 4 & 2 & 0 & -2 \\ 2 & 4 & 6 & 4 & 2 & 0 \\ 0 & 2 & 4 & 6 & 4 & 2 \\ -2 & 0 & 2 & 4 & 6 & 4 \\ -4 & -2 & 0 & 2 & 4 & 6 \end{pmatrix}.$$

The fact that  $\varphi_n$  is a pseudo-circulant linear application is simply due to the definition of  $\sigma_n$  as having the same sequence of edges and rhombuses on the edges of the metatiles combined with the way we order the set of vertices  $\{\pm\vec{v}_k, 0 \leq k < n\}$ , see Figures 3.12 and 3.13.

As for the odd case we will not prove this proposition as we will prove a stronger proposition later.

Remark that what determines  $\varphi_n$  is the edges of the metatiles, and in the Sub Rosa case these edges are all the same sequence of rhombuses called the edge word  $\Sigma(n)$ . Actually what determines  $\varphi_n$  is the edge word up to reordering so we define the abelianized edge word.

**Definition 3.5.2** (Abelianized edge word for even  $n$ ). *The abelianized edge word denoted by  $[\Sigma(n)]$  is a vector on  $m$  coordinates where  $m$  is the number of different letters in the word/alphabet, with  $[\Sigma(n)]_i$  is the number of occurrences of the  $i^{\text{th}}$  letter of the alphabet in  $\Sigma(n)$ .*

For even  $n$ , the letters that appear in  $\Sigma(n)$  are the even  $k$  from 0 to  $n-2$ . So there are  $\frac{n}{2}$  letters in  $\Sigma(n)$ , and  $[\Sigma(n)] = ([\Sigma(n)]_i)_{0 \leq i < \lfloor \frac{n}{2} \rfloor}$  with  $[\Sigma(n)]_i$  the number of edges for  $i = 0$  and the number rhombuses of angle  $2i$  for  $i > 0$  in  $\Sigma(n)$ .

From the definition of Sub Rosa edge words we can get an exact formula for the abelianized  $[\Sigma(n)]$ .

**Lemma 3.5.1** (Exact formula for the abelianized edge word for even  $n$ ). *For odd  $n$  we have*

$$[\Sigma(n)] = (n - 2i)_{0 \leq i < \frac{n}{2}} = 2 \left( \frac{n}{2} - i \right)_{0 \leq i < \frac{n}{2}}.$$

*Proof.* Recall that  $\Sigma(n)$  is defined as  $\Sigma(n) = s_e(n) \cdot \overline{s_e(2)} \cdot \overline{s_e(4)} \dots \overline{s_e(n-2)} | s_e(n-2) \cdot s_e(n-4) \dots s_e(2) \cdot \overline{s_e(n)}$  with  $s_e(k) = 024 \dots (k-2)$  which has abelianized word  $[s_e(k)] = (1)_{0 \leq i < \frac{k}{2}}$ . From this we immediately get that  $\Sigma(n)$  has  $n$  occurrences of the edge,  $n-2$  occurrences of the rhombus of  $\frac{2\pi}{n}$ , etc until 2 occurrences of the rhombus of angle  $\frac{(n-2)\pi}{n}$ . Which we can write  $[\Sigma(n)] = (n - 2i)_{0 \leq i < \frac{n}{2}}$ .  $\square$

We will use this exact formula later but for now let us focus on the link between the abelianized edge word  $[\Sigma(n)]$  and the expansion  $\varphi_n$ .

**Proposition 3.5.2** (Expansion matrix of  $\varphi_n$  for even  $n$ ). *For even  $n$ ,  $\varphi_n$  is a pseudo-circulant linear application of the form*

$$\varphi_n = \begin{pmatrix} m_0 & -m_{n-1} & \dots & -m_1 \\ m_1 & m_0 & \dots & -m_2 \\ \vdots & \ddots & \ddots & \vdots \\ m_{n-1} & m_{n-2} & \dots & m_0 \end{pmatrix}$$

$$\text{with } \forall 0 \leq i < \frac{n}{2}, m_i = [\Sigma(n)]_i$$

$$\text{and } \forall 1 \leq i < \frac{n}{2}, m_{n-i} = -[\Sigma(n)]_i.$$

*Proof.* In the Sub Rosa substitution for even  $n$  the edge of the metatiles is a succession of edges and rhombuses which are bisected tiles along an even angle (see Figure 3.14), it means that if we take the edge  $\vec{v}_0$  (or in  $\mathbb{R}^n$  the edge  $\vec{e}_0$ ) its image  $\partial\sigma(\vec{v}_0)$  is a succession of edges  $\vec{v}_0$  and rhombuses where the rhombus of angle  $\frac{2\pi}{n}$  has edges  $\vec{v}_1$  and  $-\vec{v}_{n-1}$ , and similarly the rhombus

of angle  $\frac{2k\pi}{n}$  has edges  $\vec{v}_k$  and  $-\vec{v}_{n-k}$  as in Figure 3.14. Remark also that on the edge of the metatiles we have only rhombuses with even angles but they appear in both possible orientations.

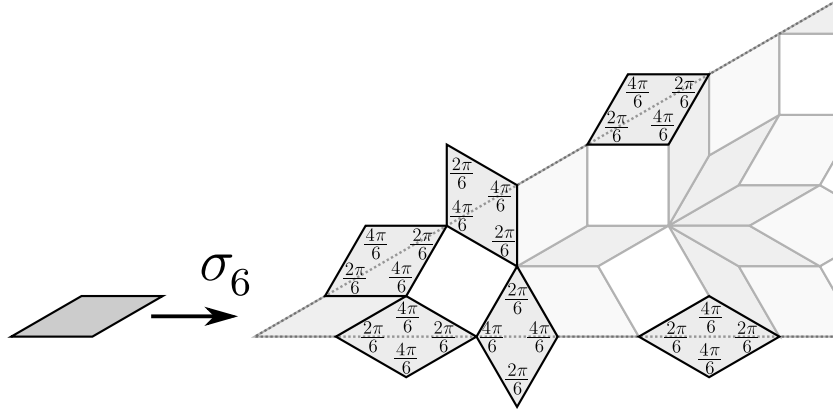


Figure 3.14: The edges and rhombuses on the edge of the metatile for even  $n$ .

□

### 3.5.3 Eigenvalues of the Sub Rosa expansion matrices

Just as for odd  $n$ , from this characterization of the expansion  $\varphi_n$  as a pseudo-circulant matrix with coefficients determined by the abelianized word  $[\Sigma(n)]$  we can compute the eigenvalues of  $\varphi_n$ .

**Definition 3.5.3** (The eigenvalue matrix for even  $n$ ). *Let us define the matrix*

$$N_n := \left( c_i \cos\left(\frac{i(2j+1)\pi}{n}\right) \right)_{0 \leq i, j < \frac{n}{2}} \quad \text{with } c_i = \begin{cases} 1 & \text{when } i = 0 \\ 2 & \text{otherwise} \end{cases}.$$

**Proposition 3.5.3** (Eigenvalues of the Sub Rosa expansion for even  $n$ ). *For even  $n$ , the Sub Rosa expansion  $\varphi_n$  admits the spaces  $\mathcal{E}_n^j$  for  $0 \leq j < \frac{n}{2}$  as eigenspaces. We denote by  $\lambda_j(n)$  the eigenvalue of  $\varphi_n$  on eigenspace  $\mathcal{E}_n^j$ . We note  $\lambda(n)$  the vector of the eigenvalues. We have*

$$[\Sigma(n)] \cdot N_n = \lambda(n).$$

which we can reformulate as

$$\begin{aligned}
\lambda_j(n) &= [\Sigma(n)]_0 + \sum_{1 \leq i < \frac{n}{2}} [\Sigma(n)]_i 2 \cos\left(\frac{i(2j+1)\pi}{n}\right) \\
&= n + \sum_{1 \leq i < \frac{n}{2}} (n - 2i) 2 \cos\left(\frac{i(2j+1)\pi}{n}\right) \\
&= n + \sum_{1 \leq i < \frac{n}{2}} 4\left(\frac{n}{2} - i\right) \cos\left(\frac{i(2j+1)\pi}{n}\right).
\end{aligned}$$

Before giving a formal proof let us point out two things:

- for even  $n$  the eigenvalue are real numbers (contrary to the odd case) which means that there is no rotation component to the expansion
- just as for the odd case, seeing  $2 \cos \frac{i(2j+1)\pi}{n}$  as the diagonal of the rhombus of angle  $\frac{2i(2j+1)\pi}{n}$  gives us a good intuition on this result.

*Proof.* The idea is the same as for the odd case. Let  $n$  be an even integer, we decompose

$$\varphi_n := \sum_{0 \leq i < \frac{n}{2}} [\Sigma(n)]_i M_i(n).$$

with  $M_0(n)$  the identity matrix (which corresponds to having a unit edge on the edge of the metatile) and for  $i \neq 0$   $M_i(n)$  the pseudo-circulant matrix (see Proposition 3.5.2) with diagonal  $i$  with value 1 and diagonal  $n - i$  with value  $-1$  (which corresponds to having a unit rhombus of angle  $\frac{2i\pi}{n}$  on the edge of the metatile).

Let  $z$  be a complex number such that  $z^n = -1$  and  $Z$  be the vector  $Z := (z^k)_{0 \leq k < n}$ . We have  $Z \cdot M_0(n) = Z$  and for  $i \neq 0$  we have

$$Z \cdot M_i(n) = (z^i - z^{n-i})Z.$$

For  $0 \leq j < \frac{n}{2}$  and  $z = e^{i\frac{(2j+1)\pi}{n}}$  we get that  $\mathcal{E}_n^j$  is an eigenspace of  $M_0(n)$  with eigenvalue 1 and for  $1 \leq i < \frac{n}{2}$  we get that  $\mathcal{E}_n^j$  is an eigenspace of  $M_i(n)$  with eigenvalue  $e^{i\frac{i(2j+1)\pi}{n}} - e^{i\frac{(n-i)(2j+1)\pi}{n}} = 2 \cos \frac{i(2j+1)\pi}{n}$ . Since all the eigenvalues are real numbers they sum and we have that  $\varphi_n$  has eigenspaces  $\mathcal{E}_n^j$  with eigenvalues

$$\lambda_j(n) = [\Sigma(n)]_0 + \sum_{1 \leq i < \frac{n}{2}} [\Sigma(n)]_i 2 \cos\left(\frac{i(2j+1)\pi}{n}\right).$$

□

Recall that the eigenvalues of the expansion  $\varphi_n$  is linked to the planarity of the substitution  $\sigma_n$ . Indeed from Proposition 3.3.3,  $|\lambda_0(n)|, |\lambda_1(n)| > 1$  is a sufficient condition for the non planarity of  $\sigma_n$ . We will now give the exact formula for the eigenvalues.

**Proposition 3.5.4** (Value of the eigenvalues  $\lambda_j(n)$  for even  $n$ ).

1. For any even  $n$  and any  $0 \leq j < \frac{n}{2}$  we have

$$\lambda_j(n) = \frac{1}{\sin^2\left(\frac{(2j+1)\pi}{2n}\right)}.$$

2. For fixed  $j$ , the sequence  $(\lambda_j(n))_{n \text{ even and } n > 2j}$  is increasing

3. For any even  $n$ , for any  $0 \leq j < \frac{n}{2}$  we have

$$\lambda_j(n) > 1.$$

*Proof.* For simplicity we define  $C'_{j,k} := \lambda_j(2k)$  and  $\theta'_{j,k} := \frac{(2j+1)\pi}{4k}$ . We will first prove the formula and then we will use it to prove the fact that the eigenvalues are increasing with  $n$  (or  $k$ ) at fixed  $j$ .

1. Let us take  $j, k$  such that  $0 \leq j < k$ . We have

$$\begin{aligned} C'_{j,k} &= 2k + \sum_{1 \leq i < k} 4(k-i) \cos \frac{i(2j+1)\pi}{2k} \\ &= 2k + \sum_{1 \leq i < k} 4(k-i) \cos(2i\theta'_{j,k}). \end{aligned}$$

Let us now prove that

$$C'_{j,k} \sin^2(\theta'_{j,k}) = 1.$$

For simplicity we write  $\theta$  for  $\theta'_{j,k}$ .

$$\begin{aligned} &C'_{j,k} \sin^2(\theta) \\ &= \left( 2k + \sum_{i=1}^{k-1} 4(k-i) \cos(2i\theta) \right) \sin^2(\theta) \end{aligned}$$

$$\begin{aligned}
&= \left( 2k + \sum_{i=1}^{k-1} 4(k-i) \cos(2i\theta) \right) \left( \frac{1 - \cos(2\theta)}{2} \right) \\
&= k(1 - \cos(2\theta)) + \sum_{i=1}^{k-1} 2(k-i) \cos(2i\theta)(1 - \cos(2\theta)) \\
&= k(1 - \cos(2\theta)) + \sum_{i=1}^{k-1} \frac{(k-i)}{2} (e^{i2i\theta} + e^{-i2i\theta})(2 - e^{i2\theta} - e^{-i2\theta}) \\
&= k(1 - \cos(2\theta)) + \sum_{i=1}^{k-1} \frac{(k-i)}{2} \\
&\quad (2e^{i2i\theta} + 2e^{-i2i\theta} - e^{i2(i+1)\theta} - e^{-i2(i+1)\theta} - e^{i2(i-1)\theta} - e^{-i2(i-1)\theta}) \\
&= k(1 - \cos(2\theta)) \\
&\quad + \sum_{i=1}^{k-1} (k-i)(2 \cos(2i\theta) - \cos(2(i+1)\theta) - \cos(2(i-1)\theta)) \\
&= k(1 - \cos(2\theta)) + \sum_{i=1}^{k-1} 2(k-i) \cos(2i\theta) \\
&\quad - \sum_{i=1}^{k-1} (k-i) \cos(2(i+1)\theta) - \sum_{i=1}^{k-1} (k-i) \cos(2(i-1)\theta) \\
&= k(1 - \cos(2\theta)) + \sum_{i=1}^{k-1} 2(k-i) \cos(2i\theta) \\
&\quad - \sum_{i=2}^k (k - (i-1)) \cos(2i\theta) - \sum_{i=0}^{k-2} (k - (i+1)) \cos(2i\theta) \\
&= k(1 - \cos(2\theta)) + \sum_{i=1}^{k-1} 2(k-i) \cos(2i\theta) \\
&\quad - \left( \sum_{i=1}^{k-1} (k - (i-1)) \cos(2i\theta) - k \cos(2\theta) + 1 \cos(2k\theta) \right) \\
&\quad - \left( \sum_{i=1}^{k-1} (k - (i+1)) \cos(2i\theta) + (k-1) - 0 \right)
\end{aligned}$$

$$\begin{aligned}
&= k(1 - \cos(2\theta)) + \sum_{i=1}^{k-1} (2(k-i) - (k-i+1) - (k-i-1)) \cos(2i\theta) \\
&\quad + k \cos(2\theta) - \cos\left(\frac{2k(2j+1)\pi}{4k}\right) - (k-1) \\
&= k(1 - \cos(2\theta)) + k \cos(2\theta) \cos\left(\frac{(2j+1)\pi}{2}\right) - k + 1 \\
&= 1.
\end{aligned}$$

With  $0 < \theta'_{j,k} < \frac{\pi}{2}$  we have the expected formula.

2. This derives from the fact that the function

$$k \mapsto \frac{1}{\sin^2\left(\frac{(2j+1)\pi}{4k}\right)}$$

has the same behaviour as

$$x \mapsto \frac{1}{\sin^2\left(\frac{1}{x}\right)}$$

and this function is strictly increasing on  $]\frac{2}{\pi}, +\infty[$ .

3. We use the formula given in 1. for any even  $n$  and any  $0 \leq j < \frac{n}{2}$  we have

$$\frac{(2j+1)\pi}{2n} \in ]0, \frac{\pi}{2}[.$$

So  $\sin^2\left(\frac{(2j+1)\pi}{2n}\right) \in ]0, 1[$  which means that

$$\lambda_j(n) > 1.$$

□

### 3.5.4 Conclusion

With the third item of Proposition 3.5.4 and Proposition 3.3.3 we get the Theorem restricted to the even case.

**Proposition 3.5.5** (Non-planarity of Sub Rosa substitutions for even  $n$ ).  
*For all even  $n \geq 4$  the Sub Rosa substitution  $\sigma_n$  is not planar and its regular tilings are not discrete planes.*



Table 3.4: Approximate values of the eigenvalues of Sub Rosa expansions for small even  $n$ .

$n$	$\lambda_0(n)$	$\lambda_1(n)$	$\lambda_2(n)$	$\lambda_3(n)$	$\lambda_4(n)$	$\lambda_6(n)$
4	6.83	1.17	-	-	-	-
6	14.93	2	1.07	-	-	-
8	26.27	3.24	1.45	1.04	-	-
10	40.86	4.85	2	1.26	1.03	-
12	58.70	6.83	2.70	1.59	1.17	1.02

*Proof.* From Proposition 3.5.4 we have that all the eigenvalues of the Sub Rosa expansions are greater than 1. From this we get that for any even  $n \geq 4$  the full space  $\mathbb{R}^n$  is an expanding stable subspace of dimension  $\geq 4$  for  $\varphi_n$ . So by Proposition 3.3.3 the substitution  $\sigma_n$  associated to  $\varphi_n$  is not planar.

See Table 3.4 for approximate values of the eigenvalues of  $\varphi_n$  for small even  $n$ . □

# Chapter 4

## Planar Rosa : substitution $n$ -fold discrete planes

### 4.1 Introduction

The Sub Rosa tilings [KR16] were good candidates for substitution discrete planes with  $n$ -fold rotational symmetry, but as stated in Theorem 1 and presented in Chapter 3 they are not discrete planes.

In this Chapter we present a new family of tilings which we call the Planar Rosa tilings which are substitution discrete planes with  $2n$ -fold rotational symmetry.

**Theorem 2** (Kari, L. 2020). *For any  $n \geq 3$  the canonical Planar Rosa tiling  $\mathcal{T}'_n$  is a substitution discrete plane with global  $2n$ -fold rotational symmetry. For any  $n \geq 3$  the Planar Rosa tilings i.e. tilings in  $X_{\sigma'_n}$ , are substitution discrete planes with local  $2n$ -fold rotational symmetry.*

The definition of the Planar Rosa substitutions denoted by  $\sigma'_n$  needs several intermediate steps and is separated between odd and even  $n$ , they can be found in Definitions 4.4.5 page 121 and 4.5.5 page 134.

For the canonical Planar Rosa tilings which are regular fixpoint tilings actually do not use the Rosa pattern as a seed but the simple star pattern.

**Definition 4.1.1** (Star pattern  $S(n)$ ). *The star pattern  $S(n)$  is the pattern of  $2n$  rhombuses of angle  $\frac{\pi}{n}$  around a vertex as shown in Figure 4.1.*

By definition of the Planar Rosa substitution  $\sigma'_n$ ,  $S(n)$  is a good seed for  $\sigma'_n$  (see Sections 4.4.6 page 129 and 4.5.6 page 142).

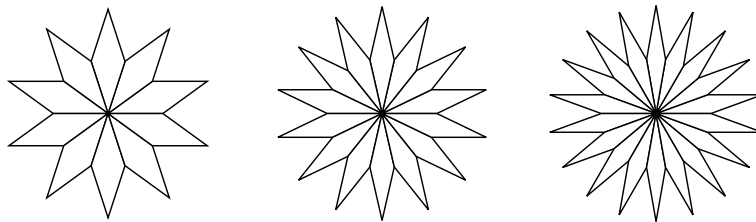


Figure 4.1: Star  $S(n)$  for  $n \in \{5, 7, 9\}$ .

**Definition 4.1.2** (Canonical Planar Rosa tilings). *For any  $n \geq 3$ , the canonical Planar Rosa tiling  $\mathcal{T}'_n$  is defined as the regular fixpoint tiling of the Planar Rosa substitution  $\sigma'_n$  from the seed  $S(n)$ .*

Examples of Planar Rosa substitutions and canonical Planar Rosa tilings are presented in Chapter 6.

In Section 4.2 we present two different strategies for the construction of Planar Rosa substitutions. In Section 4.3 we study the tileability of Sub Rosa-like metatiles given their edge-word. In Sections 4.4 and 4.5 we give the construction and proofs separately for odd  $n$  and for even  $n$ .

## 4.2 Strategy

### 4.2.1 Adapting Sub Rosa

As seen in Chapter 3, the Sub Rosa substitutions  $\sigma_n$  are easy to lift in  $\mathbb{R}^n$  and there is a nice relation between the edge word  $\Sigma(n)$  and the eigenvalues of the Sub Rosa expansion  $\varphi_n$  (Propositions 3.4.3 and 3.5.3). However with the Sub Rosa construction we get eigenvalues that are incompatible with planarity since  $\varphi_n$  is strictly expanding on a 4-dimensional subspace.

The goal here is to define Sub Rosa-like substitutions such that the associated expansion  $\varphi$  is strictly expanding along  $\mathcal{E}_n^0$  and strictly contracting on its orthogonal supplement. Recall that Sub Rosa-like substitutions are defined by their edge word  $\Sigma$ . The two key points are:

1. the construction of the edge word  $\Sigma$  to ensure planarity,
2. the tileability of the metatiles defined by their edge word  $\Sigma$ .

For a given  $n$  the idea is that we define a sequence  $(\Sigma_{(j)})_{j \in \mathbb{N}}$  of edge words such that

- there are infinitely many indices  $j$  such that the expansion  $\varphi_{(j)}$  associated to  $\Sigma_{(j)}$  is planar of slope  $\mathcal{E}_n^0$ ,
- there exists  $N \in \mathbb{N}$ , such that for any  $j \geq N$  the metatiles defined by the edge word  $\Sigma_{(j)}$  are tileable and the corresponding substitution is primitive.

We call Planar Rosa substitution denoted by  $\sigma'(n)$  the substitution defined by  $\Sigma_{(j)}$  for the smallest  $j$  such that it is both planar and tileable.

From the Planar Rosa substitution  $\sigma'(n)$  we define an associated regular fixpoint tiling with global  $2n$ -fold rotational symmetry from the seed  $S(n)$ .

### 4.2.2 Adapting $P_n(\frac{1}{2})$

In the previous Subsection we presented a strategy based on modifying the Sub Rosa substitution to get planar substitutions. Here we present another approach based on starting from a cut-and-project tiling with  $2n$ -fold rotational symmetry and approximating it by a substitution to get a substitution planar tiling. Note that here the term of approximating a tiling is not to be understood in the usual sense of cylinder topology on tilings, the main point of this approximation process is to keep the slope when lifted in  $\mathbb{R}^n$ .

As it will be seen in Chapter 5 the  $n$ -fold multigrid dual tiling  $P_n(\frac{1}{2})$  is a cut-and-project rhombus tiling with  $2n$ -fold rotational symmetry. Moreover  $P_n(\frac{1}{2})$  contains an infinite cone of angle  $\frac{\pi}{n}$  with the same sequence of unit edges and bisected rhombuses on both sides of the cone, we denote this sequence by  $\omega(n)$ . The idea now is to consider this infinite cone as some kind of metatile of infinite size. We will define larger and larger substitutions whose metatiles of angle  $\frac{\pi}{n}$  approximate this cone. There are of course a lot of details to work out as will be seen in the following sections.

These two strategies are actually two ways of looking at the construction we present in Sections 4.4 and 4.5.

## 4.3 Tileability of Sub Rosa-like metatiles

The tileability of a finite domain with a given set of prototiles is, in all generality, a NP-complete problem (see Section 2.12 for more background on this topic). However here we are interested in the tileability of a very specific kind of finite domains: Sub Rosa-like metatiles. Recall that Sub Rosa-like

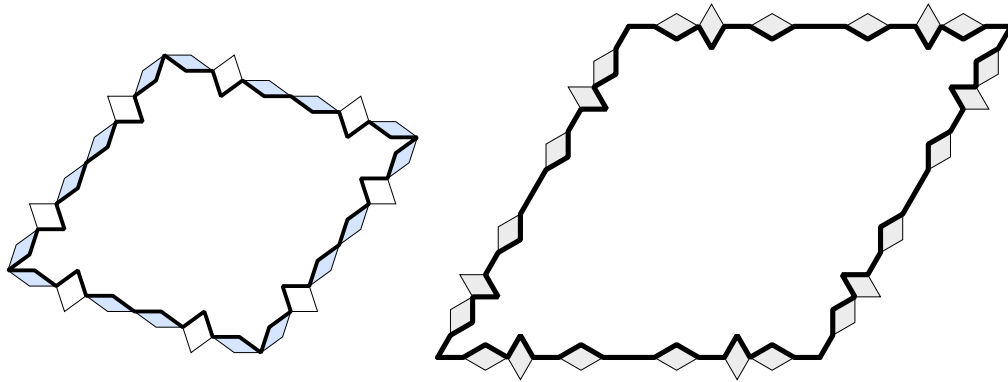


Figure 4.2: Examples of polygons defined by Sub Rosa-like metatiles for  $n \in \{5, 6\}$ .

metatiles are defined by the sequence of edges and rhombuses on their edges which is the same on all sides (up to translation and rotation) and which is called edge word and denoted by  $\Sigma$ . In this section we will use the term *pseudosubstitution* for a substitution that is defined only on the edges of the metatiles, we say that it extends to a substitution when the metatiles can be tiled with unit rhombuses.

The finite domain defined by a Sub Rosa-like metatile is a polygon (see Figure 4.2) and we aim to tile it with rhombuses which are specific cases of parallelograms. This means that we can use the Kenyon criterion for tilings polygons with parallelograms [Ken93].

The first step of the Kenyon method is to fix an origin vector on the polygon to tile. Let us note  $(a_1, \dots, a_m)$  the sequence of oriented edges when going along the edge of the parallelogram counterclockwise from the starting point and back to it. We note  $\vec{a}_j$  called *edge type* the vector of the edge  $a_j$ , all the  $\vec{a}_j$  are in the set of directions of the tiling *i.e.*  $\vec{a}_j \in \{\pm\vec{v}_k, k = 1..n\}$ .

Suppose the interior of the polygon is actually tiled. As seen in Figure 4.3 from each edge of the polygon starts a chain of rhombuses (shaded in the figure) that share the same edge type, and at the two ends of this chain are two edge of the polygon with the same edge type but opposite directions. Note that chains are also called ribbons or worms. These chains define a matching on the edges that have the following properties:

1. two edges that are matched have same absolute edge type and opposite orientation,

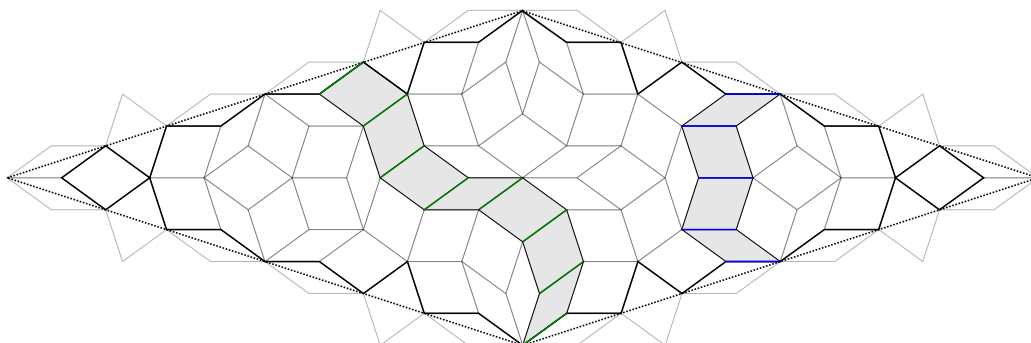


Figure 4.3: In shaded two chains of rhombuses.

2. two matched pairs of edges of the same absolute edge type cannot cross each other with respect to the cyclic ordering of the edges. Indeed two chains with the same edge type cannot cross, otherwise it would create a “flat” rhombus,
3. two matched edges must “see” each other in the parallelogram in the sense that there is a monotone increasing path according to  $\vec{a}_j^\perp$  in the interior of the parallelogram from one edge to the other. Indeed otherwise it would mean that the chain circles back on itself,
4. the matching is *peripherally monotonous*: for any two matched pairs  $\{a, a'\}$  and  $\{b, b'\}$  such that in the cyclic ordering  $a < b < a' < b'$ , we have  $[a]^\perp \cdot [b] > 0$ . That ensures that at the crossing rhombus of the two chains the rhombus actually exists.

We call *Kenyon matching* a matching on the oriented edges that follow these properties.

**Theorem 13** (Kenyon, 93). *The polygon is tileable by parallelograms if and only if a Kenyon matching exists.*

*Sketch of the proof.* See the Kenyon article for full proof [Ken93]. The main idea is that for the parallelogram to be tileable, any edge must match to an edge of same absolute type and opposite direction such that there is a chain of parallelograms between the two matched edges (see Figure 4.3). And when two such chains cross, then their crossing is a parallelogram which edges are the edges of the two matched pairs.  $\square$

In the case of our substitution tilings, we study the tileability of the polygons which are defined by the same sequence of rhombuses and edges on all four edges of the metatiles. Recall that in the edge word  $\Sigma$  of a Sub Rosa-like substitution a 0 encodes a unit edge and an integer  $k$  encodes a rhombus bisected along its angle  $\frac{k\pi}{n}$ . For  $n$  odd, the letters in the edge word are the odd integers from 1 to  $n - 2$ , and for even  $n$  the letters in the edge word are the even numbers from 0 to  $n - 2$ .

Given the constraints on Sub Rosa-like substitutions the edge word  $\Sigma$  is a palindrome and is the same on each edge of every metatyle. That is why we only consider one word. Recall that, as discussed in Chapter 3, the expansion  $\varphi$  is determined by the abelianized edge word  $[\Sigma]$ . So the expansion, and the planarity of the substitution, are determined by the abelianized edge word *i.e.* the edge word up to reordering, but for tileability the order is very important.

For technical reasons we will introduce the counting functions of the edge word:

**Definition 4.3.1** (Counting function). *Given some integer  $n \geq 3$  and an edge word  $\Sigma = u_0 u_1 \dots u_{m-1}$  of length  $m$ . For an edge/rhombus type  $i$  and a position  $x \in \{0, \dots, m\}$  we define  $f_i(x) := |u_0 \dots u_{x-1}|_i$  the number of letters  $i$  in the prefix of length  $x$  of the edge word  $\Sigma$ .*

*We also define  $f_i^{-1}(y)$  the length of the shortest prefix of  $\Sigma$  with  $y$  occurrences of the letter  $i$ . If there is no such prefix then  $f_i^{-1}(y) := +\infty$ , also if  $y < 0$  then  $f_i^{-1}(y) := -\infty$  and  $f_i^{-1}(0) := 0$ .*

*For  $i = n$  we define  $f_i(x) := 0$  and for  $n < i < 2n$  we define  $f_i(x) := -f_{2n-i}(x)$ . For these cases we do not define  $f_i^{-1}$ .*

Let us remark a few things regarding this definition:

- $f_i^{-1}$  is not an inverse function since  $f_i$  is not bijective. However for any  $i, y$  such that there is at least  $y$  occurrences of the letter  $i$  we have  $f_i(f_i^{-1}(y)) = y$ , and for any  $x$  such that  $u_{x-1} = i$  we also have  $f_i^{-1}(f_i(x)) = x$  (but but when  $u_{x-1} \neq i$  we have  $f_i^{-1}(f_i(x)) < x$ ),
- the fact that  $i$  is a edge/rhombus type means that it is either an odd number between 1 and  $n - 2$  which codes a unit rhombus of angle  $\frac{i\pi}{n}$  when  $n$  is odd or an even number between 0 and  $n - 2$  where 0 codes a unit edge and  $i \neq 0$  codes a unit rhombus of angle  $\frac{i\pi}{n}$  when  $n$  is even,

- we give a definition of  $f_i(x)$  for  $n \leq i < 2n$  because later on they will appear and we want to give them a meaning,
- we fix  $f_i^{-1}(y) = +\infty$  if there are less than  $y$  occurrences of the letter  $i$  in the edgeward for simplicity. This allows us to not have to check whether the number of occurrences of the letter  $i$  before using  $f_i^{-1}$ . We also use the convention that  $+\infty > +\infty$  for the simplicity of some statements (which have sense for values that are not infinity). We could also just say that the formulas that involve  $f_i^{-1}$  are understood only in the non-infinity case. The same goes for  $f_i^{-1}(y) = -\infty$  in the case that  $y$  is negative.

The Kenyon conditions translates into inequalities on the counting functions  $f_j$ . But for a concise formulation we need an additional definition.

**Definition 4.3.2** (Almost-balancedness). *We call a word  $u$   $n$ -almost-balanced when for any letters  $i_1 < i_2$  and any factor subword  $v$  of  $u$  we have  $|v|_{i_1} - |v|_{i_2} \geq -n$ .*

The idea is that the frequency of apparition of  $i_1$  is greater than the frequency of apparition of  $i_2$  when  $i_1 < i_2$ , so the idea is that  $|v|_{i_1} - |v|_{i_2}$  should be positive for large  $v$ , but for small factors  $v$  we can have negative values for example if we take  $v = i_2$  as subword of  $u$ . This quite unusual definition of  $n$ -almost-balancedness bounds the negative values that  $|v|_{i_1} - |v|_{i_2}$  can take. For example for a binary Sturmian word  $u$  with letters  $i_1$  and  $i_2$  and frequency of  $i_1$  larger than frequency of  $i_2$ ,  $u$  is 1-almost-balanced.

The main result of this section is the following.

**Proposition 4.3.1** (Tileability). *Let us consider a pseudosubstitution of 2-almost-balanced edge word  $\Sigma$  and counting functions  $f_i$ .*

*If for any letters  $i_1 < i_2$  we have  $f_{i_1}(m) > f_{i_2}(m) > 0$  where  $m$  is the length of the edge word  $\Sigma$  and for any prefix length  $x_1$  such that at position  $x_1 - 1$  in the edge word there is an edge or rhombus  $i_1$  we have*

$$f_{|i_2-2|}^{-1} \circ f_{i_2}(x_1) < f_{|i_1-2|}^{-1} \circ f_{i_1}(x_1), \quad (4.1)$$

*then all the metatiles of the pseudosubstitution defined by  $\Sigma$  are tileable. Which means that  $\Sigma$  actually defines a substitution.*

Recall that when  $n$  is odd the letters in the edge word are the odd integers  $1 \leq i < n$  and they represent rhombuses of angle  $\frac{i\pi}{n}$  on the edge of the



metatile, and when  $n$  is even the letters in the edge word are the even integers  $0 \leq i < n$  and 0 represents an unit edge and non-zero  $i$  represent rhombuses of angle  $\frac{i\pi}{n}$  on the edge of the metatile.

This proposition gives us a sufficient condition for tileability of the metatiles that we will use for the construction of the Planar Rosa substitutions which are planar substitutions with  $2n$ -fold rotational symmetry in Sections 4.4 and 4.5. This proposition was formulated as an implication because that is how we use it, but it is actually an equivalence.

Let us give two quick examples with  $n = 5$ . Let us first consider the edge word  $\Sigma = 1331$ , with  $i_1 = 1$ ,  $i_2 = 3$ , we have  $f_{i_1}(m) = f_{i_2}(m) = 2$  which contradicts the first condition and additionally for  $x = 4$  we have

$$f_{|i_2-2|}^{-1} \circ f_{i_2}(x) = f_1^{-1} \circ f_3(4) = f_1^{-1}(2) = 4,$$

and

$$f_{|i_1-2|}^{-1} \circ f_{i_1}(x) = f_1^{-1} \circ f_1(4) = 4,$$

which also contradicts the second condition. This implies that the narrow metatile of edge word  $\Sigma = 1331$  is not tileable.

Now let us consider the edge word  $\Sigma = 131131$ , with  $i_1 = 1$  and  $i_2 = 3$  we have  $f_{i_1}(m) = 4$  and  $f_{i_2}(m) = 2$  so the first condition holds, now we need to check

$$f_{|i_2-2|}^{-1} \circ f_{i_2}(x_1) < f_{|i_1-2|}^{-1} \circ f_{i_1}(x_1),$$

for any position  $x_1$  where there is a rhombus of type  $i_1$ .

We will now present the proof of this proposition with several lemmas and propositions to cut this in smaller pieces and make for hopefully understandable proofs.

First we will assume the metatiles to be tileable to see what conditions we get on the counting functions  $f_j$ , we will later show the converse.

**Proposition 4.3.2.** *If the metatile with angle  $\frac{k\pi}{n}$  is tileable then for any  $i_1 < i_2$  and any prefix length  $x_1$  such that at position  $x_1 - 1$  in the edge word there is a rhombus  $i_1$  we have*

$$f_{|i_2-2k|}^{-1} \circ f_{i_2}(x_1) < f_{|i_1-2k|}^{-1} \circ f_{i_1}(x_1). \quad (4.2)$$

The unwritten assumption here is that there are at least  $f_{i_2}(x_1)$  rhombuses of type  $|i_2 - 2k|$  in the edgeword, in the case that there are not enough rhombuses of type  $|i_2 - 2k|$  we have imposed the convention that  $f_{|i_2-2k|}^{-1} \circ f_{i_2}(x_1) = +\infty$  which “solves” this degenerate case.

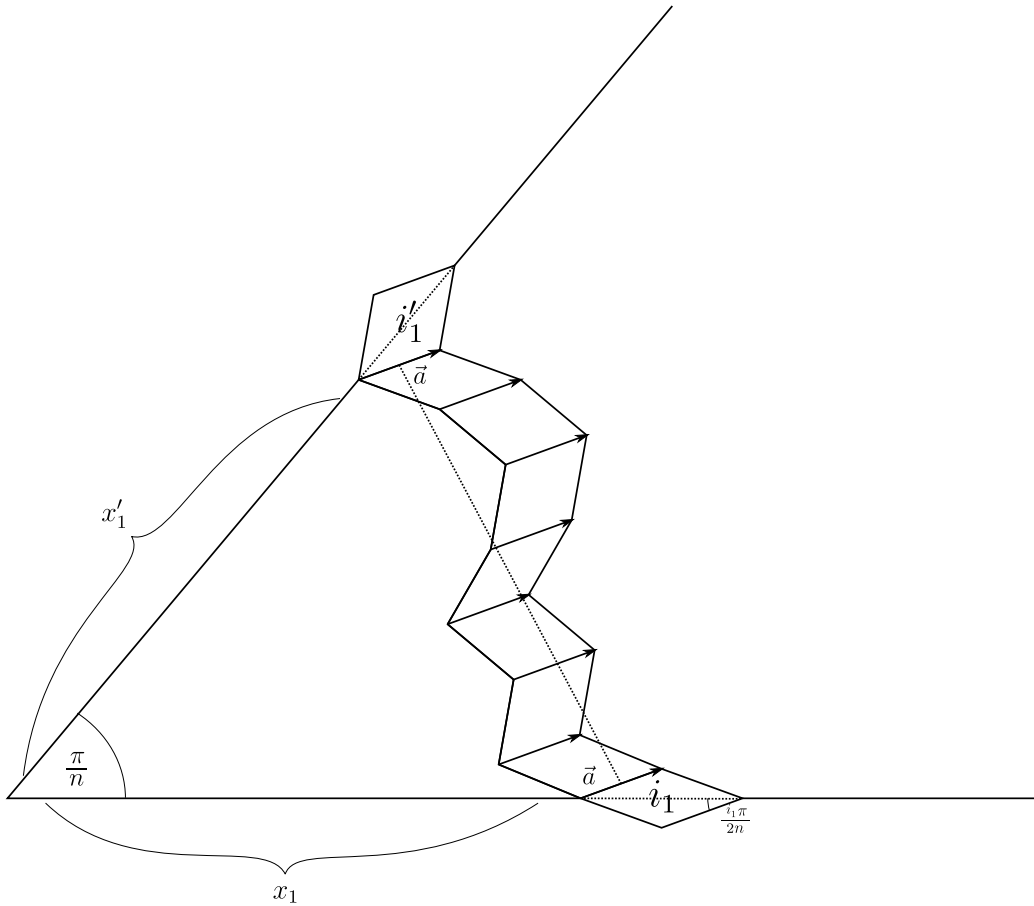


Figure 4.4: A chain of rhombuses around the narrow corner of the metatile.

*Proof.* Let us assume the metatile is tileable. Let us see how chains of parallelograms behave in our case. For simplicity consider the narrowest metatile, we assume it is tileable and that we have a valid Kenyon matching. Take a chain of edge type  $\vec{a}$  that links a rhombus of type  $i_1$  on the side 1 of the metatile to a rhombus of type  $i'_1$  on the side two as in Figure 4.4.

On side 1, the direction  $\vec{a}_1$  can only be found on the rhombuses of type  $j$ , because the direction of the edges of rhombus is determined by the general direction of the side and half the angle of the rhombus. Call  $x_1 - 1$  the index of this rhombus on side 1 (starting the indexes from the corner with side 2). There are  $f_{i_1}(x_1)$  rhombuses of type  $i_1$  between the corner and the chain on side 1. On side 2, for the same reason the direction  $-\vec{a}_1$  only appears on

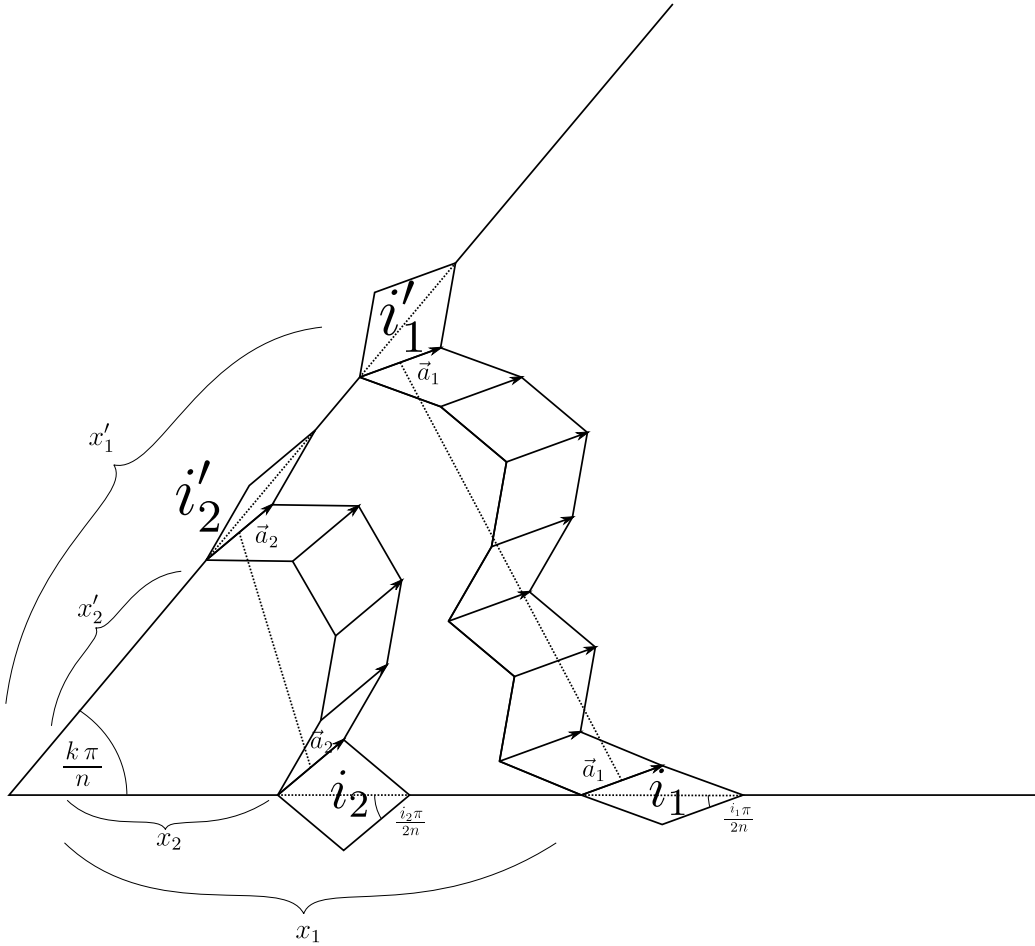


Figure 4.5: A second chain of rhombuses around the narrow corner.

the edge of  $i'_1$  rhombuses and there are  $f_{i'_1}(x'_1)$  such rhombuses between the corner and the chain. And since the matching is valid, two chains of same absolute edge type cannot cross each other (condition 2), so every rhombus  $i_1$  of side one between the corner and the chain is matched to a rhombus of type  $i'_1$  of side two also between the corner and the chain. So we have  $f_{i_1}(x_1) = f_{i'_1}(x'_1)$  that we can reformulate  $f_{i'_1}^{-1}(f_{i_1}(x_1)) = x'_1$ .

We can also remark that since the angle of the corner of the metatile is  $\frac{\pi}{n}$ , the half-angles of the rhombuses are  $\frac{i_1\pi}{2n}$  and  $\frac{i'_1\pi}{2n}$  and their sides are parallel so we have  $i'_1 = |i_1 - 2|$ . More generally around a corner of angle  $\frac{k\pi}{n}$  we would have  $i'_1 = |i_1 - 2k|$ . Now let us consider a second chain on that setting.

Take a type of rhombus  $i_2 > i_1$  and note  $x_2 - 1$  the last position at which a rhombus  $i_2$  appears between the corner and the chain of direction  $\vec{a}_1$  as in Figure 4.5. Denote  $\vec{a}_2$  the edge of the rhombus facing the corner and consider the chain that starts at this edge. As for the first chain, this one is linked to some rhombus of type  $i'_2 = |i_2 - 2|$  on side 2 which is at position  $x'_2$  and we have  $f_{i'_2}^{-1}(f_{i_2}(x_2)) = x'_2$ . But since there is no rhombus of type  $i_2$  between  $x_2$  and  $x_1 - 1$  we have  $f_{i_2}(x_2) = f_{i_2}(x_1)$ .

Since  $i_2 > i_1$  we have  $\langle \vec{a}_2^\perp | \vec{a}_1 \rangle \leq 0$  so the two chains cannot cross (see Figure 4.5), this means that  $x'_2 < x'_1$ . So overall

$$f_{i'_2}^{-1} \circ f_{i_2}(x_1) < f_{i'_1}^{-1} \circ f_{i_1}(x_1).$$

□

Now if we modify this situation a little bit. Suppose that the chains connect to the opposite side as in Figure 4.6. Then we have the following proposition.

**Proposition 4.3.3.** *If the metatile with angle  $\frac{k\pi}{n}$  is tileable then for any  $i_1 < i_2$  and any prefix length  $x_1$  such that at position  $x_1 - 1$  in the edge word there is a rhombus  $i_1$  we have*

$$f_{i_2}^{-1}\left(f_{i_2}(x_1) - f_{|i_2-2k|}(m)\right) < f_{i_1}^{-1}\left(f_{i_1}(x_1) - f_{|i_1-2k|}(m)\right). \quad (4.3)$$

.

The unwritten assumption in this statement is that that  $f_{i_2}(x_1) - f_{|i_2-2k|}(m) > 0$  (and same for  $i_1$ ), that is why we imposed the convention that  $f_i^{-1}(y) = -\infty$  for negative  $y$ .

*Proof.* The quantity  $f_{|i_2-2k|}(m)$  is the total number of rhombuses of type  $|i_2 - 2k|$  on the edge adjacent to the angle see Figure 4.6, so it is the number of rhombuses of type  $i_2$  that will be matched to rhombuses of type  $|i_2 - 2k|$  on the adjacent edge. Once we remove those rhombuses, rhombuses of type  $i_2$  match to rhombuses of type  $i_2$  on the matching edge, hence the Equation (4.3). □

Overall, if the metatile with angles  $\frac{k\pi}{n}$  and  $\frac{(n-k)\pi}{n}$  is tileable then for any  $i_1 < i_2$  and any prefix length  $x_1$  such that at position  $x_1 - 1$  in the edge word there is a rhombus  $i_1$  we have Equations (4.2) and (4.3) for the two angles. So four equations hold. Let us see how the converse goes.

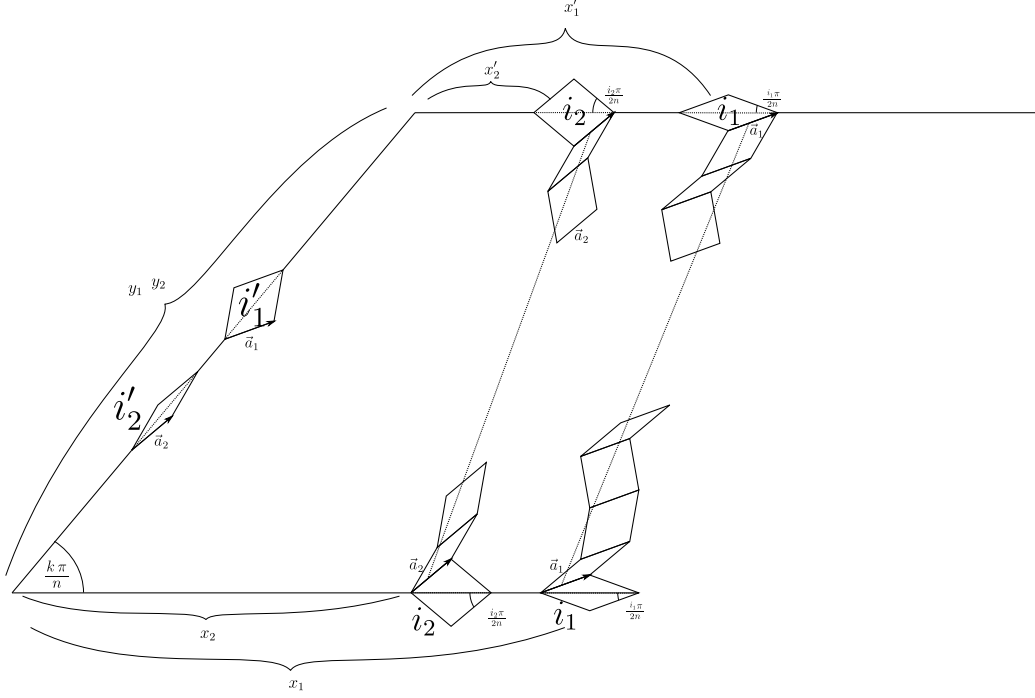


Figure 4.6: The two chains linking opposite sides.

**Proposition 4.3.4.** *Let us consider the metatile of angles  $\frac{k\pi}{n}$  and  $\frac{(n-k)\pi}{n}$ . If  $f_1 \geq f_3 \geq \dots \geq f_{n-2} > 0$  (when  $n$  is odd) or  $f_0 \geq f_2 \geq \dots \geq f_{n-2} > 0$  (when  $n$  is even) and if for any  $i_1 < i_2$  and any prefix length  $x_1$  such that at position  $x_1 - 1$  in the edge word there is a rhombus  $i_1$  we have*

$$f_{|i_2-2k|}^{-1} \circ f_{i_2}(x_1) < f_{|i_1-2k|}^{-1} \circ f_{i_1}(x_1), \quad (4.4)$$

$$f_{|i_2-2(n-k)|}^{-1} \circ f_{i_2}(x_1) < f_{|i_1-2(n-k)|}^{-1} \circ f_{i_1}(x_1), \quad (4.5)$$

$$f_{i_2}^{-1}(f_{i_2}(x_1) - f_{|i_2-2k|}(m)) < f_{i_1}^{-1}(f_{i_1}(x_1) - f_{|i_1-2k|}(m)), \quad (4.6)$$

$$f_{i_2}^{-1}(f_{i_2}(x_1) - f_{|i_2-2(n-k)|}(m)) < f_{i_1}^{-1}(f_{i_1}(x_1) - f_{|i_1-2(n-k)|}(m)), \quad (4.7)$$

then the metatile is tileable.

Let us remark once again that in the two degenerate cases ( the case of  $f_i^{-1}(y)$  with either  $y$  negative or  $y$  greater than the number of occurrences of the letter  $i$  in the full word) we have infinite values with the convention that  $-\infty < -\infty$  and  $+\infty < +\infty$ .

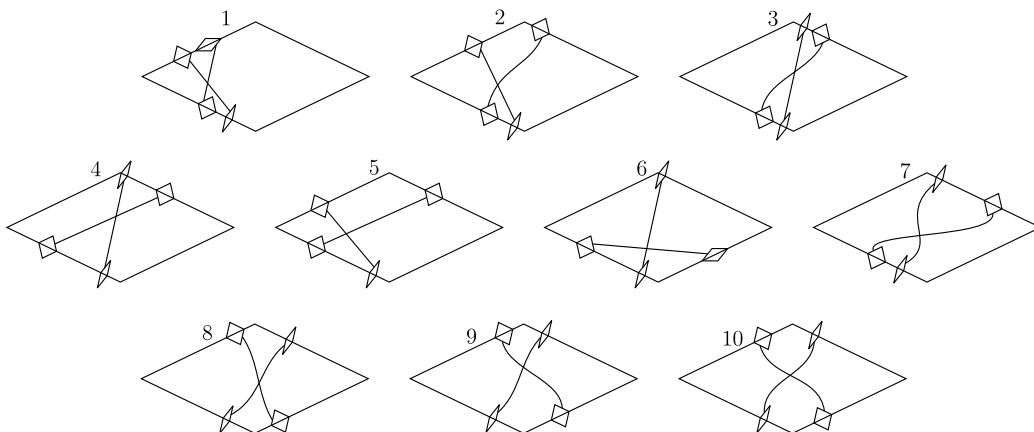


Figure 4.7: Atlas of possible (but not necessarily valid) crossing types.

*Proof of Lemma 4.3.4.* By contradiction suppose the metatile is not tileable. We will prove that one of the inequations is broken. If the metatile is not tileable, then by Theorem 13 there exists an invalid crossing of chains. Any two chains that cross are of one of the types described in Figure 4.7. The first case is the one described in the proof of Proposition 4.3.2 above and in Figure 4.5, same for the case 2. So if the invalid crossing is of type 1 or type 2 then Equation (4.4) is broken which contradicts the hypothesis.

Type 3 corresponds to Equation (4.6).

Type 4, 5 and 6 are never invalid.

Type 7 : Let us first consider the sub-case where the two rhombus whose chain cross are actually the same type of rhombus. This means that we have a situation where the two chains leaving from the two sides of a rhombus are crossing. Let us show it is never the case. For simplicity we consider  $k < n - k$ . And let us consider that the rhombus in question has (odd) angle  $\frac{i\pi}{n}$ . If  $n - k - 2i < n/2$  it means that the two directions of the sides of the rhombus have matching rhombuses on the adjacent edges of the metatile. If we call  $x$  the position of the rhombus,  $x'$  the position of the rhombus to which the left side matches and  $x''$  the position of the rhombus to which the right side matches this means that  $x' < x < x''$ . But if we have  $n - k - 2i > n/2$ , assuming that the wide angle of the metatile is to the right of the rhombus we have  $x'' < x$  because on the adjacent edge of the metatile there are rhombuses that have the exact same edge direction as our rhombus these are the rhombuses of type  $2k + i$ , so the rhombus  $x$  matches to a rhombus  $x''$  which

is more to the left. But the left side of the rhombus matches to  $x' < x$  and even  $x' < x'' < x$  because there are strictly more rhombuses of type  $|i - 2k|$  (to which the left direction matches) on the left edge of the metatile, than rhombuses of type  $i + 2k$  (which have the same direction the same are the right side) on the right edge of the metatile, so  $x'$  is offset by strictly more positions of rhombuses of type  $i$  to the left of  $x$  than  $x''$ . So the two sides of a same rhombus cannot spawn crossing worms.

Now consider that we have a crossing of that type with two different rhombuses, then if we look at the worm leaving the right side of the left rhombus it crosses the worm leaving the right side of the right rhombus (otherwise the two worms leaving the left rhombus would cross), but also the worm leaving the left side of the right rhombus crosses the worm leaving the left side of the left rhombus (for the same reason), and at least one of these two crossing is invalid and of Type 2 or 3. So by the previous result if the equations hold a crossing of type 7 is impossible.

For the following, consider that the left rhombus is of type  $i$ , the right rhombus is of type  $j$ . And the edge we are interested in are  $a$  for the left rhombus and  $b$  for the right.

Type 8 : Such a crossing is invalid only if  $\langle a^\perp | b \rangle < 0$  with  $a$  and  $b$  the direction of the edges. And this can only be possible if  $i > k$  or  $j > k$  if we consider that the angle on the metatile between the two rhombuses is  $\frac{k\pi}{n}$ . For simplicity let us assume  $i > k$ , in that case the edge direction  $a$  is matched, on an adjacent edge of the metatile, to rhombuses of type  $|2k - i| < i$ , there are more vectors of type  $|2k - i|$  than of type  $i$  so the rhombus cannot be matched to a rhombus of the opposite edge of the metatile. So such a crossing cannot be invalid.

Type 9 : Such a crossing is invalid only if  $\langle a^\perp | b \rangle < 0$  with  $a$  and  $b$  the direction of the edges. And this can only be possible if  $j > k$  if we consider that the angle on the metatile between the two rhombuses is  $\frac{(n-k)\pi}{n}$ . In that case the edge direction  $b$  is matched, on an adjacent edge of the metatile, to rhombuses of type  $|2k - j| < j$ , there are more vectors of type  $|2k - j|$  than of type  $j$  so the rhombus cannot be matched to a rhombus of the opposite edge of the metatile. So such a crossing cannot be invalid.

Type 10 : Such a crossing is invalid only if  $\langle a^\perp | b \rangle < 0$  with  $a$  and  $b$  the direction of the edges. And this can only be possible if  $i > k$  or  $j > k$  if we consider that the angle on the metatile between the two rhombuses is  $\frac{(n-k)\pi}{n}$ . For simplicity let us assume  $i > k$ , in that case the edge direction  $a$  is matched, on an adjacent edge of the metatile, to rhombuses of type  $|2k - i| <$

$i$ , there are more vectors of type  $|2k - i|$  than of type  $i$  so the rhombus cannot be matched to a rhombus of the opposite edge of the metatile. So such a crossing cannot be invalid.  $\square$

We can actually do better than this: under the almost-balancedness assumption we only need to prove the Equation (4.4) with  $k = 1$ .

First let us observe that the Equation (4.4) with  $k = 1$  implies that there are more rhombuses  $i_1$  than rhombuses  $i_2$  whenever  $i_1 < i_2$ .

**Lemma 4.3.1.** *If for any edge or rhombus type  $i_1 < i_2$  and any prefix length  $x_1$  such that at position  $x_1 - 1$  in the edge word there is a rhombus  $i_1$*

$$f_{|i_2-2|}^{-1} \circ f_{i_2}(x_1) < f_{|i_1-2|}^{-1} \circ f_{i_1}(x_1), \quad (4.8)$$

*then we have  $f_1 \geq f_3 \geq \dots \geq f_{n-2}$  when  $n$  is odd, and we have  $f_0 \geq f_2 \geq f_4 \geq \dots \geq f_{n-2}$  when  $n$  is even.*

*Proof of Lemma 4.3.1.* Let us first recall that the edge word  $\Sigma$  is a palindrome. This result would not necessarily hold otherwise.

We will prove it for the case of odd  $n$ , the case of even  $n$  is the same up to replacing the odd rhombus types by even edge or rhombus types. Take and odd  $i < n - 2$ , assume that  $f_1 \geq f_3 \geq \dots \geq f_i$ , let us prove that  $f_i \geq f_{i+2}$ . By contradiction suppose that there exists  $x_2$  such that  $f_{i+2}(x_2) \geq 1 + f_i(x_2)$ . We take  $x_2$  to be the smallest prefix length at which it holds. We have  $u_{x_2} = i + 2$ . Take  $x_1$  the smallest prefix length greater than  $x_2$  such that  $u_{x_1-1} = i$ . Such an index exists, because the first occurrence of  $i$  is before the first occurrence of  $i + 2$  from Equation (4.8), so the last occurrence of  $i$  is after the last occurrence of  $i + 2$ . By definition  $f_i(x_1) = f_i(x_2) + 1$  and  $f_{i+2}(x_1) \geq f_{i+2}(x_2)$ , so  $f_i(x_1) \leq f_{i+2}(x_1)$ . But by  $f_{|i-2|} \geq f_i$  we have  $f_{|i-2|}^{-1}(f_i(x_1)) \leq x_1$ . This is impossible because when we apply Equation (4.8) with  $i_1 = i$  and  $i_2 = i + 2$  on  $x_1$ , we get

$$f_i^{-1} \circ f_{i+2}(x_1) < f_{i-2}^{-1} \circ f_i(x_1) \leq x_1,$$

which implies  $f_{i+2}(x_1) < f_i(x_1)$ .  $\square$

From this lemma we can obtain this nice result on the counting functions.



**Lemma 4.3.2.** *If Equation (4.4) holds for  $k = 1$  then Equations (4.4) and (4.5) hold for any  $1 \leq k < n$ .*

*Proof.* Let us prove that from Equation (4.4) with  $k = 1$  we can obtain it with  $k = 2$ .

This means that we assume that for any  $i_1 < i_2$  and any  $x_1$  such that  $u_{x_1-1} = i_1$  we have

$$f_{|i_2-2|}^{-1} \circ f_{i_2}(x_1) < f_{|i_1-2|}^{-1} \circ f_{i_1}(x_1),$$

and we want to prove that for any  $i_1 < i_2$  and any  $x_1$  such that  $u_{x_1-1} = i_1$  we have

$$f_{|i_2-4|}^{-1} \circ f_{i_2}(x_1) < f_{|i_1-4|}^{-1} \circ f_{i_1}(x_1).$$

Let us take  $i_1, i_2, x_1$  such that  $i_1 < i_2$  and  $u_{x_1-1} = i_1$ . If  $i_1 > 1$  we have  $|i_1 - 4| = ||i_1 - 2| - 2|$  so it becomes straightforward with

$$f_{|i_1-4|}^{-1} \circ f_{i_1}(x_1) = f_{|i_1-4|}^{-1} \circ f_{|i_1-2|} \circ f_{|i_1-2|}^{-1} \circ f_{i_1}(x_1).$$

Otherwise we have  $i_1 = 1$  and  $i_2 \geq 3$  so we need to compare  $f_{|i_2-4|}^{-1} \circ f_{i_2}$  and  $f_3^{-1} \circ f_1$  with  $|i_2 - 4| \leq i_2$ . From Lemma 4.3.1 we have that  $f_1 \geq f_3$  and  $f_{|i_2-4|} \geq f_{i_2}$  so  $f_3^{-1} \circ f_1(k1) \geq x_1 \geq f_{|i_2-4|}^{-1} \circ f_{i_2}(x_1)$  moreover the first inequality is strict because  $u_{x_1} = 1$ , so overall  $f_3^{-1} \circ f_1(k1) \geq f_{|i_2-4|}^{-1} \circ f_{i_2}(x_1)$ .  $\square$

To also get Equations (4.6) and (4.7) we need the almost-balancedness assumption.

Under the assumption that  $u$  is 2-almost-balanced we always have Equation (4.6) and (4.7).

**Lemma 4.3.3.** *Under the assumption that the edgeward  $\Sigma$  is 2-almost-balanced (with our unusual definition 4.3.2) and if  $f_1(m) > f_3(m) > \dots > f_{n-2}(m) > 0$  (or  $f_0(m) > f_1(m) > \dots > f_{n-2}(m) > 0$  when  $n$  is even) with  $m = |\Sigma|$  the length of the whole word then for any  $0 < k < n$ , for any  $i_1 < i_2$  and for any  $x_1$  such that  $u_{x_1-1} = i_1$  we have*

$$f_{i_2}^{-1} (f_{i_2}(x_1) - f_{|i_2-2k|}(m)) < f_{i_1}^{-1} (f_{i_1}(x_1) - f_{|i_1-2k|}(m)).$$

*Proof.* Let us take such  $k, i_1, i_2, x_1$ .

Let us solve two special cases:

- if  $i_1 \geq |i_1 - 2k|$  then we never have  $f_{i_1}(x_1) > f_{|i_1-2k|}(m)$  so there exist no such  $k, i_1, i_2, x_1$ ,
- if  $|i_1 - 2k| > n - 2$  then there is no rhombus of angle  $|i_1 - 2k|$  in the edge word and either  $|i_1 - 2k| = n$  in which case  $f_{|i_1-2k|}(m) = 0$  or  $|i_1 - 2k| > n$  in which case  $f_{|i_1-2k|}(m) = -f_{2n-|i_1-2k|}(m) < 0$ . These cases actually are the same as the other because we have  $f_1(m) > f_3(m) > \dots > f_{n-2}(m) > f_n(m) > f_{n+2}(m) > \dots > f_{2n-2}(m)$  with the definition of  $f_i(m) = -f_{2n-i}(m)$  for  $i > n$ .

If we are not in these cases then we have  $|i_1 - 2k| > i_1$  so this means that  $|i_1 - 2k| = 2k - i_1$  and  $i_1 < k$ .

If  $i_2 \geq |i_2 - 2k|$  then the inequation is simple with

$$\begin{aligned} f_{i_2}(x_1) - f_{|i_2-2k|}(m) &\leq 0 \Rightarrow \\ f_{i_2}^{-1}(f_{i_2}(x_1) - f_{|i_2-2k|}(m)) &= 0 < f_{i_1}^{-1}(f_{i_1}(x_1) - f_{|i_1-2k|}(m)). \end{aligned}$$

Otherwise we have  $i_1 < i_2 < k < |i_2 - 2k| < |i_1 - 2k| \leq n - 2$ . In that case we have  $f_{|i_2-2k|}(m) > f_{|i_1-2k|}(m)$ . Since  $f_{i_1}(x_1) - f_{|i_1-2k|}(m) > 0$  there exists a  $x'_1 < x_1$  such that  $u_{x'_1} = i_1$  and  $f_{i_1}(x'_1) = f_{i_1}(x_1) - f_{|i_1-2k|}(m)$ .

Let us now remark that  $f_{i_2}(x_1) - f_{|i_2-2k|}(m) \leq f_{i_2}(x_1) - (f_{|i_1-2k|}(m) + 1) \leq f_{i_2}(x'_1)$  because  $|u_{x'_1} u_{x'_1+1} \dots u_{x_1-1}|_{i_2} \leq 2 + |u_{x'_1} u_{x'_1+1} \dots u_{x_1-1}|_{i_1}$  ( by Definition 4.3.2)

so  $|u_{x'_1} u_{x'_1+1} \dots u_{x_1-1} u_{x_1}|_{i_2} \leq 1 + |u_{x'_1} u_{x'_1+1} \dots u_{x_1-1} u_{x_1}|_{i_1}$  and

$$\begin{aligned} f_{i_2}(x_1) - f_{i_2}(x'_1) &= |u_{x'_1} u_{x'_1+1} \dots u_{x_1-1} u_{x_1}|_{i_2} \\ &\leq 1 + |u_{x'_1} u_{x'_1+1} \dots u_{x_1-1} u_{x_1}|_{i_1} \\ &\leq 1 + f_{i_1}(x_1) - f_{i_1}(x'_1) \\ &\leq 1 + f_{|i_1-2k|}(m). \end{aligned}$$

So overall

$$\begin{aligned} f_{i_2}^{-1}(f_{i_2}(x_1) - f_{|i_2-2k|}(m)) &\leq f_{i_2}^{-1} \circ f_{i_2}(x'_1) \\ &< f_{i_1}^{-1} \circ f_{i_1}(x_1) = f_{i_1}^{-1}(f_{i_1}(x_1) - f_{|i_1-2k|}(m)). \end{aligned}$$

□

## 4.4 Construction for odd $n$

### 4.4.1 Lifting and eigenvalues

Here  $n$  is an odd integer greater than 3 and we are considering Sub Rosa-like substitutions of order  $n$  *i.e.* with unit rhombus prototiles of angles  $\frac{k\pi}{n}$  and  $\frac{(n-k)\pi}{n}$ . Sub Rosa-like substitutions are lifted in the same way as Sub Rosa substitutions, we will here recall the most important definitions and propositions but proofs and explanations will be found in Section 3.4.

**Definition 4.4.1** (Decomposition of  $\mathbb{R}^n$  for odd  $n$ ). *We decompose  $\mathbb{R}^n$  as the orthogonal direct sum*

$$\mathbb{R}^n = \Delta \oplus \bigoplus_{0 \leq k < \lfloor \frac{n}{2} \rfloor} \mathcal{E}_n^k.$$

with  $\Delta := \langle (1)_{0 \leq i < n} \rangle$  and

$$\mathcal{E}_n^k := \left\langle \left( \cos\left(\frac{2i(2k+1)\pi}{n}\right) \right)_{0 \leq i < n}, \left( \sin\left(\frac{2i(2k+1)\pi}{n}\right) \right)_{0 \leq i < n} \right\rangle = \left\langle \left( e^{i\frac{2i(2k+1)\pi}{n}} \right)_{0 \leq i < n} \right\rangle.$$

Given a Sub Rosa-like substitution  $\sigma$  with expansion  $\varphi$  and edge word  $\Sigma$  we have:

**Proposition 4.4.1** (Expansion matrix of  $\varphi$  for odd  $n$ ).  *$\varphi$  is a circulant linear application of the form*

$$\varphi_n = \begin{pmatrix} m_0 & m_{n-1} & \dots & m_1 \\ m_1 & m_0 & \dots & m_2 \\ \vdots & \ddots & \ddots & \vdots \\ m_{n-1} & m_{n-2} & \dots & m_0 \end{pmatrix},$$

$$\text{with } \forall i \in \{0, 1, \dots, \lfloor \frac{n}{2} \rfloor - 1\}, m_{i \lfloor \frac{n}{2} \rfloor} = (-1)^i [\Sigma]_i, \\ \text{and } m_{-(i+1) \lfloor \frac{n}{2} \rfloor} = (-1)^{i+1} [\Sigma]_i.$$

**Definition 4.4.2** (The eigenvalue matrix for odd  $n$ ). *Let us define the matrix*

$$N_n := \left( 2 \cos\left(\frac{(2i+1)(2j+1)\pi}{2n}\right) \right)_{0 \leq i, j < \lfloor \frac{n}{2} \rfloor}.$$

**Proposition 4.4.2** (Eigenvalues of Sub Rosa-like expansions for odd  $n$ ).  
*The Sub Rosa-like expansion  $\varphi$  of edge word  $\Sigma$  admits the spaces  $\mathcal{E}_n^j$  for  $0 \leq j < \lfloor \frac{n}{2} \rfloor$  and  $\Delta$  as eigenspaces. We denote by  $\lambda_j$  its eigenvalue on eigenspace  $\mathcal{E}_n^j$  and  $\lambda_\Delta$  on  $\Delta$ . We note  $|\lambda|$  the vector of modules of the eigenvalues  $\lambda_j$ . We have  $\lambda_\Delta = 0$  and*

$$|[\Sigma] \cdot N_n| = |\lambda|.$$

*More precisely we have*

$$\lambda_j = \left( \sum_{i=0}^{\lfloor \frac{n}{2} \rfloor - 1} [\Sigma]_i 2 \cos \left( \frac{(2j+1)(2i+1)\pi}{2n} \right) \right) e^{-i \frac{(2j+1)\pi}{2n}}.$$

#### 4.4.2 Choosing the edge word

Recall that here  $n$  is a fixed odd integer. The important thing for planarity is the abelianized edge word  $[\Sigma]$  and actually mostly the rhombus frequencies.

**Definition 4.4.3** (Optimal rhombus frequency vector for odd  $n$ ). *Let us define the optimal rhombus frequency vector  $\tilde{\gamma}$  as*

$$\tilde{\gamma} := \frac{\gamma}{2\|\gamma\|^2} \quad \text{with} \quad \gamma := \left( \cos\left(\frac{(2i+1)\pi}{2n}\right) \right)_{0 \leq i < \lfloor \frac{n}{2} \rfloor}.$$

We call this vector the *optimal rhombus frequency vector* because we have:

**Lemma 4.4.1.** *With the eigenvalue matrix  $N_n$  and the optimal rhombus frequency vector  $\tilde{\gamma}$  we have*

$$\tilde{\gamma} \cdot N_n = (1, 0, \dots, 0)$$

*Proof.* Remark that  $2\gamma$  is the first line of  $N_n$ . The idea is that  $N_n$  is very similar to a Discrete Cosine Transform matrix and is orthogonal (up to renormalization). The fact that DCT is orthogonal is a classical result and we will not give a full proof.  $\square$

From this we get the following result

**Lemma 4.4.2** (Approximating the optimal rhombus frequency for odd  $n$ ).  
*There exists  $\varepsilon > 0$  such that for any  $x \in ]2, +\infty[$  and any Sub Rosa-like substitution  $\sigma$  of edge word  $\Sigma$  and eigenvalues  $\lambda_j$  we have*

$$d([\Sigma], x\tilde{\gamma}) < \varepsilon \implies \begin{cases} |\lambda_0| > 1 \\ |\lambda_1| < 1 \\ \vdots \\ |\lambda_{\lfloor \frac{n}{2} \rfloor - 1}| < 1 \end{cases} \implies \sigma \text{ is planar of slope } \mathcal{E}_n^0.$$

*Proof.* The first step is a combination of the uniform continuity of the vector-matrix product together with  $x > 2$  and

$$x\tilde{\gamma} \cdot N_n = (x, 0, 0 \dots, 0).$$

Indeed by uniform continuity there is an  $\varepsilon > 0$  such that

$$d([\Sigma], x\tilde{\gamma}) < \varepsilon \implies d([\Sigma] \cdot N_n, x\tilde{\gamma} \cdot N_n) < 1.$$

Which can be reformulated with Proposition 4.4.2 and Lemma 4.4.1 as

$$d([\Sigma], x\tilde{\gamma}) < \varepsilon \implies \begin{cases} |\lambda_0| > 1 \\ |\lambda_1| < 1 \\ \vdots \\ |\lambda_{\lfloor \frac{n}{2} \rfloor - 1}| < 1 \end{cases}.$$

And with Proposition 3.3.4 we can conclude to the planarity of  $\sigma$ . □

This means that if  $[\Sigma]$ , as a point in  $\mathbb{Z}^{\lfloor \frac{n}{2} \rfloor}$ , is close enough to the line  $\langle \gamma \rangle$  then the associated Sub Rosa-like substitution  $\sigma$  is planar.

We will now define a sequence of edge words  $(\Sigma_{(j)})_{j \in \mathbb{N}}$  such that  $[\Sigma_{(j)}]$  is infinitely often arbitrarily close to the line  $\langle \gamma \rangle$ . To approximate  $\langle \gamma \rangle$  we use the billiard word of direction  $\gamma$ , for more background on billiard words see [AMST94].

**Definition 4.4.4** (Definition of the sequence of edge words for odd  $n$ ). *Let  $\Gamma$  be the line  $\langle \gamma \rangle = \{t\gamma, t \in \mathbb{R}\}$  and  $\Gamma_{\frac{1}{2}}$  be the line  $\langle \gamma \rangle + (\frac{1}{2}, \dots, \frac{1}{2})$ .*

1. Let  $\omega$  be the one-way-infinite billiard word of line  $\Gamma_{\frac{1}{2}}$  starting on  $(\frac{1}{2}, \dots, \frac{1}{2})$ , this means that we build the bi-infinite word  $\omega$  by travelling the line and adding a letter  $2i + 1$  each time it crosses an hyperplane of type  $H_{i,k}$  with

$$H_{i,k} := \{x \in \mathbb{R}^{\lfloor \frac{n}{2} \rfloor} \mid \langle x | \vec{e}_i \rangle = k\},$$

with  $k \in \mathbb{N}$  and  $\vec{e}_i$  a vector of the canonical basis of  $\mathbb{R}^{\lfloor \frac{n}{2} \rfloor}$ . Let us stress that when the line crosses an hyperplane of normal  $\vec{e}_i$  we add a letter  $2i+1$  instead of the classical letter  $i$ , indeed the letters of  $\omega$  will represent rhombuses on the boundary of the substitution's metatiles, and in that case the rhombuses are bisected by the metatile's edge through their odd angles.

2. We define the sequence of edge words as  $(\Sigma_{(j)})_{j \in \mathbb{N}}$  as

$$\Sigma_{(j)} := \text{pref}_j(\omega) \overline{\text{pref}_j(\omega)},$$

where  $\text{pref}_j(\omega)$  is the prefix of length  $j$  of  $\omega$ , and  $\overline{\text{pref}_j(\omega)}$  is its mirror image.

3. We define the sequence of Sub Rosa-like pseudosubstitutions  $(\sigma_{(j)})_{j \in \mathbb{N}}$  where  $\sigma_{(j)}$  is the pseudosubstitution of edge words  $\Sigma_{(j)}$ . We denote by  $\varphi_{(j)}$  the expansion associated to  $\sigma_{(j)}$ .

The main result of this section is the fact that in this sequence  $(\sigma_{(j)})_{j \in \mathbb{N}}$  there are primitive planar substitutions.

**Proposition 4.4.3.** *There exists  $j$  such that  $\sigma_{(j)}$  is a primitive planar substitution of slope  $\mathcal{E}_n^0$ .*

We call the smallest such substitution Planar Rosa substitution.

**Definition 4.4.5** (The Planar Rosa substitution for odd  $n$ ). *The Planar Rosa substitution  $\sigma'_n$  is defined as  $\sigma'_n = \sigma_{(j_0)}$  with*

$$j_0 = \min\{j \in \mathbb{N} \mid \varphi_{(j)} \text{ is planar of slope } \mathcal{E}_n^0 \text{ and } \sigma_{(j)} \text{ is a primitive substitution}\}.$$

We cut this proposition in three lemmas:

**Lemma 4.4.3** (Planarity of  $\sigma_{(j)}$  for odd  $n$ ).

$$\exists^\infty j \in \mathbb{N}, \varphi_{(j)} \text{ is planar of slope } \mathcal{E}_n^0.$$

**Lemma 4.4.4** (Tileability of  $\sigma_{(j)}$  for odd  $n$ ).

$$\exists N_0 \in \mathbb{N}, \forall j \geq N_0, \sigma_{(j)} \text{ is a substitution,}$$

i.e. the metatiles defined by the edge word  $\Sigma_{(j)}$  are tileable.

**Lemma 4.4.5** ( Primitivity of  $\sigma_{(j)}$  for odd  $n$ ).

$$\exists N_1 \in \mathbb{N}, \forall j \geq N_1, \text{ if } \sigma_{(j)} \text{ is a substitution then it is primitive.}$$

We will prove these three lemmas in the next three Subsections. Note that the definition of Planar Rosa substitution implies the second part of Theorem 2 (planarity of the substitution tilings) for odd  $n$  i.e. the fact that Planar Rosa tilings are substitution discrete planes with local  $n$ -fold rotational symmetry. The first part of Theorem 2 (i.e. the regular fixpoint tiling) for odd  $n$  is proved in Section 4.4.6.

### 4.4.3 Proof of Lemma 4.4.3 (planarity)

In this subsection we prove Lemma 4.4.3. For the proof of planarity of  $\sigma_{(j)}$  we introduce the discrete billiard line  $(p_i)_{i \in \mathbb{N}}$ :

**Definition 4.4.6** (Billiard line). Let  $(p_i)_{i \in \mathbb{N}}$  be the sequence of points of  $\mathbb{Z}^{\lfloor \frac{n}{2} \rfloor}$  associated to the billiard word  $\omega$  with  $p_0 = 0$ . This means that for all  $j$ ,

$$\omega_j = 2i + 1 \quad \implies \quad p_{j+1} - p_j = \vec{e}_i.$$

The choice of having the word  $\omega$  and the sequence of points  $(p_i)_{i \in \mathbb{N}}$  be associated to the line  $\Gamma_{\frac{1}{2}}$  instead of the line  $\Gamma$  is motivated by the fact that the exact sequence of rhombus  $\omega$  appears in the De Bruijn multigrid tiling  $P_n(\frac{1}{2})$  and we will use it in Subsection 4.4.4 to prove the tileability of metatiles.

Remark that the definition of  $\Sigma_{(j)}$  ensures that it is a palindromic word and that  $[\Sigma_{(j)}] = 2p_j$ .

**Proposition 4.4.4.** The sequence  $(p_i)_{i \in \mathbb{N}}$  approximates the line  $\Gamma$ , which means that for any positive  $\varepsilon$  there are infinitely many points  $p_i$  that are  $\varepsilon$ -close to the line  $\Gamma$

$$\forall \varepsilon > 0, \exists^\infty i > 0, d(p_i, \Gamma) < \varepsilon.$$

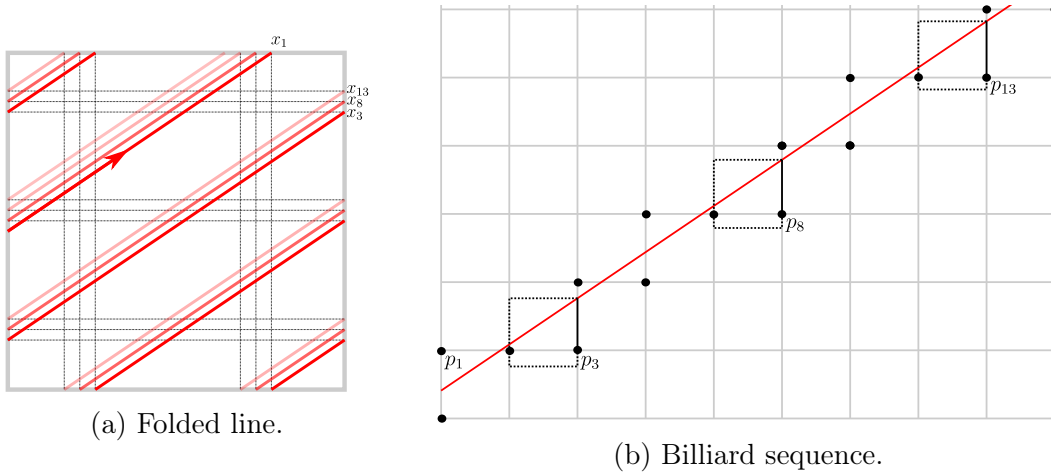


Figure 4.8: Ideas for the proof of Theorem 15.

**Corollary 4.4.1.** *The sequence  $([\Sigma_{(i)}])_{i \in \mathbb{N}}$  approximates the line  $\Gamma$ , which means that for any positive  $\varepsilon$  there are infinitely many abelianized edge word  $[\Sigma_{(i)}]$  that are  $\varepsilon$ -close to the line  $\Gamma$*

$$\forall \varepsilon > 0, \exists^\infty i > 0, d([\Sigma_{(i)}], \Gamma) < \varepsilon.$$

The corollary is just a rewriting of the fact that by definition  $[\Sigma_{(j)}] = 2p_j$ .

There are several ways we could present this proposition. We could use a linear flow approach based on [HK03] (Part 1, chapter 5) or we could use a cut-and-project approach by rewriting Theorem 7.2 of [BG13] with the formalism of [Har04] as:

**Theorem 14.** *Let  $\Lambda$  be a canonical cut and project set with the cut-and-project scheme  $(\mathcal{V}, \mathcal{W}, \mathcal{R}, \mathbb{Z}^n)$  where  $\mathcal{V} \oplus \mathcal{W} \oplus \mathcal{R} = \mathbb{R}^n$ . Let  $(x_i)_{i \in \mathbb{N}}$  be an exhaustive sequence of the points of  $\Lambda$  ordered by increasing norm i.e.  $\Lambda = \{x_i, i \in \mathbb{N}\}$  and  $\forall i, \|x_{i+1}\| \geq \|x_i\|$ . Then the sequence  $(\pi_{\mathcal{V}^\perp}(x_i))_{i \in \mathbb{N}}$  is uniformly distributed in the window  $\Omega$ .*

But we use a known result on billiard words and discrete lines.

**Theorem 15 (folk.).** *Let  $(p_i)_{i \in \mathbb{N}}$  be a billiard sequence of line  $\Gamma$  and  $\pi$  be the orthogonal projection onto  $\Gamma^\perp$ . Every projected point  $\pi(p_i)$  is an accumulation point of the projected sequence  $(\pi(p_i))_{i \in \mathbb{N}}$ .*



*Proof.* The idea is to first consider the folded line  $\Gamma$  in the torus as seen in Figure 4.8a, and consider the sequence  $(x_i)_{i \in \mathbb{N}}$  of the intersection points of  $\Gamma$  with the boundary of the torus. This sequence has the property that each of its points is an accumulation point of the sequence, this can be proved by Poincaré Recurrence Theorem applied to the translation  $\Gamma(t, x)$  in the torus. Then we only need remark that the sequence  $(\pi(p_i))$  and  $(x_i)$  very similar: if there are two points  $x_{i_1}$  and  $x_{i_2}$  that are on the same hyper-facet of the torus and that are  $\varepsilon$ -close, then the corresponding  $\pi(p_{i_1})$  and  $\pi(p_{i_2})$  are also  $\varepsilon$ -close as is illustrated with points  $x_3, x_8, x_{13}$  and  $p_3, p_8, p_{13}$  in Figure 4.8. The result follows.  $\square$

Combining Corollary 4.4.1 and Lemma 4.4.2 we get Lemma 4.4.3

#### 4.4.4 Proof of Lemma 4.4.4 (tileability)

In this subsection we prove Lemma 4.4.4:  $n$  is a fixed integer and we prove that for the sequence of pseudosubstitutions  $(\sigma_{(j)})_{j \in \mathbb{N}}$  defined by their edge word  $\Sigma_{(j)}$  there exists an integer  $N_0$  such that for any  $j \geq N_0$ ,  $\sigma_{(j)}$  is a substitution *i.e.* the metatiles defined by the pseudosubstitution are tileable.

Let us recall that  $\Sigma_{(j)}$  is defined as

$$\Sigma_{(j)} := \overline{pref_j(\omega)pref_j(\omega)},$$

where  $\omega$  is the billiard word of direction  $\gamma$ . This means that the corners of metatiles have  $v = pref_j(\omega)$  on both sides as shown in Figure 4.9.

Let us fix  $j$ , with the counting functions  $f_i(x)$  of the edge word  $\Sigma_{(j)}$  as defined in Section 4.3 we can apply Proposition 4.3.1 which means that if we have :

- $\Sigma_{(j)}$  is 2-almost-balanced (Definition 4.3.2 page 107)
- for any odd  $i_1 < i_2$  and any position  $x_1$  such that at position  $x_1$  in the edge word  $\Sigma_{(j)}$  there is a rhombus  $i_1$  we have

$$f_{|i_2-2|}^{-1} \circ f_{i_2}(x_1) < f_{|i_1-2|}^{-1} \circ f_{i_1}(x_1),$$

then the metatiles defined by edge word  $\Sigma_{(j)}$  are tileable which means that  $\sigma_{(j)}$  is a substitution.

**Lemma 4.4.6** (The edge word are 2-almost-balanced). *For any  $j$  the edge word  $\Sigma_{(j)}$  is 2-almost-balanced.*

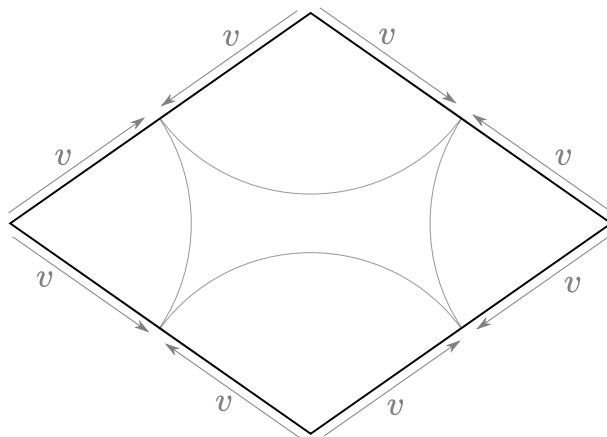


Figure 4.9: Sketch of the metatile with  $v = \text{pref}_j(\omega)$  for some  $j$ .

*Proof.* Recall that 2-almost-balancedness is that for any letters  $i_1 < i_2$  and any factor subword  $v$  of  $\Sigma_{(j)}$  we have  $|v|_{i_1} - |v|_{i_2} > -2$ . This is a direct consequence of the fact that  $\omega$  is a billiard word so it is 1-almost-balanced and that any factor subword  $v$  of  $\Sigma_{(j)}$  can be decomposed of as  $v = v_0 \cdot v_1$  with  $v_0$  a factor of  $\omega$  and  $v_1$  the mirror image of a factor of  $\omega$ .

Remark that n-almost-balancedness takes only one factor at a time (as a difference to the usual balancedness on word which takes two factors and counts the difference of number of a letter on these two factors), so it works well with projection on a subset of letters. And we can see the 1-almost-balancedness of general billiard word as a consequence of the 1-almost-balancedness of 2-letters billiard words *i.e.* Sturmian words. The 1-almost-balancedness of Sturmian words derives from the fact that they are 1-balanced (in the usual sense).  $\square$

So for the tileability of metatiles we now need only to prove the second item: the inequality on the counting functions. And for that we will split it in two: the first half of the edge word (position  $x_1 < j$ ) and the second half (position  $x_1 \geq j$ ).

### The first half: the corner

Here we look at the case  $x_1 < j$ .

The key point is that if the inequality

$$f_{|i_2-2|}^{-1} \circ f_{i_2}(x_1) < f_{|i_1-2|}^{-1} \circ f_{i_1}(x_1),$$

were broken for  $x_1 \leq j$  and with position  $x_1$  such that in the edge word there is a rhombus  $i_1$  at position  $x_1$  then the full cone of angle  $\frac{\pi}{n}$  and edge words  $\omega$  would not be tileable.

We denote by  $\tilde{f}_i(x)$  the counting function for the infinite edge word  $\omega$ . We have by definition  $\tilde{f}_i(x) = f_i(x)$  for any  $x < j$ . And assuming that the infinite cone is tileable then  $\tilde{f}_{|i-2|}^{-1} \circ \tilde{f}_i(x) \leq x$  so we actually have  $f_{|i-2|}^{-1} \circ f_i(x) = \tilde{f}_{|i-2|}^{-1} \circ \tilde{f}_i(x)$ .

So we if the inequality is broken in the first half of the edge word and the cone is tileable then we also break the inequality of the counting function of the infinite cone which is impossible because it is tileable.

**Lemma 4.4.7** (The infinite cone is tileable). *The infinite cone of angle  $\frac{\pi}{n}$  and edge words  $\omega$  is tileable.*

*Proof.* This is due to the fact that the cone appears in the multigrid dual tiling  $P_n(\frac{1}{2})$  which is a rhombus tiling as stated in Theorem 3 and proved in Chapter 5. Let us now prove that the infinite cone indeed appears in  $P_n(\frac{1}{2})$ .

In order to prove this we look at the vertical half line  $i\mathbb{R}^+$  in  $P_n(\frac{1}{2})$ , in the multigrid  $G_n(\frac{1}{2})$  on the vertical half line we have a succession of intersection points which correspond in the dual tiling to a succession of rhombuses which turns out to be exactly  $\omega$ .

The exact position of the intersection points of the line  $\Gamma_{\frac{1}{2}}$  with some hyperplane  $H_{i,k} = \{x \in \mathbb{R}^{\lfloor \frac{n}{2} \rfloor} \mid \langle x | \vec{e}_i \rangle = k\}$  is

$$\Gamma_{\frac{1}{2}} \cap H_{i,k} = \left(\frac{1}{2}, \dots, \frac{1}{2}\right) + \frac{k - \frac{1}{2}}{\cos\left(\frac{(2i+1)\pi}{2n}\right)} \gamma.$$

This comes from the fact that the  $i^{\text{th}}$  coordinate of vector  $\gamma$  is  $\gamma_i = \cos\left(\frac{(2i+1)\pi}{2n}\right)$  and that the vector from  $(\frac{1}{2}, \dots, \frac{1}{2})$  to  $H_{i,k}$  is  $(k - \frac{1}{2})\vec{e}_i$ .

And in  $P_n(\frac{1}{2})$  a rhombus of angle  $\frac{(2i+1)\pi}{n}$  on the vertical half-line corresponds in the multigrid  $G_n(\frac{1}{2})$  to an intersection of the grids of orientation  $\zeta^{i'}$  and  $\zeta^{n-i'}$  for  $i' = \frac{n-(2i+1)}{2}$ ,  $H(\zeta^{i'}, \frac{1}{2}) \cap H(\zeta^{n-i'}, \frac{1}{2})$  where  $\zeta = e^{i\frac{\pi}{2n}}$  and these intersection points are exactly at positions  $I_i$  on the vertical half-line with

$$I_i := \left\{ \frac{k - \frac{1}{2}}{\cos\left(\frac{(2i+1)\pi}{n}\right)}, k \in \mathbb{N} \right\}.$$

Overall the succession of letters in the billiard word  $\omega$  and the succession of rhombuses on the vertical half-line in  $P_n(\frac{1}{2})$  are the same.

By  $2n$ -fold rotational symmetry of  $P_n(\frac{1}{2})$  there is the same sequence of rhombuses on the rotated half-line  $ie^{i\frac{\pi}{n}}\mathbb{R}^+$ , so we have an infinite cone of angle  $\frac{\pi}{n}$  with edge word  $\omega$  on both sides in  $P_n(\frac{1}{2})$ . □

Overall the inequality

$$f_{|i_2-2|}^{-1} \circ f_{i_2}(x_1) < f_{|i_1-2|}^{-1} \circ f_{i_1}(x_1),$$

holds for any  $i_1 < i_2$  and any  $x_1 < j$  such that there is a rhombus  $i_1$  at position  $x_1$  in the edge word  $\Sigma_{(j)}$ .

We now have to look at the second half of the edge word, and here things get tricky.

### The second half: the middle

Here the idea is to look at the a new function  $g_{i_1, i_2}(x)$  with  $i_1 < i_2$  defined as

$$g_{i_1, i_2}(x) := f_{|i_1-2|}^{-1} \circ f_{i_1}(x) - f_{|i_2-2|}^{-1} \circ f_{i_2}(x).$$

The tilability of the metatiles of edge word  $\Sigma_{(j)}$  is now reduced to  $g_{i_1, i_2}(x) > 0$  for any  $x \geq j$  such that at there is a rhombus of type  $i_1$  on position  $x$  in  $\Sigma_{(j)}$ .

The idea is that since the frequency of apparition of  $i_1$  in the word  $\omega$  (and in the word  $\Sigma_{(j)}$ ) is strictly bigger than the frequency of apparition of  $i_2$  the idea is that  $g_{i_1, i_2}(x)$  has a general increasing trend and (if  $\Sigma_{(j)}$  is long enough) there is a  $N_0$  such that for any  $x > N_0$ ,  $g_{i_1, i_2}(x) > 0$ .

Once we get that we only need to take  $j > N_0$  and then the metatiles defined by  $\Sigma_{(j)}$  are tileable because the for any  $x \geq j > N_0$  we have  $g_{i_1, i_2}(x) > 0$ .

Now for the positivity of  $g_{i_1, i_2}(x)$ . Let us recall that by construction of  $\omega$  we have  $\tilde{f}_{2k+1}(x) \approx x \frac{\gamma_k}{\|\gamma\|}$  and by definition of  $\Sigma_{(j)}$  there is a  $\delta$  only dependent on the dimension  $n$  such that  $|f_{2k+1}(x) - x \frac{\gamma_k}{\|\gamma\|}| < \delta$  for any  $k$  and  $x$ . For example  $\delta = 2\sqrt{n}$  works. This means that

$$\left| g_{i_1, i_2}(x) - x \left( \frac{\gamma_{i_1}'}{\gamma_{i_1}''} - \frac{\gamma_{i_2}'}{\gamma_{i_2}''} \right) \right| < 2\delta + \frac{\delta \|\gamma\|}{\gamma_{i_1}''} + \frac{\delta \|\gamma\|}{\gamma_{i_2}''},$$

with  $i'_1 = \lfloor \frac{i_1}{2} \rfloor$ ,  $i''_1 = |i'_1 - 2|$ ,  $i'_2 = \lfloor \frac{i_2}{2} \rfloor$ ,  $i''_2 = |i'_2 - 2|$ . Remark that with

$$\gamma = \left( \cos\left(\frac{(2i+1)\pi}{2n}\right) \right)_{0 \leq i < \lfloor \frac{n}{2} \rfloor},$$

we have that  $\frac{\gamma_{i'_1}}{\gamma_{i''_1}} - \frac{\gamma_{i'_2}}{\gamma_{i''_2}} > 0$  for  $i_1 < i_2$ . Which means that for

$$x > \frac{2\delta + \frac{\delta\|\gamma\|}{\gamma_{i''_1}} + \frac{\delta\|\gamma\|}{\gamma_{i''_2}}}{\frac{\gamma_{i'_1}}{\gamma_{i''_1}} - \frac{\gamma_{i'_2}}{\gamma_{i''_2}}},$$

we have  $g_{i_1, i_2}(x) > 0$  (and this bound is finite).

Now take

$$N_0 := \max_{i_1 < i_2} \left( \frac{2\delta + \frac{\delta\|\gamma\|}{\gamma_{i''_1}} + \frac{\delta\|\gamma\|}{\gamma_{i''_2}}}{\frac{\gamma_{i'_1}}{\gamma_{i''_1}} - \frac{\gamma_{i'_2}}{\gamma_{i''_2}}} \right).$$

For any  $x > N_0$  and any  $i_1 < i_2$  we have  $g_{i_1, i_2}(x) > 0$ .

Overall for any  $j > N_0$  the metatiles defined by the edge word  $\Sigma_{(j)}$  are tileable which means that  $\sigma_{(j)}$  is a substitution.

#### 4.4.5 Proof of Lemma 4.4.5 (primitivity)

In this subsection we prove Lemma 4.4.5, recall that  $n$  is a fixed odd integer.

Let  $N_1$  be the index of the first occurrence of the rhombus on angle  $\frac{(n-2)\pi}{n}$  in the word  $\omega$ . For any  $j \geq N_1$  the pseudosubstitution  $\sigma_{(j)}$  is primitive (if it is a substitution). Remark that here we are only interested in the primitivity of  $\sigma_{(j)}$  if it is a substitution and not in the tileability of the metatiles.

Let us fix some  $j \geq N_1$ , by definition on  $\omega$  and of  $\Sigma_{(j)}$ ,  $\Sigma_{(j)}$  contains all the types of rhombuses *i.e.* all the rhombus with odd angle  $2i + 1$  bisected by the edge. So for a tile  $t$ , on the boundary of  $\sigma_{(j)}(t)$  there are every type of rhombus in two orientations (because there are two edges orientation on a rhombus tile). Now if we look at the tiles of the boundary of  $\sigma_{(j)}^2(t)$  we have every type of rhombus in every orientation as shown in Figure 4.10, because on the boundary rhombuses of  $\sigma_{(j)}(t)$  there are all the edge orientations.

So for  $j \geq N_1$ ,  $\sigma_{(j)}$  is primitive of order at most 2 (if it is a substitution).

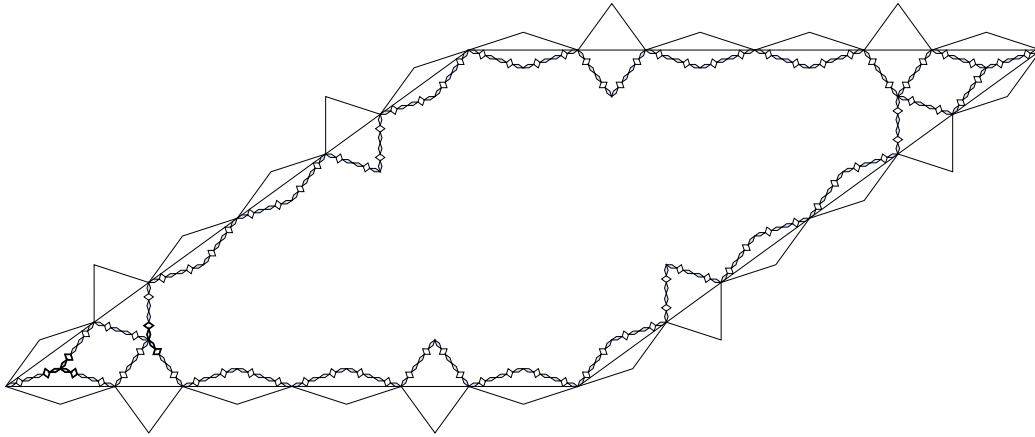


Figure 4.10: Primitivity of  $\sigma_{(j)}$  for  $n = 5$  and  $j = 3$ .

This then concludes the proof of Proposition 4.4.3 which implies that the Planar Rosa substitutions are well defined.

Note that actually the Planar Rosa substitutions are primitive of order 1 but the proof is quite tricky, for even  $n$  we give in Subsection a proof from which we can derive a proof of primitivity of order 1 for Planar Rosa for odd  $n$ .

#### 4.4.6 Regular fixpoint tiling

Here we complete the proof of Theorem 2 for odd  $n$ . The one thing to prove is that the star  $S(n)$  is indeed a regular seed for  $\sigma'_n$ .

The fact that  $S(n)$  is a seed is straightforward, indeed in the definition of  $\sigma'_n$  we have the fact that on the edges of the metatiles there is a sequence of bisected rhombuses starting by a bisected rhombus of angle  $\frac{\pi}{n}$ . This means that in the  $\frac{\pi}{n}$  angle of the metatiles we have two rhombuses of angle  $\frac{\pi}{n}$  (which overlap out of the metatiles) can be seen in Figure 4.10. From that we immediately get that at the centre of  $\sigma'_n(S(n))$  we have  $S(n)$ , hence it is a seed.

Regularity is a bit more tricky because we have no exact description of the tiles. What we show is that for any prototile  $t$ ,  $S(n)$  appears in  $\sigma_n'^n(t)$  for any tile  $t$ . The idea is that for any tile  $t$  there is an interior vertex in  $\sigma_n'(t)$ , around this vertex are at least three tiles of angles  $\frac{k_0\pi}{n}$ ,  $\frac{k_1\pi}{n}$  and  $\frac{k_2\pi}{n}$  with  $1 \leq k_0, k_1, k_2 \leq n - 1$ . And in the  $k$ th image of an angle  $\frac{k\pi}{n}$  there is a

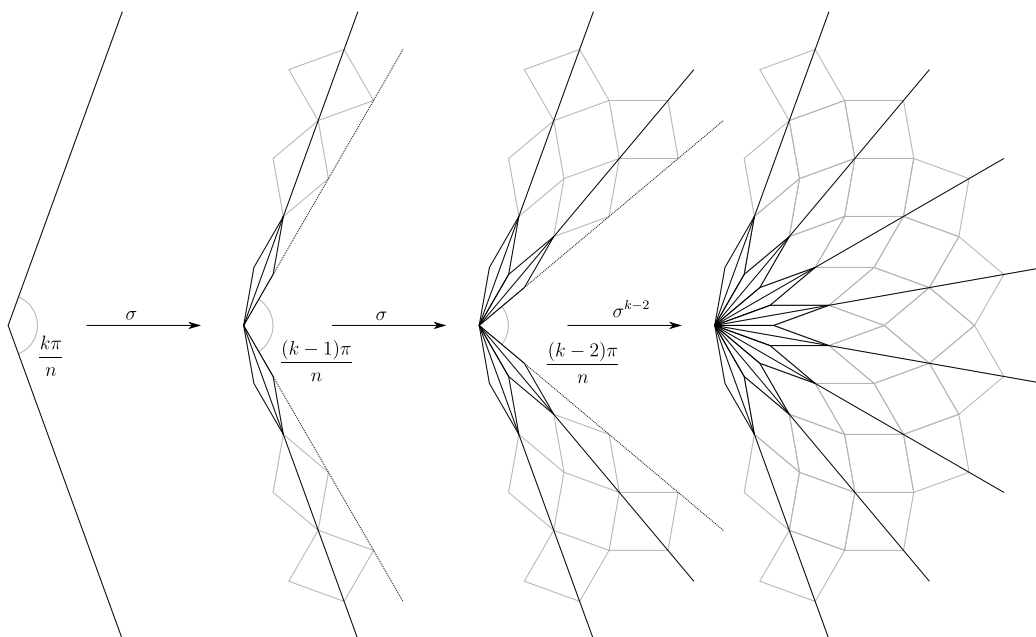


Figure 4.11: Corners of metatiles.

portion of the star  $S(n)$  as shown in Figure 4.11. So in  $\sigma'_n{}^{\max(k_0, k_1, k_2)}(\sigma'_n(t))$  there is the star  $S(n)$ , since  $\max(k_0, k_1, k_2) \leq n - 1$  and  $S(n) \subset \sigma'_n(S(n))$  then  $\text{starn} \subset \sigma'_n{}^n(t)$ , hence  $S(n)$  is a regular seed for  $\sigma'_n$ . This concludes the proof of Theorem 2 for odd  $n$ .

## 4.5 Construction for even $n$

The construction for even  $n$  is very similar to the one for odd  $n$ , much as it was for the Sub Rosa substitutions. We will here mostly just state the definitions and propositions. The only thing that is very different is the proof of the primitivity of Planar Rosa substitutions.

### 4.5.1 Lifting and eigenvalues

Sub Rosa-like substitutions for even  $n$  are lifted exactly as the Sub Rosa substitutions in Chapter 3.

Sub Rosa-like substitutions are defined as having the same sequence of rhombuses and edges on the edges of the metatiles (up to translation and

rotation). In particular this means as seen in Section 3.3 that Sub Rosa-like expansions  $\varphi$  are lifted to linear applications of  $\mathbb{Z}^n$ .

**Definition 4.5.1** (Decomposition of  $\mathbb{R}^n$  for even  $n$ ). *We decompose  $\mathbb{R}^n$  as the orthogonal direct sum*

$$\mathbb{R}^n = \bigoplus_{0 \leq k < \frac{n}{2}} \mathcal{E}_n^k,$$

$$\mathcal{E}_n^k := \left\langle \left( \cos\left(\frac{i(2k+1)\pi}{n}\right) \right)_{0 \leq i < n}, \left( \sin\left(\frac{i(2k+1)\pi}{n}\right) \right)_{0 \leq i < n} \right\rangle = \left\langle \left( e^{i\frac{i(2k+1)\pi}{n}} \right)_{0 \leq i < n} \right\rangle.$$

**Proposition 4.5.1** (Sub Rosa-like expansion matrix for even  $n$ ). *For even  $n$ , the Sub Rosa-like expansion  $\varphi$  of edge word  $\Sigma$  is a pseudo-circulant linear application of the form*

$$\varphi_n = \begin{pmatrix} m_0 & -m_{n-1} & \dots & -m_1 \\ m_1 & m_0 & \dots & -m_2 \\ \vdots & \ddots & \ddots & \vdots \\ m_{n-1} & m_{n-2} & \dots & m_0 \end{pmatrix},$$

$$\begin{aligned} &\text{with } \forall i \in \{0, \dots, \frac{n}{2}\}, m_i = [\Sigma]_i, \\ &\text{and } \forall i \in \{1, \dots, < \frac{n}{2}\}, m_{n-i} = -[\Sigma]_i. \end{aligned}$$

**Definition 4.5.2** (The eigenvalue matrix for even  $n$ ). *Let us define the matrix*

$$N_n := \left( c_i \cos\left(\frac{i(2j+1)\pi}{n}\right) \right)_{0 \leq i, j < \frac{n}{2}} \quad \text{with } c_i = \begin{cases} 1 & \text{when } i = 0 \\ 2 & \text{otherwise} \end{cases}.$$

**Proposition 4.5.2** (Eigenvalues of Sub Rosa-like expansions for even  $n$ ). *For even  $n$ , the Sub Rosa-like expansion  $\varphi$  of edge word  $\Sigma$  admits the spaces  $\mathcal{E}_n^j$  for  $0 \leq j < \frac{n}{2}$  as eigenspaces. We denote by  $\lambda_j$  the eigenvalue of  $\varphi$  on eigenspace  $\mathcal{E}_n^j$ . We note  $\lambda$  the vector of the eigenvalues. We have*

$$[\Sigma] \cdot N_n = \lambda,$$

which we can reformulate as

$$\lambda_j = [\Sigma]_0 + \sum_{1 \leq i < \frac{n}{2}} [\Sigma]_i 2 \cos\left(\frac{i(2j+1)\pi}{n}\right).$$



## 4.5.2 Choosing the edge word

The idea here is the same as in the odd case, we define an optimal rhombus frequency vector  $\gamma$  and its associated infinite billiard word  $\omega$ . From this we define a sequence of longer and longer edge words as  $\overline{pref_j(\omega)pref_j(\omega)}$  and we prove that in this sequence there is an edge word which defines a primitive substitution which is planar for slope  $\mathcal{E}_n^0$ . We call Planar Rosa substitution  $\sigma'_n$  the substitution induced by the smallest suitable edge word.

Recall that here  $n$  is a fixed even integer. And that the important thing for planarity is the abelianized edge word  $[\Sigma]$  and actually mostly the rhombus frequencies.

**Definition 4.5.3** (Optimal rhombus frequency vector for even  $n$ ). *Let us define the optimal rhombus frequency vector  $\tilde{\gamma}$  as*

$$\tilde{\gamma} := \frac{2\gamma}{n} \quad \text{with} \quad \gamma := \left( \cos\left(\frac{i\pi}{n}\right) \right)_{0 \leq i < \frac{n}{2}}.$$

We call this vector the optimal rhombus frequency vector because of the two following lemmas:

**Lemma 4.5.1.** *With the eigenvalue matrix  $N_n$  and the optimal rhombus frequency vector  $\tilde{\gamma}$  we have*

$$\tilde{\gamma} \cdot N_n = (1, 0, \dots, 0).$$

*Proof.* Remark that  $\gamma$  is very similar to the first column of  $N_n$ , the only difference are the coefficients  $c_i$ . The idea is that  $N_n$  is very similar to a Discrete Cosine Transform matrix and is orthogonal (up to renormalization). We will not give a full proof.  $\square$

**Lemma 4.5.2** (Approximating the optimal rhombus frequency for even  $n$ ). *There exists  $\varepsilon > 0$  such that for any  $x \in ]2, +\infty[$  and any Sub Rosa-like substitution  $\sigma$  of edge word  $\Sigma$  and eigenvalues  $\lambda_j$  we have*

$$d([\Sigma], x\tilde{\gamma}) < \varepsilon \implies \begin{cases} |\lambda_0| > 1 \\ |\lambda_1| < 1 \\ \vdots \\ |\lambda_{\frac{n}{2}-1}| < 1 \end{cases} \implies \sigma \text{ is planar of slope } \mathcal{E}_n^0.$$

The proof is the same as for odd  $n$ .

As in the case of odd  $n$ , we will now define a sequence of edge words  $(\Sigma_{(j)})_{j \in \mathbb{N}}$  such that  $[\Sigma_{(j)}]$  is infinitely often arbitrarily close to the line  $\langle \gamma \rangle$ . To approximate  $\langle \gamma \rangle$  we use the billiard word of direction  $\gamma$ , for more background on billiard words see [AMST94].

**Definition 4.5.4** (Definition of the sequence of edge words for even  $n$ ). *Let  $\Gamma$  be the line  $\langle \gamma \rangle = \{t\gamma, t \in \mathbb{R}\}$  and  $\Gamma_{\frac{1}{2}}$  be the line  $\langle \gamma \rangle + (\frac{1}{2}, \dots, \frac{1}{2})$ .*

1. *Let  $\omega$  be the one-way-infinite billiard word of line  $\Gamma_{\frac{1}{2}}$  starting on  $(\frac{1}{2}, \dots, \frac{1}{2})$ , this means that we build the bi-infinite word  $\omega$  by travelling the line and adding a letter  $2i$  each time it crosses an hyperplane of type  $H_{i,k}$  with*

$$H_{i,k} := \{x \in \mathbb{R}^{\lfloor \frac{n}{2} \rfloor} \mid \langle x | \vec{e}_i \rangle = k\},$$

*with  $k \in \mathbb{N}$  and  $\vec{e}_i$  a vector of the canonical basis of  $\mathbb{R}^{\lfloor \frac{n}{2} \rfloor}$ . Let us stress that when the line crosses an hyperplane of normal  $\vec{e}_i$  we add a letter  $2i$  instead of the classical letter  $i$ , indeed the letters of  $\omega$  will represent rhombuses on the boundary of the substitution's metatiles, and in that case the rhombuses are bisected by the metatile's edge through their an even angle (and 0 represents a simple edge).*

2. *We define the sequence of edge words as  $(\Sigma_{(j)})_{j \in \mathbb{N}}$  as*

$$\Sigma_{(j)} := \text{pref}_j(\omega) \overline{\text{pref}_j(\omega)},$$

*where  $\text{pref}_j(\omega)$  is the prefix of length  $j$  of  $\omega$ , and  $\overline{\text{pref}_j(\omega)}$  is its mirror image.*

3. *We define the sequence of Sub Rosa-like pseudosubstitutions  $(\sigma_{(j)})_{j \in \mathbb{N}}$  where  $\sigma_{(j)}$  is the pseudosubstitution of edge words  $\Sigma_{(j)}$ . We denote by  $\varphi_{(j)}$  the expansion associated to  $\sigma_{(j)}$ .*

The main result of this section is the fact that in this sequence  $(\sigma_{(j)})_{j \in \mathbb{N}}$  there are primitive planar substitutions with the corner condition. We call *corner condition* the fact that there is a  $\frac{\pi}{n}$  rhombus on each side in each corner, see Figure 4.12. This additional condition is necessary for the regular fixpoint tiling (see Subsection 4.5.6).

**Proposition 4.5.3.** *There exists  $j$  such that  $\sigma_{(j)}$  is a primitive planar substitution of slope  $\mathcal{E}_n^0$  with the corner condition.*

We call the smallest such substitution Planar Rosa substitution.

**Definition 4.5.5** (The Planar Rosa substitution for even  $n$ ). *The Planar Rosa substitution  $\sigma'_n$  is defined as  $\sigma'_n = \sigma_{(j_0)}$  with*

$$j_0 = \min\{j \in \mathbb{N} \mid \varphi_{(j)} \text{ is planar of slope } \mathcal{E}_n^0 \text{ and} \\ \sigma_{(j)} \text{ is a primitive substitution with the corner condition}\}.$$

We cut this proposition in three lemmas:

**Lemma 4.5.3** (Planarity of  $\sigma_{(j)}$  for even  $n$ ).

$$\exists^\infty j \in \mathbb{N}, \varphi_{(j)} \text{ is planar of slope } \mathcal{E}_n^0.$$

**Lemma 4.5.4** (Tileability of  $\sigma_{(j)}$  for even  $n$ ).

$$\exists N_0 \in \mathbb{N}, \forall j \geq N_0, \sigma_{(j)} \text{ is a substitution with the corner condition,}$$

*i.e. the metatiles defined by the edge word  $\Sigma_{(j)}$  are tileable with the corner condition.*

**Lemma 4.5.5** (Primitivity of  $\sigma_{(j)}$  for even  $n$ ).

$$\exists N_1 \in \mathbb{N}, \forall j \geq N_1, \text{ if } \sigma_{(j)} \text{ is a substitution with the corner condition} \\ \text{then it is primitive.}$$

We will prove these three lemmas in the next three Subsections. Note that the definition of Planar Rosa substitution implies the second part of Theorem 2 for even  $n$  *i.e.* the fact that Planar Rosa tilings are substitution discrete planes with local  $n$ -fold rotational symmetry. The first part of Theorem 2 (*i.e.* the regular fixpoint tiling) for even  $n$  is proved in Section 4.5.6.

### 4.5.3 Proof of Lemma 4.5.3 (planarity)

In this subsection we prove Lemma 4.5.3, recall that  $n$  is a fixed even integer. The proof for planarity works exactly as for the odd case.

**Definition 4.5.6** (Billiard line). *Let  $(p_i)_{i \in \mathbb{N}}$  be the sequence of points of  $\mathbb{Z}^{\frac{n}{2}}$  associated to the billiard word  $\omega$  with  $p_0 = 0$ . This means that for all  $j$ ,*

$$\omega_j = 2i \quad \implies \quad p_{j+1} - p_j = \vec{e}_i.$$

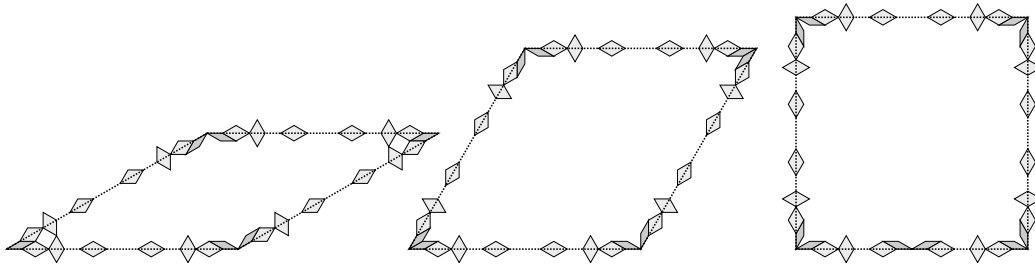


Figure 4.12: The corner condition : the  $\frac{\pi}{n}$  rhombus on each side in each corner of each metatile for  $n = 6$ .

**Proposition 4.5.4.** *The sequence  $(p_i)_{i \in \mathbb{N}}$  approximates the line  $\Gamma$ , which means that for any positive  $\varepsilon$  there are infinitely many points  $p_i$  that are  $\varepsilon$ -close to the line  $\Gamma$*

$$\forall \varepsilon > 0, \exists^\infty i > 0, d(p_i, \Gamma) < \varepsilon.$$

**Corollary 4.5.1.** *The sequence  $([\Sigma_{(i)}])_{i \in \mathbb{N}}$  approximates the line  $\Gamma$ , which means that for any positive  $\varepsilon$  there are infinitely many abelianized edge word  $[\Sigma_{(i)}]$  that are  $\varepsilon$ -close to the line  $\Gamma$*

$$\forall \varepsilon > 0, \exists^\infty i > 0, d([\Sigma_{(i)}], \Gamma) < \varepsilon.$$

The corollary is just a rewriting of the fact that by definition  $[\Sigma_{(j)}] = 2p_j$ . The proof for the proposition is the same as for the odd case (Proposition 4.4.4 page 122).

From this we get Lemma 4.5.3.

#### 4.5.4 Proof of Lemma 4.5.4 (tileability)

In this subsection we prove Lemma 4.5.4, recall that  $n$  is a fixed even integer. The proof for tileability is very similar to the odd case but there is one slight difference, we have the additional corner condition: on each corner along each meta-edge there is a  $\frac{\pi}{n}$  rhombus (see Figure 4.12). Remark that for the  $\frac{\pi}{n}$  corner of the narrowest metatile we have only one  $\frac{\pi}{n}$  rhombus, for every other corner of metatiles we have two  $\frac{\pi}{n}$  rhombuses: one on each side.

We recall that the edge word is  $\Sigma_{(j)} = \overline{pref_j(\omega)pref_j(\omega)}$  where  $\omega$  is a billiard word of direction  $\gamma$ . This means that in each corner of each metatile we have a portion of cone with edge word  $pref_j(\omega)$  on both sides and with

rhombus  $\frac{\pi}{n}$  in the corner as in Figure 4.12. We have no problem of tileability in these portions of cone due to the fact that the infinite cone with edge word  $\omega$  and with rhombus  $\frac{\pi}{n}$  in the corner is tileable, this comes from the fact that it appears in the multigrid dual tiling  $P_n(\frac{1}{2})$ .

Let us fix  $j$ , with the counting functions  $f_i(x)$  of the edge word  $\Sigma_{(j)}$  as defined in Section 4.3 we can apply Proposition 4.3.1 which means that if we have :

- $\Sigma_{(j)}$  is 2-almost-balanced (Definition 4.3.2 page 107)
- for any even  $i_1 < i_2$  and any position  $x_1$  such that at position  $x_1$  in the edge word  $\Sigma_{(j)}$  there is a rhombus  $i_1$  we have

$$f_{|i_2-2|}^{-1} \circ f_{i_2}(x_1) < f_{|i_1-2|}^{-1} \circ f_{i_1}(x_1),$$

then the metatiles defined by edge word  $\Sigma_{(j)}$  are tileable which means that  $\sigma_{(j)}$  is a substitution.

Remark that here the counting function and the edge word do not take into account the extra condition of having a  $\frac{\pi}{n}$  rhombus on each side of each corner. We will address that in the next few paragraphs.

Let us recall that  $\Sigma_{(j)}$  is 2-almost-balanced (see Lemma 4.4.6), so we only need to prove the second condition which we split between the first half  $x_1 < j$  and the second half  $x_1 \geq j$ .

### The first half: the corners

As explained above, the inequality in the first half of the edge word is due to the fact that the infinite cone of angle  $\frac{\pi}{n}$  with edge word  $\omega$  on both sides is tileable because it appears in the multigrid tiling  $P_n(\frac{1}{2})$ , see Section 2.6 page 43 for a definition of multigrids and see Chapter 5 page 144 for the proof of the fact that  $P_n(\frac{1}{2})$  is a rhombus tiling with global  $2n$ -fold rotational symmetry.

**Lemma 4.5.6** (The infinite cone is tileable). *The infinite cone of angle  $\frac{\pi}{n}$  and edge word  $\omega$  on both sides is tileable with rhombus tiles.*

*Proof.* In the multigrid  $P_n(\frac{1}{2})$  the sequence  $\omega$  of edges and rhombuses appears on the horizontal half line  $\mathbb{R}^+$ , indeed in the multigrid  $G_n(\frac{1}{2})$  the horizontal half line  $\mathbb{R}^+$  crosses either vertical grid lines (which correspond in the dual tiling to edges on the horizontal half line) or crossing points of two grid lines

$H(\zeta^i, \frac{1}{2}) \cap H(\zeta^{n-i}, \frac{1}{2})$  with  $\zeta = e^{i\frac{\pi}{n}}$  which corresponds to a rhombus of angle  $\frac{2i\pi}{n}$ . Edges appears in positions  $I_0$  with

$$I_0 := \{k - \frac{1}{2}, k > 1\},$$

and rhombuses of angle  $\frac{2i\pi}{n}$  appear in position  $I_i$  with

$$I_i = \left\{ \frac{k - \frac{1}{2}}{\cos(\frac{i\pi}{n})}, k > 1 \right\}.$$

These positions are exactly the coordinates of the intersection of the line  $\Gamma_{\frac{1}{2}}$  with the hyperplanes  $H(i, k)$  (recall the Definition of  $\omega$  as the billiard word of line  $\Gamma_{\frac{1}{2}}$ ), so indeed  $\omega$  appears on the horizontal half-line in  $P_n(\frac{1}{2})$ .

By global  $2n$ -fold rotational symmetry of  $P_n(\frac{1}{2})$  we get that  $\omega$  also appears on the rotated half line  $\zeta\mathbb{R}$ . So the cone of angle  $\frac{\pi}{n}$  and edge word  $\omega$  on both sides indeed appears in  $P_n(\frac{1}{2})$ .  $\square$

### The second half: the middle

Here the same proof as for odd  $n$  works.

The main point is to define  $g_{i_1, i_2}(x)$  for even  $i_1 < i_2$  as

$$g_{i_1, i_2}(x) := f_{|i_1-2|}^{-1} \circ f_{i_1}(x) - f_{|i_2-2|}^{-1} \circ f_{i_2}(x).$$

As the functions  $f_{i_1}$  is determined by the edge word  $\Sigma_{(j)}$  which approximates the line  $\Gamma$  (though it approximates it only half as well as  $\omega$  due to the definition of the edgeword as  $\Sigma_{(j)} = \overline{\text{pref}_j(\omega)\text{pref}_j(\omega)}$ ) so we get the existence of a  $\delta$  such that

$$\left| g_{i_1, i_2}(x) - x \left( \frac{\gamma_{i_1'}}{\gamma_{i_1''}} - \frac{\gamma_{i_2'}}{\gamma_{i_2''}} \right) \right| < 2\delta + \frac{\delta\|\gamma\|}{\gamma_{i_1''}} + \frac{\delta\|\gamma\|}{\gamma_{i_2''}},$$

with  $i_1' := \frac{i_1}{2}$ ,  $i_1'' := |i_1' - 2|$ ,  $i_2' := \frac{i_2}{2}$  and  $i_2'' := |i_2' - 2|$ .

With  $\gamma = (\cos(\frac{i\pi}{n}))_{0 \leq i < \frac{n}{2}}$  and  $i_1 < i_2$  we have

$$\frac{\gamma_{i_1'}}{\gamma_{i_1''}} - \frac{\gamma_{i_2'}}{\gamma_{i_2''}} > 0,$$

so we can define  $N_0$  as in the odd case.

For  $x > N'_0$  we have  $g_{i_1, i_2}(x) > 0$  for any  $i_1 < i_2$  with

$$N'_0 := \max_{i_1 < i_2} \left( \frac{2\delta + \frac{\delta \|\gamma\|}{\gamma_{i_1}''} + \frac{\delta \|\gamma\|}{\gamma_{i_2}''}}{\frac{\gamma_{i_1}'}{\gamma_{i_1}''} - \frac{\gamma_{i_2}'}{\gamma_{i_2}''}} \right).$$

Remark that in the definition of  $N'_0$  in the max it is implicit that  $i_1$  and  $i_2$  are edges or rhombus types, so they are even numbers between 0 and  $n - 2$ . This means that  $N'_0$  is a maximum of a finite set of real numbers, which means that it is indeed a real number (and not infinity).

### The corner condition: the $\frac{\pi}{n}$ rhombuses in the corners

There are two ways to prove that the metatiles are tileable in such a way that there is a  $\frac{\pi}{n}$  rhombus on each side in each corner: we can either modify the framework we introduced to prove tileability to adapt to this case, or we can start from the tileability of the meta-tiles without this condition and look at the conditions on the Kenyon matching to ensure that it is possible to have a  $\frac{\pi}{n}$  rhombus on each side in each corner.

Since the framework we introduced for tileability in Section 4.3 is quite difficult to modify (and to re-prove all the results) we will adopt the second approach. However we could just consider that the first two letters in the edge-word are merged and not re-prove all the results, we still would have the fact that  $g_{i_1, i_2}(x) > 0$  for  $x > N_0$  for some  $N_0$  (possibly a greater value than the  $N_0$  without the condition) and we would still have the tileability in the corners from the fact that in the multigrid dual tiling  $P_n(\frac{1}{2})$  we have a star of narrow rhombuses at the centre so we have the infinite cone with  $\frac{\pi}{n}$  rhombus on each sides of the corner.

For the sake of completeness we will still present the second approach. For the metatiles to be tileable with a rhombus  $\frac{\pi}{n}$  on each side in each corner it is sufficient to have, in the Kenyon matching, the fact that the chains that leave from the first edge and from the first rhombus cross as in Figure 4.13

Let us consider the metatile corner  $\frac{k\pi}{n}$ . There are actually four cases:

1.  $1 \leq k < \frac{n}{2}$  in which case both the edge 0 and the rhombus 2 match to the adjacent side of the metatile. In that case the two chains cross because 0 is matched to the first rhombus of type  $2k$  and 2 to the first rhombus of type  $2k - 2$ . Since  $2k > 2k - 2$  we have that the first

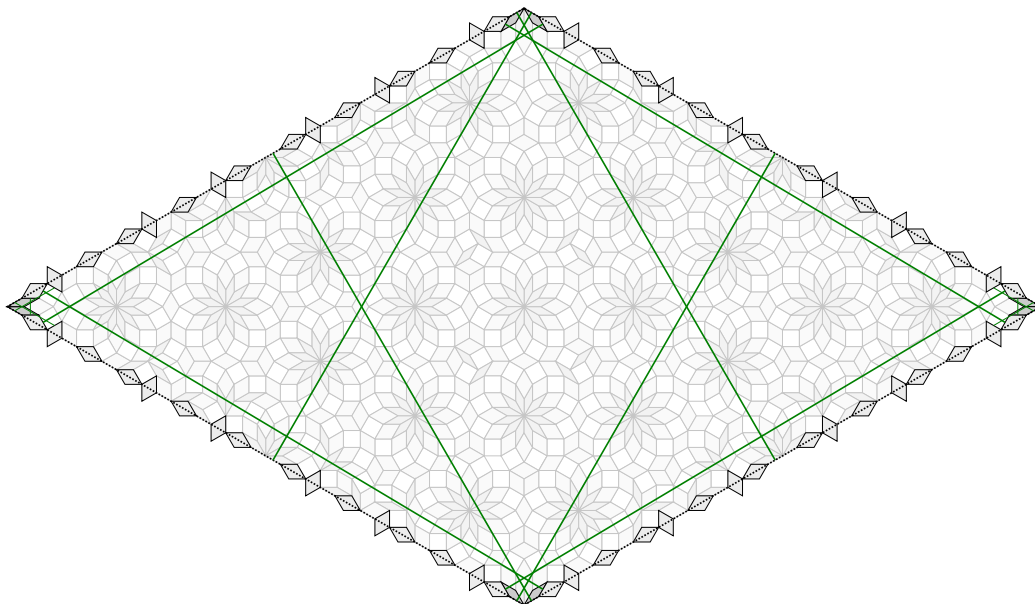


Figure 4.13: The chains in the corner for Planar Rosa 6.

occurrence of  $2k - 2$  is before the first occurrence of  $2k$  in the edge word  $\Sigma_{(j)}$ . Which means that the chains leaving the first 0 and the first 2 cross.

2.  $k = \frac{n}{2}$  in which case the edge 0 matches to the opposite side of the metatile and the rhombus 2 to the adjacent side of the metatile which means that the chains leaving the first 0 and the first 2 cross.
3.  $k = \frac{n}{2} + 1$  in which case both 0 and 2 match to the opposite side of the metatile, but there is no edge parallel to 2 on the adjacent side of the metatile. Which means that the first 2 is matched to the first 2 of the opposite side but the first 0 is not matched to the first 0 of the opposite side so the chains cross.
4.  $\frac{n}{2} + 1 < k \leq n - 1$  in which case both 0 and 2 match to the opposite side of the metatile and both have parallel edges on the adjacent side of the metatile. On the adjacent side, the edge direction 0 appears on rhombuses  $2k'$  with  $k' := n - k$  and the edge direction of 2 appears on rhombuses  $2(k' + 1)$ . Let us now look at where the chains of the first 0 and the first 1 appear. On the adjacent side there are  $f_{2k'}(2j)$



rhombuses of type  $2k'$  and  $f_{2(k'+1)}(2j)$  rhombuses of type  $2(k' + 1)$  because the length of the edge  $\Sigma_{(j)}$  is  $2j$ . So the first 0 is matched to  $f_0^{-1}(f_{2k'}(2j) + 1)$  and the first 2 is matched to  $f_2^{-1}(f_{2(k'+1)}(2j) + 1)$ . For the two chains to cross we need

$$f_0^{-1}(f_{2k'}(2j) + 1) > f_2^{-1}(f_{2(k'+1)}(2j) + 1)$$

Now is the time we recall that since  $\Sigma_{(j)}$  is defined as  $\overline{pref_j(\omega)pref_j(\omega)}$  the counting functions have a simple approximate value. More precisely there exist a bound  $\delta > 0$  such that

$$\begin{aligned} |f_0^{-1}(f_{2k'}(2j) + 1) - 2j \frac{\gamma_{k'}}{\gamma_0}| &\leq \delta \\ |f_2^{-1}(f_{2(k'+1)}(2j) + 1) - 2j \frac{\gamma_{k'+1}}{\gamma_1}| &\leq \delta \end{aligned}$$

So we have

$$\left| f_0^{-1}(f_{2k'}(2j) + 1) - f_2^{-1}(f_{2(k'+1)}(2j) + 1) - 2j \left( \frac{\gamma_{k'}}{\gamma_0} - \frac{\gamma_{k'+1}}{\gamma_1} \right) \right| \leq 2\delta$$

However with  $0 < k' < \frac{n}{2} - 1$  and  $\gamma_i = \cos(\frac{i\pi}{n})$  we have

$$\frac{\gamma_{k'}}{\gamma_0} - \frac{\gamma_{k'+1}}{\gamma_1} = \cos(\frac{k'\pi}{n}) - \frac{\cos(\frac{(k'+1)\pi}{n})}{\cos(\frac{\pi}{n})} > 0$$

Indeed we have  $\cos(\frac{(k'+1)\pi}{n}) = \cos(\frac{k'\pi}{n})\cos(\frac{\pi}{n}) - \sin(\frac{k'\pi}{n})\sin(\frac{\pi}{n})$  and with  $0 < k' < \frac{n}{2} - 1$  we get  $\cos(\frac{(k'+1)\pi}{n}) < \cos(\frac{k'\pi}{n})\cos(\frac{\pi}{n})$ .

Overall this means that there exists  $N_0''$  (which we can define in a similar way as  $N_0'$  in the previous subsection) such that for any  $j > N_0''$  the chains of the first 0 and the first 2 cross in every metatile corner of angle  $k > \frac{n}{2} + 1$

Overall we get the existence of  $N_0''$  such that for any  $j > N_0''$  if the metatiles are tileable then they are tileable with a rhombus on each side in every corner of every metatile.

Now take  $N_0 = \max(N_0', N_0'')$  for any  $j > N_0$ ,  $\sigma_{(j)}$  is a substitution with a rhombus on each side of every corner of every metatile.

### 4.5.5 Proof of Lemma 4.5.5 (primitivity)

In this subsection we prove Lemma 4.5.5, recall that  $n$  is a fixed even integer.

The proof of primitivity is very different than the proof for odd  $n$ , indeed for odd  $n$  we only used the boundary of the metatiles because all rhombus types appear in the edgeward in the odd case. However for the even case on the boundary only the rhombuses with even angles appear in the edge-word. So we will give a proof that needs the interior of the tiles.

What we will prove is that there exists  $N_1$  such that for any  $j > N_1$  if  $\sigma_{(j)}$  is a substitution (with  $\frac{\pi}{n}$  rhombus on each side of each corner of every metatile) then it is primitive of order 2. To prove that the first step is that the  $\frac{\pi}{n}$  rhombus appears in the image of any tile for our substitution since we imposed it. The second step is that for the for  $j > N_1$  for some  $N_1$  the image of the  $\frac{\pi}{n}$  rhombus contains every tile in every orientation.

The idea is that in the infinite cone of angle  $\frac{\pi}{n}$  and with  $\omega$  on both sides there are all the rhombus types in every orientation. This is simply due to the fact that in the multigrad dual tiling  $P_n(\frac{1}{2})$  a rhombus type (and an orientation) is the dual of a specific grid-line crossing, for example a rhombus with sides  $\zeta^i$  and  $\zeta^j$  is the dual of a crossing  $H(\zeta^i, \frac{1}{2}) \cap H(\zeta^j, \frac{1}{2})$ , and in the infinite cone every two grids cross. So in the infinite cone in the dual tiling there are every rhombuses in all orientations.

Now for each rhombus and orientation (which we denote by  $t$ ) we take its position closest to the corner in the infinite cone and we look at the two chains of rhombuses which cross on this rhombus, more specifically we look at which positions on the edge  $\omega$  these chain enter the cone. Now denote by  $j_t$  the maximum of the four positions (of entry of the chains that cross at  $t$ ). For any  $j \geq j_t$ , if the metatile of angle  $\frac{\pi}{n}$  and of edge word  $\Sigma_{(j)}$  is tileable then it contains the rhombus and orientation  $t$  because the Kenyon matching of the metatile contains a crossing that forces rhombus  $t$ . With  $\mathbf{T}$  the set of all rhombus prototiles (in every orientation) we define

$$N_1 := \max_{t \in \mathbf{T}} j_t.$$

From that we get that for any  $j \geq N_1$ , if  $\sigma_{(j)}$  is a substitution (with a  $\frac{k\pi}{n}$  rhombus on each side in every corner of every metatile) then it is primitive of order 2.

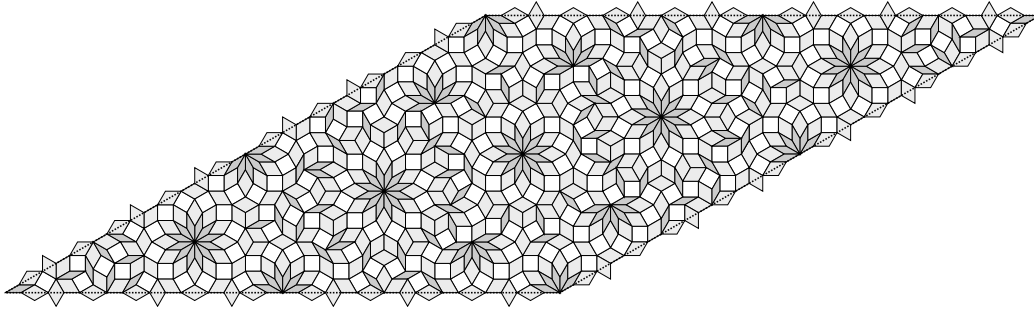


Figure 4.14: The narrowest metatile for Planar Rosa 6 (*i.e.* metatile of angle  $\frac{\pi}{6}$ ).

### 4.5.6 Regular fixpoint tiling

Here we complete the proof of Theorem 2 for even  $n$ . Just as in the odd case, the one thing to prove is that the star  $S(n)$  is indeed a regular seed for  $\sigma'_n$ .

The fact that  $S(n)$  is a seed is straightforward, indeed in the definition of  $\sigma'_n$  we have the fact that on the edges of the metatiles there is a sequence of unit edges and bisected rhombuses starting by a unit edge. This means that in the  $\frac{\pi}{n}$  angle of the metatile we have one rhombus of angle  $\frac{\pi}{n}$  as shown in Figure 4.14. From that we immediately get that at the centre of  $\sigma'_n(S(n))$  we have  $S(n)$ , hence it is a seed.

Regularity is a bit more tricky because we have no exact description of the tiles. What we show is that for any prototile  $t$ ,  $S(n)$  appears in  $\sigma_n^{1+\frac{n}{2}}(t)$  for any tile  $t$ . The idea is that for any tile  $t$  there is a interior vertex in  $\sigma'_n(t)$ , around this vertex are three tiles of angles  $\frac{k_0\pi}{n}$ ,  $\frac{k_1\pi}{n}$  and  $\frac{k_2\pi}{n}$  with  $1 \leq k_0, k_1, k_2 \leq n - 1$ . And in the  $\lceil \frac{k}{2} \rceil^{th}$  image of an angle  $\frac{k\pi}{n}$  there is a portion of the star  $S(n)$  as shown in Figure 4.11. So in  $\sigma_n^{k_3}(\sigma'_n(t))$  there is the star  $S(n)$ , with  $k_3 = \max(\lceil \frac{k_0}{2} \rceil, \lceil \frac{k_1}{2} \rceil, \lceil \frac{k_2}{2} \rceil) \leq \frac{n}{2}$ . From this we get that  $\sigma_n^{1+\frac{n}{2}}(t)$  contains  $S(n)$ , which means that  $S(n)$  is a regular seed. This concludes the proof of Theorem 2 for even  $n$ .

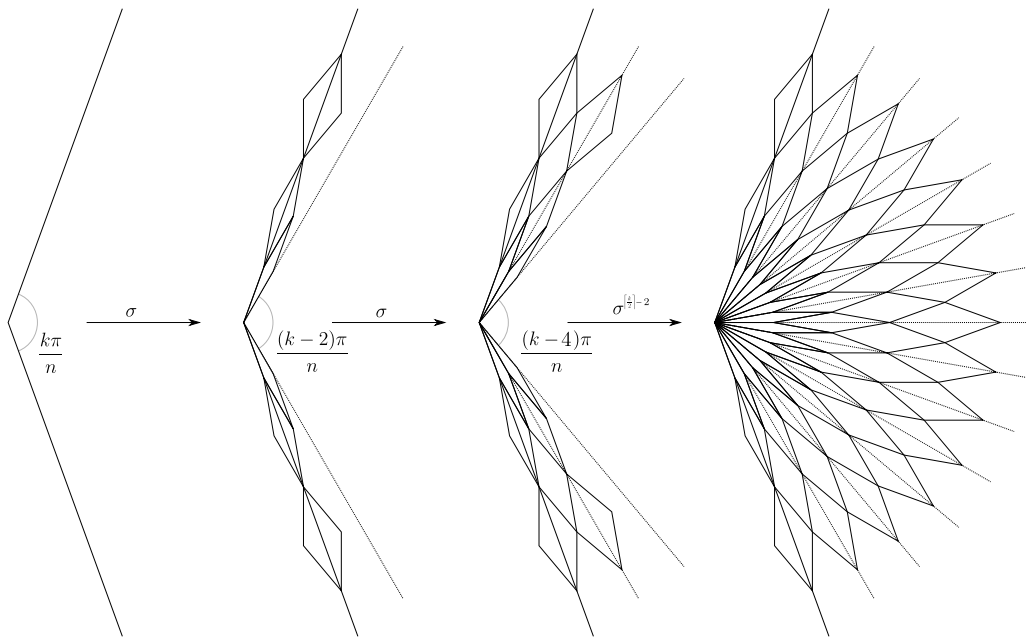


Figure 4.15: Corners of metatiles.

# Chapter 5

## Regular $n$ -fold multigrids and their dual tilings

In this chapter we present our result on multigrids, their dual tilings and the link with the substitution planar tilings presented in Chapter 4, these results were submitted and accepted to Automata2021 [Lut21a]. Recall that the definitions for multigrids and their dual tilings can be found in Section 2.6 page 43.

### 5.1 Main result

The main result of this chapter is on the properties of some specific  $n$ -fold multigrid dual tilings.

**Theorem 3** ([Lut21a]).

1. For any  $n \geq 4$  the  $n$ -fold multigrid dual tiling  $P_n(\frac{1}{2})$  is a quasiperiodic rhombus cut-and-project tiling with global  $2n$ -fold rotational symmetry.
2. For any **odd**  $n \geq 5$  the  $n$ -fold multigrid dual tiling  $P_n(\frac{1}{n})$  is a quasiperiodic rhombus cut-and-project tiling with global  $n$ -fold rotational symmetry.

Theorem 3 is actually a corollary of a more technical result on the regularity of  $n$ -fold multigrids.

**Theorem 16** ([Lut21a]).

1. for any  $n \geq 3$  and any non-zero rational offset  $r \in \mathbb{Q} \cap ]0, 1[$  the  $n$ -fold multigrid  $G_n(r)$  is regular
2. for any **odd**  $n \geq 3$  and any tuple of non-zero rational offsets  $\gamma = (\gamma_i)_{0 \leq i < n} \in (\mathbb{Q} \cap ]0, 1])^n$  the  $n$ -fold multigrid  $G_n(\gamma)$  is regular

See Figures 5.1 and 5.3 or Chapter 6 page 157 for examples of tilings  $P_n(\frac{1}{2})$  and  $P_n(\frac{1}{n})$ , these figures have been produced using a SageMath program which is available in [Lut21b]. Remark that Theorem 16 is not an exact characterization of regular  $n$ -fold multigrid but rather an easily checked sufficient condition for regularity. In [DB81] N. G. de Bruijn gives an exact characterization of regular pentagrids in the specific Penrose case (sum of the offsets is an integer), but this characterization is not easily generalized to the non-Penrose case and to all  $n$ -fold multigrids.

The fact that the grids  $G_n(\frac{1}{2})$  are regular and that their dual tilings  $P_n(\frac{1}{2})$  are rhombus tilings is used in Chapter 4 for the construction of the Planar Rosa substitutions.

In Section 5.2 we show how Theorem 3 is a corollary of Theorem 16, in Section 5.3 we present the link between the regularity of multigrids and some trigonometric diophantine equations, in Section 5.4 we present the result of Conway and Jones on trigonometric diophantine equations and in Section 5.5 we give the proof of Theorem 16.

## 5.2 From regular $n$ -fold multigrids to tilings with global $n$ -fold symmetry

Let  $n \geq 3$  be an integer. By Theorem 16 the multigrid  $G_n(\frac{1}{2})$  and  $G_n(\frac{1}{n})$  are regular, so their dual tilings  $P_n(\frac{1}{2})$  and  $P_n(\frac{1}{n})$  are edge-to-edge rhombus tilings. As mentioned in Section 2.6, the multigrid dual tilings are cut-and-project [GR86] and therefore also uniformly recurrent.

Let us remark that the dualization process commutes with rotations around the origin, so if a multigrid has some rotational symmetry around the origin then so does its dual tiling.

So for odd  $n$ ,  $P_n(\frac{1}{n})$  has global  $n$ -fold rotational symmetry because the grid also has global  $n$ -fold rotational symmetry, indeed applying the rotation of angle  $\frac{2\pi}{n}$  centered on the origin to the multigrid sends  $\zeta_n^k$  to  $\zeta_n^{k+1}$  and since the offset is the same on all directions the rotated multigrid is the same as

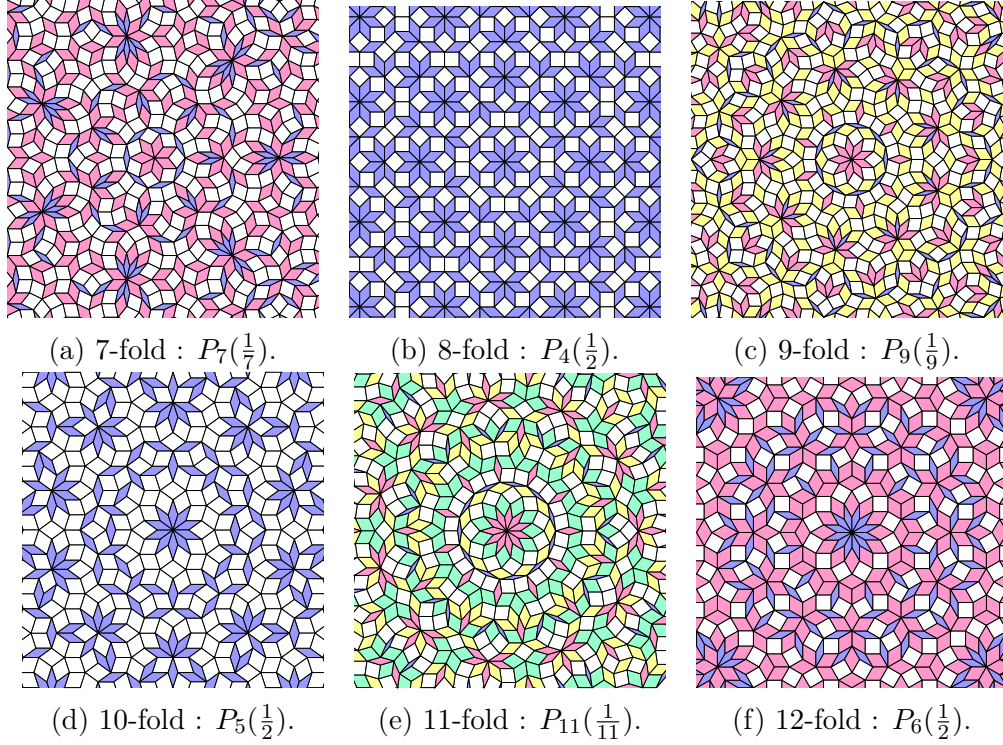


Figure 5.1: Central patch of the multigrad dual tiling with exactly  $n$ -fold rotational symmetry for  $n \in \{7, 8, 9, 10, 11, 12\}$ .

the original one. However this does not hold for even  $n$  since in that case we chose  $\zeta_n = e^{i\frac{\pi}{n}}$  so we have  $\zeta_n^n = e^{i\pi} = -1 = -\zeta_n^0$  so the grid of offset  $\frac{1}{n}$  for even  $n \geq 4$  does not have any rotational symmetry.

Also for odd  $n$ ,  $P_n(\frac{1}{2})$  has global  $2n$ -fold rotational symmetry because the image of  $\zeta_n^0$  by the rotation of angle  $\frac{\pi}{n}$  is

$$e^{i\frac{\pi}{n}} = -e^{i\frac{(n+1)\pi}{n}} = -e^{i\frac{2\lceil\frac{n}{2}\rceil\pi}{n}} = -\zeta_n^{\lceil\frac{n}{2}\rceil}$$

so with  $1 - \frac{1}{2} = \frac{1}{2}$  (*i.e.* the offset in direction  $\zeta_n^i$  and in its reverse direction  $-\zeta_n^i$  is the same) we get global  $2n$ -fold rotational symmetry for  $G_n(\frac{1}{2})$  and  $P_n(\frac{1}{2})$ . For even  $n$  we use also the fact that with offset  $\frac{1}{2}$  we get that the offset along  $\zeta_n^i$  is the same as along the opposite direction  $-\zeta_n^i$  together with  $\zeta_n = e^{i\frac{\pi}{n}}$  which means that  $\zeta_n^{n+i} = -\zeta_n^i$  to get global  $2n$ -fold rotational symmetry for  $G_n(\frac{1}{2})$  and  $P_n(\frac{1}{2})$ .

When we combine these with the crystallographic restriction which implies that for any  $n \geq 4$  these tilings are non-periodic we get Theorem 3. Remark that for even  $n$ ,  $P_n(\frac{1}{2})$  has global  $2n$ -fold rotational symmetry and  $P_{\frac{n}{2}}(\frac{1}{2})$  has exactly  $n$ -fold global rotational symmetry. So for any  $n$  there exists a tiling with exactly  $n$ -fold global rotational symmetry, see the examples for  $n \in \{7, 8, 9, 10, 11, 12\}$  in Figure 5.1, and for  $n = 23$  in Figure 5.3.

Remark also that for odd  $n$ , for any  $r \in \mathbb{Q} \cap ]0, 1[$  the multigrid  $G_n(r)$  is regular and the multigrid dual tiling  $P_n(r)$  has global  $n$ -fold rotational symmetry, except the specific case  $r = \frac{1}{2}$  that has global  $2n$ -fold rotational symmetry. The choice of  $r = \frac{1}{n}$  is mainly due to the fact that the canonical Penrose rhombus tiling is  $P_5(\frac{1}{5})$  so  $P_n(\frac{1}{n})$  is in that sense a generalization of the canonical Penrose rhombus tiling.

Note that Theorem 3 is stated for  $n > 3$  because for  $n = 3$  the multigrid dual tilings with offset  $\frac{1}{2}$  and  $\frac{1}{3}$  are periodic.

### 5.3 Regularity of $n$ -fold multigrids and trigonometric equations

In this section we present the link between the regularity or singularity of  $n$ -fold multigrids and some trigonometric equations.

**Proposition 5.3.1** (Regularity of multigrids and trigonometric equations). *Let  $n \in \mathbb{N}$ , and  $\gamma_0, \gamma_1, \dots, \gamma_{n-1}$  be offsets in  $[0, 1[$ . Assume that for any  $p, q$  such that  $0 < q < p < n$  and any  $r_0 \in \mathbb{Z} - \gamma_0$ ,  $r_q \in \mathbb{Z} - \gamma_q$  and  $r_p \in \mathbb{Z} - \gamma_p$  we have either Inequation (5.1) when  $n$  is odd, or Inequation (5.2) when  $n$  is even.*

$$(n \text{ odd}) \quad r_0 \sin \frac{2(p-q)\pi}{n} + r_p \sin \frac{2q\pi}{n} - r_q \sin \frac{2p\pi}{n} \neq 0 \quad (5.1)$$

$$(n \text{ even}) \quad r_0 \sin \frac{(p-q)\pi}{n} + r_p \sin \frac{q\pi}{n} - r_q \sin \frac{p\pi}{n} \neq 0 \quad (5.2)$$

Then the grid  $G_n(\gamma_0, \gamma_1, \dots, \gamma_{n-1})$  is regular.

*Proof.* We will prove this proposition by contradiction *i.e.* we assume a grid is singular and we show that it implies the existence of  $r_0, r_p, r_q$  such that the Inequation (5.1) is contradicted if  $n$  is odd, and Inequation (5.2) is contradicted if  $n$  is even.

We will actually prove it for odd  $n$ , the proof for even  $n$  is exactly the same and it is only needed to replace the formula of  $\zeta_n^k$  which in the even



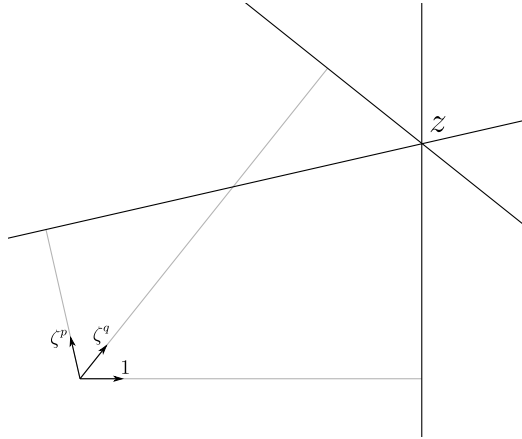


Figure 5.2: Intersection of three lines (in a singular multigrad).

case is  $e^{i\frac{k\pi}{n}}$  instead of  $e^{i\frac{2k\pi}{n}}$ , which means that in the angles we remove the factor 2.

Let  $n$  be an odd integer and let  $\gamma_0, \gamma_1, \dots, \gamma_{n-1} \in [0, 1[$  such that  $G_n(\gamma_0, \gamma_1, \dots, \gamma_{n-1})$  is singular. This means that there exist  $z \in \mathbb{C}$  at the intersection of three lines, up to relabeling and rotation we chose to consider it is at the intersection of  $H(\zeta_n^0, \gamma_0)$ ,  $H(\zeta_n^q, \gamma_q)$  and  $H(\zeta_n^p, \gamma_p)$  for some  $0 < q < p < n$ , see Figure 5.2. This means that there exist  $k_0, k_q, k_p \in \mathbb{Z}$  such that

$$\begin{cases} \operatorname{Re}(z) = k_0 - \gamma_0 \\ \operatorname{Re}(z \cdot \bar{\zeta}_n^q) = k_q - \gamma_q \\ \operatorname{Re}(z \cdot \bar{\zeta}_n^p) = k_p - \gamma_p \end{cases}$$

Write  $z = k_0 - \gamma_0 + iy$ ,  $\zeta_n = e^{\frac{2i\pi}{n}}$  and rewrite  $k_0 - \gamma_0$ ,  $k_p - \gamma_p$ ,  $k_q - \gamma_q$  as  $r_0$ ,  $r_p$ ,  $r_q$ . Now we have

$$\begin{cases} z = r_0 + iy \\ r_0 \cos \frac{2q\pi}{n} + y \sin \frac{2q\pi}{n} = r_q \\ r_0 \cos \frac{2p\pi}{n} + y \sin \frac{2p\pi}{n} = r_p \end{cases}$$

Let us now cancel out the  $y$  terms by substituting the third line by  $\sin \frac{2p\pi}{n}$

times the seconde equality minus  $\sin \frac{2q\pi}{n}$  times the third equality.

$$\begin{cases} z = r_0 + iy \\ r_0 \cos \frac{2q\pi}{n} + y \sin \frac{2q\pi}{n} = r_q \\ r_0(\cos \frac{2q\pi}{n} \sin \frac{2p\pi}{n} - \cos \frac{2p\pi}{n} \sin \frac{2q\pi}{n}) = r_q \sin \frac{2p\pi}{n} - r_p \sin \frac{2q\pi}{n} \end{cases}$$

Now let us study the third line to simplify it.

$$\begin{aligned} r_0 \cos \frac{2q\pi}{n} \sin \frac{2p\pi}{n} - r_0 \cos \frac{2p\pi}{n} \sin \frac{2q\pi}{n} &= r_q \sin \frac{2p\pi}{n} - r_p \sin \frac{2q\pi}{n} \\ \Leftrightarrow r_0 \left( \cos \frac{2q\pi}{n} \sin \frac{2p\pi}{n} - \cos \frac{2p\pi}{n} \sin \frac{2q\pi}{n} \right) &= r_q \sin \frac{2p\pi}{n} - r_p \sin \frac{2q\pi}{n} \\ \Leftrightarrow r_0 \sin \frac{2(p-q)\pi}{n} + r_p \sin \frac{2q\pi}{n} - r_q \sin \frac{2p\pi}{n} &= 0. \end{aligned}$$

Overall we obtain

$$r_0 \sin \frac{2(p-q)\pi}{n} + r_p \sin \frac{2q\pi}{n} - r_q \sin \frac{2p\pi}{n} = 0,$$

which is exactly the contradiction of Inequation (5.1).  $\square$

In the next section we consider the solutions to these kind of trigonometric equations.

## 5.4 Trigonometric diophantine equations

We call *rational angles* the set  $\pi\mathbb{Q}$ . We consider now equations of the type

$$A \cos(a) + B \cos(b) + C \cos(c) = 0 \tag{5.3}$$

with  $a, b$  and  $c$  rational angles.

In the previous paragraph we had sine instead of cosine but we can always convert sine to cosine, and we had  $A \in \mathbb{Z} - \gamma$  for some real number  $0 \leq \gamma < 1$  and similarly for  $B$  and  $C$  but now we will consider  $A, B$  and  $C$  to be rationals.

**Theorem 17** ([CJ76]). *Suppose we have at most four distinct rational angles strictly between 0 and  $\frac{\pi}{2}$  for which some rational linear combination of their cosines has rational value but no proper subset has this property.*

Then the appropriate linear combination is proportional to one from the following list:

$$\cos\left(\frac{\pi}{3}\right) = \frac{1}{2} \quad (5.4)$$

$$-\cos(\varphi) + \cos\left(\frac{\pi}{3} - \varphi\right) + \cos\left(\frac{\pi}{3} + \varphi\right) = 0 \quad (0 < \varphi < \frac{\pi}{6}) \quad (5.5)$$

$$\cos\left(\frac{\pi}{5}\right) - \cos\left(\frac{2\pi}{5}\right) = \frac{1}{2} \quad (5.6)$$

$$\cos\left(\frac{\pi}{7}\right) - \cos\left(\frac{2\pi}{7}\right) + \cos\left(\frac{3\pi}{7}\right) = \frac{1}{2} \quad (5.7)$$

$$\cos\left(\frac{\pi}{5}\right) - \cos\left(\frac{\pi}{15}\right) + \cos\left(\frac{4\pi}{15}\right) = \frac{1}{2} \quad (5.8)$$

$$-\cos\left(\frac{2\pi}{5}\right) + \cos\left(\frac{2\pi}{15}\right) - \cos\left(\frac{7\pi}{15}\right) = \frac{1}{2} \quad (5.9)$$

$$\cos\left(\frac{\pi}{7}\right) + \cos\left(\frac{3\pi}{7}\right) - \cos\left(\frac{\pi}{21}\right) + \cos\left(\frac{8\pi}{21}\right) = \frac{1}{2} \quad (5.10)$$

$$\cos\left(\frac{\pi}{7}\right) - \cos\left(\frac{2\pi}{7}\right) + \cos\left(\frac{2\pi}{21}\right) - \cos\left(\frac{5\pi}{21}\right) = \frac{1}{2} \quad (5.11)$$

$$-\cos\left(\frac{2\pi}{7}\right) + \cos\left(\frac{3\pi}{7}\right) + \cos\left(\frac{4\pi}{21}\right) + \cos\left(\frac{10\pi}{21}\right) = \frac{1}{2} \quad (5.12)$$

$$-\cos\left(\frac{\pi}{15}\right) + \cos\left(\frac{2\pi}{15}\right) + \cos\left(\frac{4\pi}{15}\right) - \cos\left(\frac{7\pi}{15}\right) = \frac{1}{2} \quad (5.13)$$

See the original article [CJ76] for the proof. The proof is based on a more general result on vanishing sums of roots of unity. And this is proved using complex numbers and the theory of vanishing formal sums. If we adapt this result for sum of three cosines that have value zero we get.

**Corollary 5.4.1.** *Let  $a \leq b \leq c$  be rational angles strictly between 0 and  $\frac{\pi}{2}$  and not all equal, and let  $A, B, C$  be non-zero rationals.*

*If  $A \cos(a) + B \cos(b) + C \cos(c) = 0$  then either*

$$\begin{cases} a = \frac{\pi}{5} \\ b = \frac{\pi}{3} \\ c = \frac{2\pi}{5} \\ B = C = -A \end{cases} \quad \text{or} \quad \begin{cases} 0 < a < \frac{\pi}{6} \\ b = \frac{\pi}{3} - a \\ c = \frac{\pi}{3} + a \\ B = C = -A \end{cases}$$

*Proof.* We just need to apply Theorem 17. First remark that there is no solution for  $A \cos(a) + B \cos(b) = 0$  with  $a$  and  $b$  distinct and strictly between 0 and  $\frac{\pi}{2}$ , and  $A$  and  $B$  non zero. Now with  $0 < a < b < c < \frac{\pi}{2}$ , we have either a combination of Equations (5.4) and (5.6) (first case) or Equation (5.5) (second case).  $\square$

And in the case that one of the angle is 0, we get the following.

**Corollary 5.4.2.** *Let  $a \leq b$  be rational angles strictly between 0 and  $\frac{\pi}{2}$  and not all equal, and let  $A, B, C$  be non-zero rationals.*

*If  $A \cos(a) + B \cos(b) = C$  then either*

$$\begin{cases} a = \frac{\pi}{5} \\ b = \frac{2\pi}{5} \\ A = -B = 2C \end{cases} \quad \text{or} \quad \begin{cases} a = b = \frac{\pi}{3} \\ A + B = 2C \end{cases}$$

*Proof.* Just as above we just apply Theorem 17. □

## 5.5 Proof of Theorem 16

Here we use Proposition 5.3.1 and Corollary 5.4.1 to prove Theorem 16.

### 5.5.1 For odd $n$

First let us remark that in Theorem 16 the first statement when restricted to odd  $n$  is a strict subcase of the second statement, so here we will prove the second statement which is as follows: for any odd  $n \geq 3$  and any tuple of non-zero rational offsets  $\gamma = (\gamma_i)_{0 \leq i < n} \in (\mathbb{Q} \cap ]0, 1])^n$  the  $n$ -fold multigrig  $G_n(\gamma)$  is regular. We reformulate this with Proposition 5.3.1 as: for any odd  $n \geq 3$ , for any  $0 < p < q < n$  and any three non-zero rational offsets  $\gamma_0, \gamma_p, \gamma_q$ , for any  $r_0 \in \mathbb{Z} - \gamma_0, r_p \in \mathbb{Z} - \gamma_p$  and  $r_q \in \mathbb{Z} - \gamma_q$  we have

$$r_0 \sin \frac{2(p-q)\pi}{n} + r_p \sin \frac{2q\pi}{n} - r_q \sin \frac{2p\pi}{n} \neq 0.$$

Actually we prove a slightly reformulated version: for any odd  $n \geq 3$ , for any  $0 < p < q < n$  and any three non-zero rationals  $r_0, r_p, r_q \in \mathbb{Q} \setminus \{0\}$  we have

$$r_0 \sin \frac{2(p-q)\pi}{n} + r_p \sin \frac{2q\pi}{n} - r_q \sin \frac{2p\pi}{n} \neq 0.$$

To apply Corollary 5.4.1 we first need to translate the formula with sine and with angles in  $]0, 2\pi[$  as a formula with cosine and angles in  $]0, \frac{\pi}{2}[$ .

**Lemma 5.5.1** (Sine and Cosine). *For  $\theta \in [0, 2\pi[$  we have*

$$\sin(\theta) = (-1)^{\lfloor \frac{\theta}{\pi} \rfloor} \cos \left( (-1)^{\lfloor \frac{2\theta}{\pi} \rfloor} \left( \lfloor \frac{\theta}{\pi} \rfloor \pi + \frac{\pi}{2} - \theta \right) \right)$$

*and  $(-1)^{\lfloor \frac{2\theta}{\pi} \rfloor} \left( \lfloor \frac{\theta}{\pi} \rfloor \pi + \frac{\pi}{2} - \theta \right) \in [0, \frac{\pi}{2}[$ .*

*Proof.* This result is just a rewriting of :

- if  $0 \leq \theta < \frac{\pi}{2}$  then  $\sin(\theta) = \cos(\frac{\pi}{2} - \theta)$  and  $(\frac{\pi}{2} - \theta) \in [0, \frac{\pi}{2}]$
- if  $\frac{\pi}{2} \leq \theta < \pi$  then  $\sin(\theta) = \cos(\theta - \frac{\pi}{2})$  and  $(\theta - \frac{\pi}{2}) \in [0, \frac{\pi}{2}]$
- if  $\pi \leq \theta < \frac{3\pi}{2}$  then  $\sin(\theta) = -\cos(\frac{3\pi}{2} - \theta)$  and  $(\frac{3\pi}{2} - \theta) \in [0, \frac{\pi}{2}]$
- if  $\frac{3\pi}{2} \leq \theta < 2\pi$  then  $\sin(\theta) = -\cos(\theta - \frac{3\pi}{2})$  and  $(\theta - \frac{3\pi}{2}) \in [0, \frac{\pi}{2}]$

□

We define  $\varepsilon(\theta) := (-1)^{\lfloor \frac{\theta}{\pi} \rfloor}$  and  $\varphi(\theta) := (-1)^{\lfloor \frac{2\theta}{\pi} \rfloor} (\lfloor \frac{\theta}{\pi} \rfloor \pi + \frac{\pi}{2} - \theta)$ . Remark that this means that  $\theta = \lfloor \frac{\theta}{\pi} \rfloor \pi + \frac{\pi}{2} - (-1)^{\lfloor \frac{2\theta}{\pi} \rfloor} \varphi(\theta)$ .

Let  $n, p, q$  be integers such that  $n$  is odd,  $n \geq 3$  and  $0 < q < p < n$ . By contradiction suppose that there exists  $r_0, r_p$  and  $r_q$  non-zero rationals such that

$$r_0 \sin(\frac{2(p-q)\pi}{n}) + r_p \sin(\frac{2q\pi}{n}) - r_q \sin(\frac{2p\pi}{n}) = 0.$$

By Lemma 5.5.1 we have

$$r_0 \varepsilon(\frac{2(p-q)\pi}{n}) \cos(\varphi(\frac{2(p-q)\pi}{n})) + r_p \varepsilon(\frac{2q\pi}{n}) \cos(\varphi(\frac{2q\pi}{n})) - r_q \varepsilon(\frac{2p\pi}{n}) \cos(\varphi(\frac{2p\pi}{n})) = 0.$$

Which we reformulate as

$$r'_0 \cos(\theta_0) + r'_p \cos(\theta_q) + r'_q \cos(\theta_p) = 0$$

with  $r'_0 := r_0 \varepsilon(\frac{2(p-q)\pi}{n})$ ,  $r'_p := r_p \varepsilon(\frac{2q\pi}{n})$ ,  $r'_q := -r_q \varepsilon(\frac{2p\pi}{n})$  and  $\theta_0 := \varphi(\frac{2(p-q)\pi}{n})$ ,  $\theta_q := \varphi(\frac{2q\pi}{n})$ ,  $\theta_p := \varphi(\frac{2p\pi}{n})$ .

Remark that for odd  $n$  and any  $0 < k < n$  we have  $\frac{2k\pi}{n} \notin \{0, \frac{\pi}{2}, \pi, \frac{3\pi}{2}\}$ , so  $\varphi(\frac{2k\pi}{n}) \notin \{0, \frac{\pi}{2}\}$ . This implies that  $0 < \theta_0, \theta_p, \theta_q < \frac{\pi}{2}$ .

Moreover for odd  $n$  we have that  $\theta_0, \theta_p, \theta_q$  are not all equal. By contradiction if  $\theta_0 = \theta_p = \theta_q$  we have that  $\frac{2p\pi}{n}, \frac{2q\pi}{n}, \frac{2(p-q)\pi}{n} \in \varphi^{-1}(\{\theta_0\}) = \{\frac{\pi}{2} - \theta_0, \frac{\pi}{2} + \theta_0, \frac{3\pi}{2} - \theta_0, \frac{3\pi}{2} + \theta_0\}$  which is impossible. So we have

$$r'_0 \cos(\theta_0) + r'_p \cos(\theta_q) + r'_q \cos(\theta_p) = 0$$

with non-zero rationals  $r'_0, r'_p, r'_q$  and with three angles strictly between 0 and  $\frac{\pi}{2}$  and not all equal.

So we can apply Corollary 5.4.1 and we now have two cases:

1.  $\{\theta_0, \theta_p, \theta_q\} = \{\frac{\pi}{5}, \frac{\pi}{3}, \frac{2\pi}{5}\}$

2.  $\{\theta_0, \theta_p, \theta_q\} = \{\theta, \frac{\pi}{3} - \theta, \frac{\pi}{3} + \theta\}$  for some  $0 < \theta < \frac{\pi}{6}$

Let us now show that both cases lead to a contradiction. In the first case we have that  $\{\frac{2p\pi}{n}, \frac{2q\pi}{n}, \frac{2(p-q)\pi}{n}\} = \{\theta_1, \theta_2, \theta_3\}$  with

$$\begin{aligned}\theta_1 &\in \varphi^{-1}(\{\frac{\pi}{5}\}) = \{\frac{3\pi}{10}, \frac{7\pi}{10}, \frac{13\pi}{10}, \frac{17\pi}{10}\} \\ \theta_2 &\in \varphi^{-1}(\{\frac{\pi}{3}\}) = \{\frac{\pi}{6}, \frac{5\pi}{6}, \frac{7\pi}{6}, \frac{11\pi}{6}\} \\ \theta_3 &\in \varphi^{-1}(\{\frac{2\pi}{5}\}) = \{\frac{\pi}{10}, \frac{9\pi}{10}, \frac{11\pi}{10}, \frac{19\pi}{10}\}\end{aligned}$$

This is impossible because by definition  $\frac{2p\pi}{n} = \frac{2q\pi}{n} + \frac{2(p-q)\pi}{n}$  and we have no  $\theta_1, \theta_2, \theta_3$  as defined above such that one is the sum of the two other.

In the second case we have that  $\{\theta_0, \theta_p, \theta_q\} = \{\theta, \frac{\pi}{3} - \theta, \frac{\pi}{3} + \theta\}$  for some  $0 < \theta < \frac{\pi}{6}$ . Now we use  $\frac{2p\pi}{n} = \frac{2q\pi}{n} + \frac{2(p-q)\pi}{n}$  and by definition we have

$$\begin{aligned}\frac{2p\pi}{n} &= \lfloor \frac{2p}{n} \rfloor \pi + \frac{\pi}{2} - (-1)^{\lfloor \frac{4p}{n} \rfloor} \theta_p = \lfloor \frac{2p}{n} \rfloor \pi + \frac{\pi}{2} \pm \theta_p \\ \frac{2q\pi}{n} &= \lfloor \frac{2q}{n} \rfloor \pi + \frac{\pi}{2} - (-1)^{\lfloor \frac{4q}{n} \rfloor} \theta_q = \lfloor \frac{2q}{n} \rfloor \pi + \frac{\pi}{2} \pm \theta_q \\ \frac{2(p-q)\pi}{n} &= \lfloor \frac{2(p-q)}{n} \rfloor \pi + \frac{\pi}{2} - (-1)^{\lfloor \frac{4(p-q)}{n} \rfloor} \theta_0 = \lfloor \frac{2(p-q)}{n} \rfloor \pi + \frac{\pi}{2} \pm \theta_0\end{aligned}$$

By assembling these two we get

$$(\lfloor \frac{2p}{n} \rfloor - \lfloor \frac{2q}{n} \rfloor - \lfloor \frac{2(p-q)}{n} \rfloor - 1)\pi + \frac{\pi}{2} = \pm \theta_p \pm \theta_0 \pm \theta_q$$

And with  $\{\theta_0, \theta_p, \theta_q\} = \{\theta, \frac{\pi}{3} - \theta, \frac{\pi}{3} + \theta\}$  we get

$$(\pm \theta_p \pm \theta_0 \pm \theta_q) \in \{\pm 3\theta, \pm \theta, \pm \frac{2\pi}{3} \pm \theta\}$$

However this is impossible since for  $0 < \theta < \frac{\pi}{6}$ , we have

$$(\mathbb{Z}\pi + \frac{\pi}{2}) \cap \{\pm 3\theta, \pm \theta, \pm \frac{2\pi}{3} \pm \theta\} = \emptyset$$

By contradiction we proved that for odd  $n$ , any  $n$ -fold multigrid with non-zero rational offsets is regular.

## 5.5.2 For even $n$

Let us now prove the first statement of Theorem 16 for even  $n$  which is: for any even  $n \geq 4$  and any non-zero rational offset  $r \in \mathbb{Q} \cap ]0, 1[$  the  $n$ -fold multigrid  $G_n(r)$  is regular. We reformulate it using Proposition 5.3.1 as:

for any even  $n \geq 4$  and any non-zero rational offset  $r \in \mathbb{Q} \cap ]0, 1[$ , for any  $0 < q < p < n$  and any  $r_0 \in \mathbb{Z} - r$ ,  $r_p \in \mathbb{Z} - r$  and  $r_q \in \mathbb{Z} - r$  we have

$$r_0 \sin \frac{(p-q)\pi}{n} + r_p \sin \frac{q\pi}{n} - r_q \sin \frac{p\pi}{n} \neq 0.$$

We will prove this by contradiction. Let  $n \geq 4$  be an even integer and  $r$  be a non-zero rational offset. Suppose that there exists  $p, q, r_0, r_p, r_q$  with  $p, q$  integers,  $0 < q < p < n$  and  $r_0 \in \mathbb{Z} - r$ ,  $r_p \in \mathbb{Z} - r$  and  $r_q \in \mathbb{Z} - r$ , such that

$$r_0 \sin \frac{(p-q)\pi}{n} + r_p \sin \frac{q\pi}{n} - r_q \sin \frac{p\pi}{n} = 0.$$

We apply Lemma 5.5.1 with the fact that since  $0 < \frac{p\pi}{n}, \frac{q\pi}{n}, \frac{(p-q)\pi}{n} < \pi$  we have  $\varepsilon(\frac{k\pi}{n}) = 1$  and  $\varphi(\frac{k\pi}{n}) = (-1)^{\lfloor \frac{2k}{n} \rfloor} (\frac{\pi}{2} - \theta)$  for  $k \in \{p, q, (p-q)\}$ . We obtain

$$r_0 \cos \theta_0 + r_p \cos \theta_q - r_q \cos \theta_p = 0$$

with  $\theta_0 = \varphi(\frac{(p-q)\pi}{n})$ ,  $\theta_p = \varphi(\frac{p\pi}{n})$  and  $\theta_q = \varphi(\frac{q\pi}{n})$ . And since  $0 < \frac{p\pi}{n}, \frac{q\pi}{n}, \frac{(p-q)\pi}{n} < \pi$  we have  $\theta_0, \theta_p, \theta_q \in [0, \frac{\pi}{2}[$ . In particular since  $n$  is even we can have  $\frac{p\pi}{n} = \frac{\pi}{2}$  which means that we can have  $\theta_p = 0$  (and also for  $\theta_0$  or  $\theta_q$ ). Note also that with  $n$  even (contrary to the odd case) we can have  $\theta_0 = \theta_p = \theta_q$ , for example with  $n = 6$ ,  $q = 2$  and  $p = 4$  we have  $\theta_0 = \theta_p = \theta_q = \frac{\pi}{6}$ . Which means that now we have a disjunction of four cases:

1.  $\theta_0 = \theta_p = \theta_q$
2.  $0 < \theta_0, \theta_p, \theta_q < \frac{\pi}{2}$  and not all equal
3. two of the angles are 0 and the other one is not
4. one of the angles is 0 and the other two are not

The first case reduces to  $(r_0 + r_p - r_q) \cos \theta_0 = 0$  and with  $\theta_0 \in [0, \frac{\pi}{2}[$  we have  $\cos \theta_0 \neq 0$  so  $(r_0 + r_p - r_q) = 0$  but this is impossible because  $(r_0 + r_p - r_q) \in \mathbb{Z} - r$  and  $0 \notin (\mathbb{Z} - r)$  for  $r \in (\mathbb{Q} \cap ]0, 1[)$ .

The second case is the same as the one discussed in Subsection 5.5.1 above, the main thing we used in the proof for odd  $n$  is the fact that  $\frac{2p\pi}{n} = \frac{2q\pi}{n} + \frac{2(p-q)\pi}{n}$  but we have the same for even  $n$  with  $\frac{p\pi}{n} = \frac{q\pi}{n} + \frac{(p-q)\pi}{n}$ . So the proof holds and this case is impossible.

The third case is impossible because for two angles to be 0, we need two of  $\{\frac{p\pi}{n}, \frac{q\pi}{n}, \frac{(p-q)\pi}{n}\}$  to be  $\frac{\pi}{2}$  but this is impossible with  $0 < q < p < n$ .

The fourth case reduces to  $A \cos a + B \cos b = C$  with  $A, B, C \in \mathbb{Z} - r \subset \mathbb{Q}$  so we can apply Corollary 5.4.2 and we get that either  $a = b = \frac{\pi}{3}$  or  $a = \frac{\pi}{5}$  and  $b = \frac{2\pi}{5}$ . The first subcase is impossible because  $\{\theta_0, \theta_p, \theta_q\} = \{0, \frac{\pi}{3}\}$  implies  $\{\frac{p\pi}{n}, \frac{q\pi}{n}, \frac{(p-q)\pi}{n}\} \subseteq \{\frac{\pi}{6}, \frac{\pi}{2}, \frac{5\pi}{6}\}$  and this is incompatible with  $\frac{p\pi}{n} = \frac{q\pi}{n} + \frac{(p-q)\pi}{n}$ . The second subcase is also impossible for the same reason as (up to interchanging  $\theta_0, \theta_p$  and  $\theta_q$ ) we would have  $\theta_0 = 0, \theta_p = \frac{\pi}{5}$  and  $\theta_q = \frac{2\pi}{5}$  which means that  $\frac{(p-q)\pi}{n} = \frac{\pi}{2}, \frac{p\pi}{n} \in \{\frac{3\pi}{10}, \frac{7\pi}{10}\}$  and  $\frac{q\pi}{n} \in \{\frac{\pi}{10}, \frac{9\pi}{10}\}$  and this is incompatible with  $\frac{p\pi}{n} = \frac{q\pi}{n} + \frac{(p-q)\pi}{n}$ .

Note that only in the first case we use the fact that the offset are all the same  $r \in \mathbb{Q} \cap ]0, 1[$ , the three other case work for any non-zero rational offsets as for the odd cases. And actually we could refine the condition because what is important here is that  $0 \notin (\mathbb{Z} - \gamma_0 - \gamma_q + \gamma_p)$  with  $\gamma_0, \gamma_p$  and  $\gamma_q$  the rational offsets. So for even  $n$  if we have a tuple of rational offsets  $\gamma = (\gamma_i)_{0 \leq i < n}$  such that for any distinct  $i, j, k$  we have  $\gamma_i - \gamma_j - \gamma_k \neq 0$  then the multigrid  $G_n(\gamma)$  is regular.



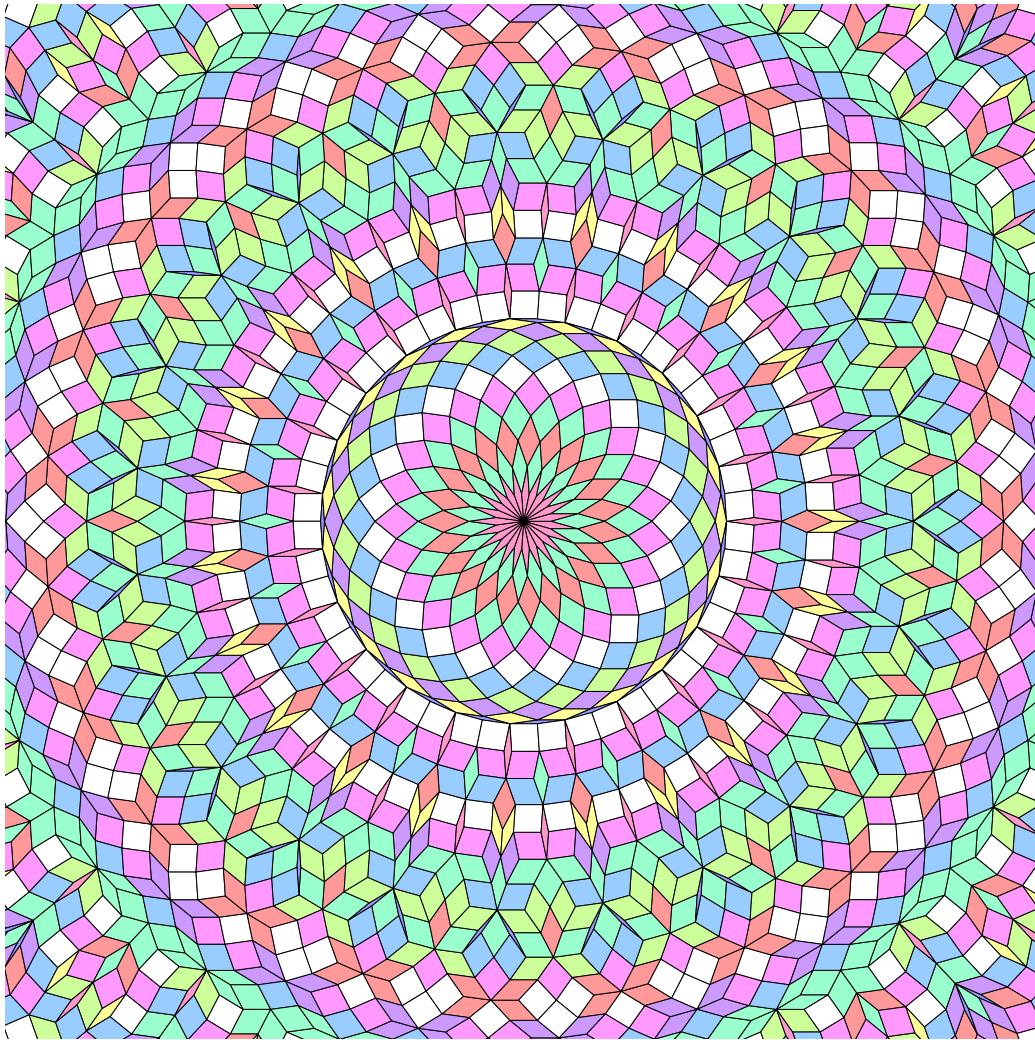


Figure 5.3: A central patch of the multigrad dual tiling  $P_{23}(\frac{1}{23})$  with 23-fold rotational symmetry.

# Chapter 6

## Examples of tilings

In this chapter we present examples of rhombus edge-to-edge tilings that can be lifted in some  $\mathbb{R}^n$ . Some of these tilings are discrete planes and some are not, some of these tilings are substitution tilings and some are not necessarily (no substitution was found for them). I have decided to classify them by the dimension  $n$  to which we lift them (which means that they have  $n$  edge directions and that they have at most  $2n$ -fold rotational symmetry), for simplicity we call them  $n$ -fold tilings.

Note that here we present specific tilings rather than necessarily tiling spaces and that all the tilings we present have global  $n$ -fold or  $2n$ -fold rotational symmetry, in the figures the center of symmetry is at the center of the figure.

In the following tilings the colours are not labels, they are just there to help differentiate the different tile shapes and also to help recognize patterns. The choice of colours for tilings is always complicated and the notion of good choice of colours is highly subjective. The Sub Rosa tilings for  $n \in \{4, 6, 7\}$  are in shades of grey, the Planar Rosa tilings (and Sub Rosa 5 because it is equal to Planar Rosa 5) are in light “pastel” colours and the multigrid duals are in stronger colours.

The  $n$ -fold multigrid dual tilings figures presented in this chapter were computed using the SageMath program publicly available in [Lut21b].

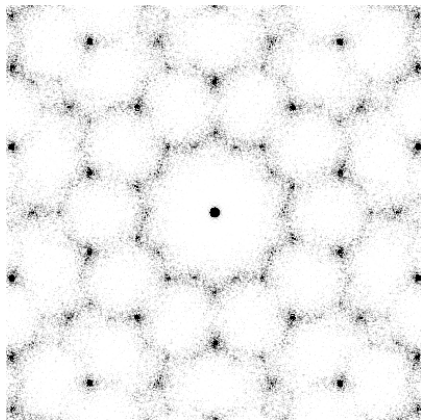
In this chapter we also show experimental diffraction patterns that we compute from fragments of the tilings, see Figures 6.10, 6.16, 6.23 and 6.34.

These diffraction patterns confirm that the  $n$ -fold multigrid dual tilings (including Ammann-Beenker and Penrose) have pure-point diffraction pat-

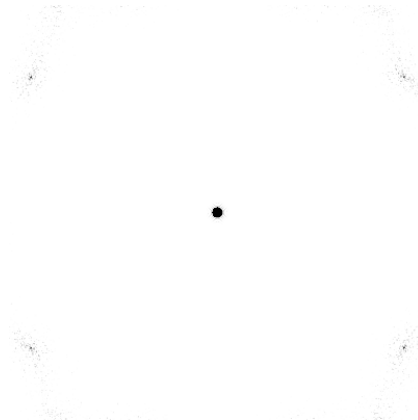
tern which was expected since they are canonical cut-and-project tilings.

The experimental diffraction patterns for the Planar Rosa tilings seem to be essentially discrete which was expected since they are quasiperiodic discrete planes. Given the size of the fragments (a few tens of thousands of vertices) compared to the size of the substitution (a few hundred vertices in the biggest metatiles) these experimental diffraction patterns are not conclusive. Note also that the way we tile the interior of the Planar Rosa metatiles affects the diffraction pattern, and especially when we use a “small” fragment to compute the diffraction pattern.

The experimental diffraction patterns for the Sub Rosa tilings (for  $n \neq 5$ ) are comparatively “noisy” and do not seem to be essentially discrete : there are bright peaks but a lot of small peaks around. The fact that there are bright peaks even if the tilings are not discrete planes is probably due to the fact that the Sub Rosa tilings are quasiperiodic (and even linearly recurrent) so they still have some long-range order. Note also that the diffraction pattern of a small fragment of any edge-to-edge rhombus tiling (even a random tiling) has peaks, see for example the diffraction pattern of a fragment of a random tiling with rhombus tiles Figure 6.1. So the peaks in the experimental diffraction patterns of Sub Rosa tilings might be due in big part to the fact that we did not use large enough fragments.



(a) Fragment of 2000 vertices.



(b) Fragment of 20000 vertices.

Figure 6.1: The diffraction patterns of two fragments of different size of the same random tiling. Though there is no long-range order in this tiling, the diffraction pattern of the small fragment has bright peaks.

## 6.1 4-fold tilings

In this section we present three rhombus tilings which have 4 edge directions and that we lift in  $\mathbb{R}^4$ .

The first tiling we present is the canonical Ammann-Beenker tiling which has global 8-fold rotational symmetry and is both a tetragrid dual tiling (hence a cut-and-project tiling) and a substitution tiling. The second tiling we present is the canonical Sub Rosa 4 tiling which is a substitution tiling with global 8-fold rotational symmetry but is not a discrete plane. The third tiling we present is the Planar Rosa 4 tiling which is a substitution discrete plane with global 8-fold rotational symmetry.

The Ammann-Beenker tiling and the Planar Rosa 4 tiling have the same slope  $\mathcal{E}_4^0$ . Note also that the Ammann-Beenker substitution is much smaller than the Planar Rosa substitution which means that it is much easier to work with, however the Ammann-Beenker substitution breaks the symmetries of the tiles (the image of the square tile by the substitution does not have the symmetries of the square, see Figure 6.2) which means that in essence the Ammann-Beenker substitution is applied on labelled tiles (each square has an orientation) whereas the Planar Rosa 4 substitution preserves the symmetries of the tiles (see Figure 6.7).

### 6.1.1 Ammann-Beenker

The Ammann-Beenker (canonical) tiling was already presented in Section 2.8 page 52. In particular it is both the tetragrid or 4-fold multigrad dual tiling  $P_4(\frac{1}{2})$  and the fixpoint of the substitution  $\sigma_{AB}$  from the star  $S(4)$ .

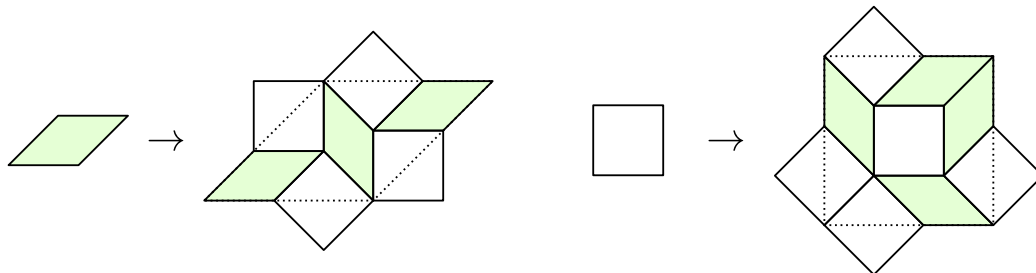


Figure 6.2: The Ammann-Beenker substitution.

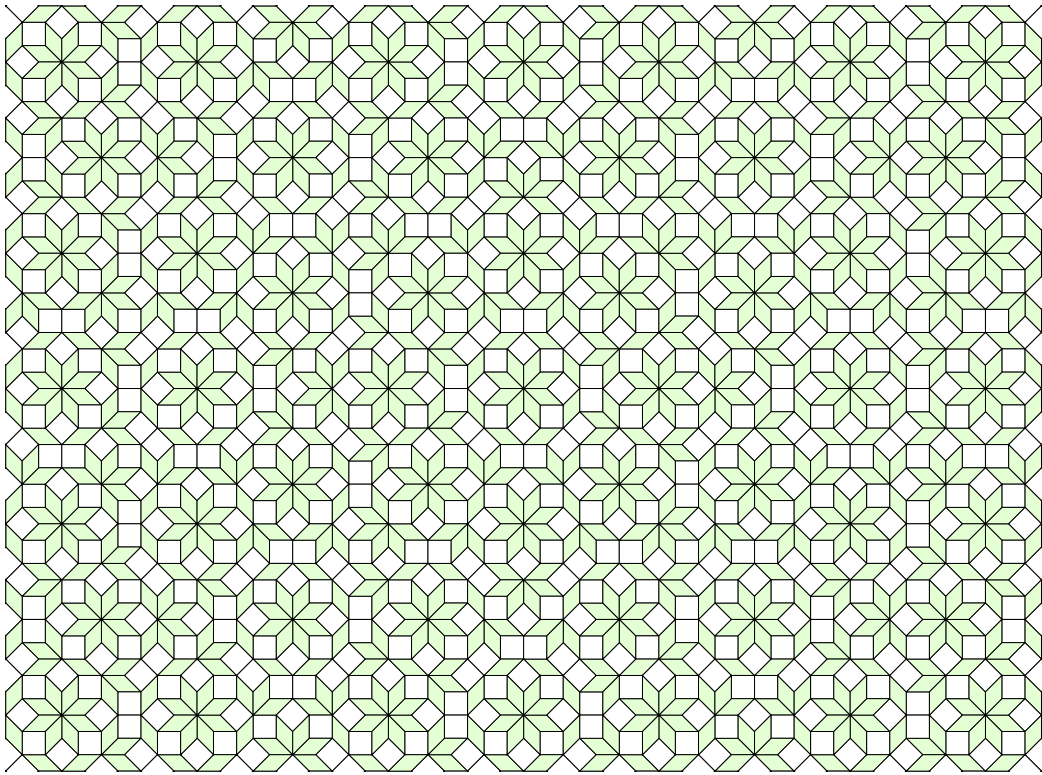


Figure 6.3: A fragment of the (canonical) Amman-Beenker tiling.

### 6.1.2 Sub Rosa 4

The (canonical) Sub Rosa 4 tiling (see Figures 6.5 and 6.6) is the regular fixpoint of the Sub Rosa substitution  $\sigma_4$  (see Figure 6.4) from the rosa  $R(4)$  (or equivalently from the star  $S(4)$ ) and is not a discrete plane.

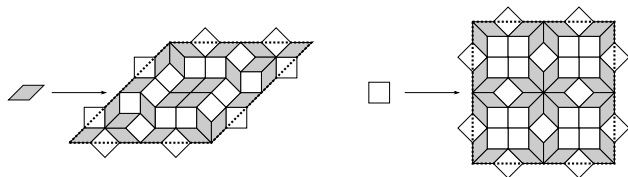


Figure 6.4: The Sub Rosa substitution  $\sigma_4$ .

The fact that it is not a discrete plane is stated in Theorem 1 and discussed and proved in Chapter 3, it is due to the fact that the underlying expansion  $\varphi_4$  is strictly expanding along the full space  $\mathbb{R}^4$ . More precisely  $\varphi_4$  has eigenspaces  $\mathcal{E}_4^0$  and  $\mathcal{E}_4^1$  with eigenvalues  $\lambda_0 \approx 6.83$  and  $\lambda_1 \approx 1.17$ , for more details on this see Section 3.5 page 91.

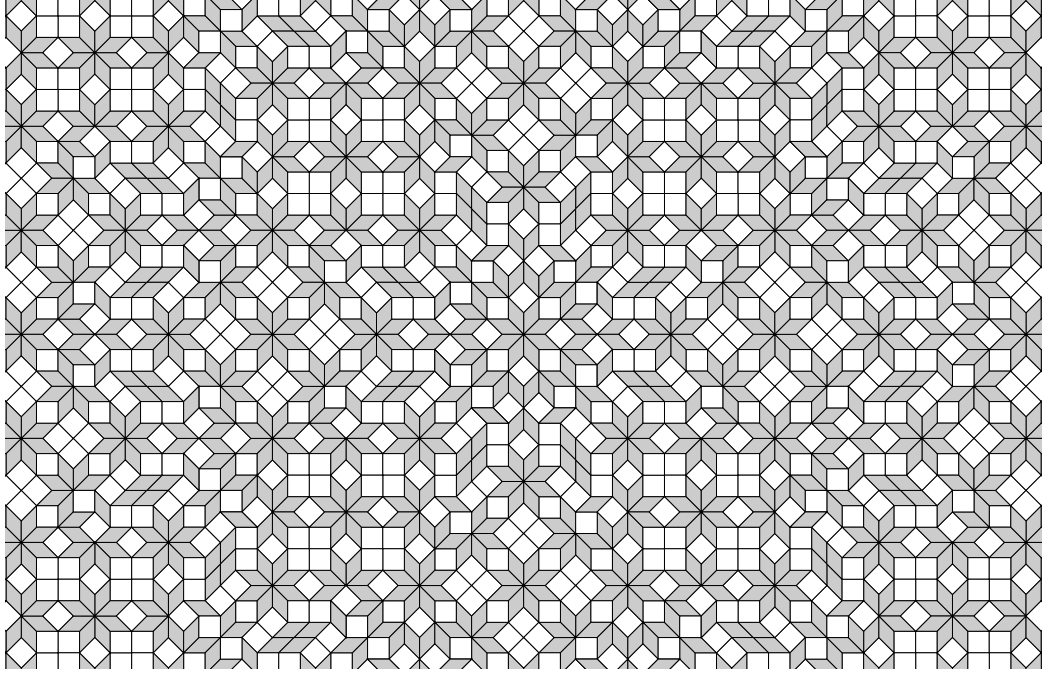


Figure 6.5: A fragment of the (canonical) Sub Rosa 4 tiling.

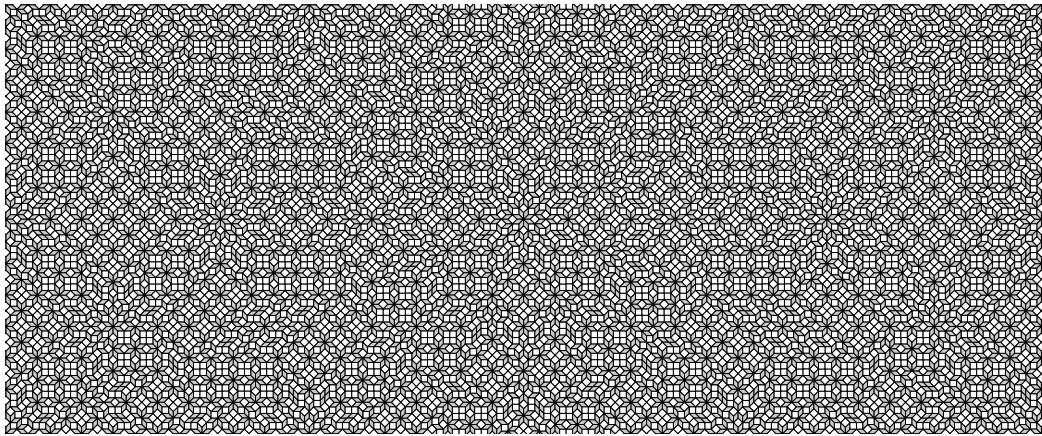


Figure 6.6: A bigger fragment of the Sub Rosa 4 tiling.

### 6.1.3 Planar Rosa 4

The (canonical) Planar Rosa 4 tiling is the regular fixpoint of the Planar Rosa substitution  $\sigma'_4$  from the star  $S(4)$  and is discrete plane. See Figure 6.7 for the substitution  $\sigma'_4$  and see Figures 6.8 and 6.9 for the (canonical) Planar Rosa 4 tiling.

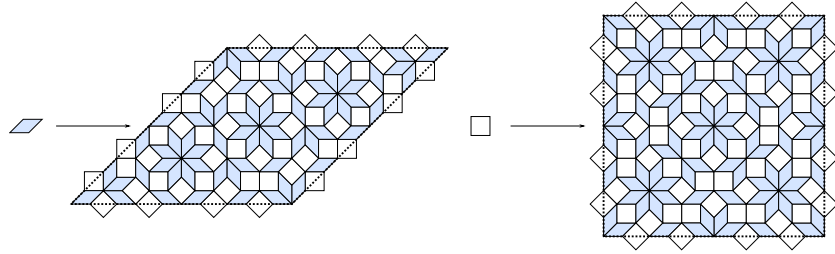


Figure 6.7: The Planar Rosa 4 substitution  $\sigma'_4$ .

The substitution  $\sigma'_4$  is defined by its edgeword  $\Sigma$  which is of the form  $\Sigma_{(j)} = \text{pref}_j(\omega)\overline{\text{pref}_j(\omega)}$  with  $\omega$  the infinite billiard word of direction  $\gamma = (\cos \frac{i\pi}{4})_{0 \leq i < 2}$ . For more details see Subsection 4.5.2 page 132.

$$\omega = 02020020202002020020202002020020202002020200202002020 \dots$$

In Table 6.1 we present the edgewords  $\Sigma_{(j)}$  of the candidates for  $\sigma'_4$ .  $\sigma'_4$  is the first one that is both planar and tileable as a primitive substitution with the corner condition, for more details see Subsection 4.5.2.

Table 6.1: Edgeword, approximate eigenvalues, planarity and tileability of candidates for  $\sigma'_4$ .

$\Sigma_{(j)}$	$\lambda_0$	$\lambda_1$	Planar	Tileable
00	2	2	No	No
0220	4.83	-0.83	Yes	No
020020	6.83	1.17	No	Yes
02022020	9.66	-1.66	No	No
0202002020	11.66	0.34	Yes	Yes

So  $\sigma'_4$  is defined by its edgeword  $\Sigma_{(5)} = 0202002020$ . See Figure 6.7 for the substitution  $\sigma'_4$  and Figure 6.8 for the Planar Rosa 4 tiling.

Remark that the edgeword  $\Sigma_{(3)}$  defines the Sub Rosa 4 substitution and as discussed before it is not planar.



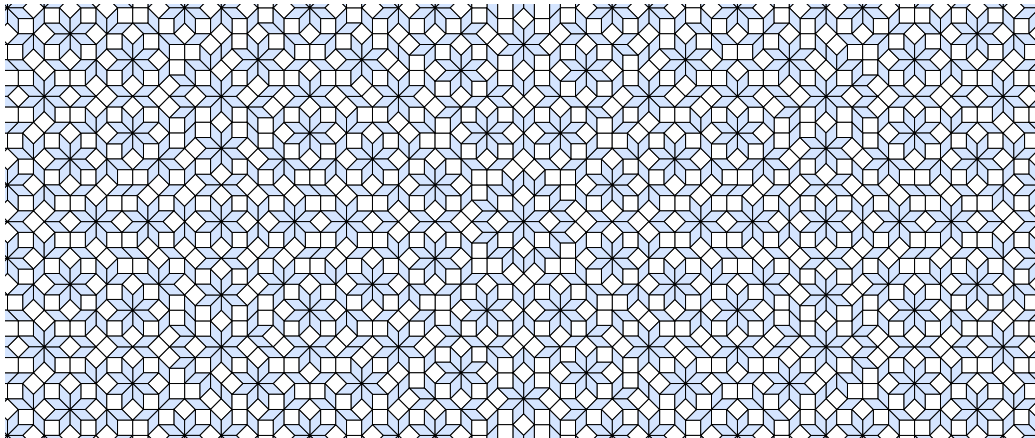


Figure 6.8: A small central fragment of the Planar Rosa 4 tiling.

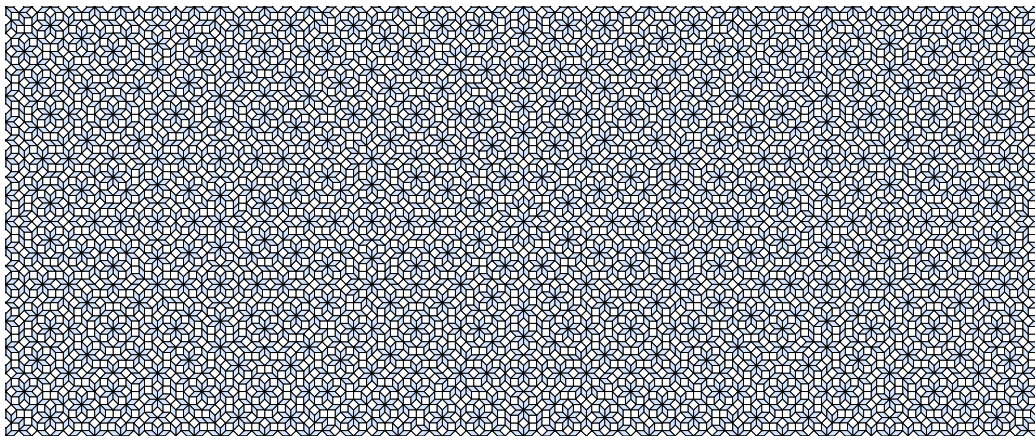


Figure 6.9: A bigger central fragment of the Planar Rosa 4 tiling

### 6.1.4 Diffraction patterns of 4-fold tiling

In Figure 6.10 we show experimental diffraction patterns computed from fragments of the Ammann-Beenker, Sub Rosa 4 and Planar Rosa 4 tilings.

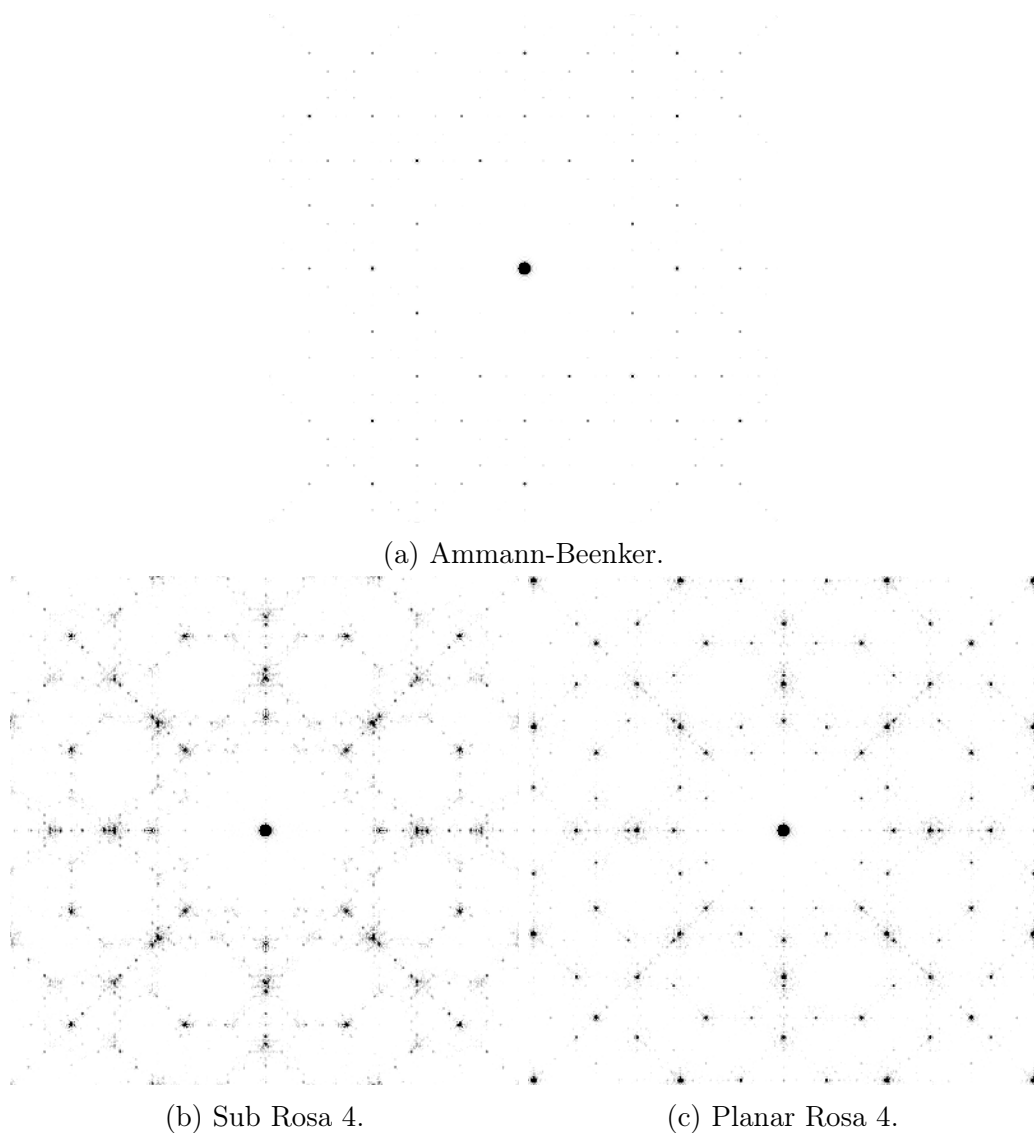


Figure 6.10: Experimental diffraction patterns from central fragments of 4-fold tilings with 20000 vertices.

The experimental diffraction pattern of the Ammann-Beenker tiling (Figure 6.10a) is pure-point and shows a strong long-range order which was expected because it is a cut-and-project tiling.

The experimental diffraction pattern of the Planar Rosa 4 tiling (Figure 6.10c) seems to be essentially discrete and suggests that the Planar Rosa 4 tiling has long-range order.

The experimental diffraction pattern of the Sub Rosa 4 tiling (Figure 6.10b) does not seem to be essentially discrete (though there are some bright peaks there are quite a lot a small peaks) which suggests that it has little long-range order .

## 6.2 5-fold tilings

In this section we present three rhombus tilings which have 5 edge directions and that we lift in  $\mathbb{R}^5$ . The first tiling we present is the Penrose rhombus tiling which has global 5-fold rotational symmetry and is both a pentagrid (5-fold multigrid) dual tiling and a substitution tiling, the second is the Anti-Penrose rhombus tiling which has global 10-fold rotational symmetry and is also a pentagrid but (to our knowledge) is not a substitution tiling, the third tiling we present is both the Sub Rosa 5 and Planar Rosa 5 tiling (both construction give the same substitution  $\sigma_5 = \sigma'_5$  and same canonical tiling) which is a substitution discrete plane with global 10-fold rotational symmetry.

Note that all three tilings have the same slope  $\mathcal{E}_5^0$ . Note also that the Penrose substitution is much smaller than the Sub Rosa 5 (and Planar Rosa 5) substitution, however the Penrose substitution breaks the symmetries of the tiles whereas the Sub Rosa 5 (and Planar Rosa 5) substitution preserves the symmetries of the tiles.

### 6.2.1 Penrose

The canonical Penrose tiling was discussed details in Section 2.7 page 46, here we will just recall that it can be defined as the pentagrid (5-fold multigrid) dual tiling  $P_5(\frac{1}{5})$ . This tiling is cut-and-project, has global 5-fold rotational symmetry and is also a substitution tiling.

Remark however that in the Penrose substitution (see Figure 2.31 page 50) the image of two parallel edges are not parallel and that the substitution

does not preserve the symmetries of the tiles. This means that in essence the substitution is applied on labelled tiles (and can not be applied to any patch of tiles) and is hard to manipulate when lifted in  $\mathbb{R}^5$  in the sense that its expansion does not naturally lift to a linear application. No “nice” substitution (in the sense that it would preserve the symmetries of the tile and be easily lifted in  $\mathbb{R}^5$ ) is known for the Penrose tiling.

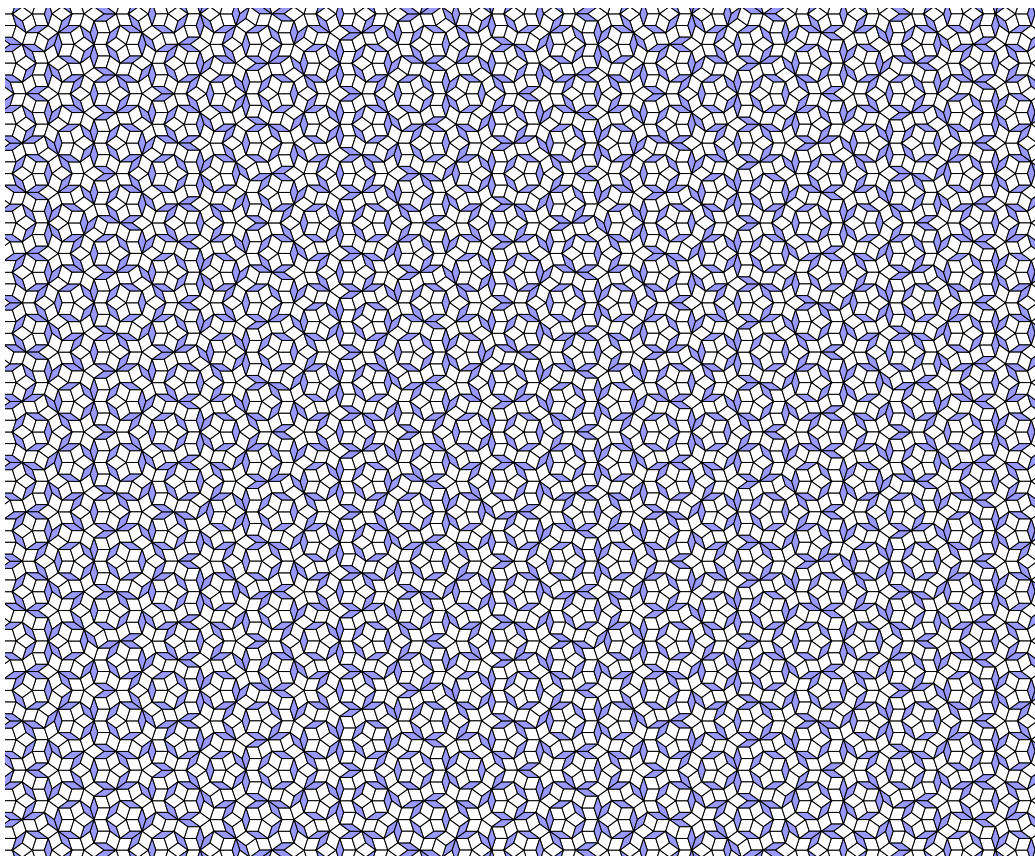


Figure 6.11: The (canonical) Penrose tiling.

### 6.2.2 Anti-Penrose

The pentagrid dual tiling  $P_5(\frac{1}{2})$  is sometimes called Anti-Penrose rhombus tiling and is a cut-and-project tiling with global 10-fold rotational symmetry.

To our knowledge it is unknown whether it is a substitution tiling or not.

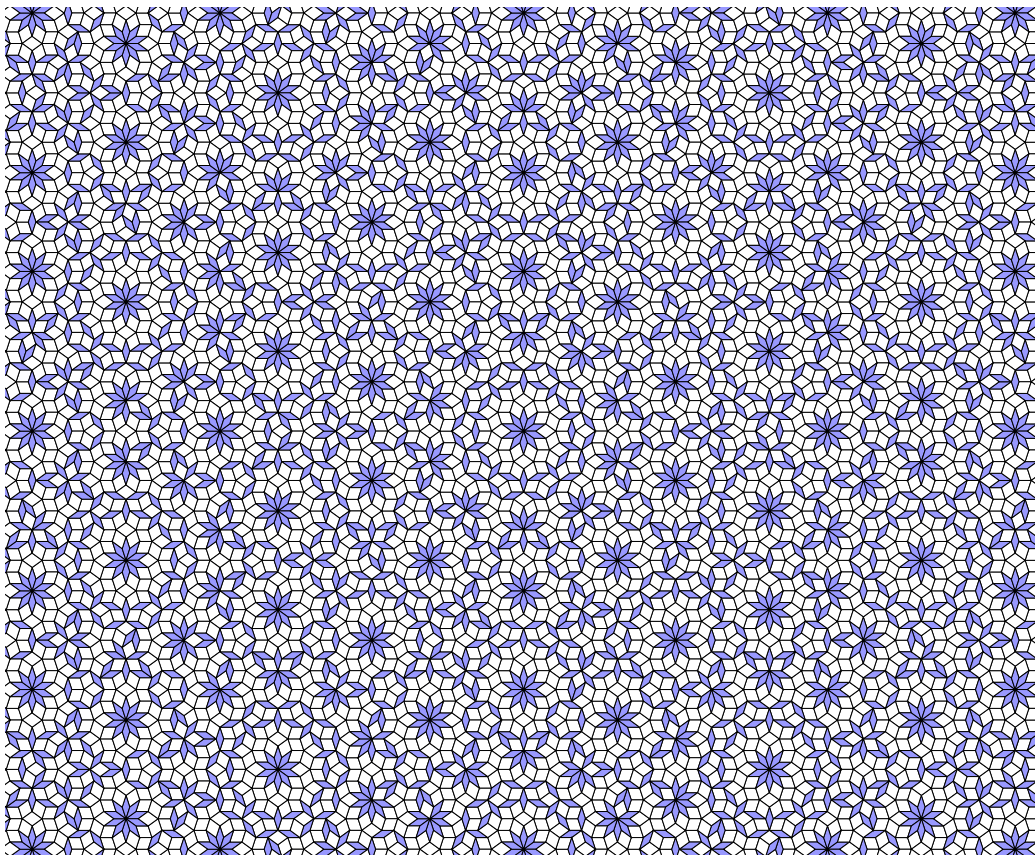


Figure 6.12: The Anti-Penrose tiling.

### 6.2.3 Sub Rosa 5

The Sub Rosa 5 tiling is a regular fixpoint for the Sub Rosa substitution  $\sigma_5$  from the rosa  $R(5)$  (or equivalently from the star  $S(5)$ ) and is a discrete plane of slope  $\mathcal{E}_5^0$ . The fact that it is a discrete plane is stated in Theorem 1 and discussed and proved in Chapter 3 and is due to the fact that the underlying expansion  $\varphi_5$  is strictly expanding along  $\mathcal{E}_5^0$  and strictly contracting along the orthogonal subspace. The Sub Rosa expansion  $\varphi_5$  has two 2-dimensional eigenspaces  $\mathcal{E}_5^0$  and  $\mathcal{E}_5^1$  and one 1-dimensional eigenspace  $\Delta$  with eigenvalues  $\lambda_0$ ,  $\lambda_1$  and  $\lambda_\Delta$ . We have:

$$|\lambda_0| \approx 9.96 \quad |\lambda_1| \approx 0.90 \quad \lambda_\Delta = 0.$$



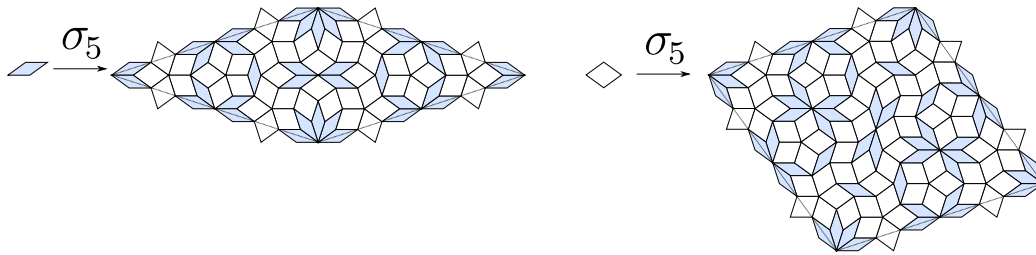


Figure 6.13: The Sub Rosa 5 substitution  $\sigma_5$ .

The substitution  $\sigma_5$  is represented in Figure 6.13 and a fragment of the Sub Rosa 5 tiling is represented in Figure 6.14.

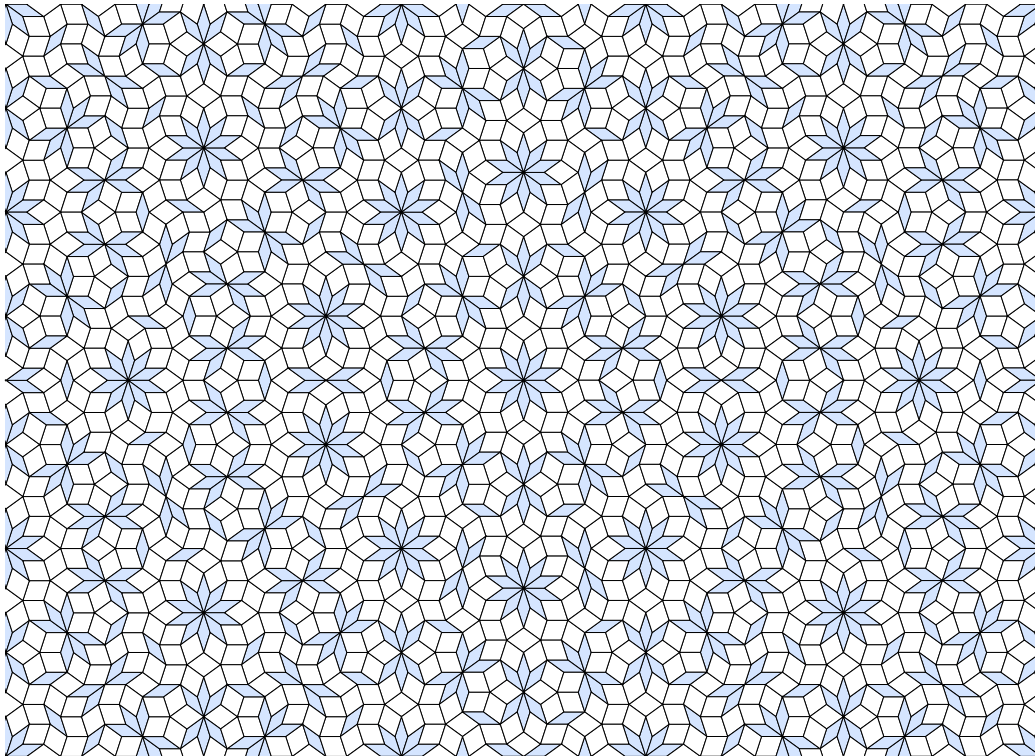


Figure 6.14: The Sub Rosa 5 tiling.

### 6.2.4 Planar Rosa 5

The Planar Rosa 5 tiling is the regular fixpoint of the Planar Rosa substitution  $\sigma'_5$  from the star  $S(5)$  and is discrete plane.

The substitution  $\sigma'_5$  is defined by its edgeword  $\Sigma$  which is of the form  $\Sigma_{(j)} = \overline{pref_j(\omega)pref_j(\omega)}$  with  $\omega$  the infinite billiard word of direction  $\gamma = (\cos \frac{(2i+1)\pi}{10})_{0 \leq i < 5}$ . For more details see Section 4.4 page 118.

$$\omega = 1313113113131131131131311313113113131131311311313113131131131131 \dots$$

In Table 6.2 we show the edgewords  $\Sigma_{(j)}$  of the candidates for  $\sigma'_5$ .  $\sigma'_5$  is the first one that is both planar and tileable as a primitive substitution.

Table 6.2: Edgeword, approximate eigenvalues, planarity and tileability of candidates for  $\sigma'_5$ .

$\Sigma_{(j)}$	$ \lambda_0 $	$ \lambda_1 $	$\lambda_\Delta$	Planar	Tileable
11	3.80	2.35	0	No	No
1331	4.16	1.45	0	No	No
131131	9.96	0.90	0	Yes	Yes

So actually  $\sigma'_5$  is defined as having edge word 131131 which is the same as the edgeword of the Sub Rosa substitution  $\sigma_5$  presented in Figure 6.13. We can therefore define it as identical to Sub Rosa 5 (see Figure 6.14), however any way of tiling the Sub Rosa-like metatiles would work.

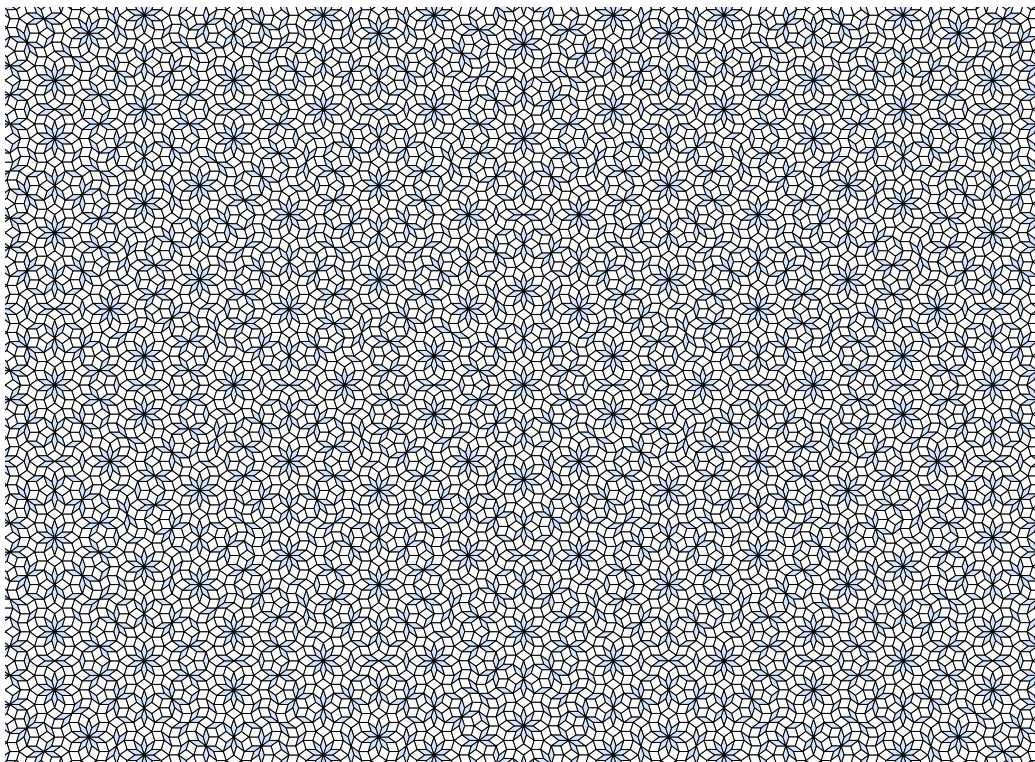


Figure 6.15: A bigger fragment of the (canonical) Sub Rosa 5 tiling.

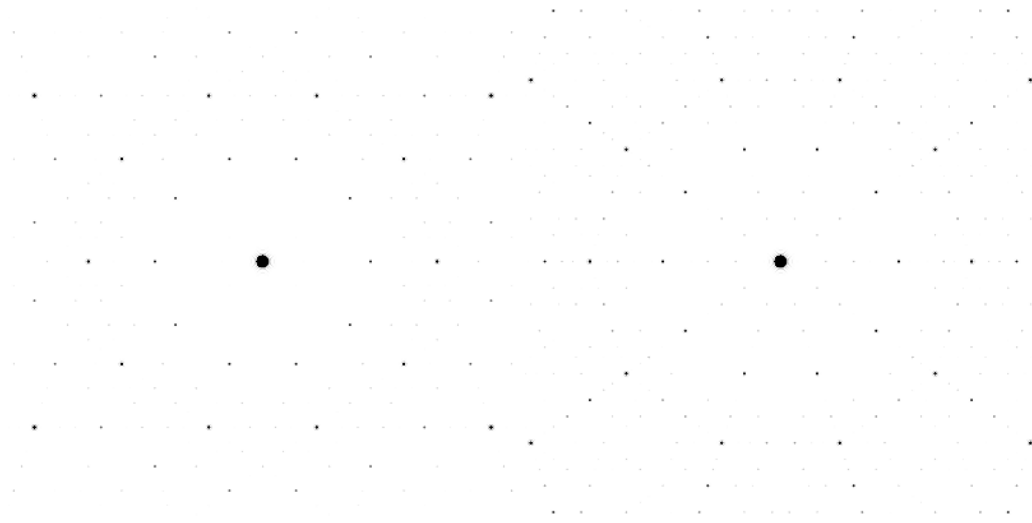
### 6.2.5 Diffraction patterns of 5-fold tilings

In Figure 6.16 we show experimental diffraction patterns computed from fragments of the Penrose, Anti-Penrose and Sub Rosa 5 tilings, recall that Planar Rosa 5 and Sub Rosa 5 are the same tiling.

The Penrose and the Anti-Penrose tilings have pure-point diffraction patterns and the Sub Rosa 5 / Planar Rosa 5 tiling seems to have essentially discrete diffraction pattern.

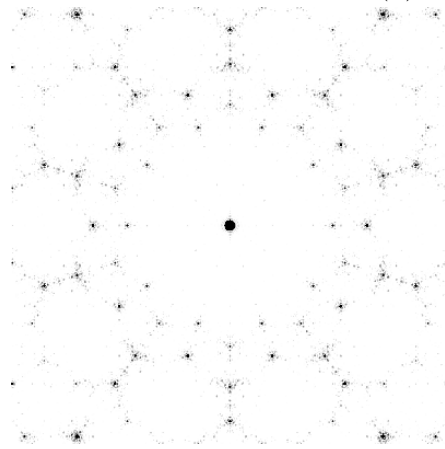
This illustrates the fact that the Penrose and Anti-Penrose tilings which are canonical cut-and-project have strong long-range order and the Sub Rosa 5 / Planar Rosa 5 tiling which is a quasiperiodic discrete plane also has long-range order.





(a) Penrose.

(b) Anti-Penrose.



(c) Sub Rosa 5 and Planar Rosa 5.

Figure 6.16: Experimental diffraction patterns from central fragments of 5-fold tilings with 30000 vertices.

## 6.3 6-fold tilings

In this section we present 3 rhombus tilings which have 6 edge directions and which we lift in  $\mathbb{R}^6$ .

The first tiling we present is the 6-fold multigrad dual tiling  $P_6(\frac{1}{2})$  which is cut-and-project and has global 12-fold rotational symmetry however to our knowledge it is not a substitution tiling, the second tiling we present is the (canonical) Sub Rosa 6 tiling which is a substitution tiling with global 12-fold rotational symmetry however it is not a discrete plane, and the third tiling we present is the (canonical) Planar Rosa 6 tiling which is a substitution discrete plane with global 12-fold rotational symmetry.

Note that  $P_6(\frac{1}{2})$  and the (canonical) Planar Rosa 6 tiling have the same slope  $\mathcal{E}_6^0$ .

### 6.3.1 $P_6(\frac{1}{2})$

The tiling  $P_6(\frac{1}{2})$  in Figure 6.17 is a cut-and-project rhombus tiling with 12-fold rotational symmetry.

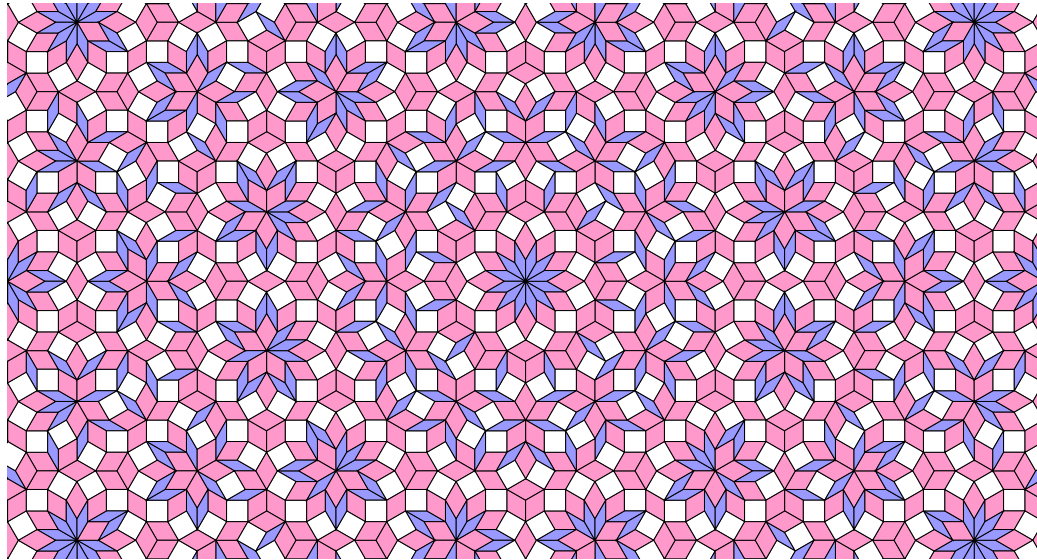


Figure 6.17:  $P_6(\frac{1}{2})$ .

### 6.3.2 Sub Rosa 6

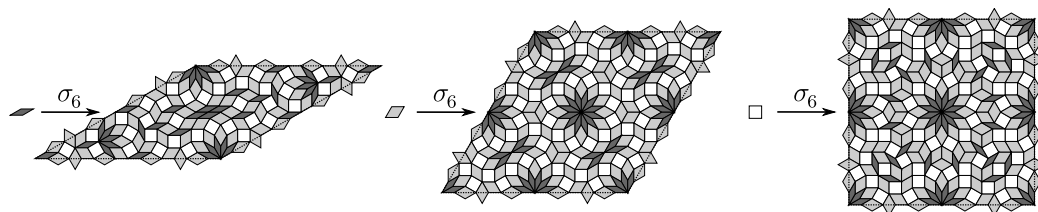


Figure 6.18: The  $\sigma_6$  substitution.

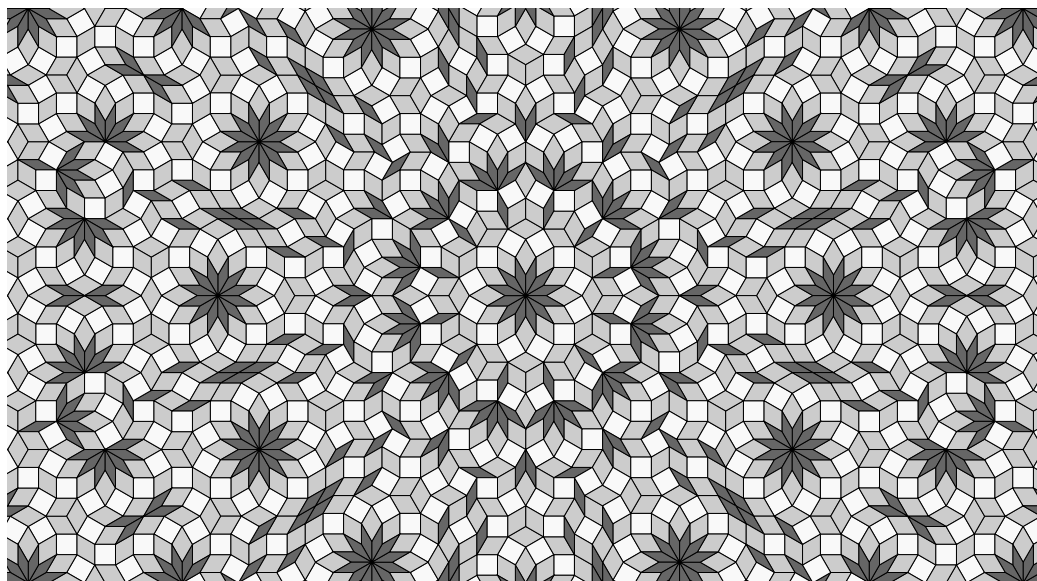


Figure 6.19: A small central fragment of the Sub Rosa 6 tiling.

The Sub Rosa 6 tiling of Figure 6.19 is defined as the fixpoint tiling of substitution  $\sigma_6$  represented in Figure 6.18 from the rosa  $R(6)$  (or equivalently from the star  $S(6)$ ). This substitution and its tilings are not planar, indeed the underlying expansion  $\varphi_6$  is expanding on the whole space  $\mathbb{R}^6$  more precisely on eigenspaces  $\mathcal{E}_6^0, \mathcal{E}_6^1$  and  $\mathcal{E}_6^2$  it has eigenvalues  $\lambda_0 \approx 14.93$ ,  $\lambda_1 = 2$  and  $\lambda_2 \approx 1.07$ . For more details see Section 3.5 page 91.

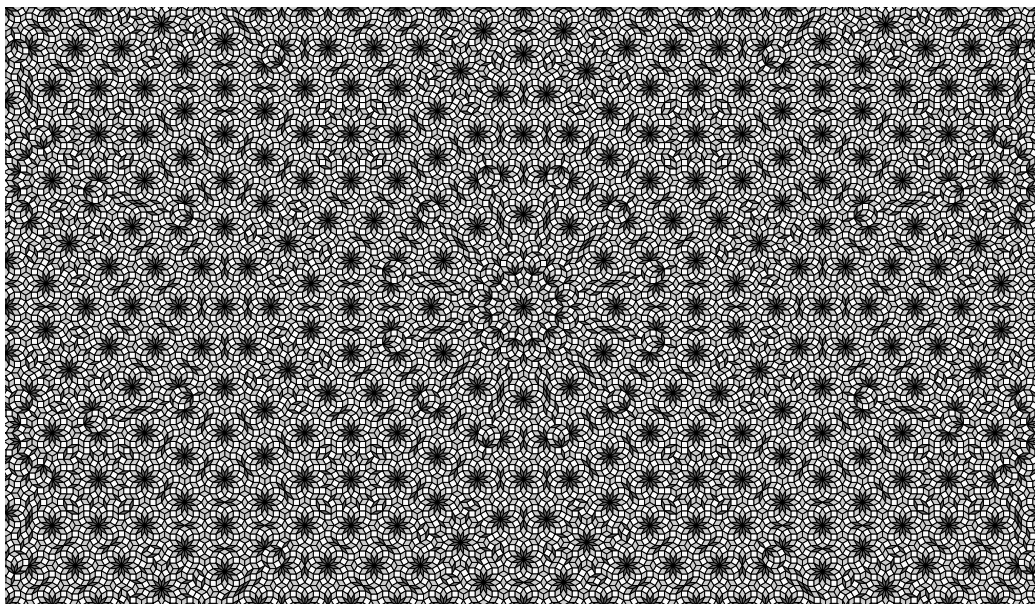


Figure 6.20: A bigger central fragment of the Sub Rosa 6 tiling.

### 6.3.3 Planar Rosa 6

The Planar Rosa 6 tiling in Figure 6.22 is defined as the fixpoint tiling of substitution  $\sigma'_6$  represented in Figure 6.21 from the star  $S(6)$ . By definition of  $\sigma'_6$  this tiling is a discrete plane and it has 12-fold rotational symmetry.

The substitution  $\sigma'_6$  is defined by its edgeward  $\Sigma$  which is of the form  $\Sigma_{(j)} = \overline{pref_j(\omega)pref_j(\omega)}$  with  $\omega$  the infinite billiard word of direction  $\gamma = (\cos \frac{i\pi}{6})_{0 \leq i < 3}$ . For more details see Subsection 4.5.2 page 132.

$$\omega = 024020240204202040202402024020420204020240204202042002 \dots$$

In Table 6.3 we show the candidates for  $\sigma'_6$ .  $\sigma'_6$  is the first one that is both planar and tileable as a primitive substitution with the corner condition.

So  $\sigma'_6$  is defined by its edgeward  $\Sigma_{(14)} = 0240202402042002402042020420$ . See Figure 6.21 for the substitution  $\sigma'_6$  and Figure 6.22 for the Planar Rosa 6 tiling.

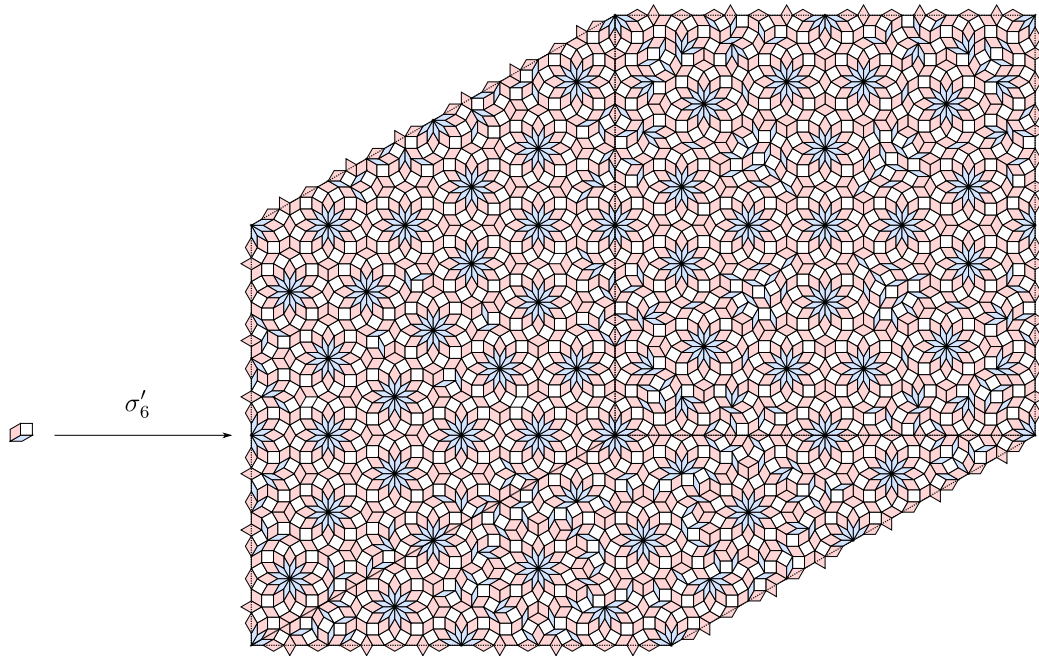


Figure 6.21: The  $\sigma'_6$  substitution.

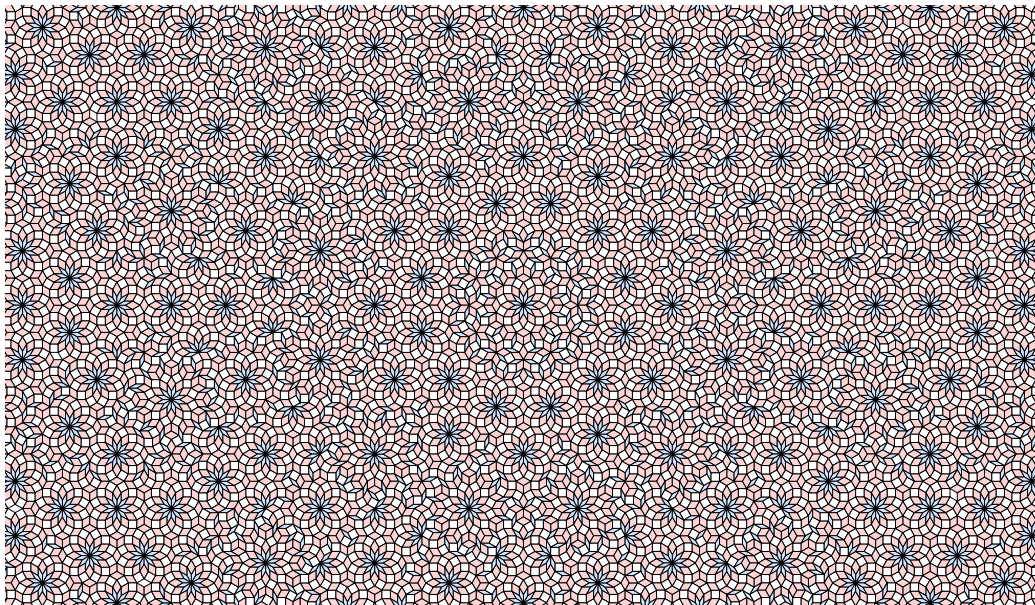


Figure 6.22: The Planar Rosa 6 tiling.

Table 6.3: Edgeward, approximate eigenvalues, planarity and tileability of candidates for  $\sigma'_6$ .

$\Sigma_{(j)}$	$\lambda_0$	$\lambda_1$	$\lambda_2$	Planar	Tileable
00	2	2	2	No	No
0220	5.46	2	-1.46	No	No
024420	7.46	-2	0.54	No	No
02400420	9.46	0	2.54	No	No
0240220420	12.92	0	-0.93	Yes	No
024020020420	14.93	2	1.07	No	Yes
02402022020420	18.39	2	-2.39	No	No
0240202442020420	20.39	-2	-0.39	No	No
024020240042020420	20.39	0	1.61	No	Yes
02402024022042020420	25.85	0	-1.86	No	No
0240202402002042020420	27.85	2	0.14	No	Yes
024020240204402042020420	29.86	-2	2.14	No	No
02402024020422402042020420	33.32	-2	-1.32	No	No
0240202402042002402042020420	35.32	0	0.68	Yes	Yes

### 6.3.4 Diffraction patterns of 6-fold tilings

In Figure 6.23 we show experimental diffraction patterns computed from fragments of the multigrad dual tiling  $P_6(\frac{1}{2})$ , the Sub Rosa 6 tiling and the Planar Rosa 6 tiling.

The  $P_6(\frac{1}{2})$  tiling has a pure-point diffraction pattern because it is a canonical cut-and-project tiling and has strong long-range order.

The Planar Rosa 6 tiling seems to have an essentially discrete diffraction pattern and the Sub Rosa 6 tiling does not seem to have an essentially discrete diffraction pattern.

These two diffraction pattern are not quite as different as the diffraction pattern of the 4-fold tilings, this might be due to the size of the fragment we uses to compute these diffraction pattern, it would seem that with high-order rotational symmetry and big substitutions we might need significantly bigger fragments to have significatively different diffraction pattern.

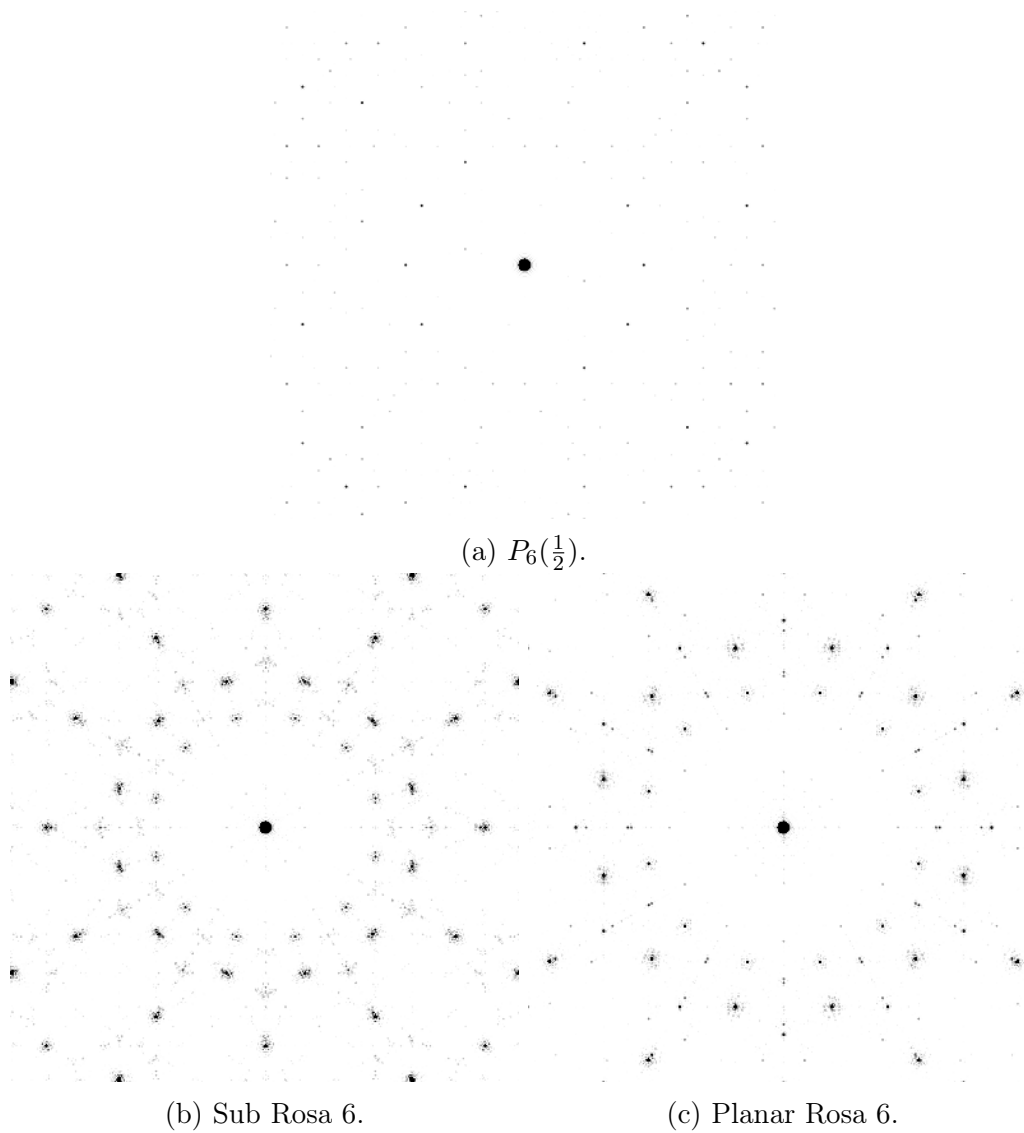


Figure 6.23: Experimental diffraction patterns computed from central fragments of 6-fold tilings with 30000 vertices.

## 6.4 7-fold tilings

In this section we present five rhombus tilings that can be lifted in  $\mathbb{R}^7$ , this means that they have 7 edge directions.

The first two tiling we present are the 7-fold multigrid dual tilings  $P_7(\frac{1}{7})$  and  $P_7(\frac{1}{2})$  which are cut-and-project tilings with respectively 7-fold and 14-fold global rotational symmetry but to our knowledge they are not substitution tilings. The third tiling we present is the (canonical) Sub Rosa 7 tiling which is a substitution tiling with global 14-fold rotational symmetry but it is not a discrete plane. The fourth tiling we present is the (canonical) Planar Rosa 7 tiling which is a substitution discrete plane with 14-fold rotational symmetry. The fifth and last tiling we present is an alternative substitution discrete plane with 14-fold rotational symmetry that has a smaller scaling factor than the Planar Rosa 7 substitution.

Note that  $P_7(\frac{1}{7})$ ,  $P_7(\frac{1}{2})$ , the Planar Rosa 7 tiling and the alternative 7-fold substitution discrete plane we present all have the same slope  $\mathcal{E}_7^0$ .

### 6.4.1 $P_7(\frac{1}{7})$ and $P_7(\frac{1}{2})$

The multigrid dual tilings  $P_7(\frac{1}{7})$  and  $P_7(\frac{1}{2})$  are quasiperiodic cut-and-project rhombus tilings with respectively 7-fold and 14-fold global rotational symmetry.



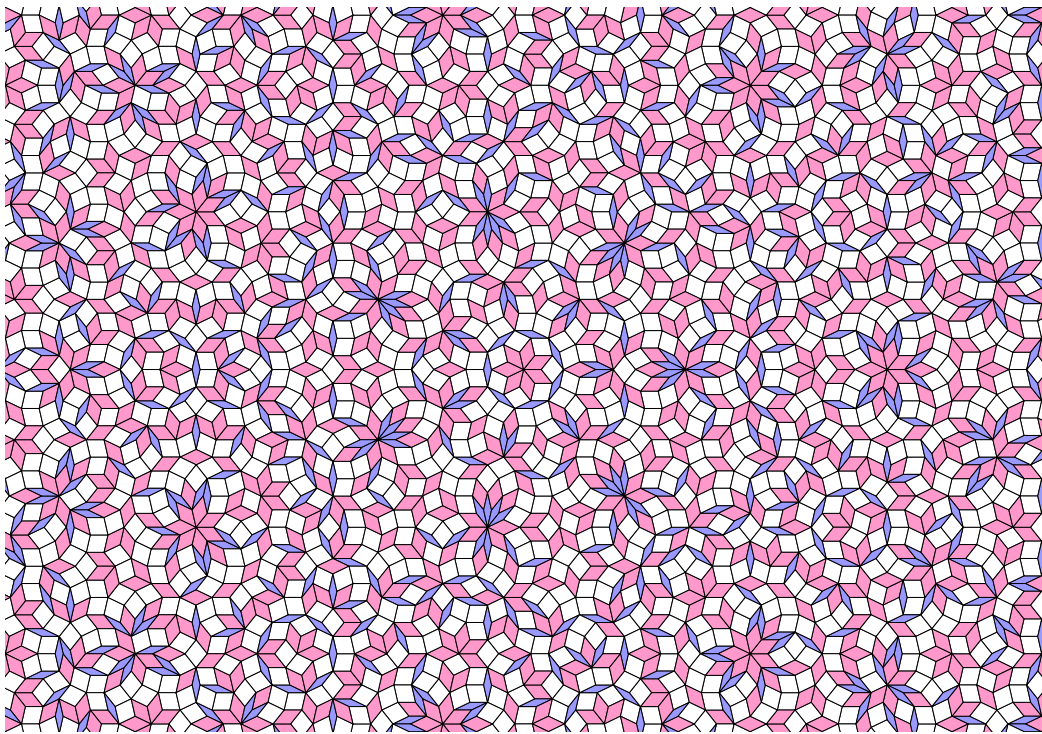


Figure 6.24:  $P_7(\frac{1}{7})$ .

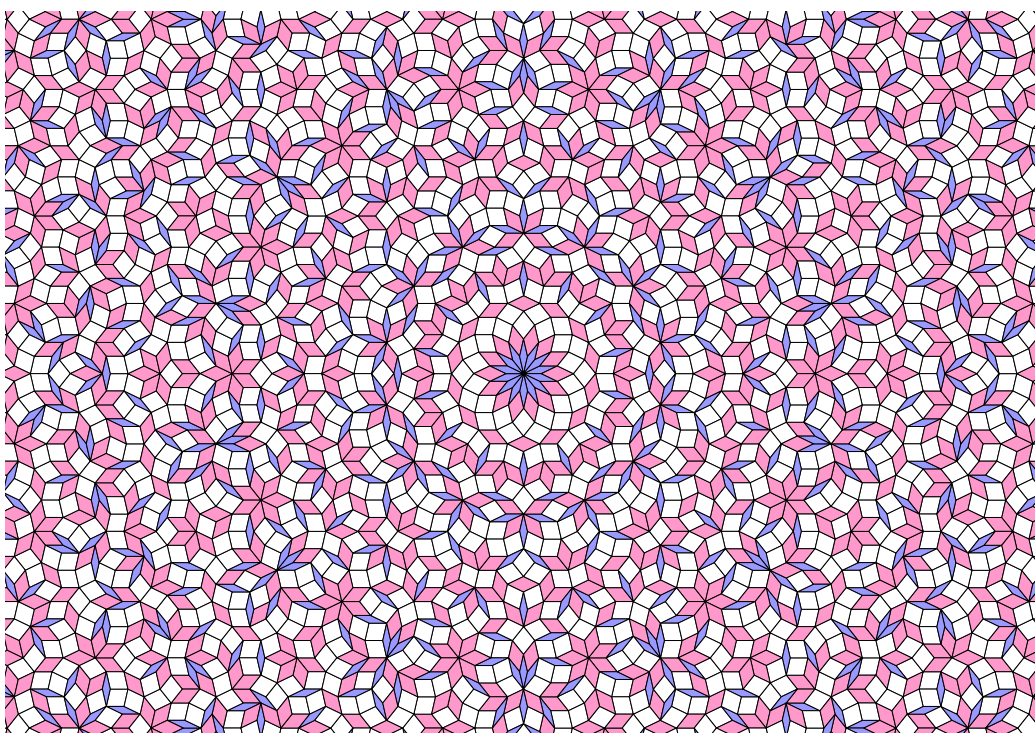


Figure 6.25:  $P_7(\frac{1}{2})$ .

## 6.4.2 Sub Rosa 7

The Sub Rosa 7 tiling is the fixpoint tiling of substitution  $\sigma_7$  represented in Figure 6.26 from the seed  $R(7)$ . This tiling has global 14-fold rotational symmetry but is not a discrete plane because the underlying expansion  $\varphi_7$  is strictly expanding along a subspace of dimension 4.

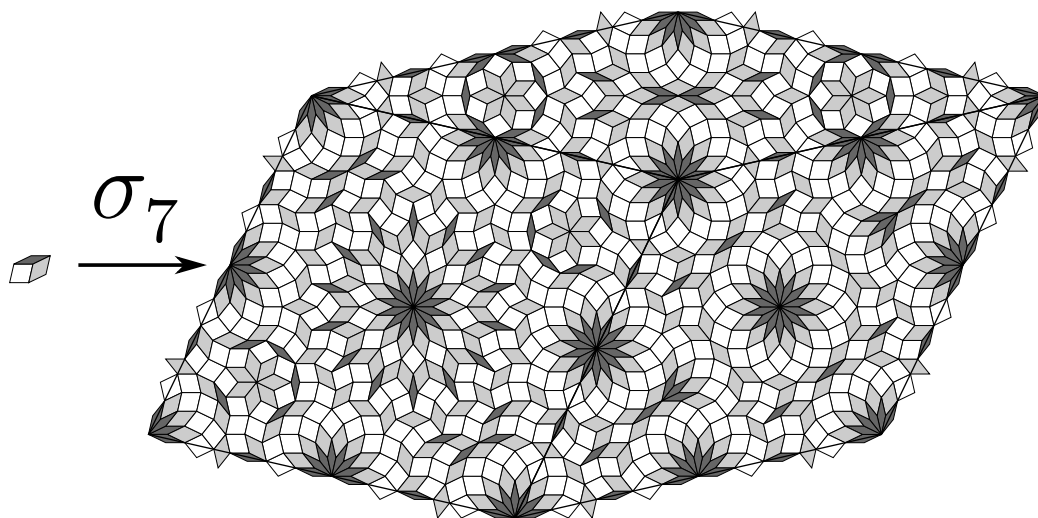


Figure 6.26: The substitution  $\sigma_7$ .

As detailed in Section 3.4 page 80 we decompose  $\mathbb{R}^7$  as the direct sum  $\mathcal{E}_7^0 \oplus \mathcal{E}_7^1 \oplus \mathcal{E}_7^2 \oplus \Delta$ , where  $\mathcal{E}_7^i$  and  $\Delta$  are eigenspaces of  $\varphi_7$ .  $\varphi_7$  has eigenvalues  $\lambda_0, \lambda_1, \lambda_2$  and  $\lambda_\Delta$  with

$$|\lambda_0| \approx 19.69$$

$$|\lambda_1| \approx 2.01$$

$$|\lambda_2| \approx 0.53$$

$$\lambda_\Delta = 0.$$

So  $\varphi_7$  is strictly expanding along  $\mathcal{E}_7^0 \oplus \mathcal{E}_7^1$  and is therefore not planar.

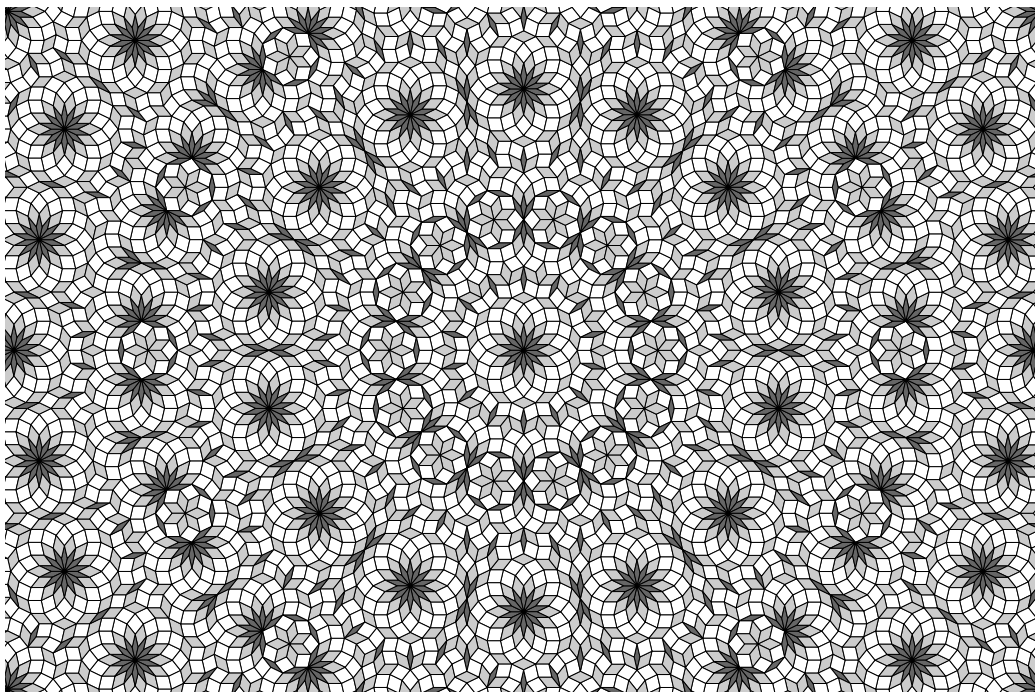


Figure 6.27: A fragment of the tiling Sub Rosa 7.

### 6.4.3 Planar Rosa 7

The Planar Rosa 7 tiling is the fixpoint tiling of substitution  $\sigma'_7$  represented in Figure 6.28 from the seed  $S(7)$ . By definition of  $\sigma'_7$  it is a discrete plane and it has global 14-fold rotational symmetry.

The substitution  $\sigma'_7$  is defined by its edgeword  $\Sigma$  which is of the form  $\Sigma_{(j)} = \text{pref}_j(\omega)\overline{\text{pref}_j(\omega)}$  with  $\omega$  the infinite billiard word of direction  $(\cos \frac{(2i+1)\pi}{14})_{0 \leq i < 3}$ . For more details see Section 4.4 page 118.

$$\omega = 13513135131135131531315131351313151313513153113513131531135 \dots$$

In Table 6.4 we show the candidates for  $\sigma'_7$ .  $\sigma'_7$  is the first one that is both planar and tileable as a primitive substitution.

So  $\sigma'_7$  is defined by its edgeword  $\Sigma = \Sigma_{(11)} = 1351313513113153131531$ . This substitution is huge: it has a scaling factor of approximately 35.48 and it has 22 bisected rhombuses on the edge of the metatiles. However we can find a smaller planar substitution if we deviate from the Planar Rosa construction.

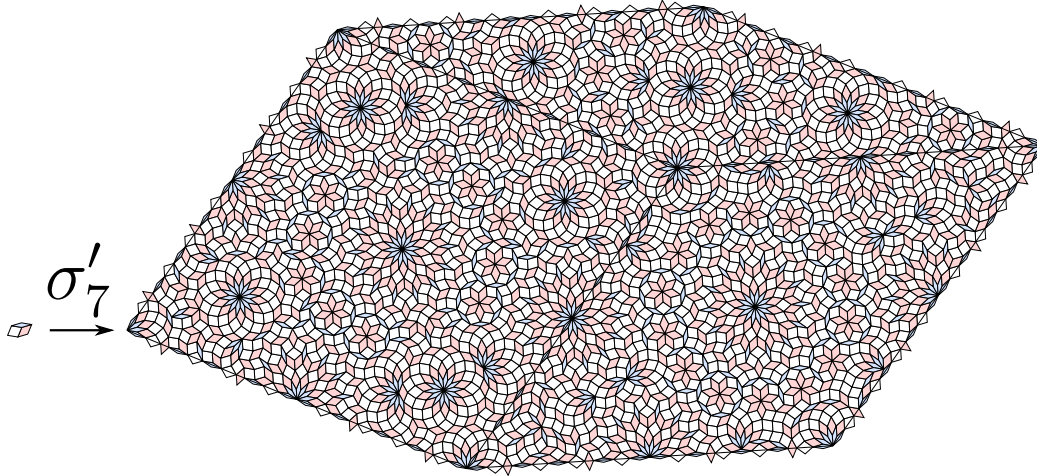


Figure 6.28: The substitution  $\sigma'_7$ .

Table 6.4: Edgeward, approximate modulus of eigenvalue, planarity and tileability of candidates for  $\sigma'_7$ .

$\Sigma_{(j)}$	$ \lambda_0 $	$ \lambda_1 $	$ \lambda_2 $	$\lambda_\Delta$	Planar	Tileable
11	3.90	3.13	1.73	0	No	No
1331	7.03	1.40	2.16	0	No	No
135531	8.76	2.51	0.96	0	No	No
13511531	12.66	0.62	2.70	0	No	No
1351331531	15.79	1.11	1.20	0	No	No
135131131531	19.69	2.01	0.53	0	No	Yes
13513133131531	22.81	0.28	3.37	0	No	No
1351313553131531	24.55	3.62	0.24	0	No	No
135131351153131531	28.45	0.50	1.50	0	No	Yes
13513135133153131531	31.58	2.23	2.40	0	No	No
1351313513113153131531	35.48	0.90	0.67	0	Yes	Yes



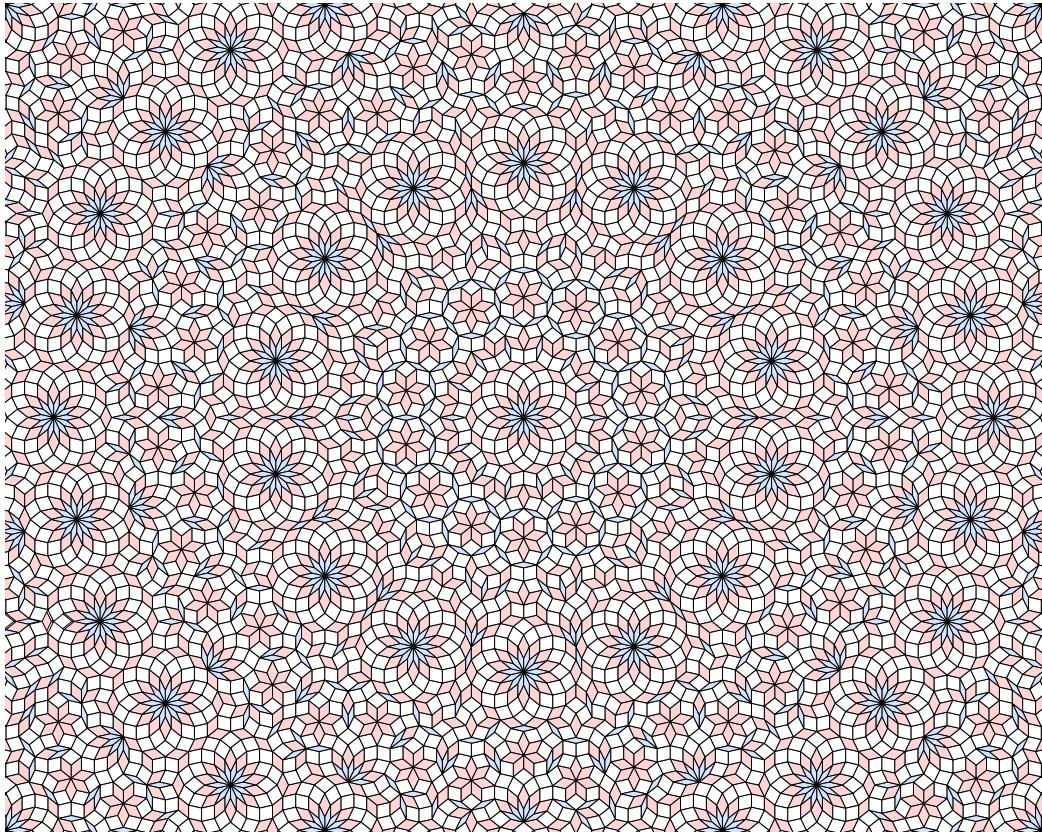


Figure 6.29: A small fragment of the tiling Planar Rosa 7.

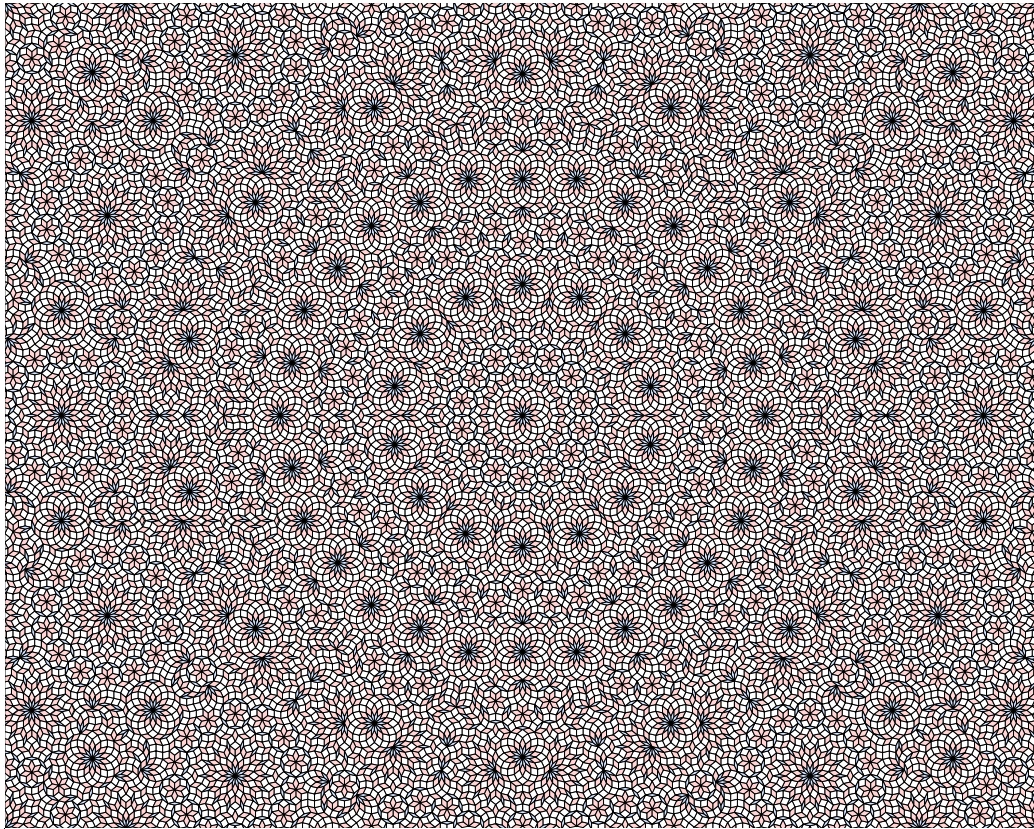


Figure 6.30: A bigger fragment of the tiling Planar Rosa 7.

#### 6.4.4 A smaller planar 7-fold Sub Rosa-like substitution

The Sub Rosa-like substitution  $\sigma_7''$  in Figure 6.31 is primitive and is planar of slope  $\mathcal{E}_7^0$ . The alternative 7-fold tiling in Figure 6.32 is the regular fixpoint of  $\sigma_7''$  from the star  $S(7)$  and it is a substitution discrete plane of slope  $\mathcal{E}_7^0$  with global 14-fold rotational symmetry.

$\sigma_7''$  is defined by its edge word  $\Sigma'' = 135131531$ , it is indeed a Sub Rosa-like substitution because it is defined by a palindromic edge word but remark that it is a palindrome of odd length, we can actually define it from the billiard word  $\omega$  as  $\Sigma'' = \text{pref}_4(\omega)\omega_4\overline{\text{pref}_4(\omega)} = \omega_0\omega_1\omega_2\omega_3\omega_4\omega_3\omega_2\omega_1\omega_0$ .

The underlying expansion  $\varphi_7''$  has eigenvalues  $\lambda_0, \lambda_1, \lambda_2, \lambda_\Delta$  on eigenspaces  $\mathcal{E}_7^0, \mathcal{E}_7^1, \mathcal{E}_7^2$  and  $\Delta$  with

$$|\lambda_0| \approx 14.23 \quad |\lambda_1| \approx 0.25 \quad |\lambda_2| \approx 0.75 \quad \lambda_\Delta = 0.$$

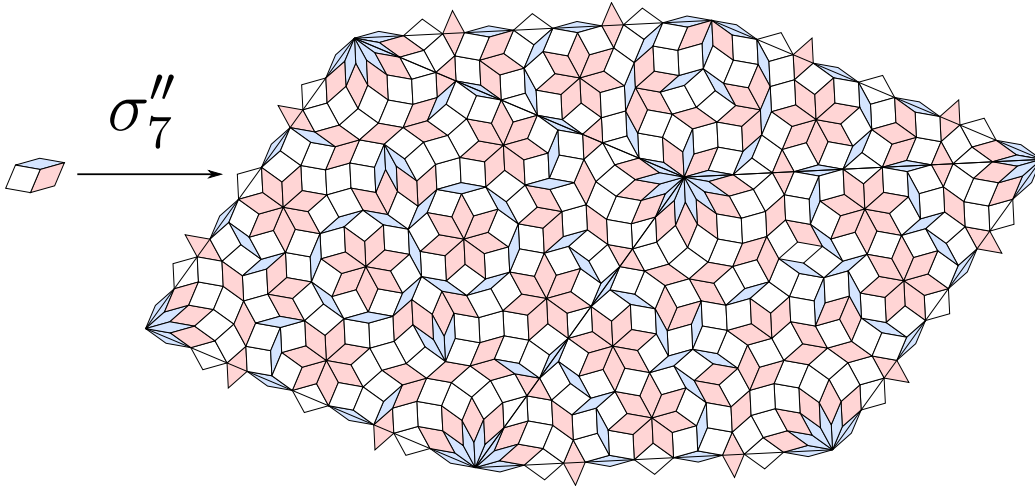


Figure 6.31: The substitution  $\sigma_7''$ .

Remark also that the metatiles of  $\sigma_7''$  do not have all the symmetries of the tiles. The metatiles  $(\frac{\pi}{7}, \frac{6\pi}{7})$  and  $(\frac{5\pi}{7}, \frac{4\pi}{7})$  both have an octagonal pattern at the very center which breaks the reflection symmetry around the long diagonal, however they preserve the symmetry around the short diagonal. The metatile  $(\frac{3\pi}{7}, \frac{4\pi}{7})$  has the symmetries of the tile.



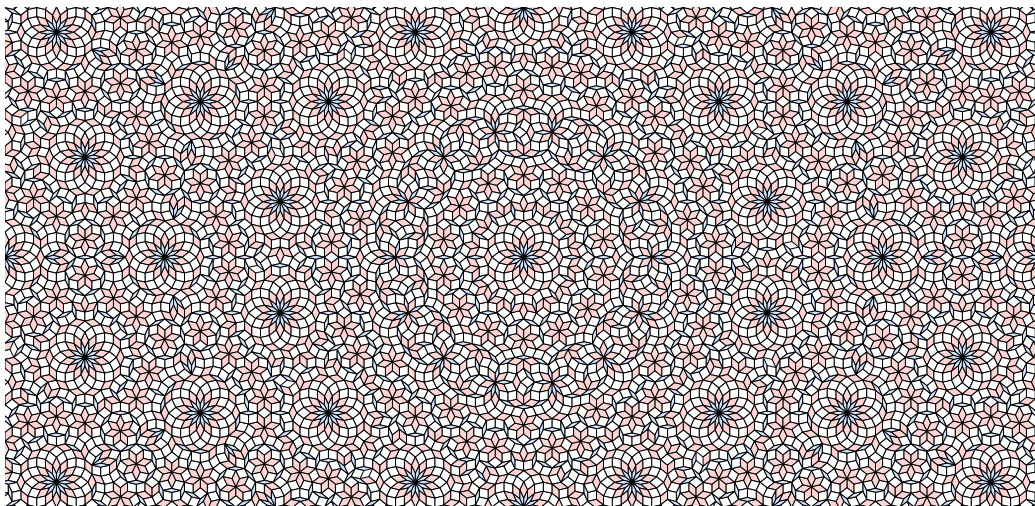


Figure 6.32: A smaller fragment of the fixpoint tiling of  $\sigma_7''$  from the seed  $S(7)$ .

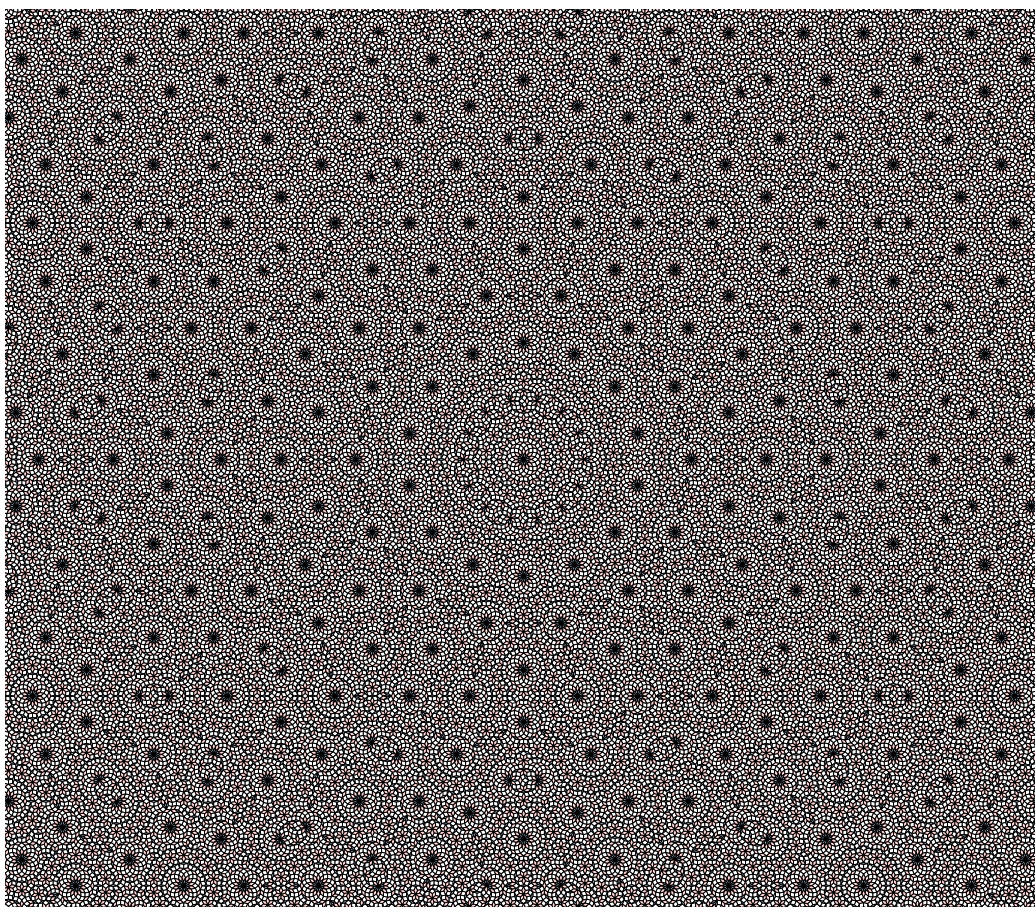


Figure 6.33: A big fragment of the fixpoint tiling of  $\sigma_7''$  from the seed  $S(7)$ .

### 6.4.5 Diffraction pattern of 7-fold tilings

In Figure 6.34 we show the experimental diffraction patterns computed from fragments of these tilings.

The 7-fold dual tilings  $P_7(\frac{1}{7})$  and  $P_7(\frac{1}{2})$  have very similar pure-point diffraction patterns (Figures 6.34a and 6.34b) which show their strong long-range order.

The Planar Rosa 7 tiling and the  $\sigma_7''$  fixpoint tiling seem to have essentially discrete diffraction patterns (Figures 6.34d and 6.34e) which suggests that they still have long-range order.

The Sub Rosa 7 tiling does not seem to have an essentially discrete diffraction pattern (Figure 6.34c), though there seem to be some peaks there are more like clouds of small peaks.

Note that the Planar Rosa 7 tiling diffraction pattern and the  $\sigma_7''$  fixpoint tiling diffraction pattern have quite a lot of “noise” (*i.e.* small peaks around the bright peaks), this is probably due to the fact that computed the diffraction pattern of relatively small fragments. Note that with small fragments (relatively to the size of the substitution) the diffraction pattern the “noise” of the diffraction pattern is strongly dependent on the way the interior of the metatiles of the substitution are tiled.

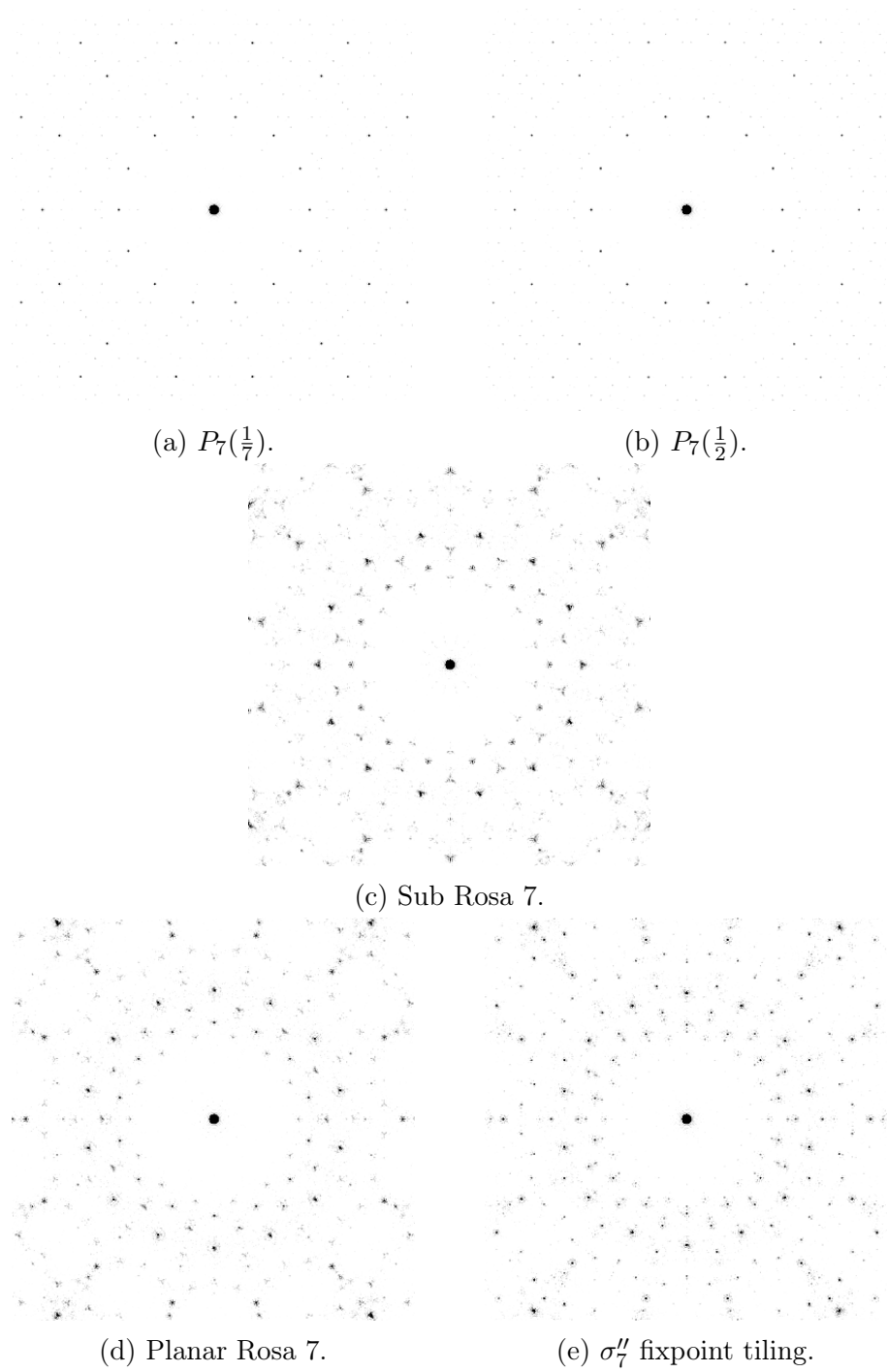


Figure 6.34: Experimental diffraction patterns computed from central fragments of 7-fold tilings with 30000 vertices.

## 6.5 Other examples of multigrid dual tilings

Examples of multigrid dual tilings have been provided in Chapter 5 in Figures 5.1, 5.3 and previously in this chapter. We will give two additional examples which are  $P_{10}(\frac{1}{2})$  and  $P_{11}(\frac{1}{2})$  in Figures 6.36 and 6.37.

The point of these figures is that they are the first two tilings  $P_n(\frac{1}{2})$  that do not have the rosa pattern  $R(n)$  at their centre. For  $n < 10$  the tiling  $P_n(\frac{1}{2})$  contains the rosa pattern  $R(n)$  at its centre, however for  $n \geq 10$  it is no longer the case.

The rosa patterns are defined in Definition 3.1.1 page 68 and the rosa patterns  $R(10)$  and  $R(11)$  are depicted in Figure 6.35. In the multigrid dual tilings  $P_{10}(\frac{1}{2})$  and  $P_{11}(\frac{1}{2})$  the last layer (pink-red tiles) of the rosa  $R(n)$  is missing.

Remark that this translates to Planar Rosa substitutions: for  $n \geq 10$  we cannot have a portion of the rosa pattern  $R(n)$  in each corner of each metatile. This is due to the fact that for  $n \geq 10$  the infinite billiard word does not start with the sequence  $135 \dots (n-2)$  (or  $0246 \dots (n-2)$  when  $n$  is even) and therefore the sequence of rhombuses on the edges of the metatiles is incompatible with a rosa pattern. This is the reason why we defined the Planar Rosa tilings from the seed  $S(n)$  instead of  $R(n)$ .

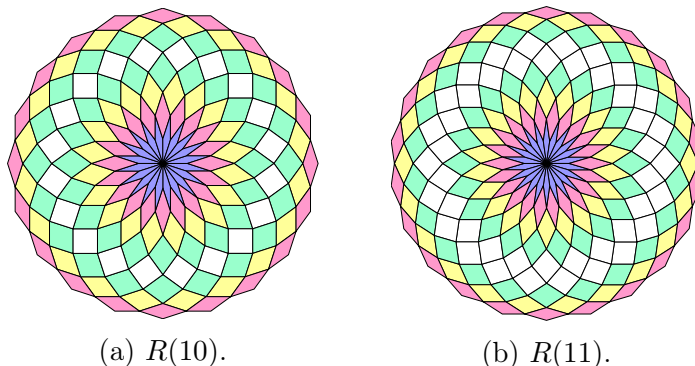


Figure 6.35: The rosa patterns.



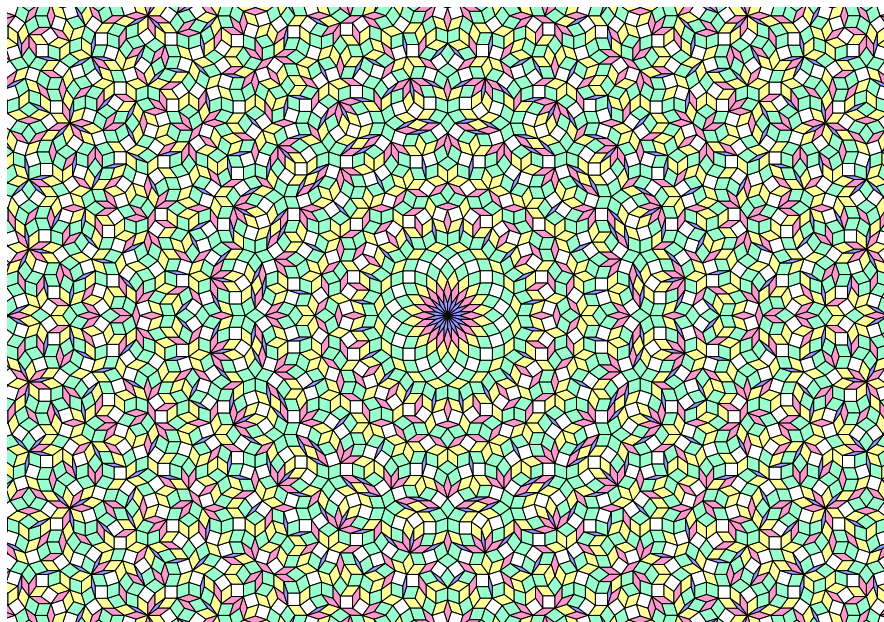


Figure 6.36:  $P_{10}(\frac{1}{2})$ .

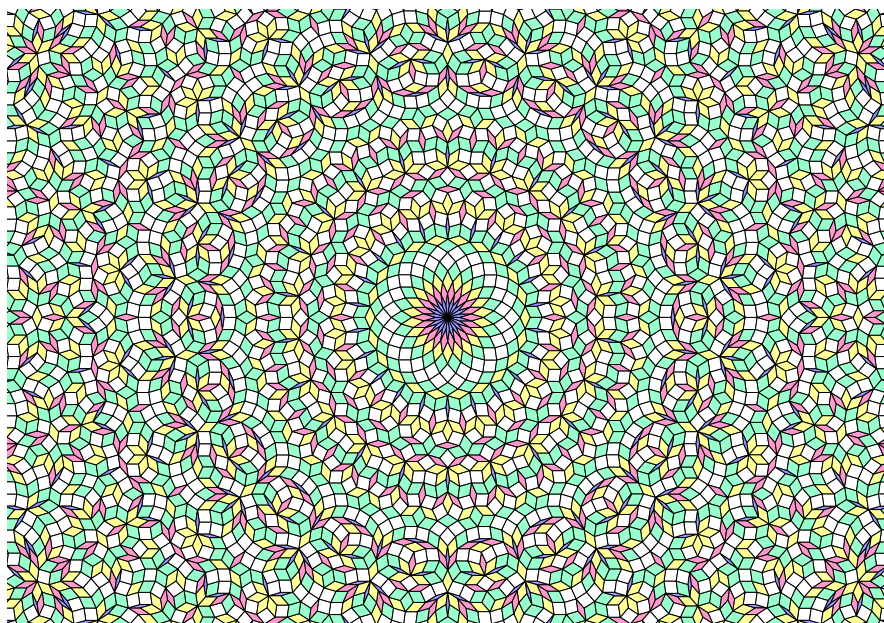


Figure 6.37:  $P_{11}(\frac{1}{2})$ .

# Chapter 7

## Conjectures and future work

### 7.1 Planar Rosa substitution tilings

**Conjecture 1.** *The Planar Rosa substitution tilings are cut-and-project substitution tilings with  $2n$ -fold rotational symmetry.*

In Theorem 2 we stated that the Planar Rosa substitution tilings are substitution discrete planes with  $2n$ -fold rotational symmetry. The difference between a discrete plane of slope  $\mathcal{E}$  and a cut-and-project tiling of slope  $\mathcal{E}$  is the properties of the window  $\Omega$  which is the projection of the vertex set onto the orthogonal subspace  $\mathcal{E}^\perp$ . For a cut-and-project tiling the vertex set  $V$  is exactly the projection on  $\mathcal{E}$  of set of point of  $\mathbb{Z}^n$  that project inside  $\Omega$

$$V = \{\pi_{\mathcal{E}}(x), x \in \mathbb{Z}^n | \pi_{\mathcal{E}^\perp}(x) \in \Omega\},$$

and for generic cut-and-project tilings  $\Omega$  is the closure of its interior. For discrete planes the only conditions are that all the vertices project inside  $\Omega$  and that  $\Omega$  is bounded.

In our case which is not generic we decompose the orthogonal subspace in a rational subspace  $\mathcal{R}$  and a totally irrational subspace  $\mathcal{E}'$  in which case  $\Omega$  takes finitely many values on  $\mathcal{R}$  and for each value  $x_i$  on  $\mathcal{R}$  we denote  $\Omega_i$  the projection of the points of  $\Omega$  that have  $\mathcal{R}$  value  $x_i$ . The condition is that each  $\Omega_i$  is the closure of its interior, see [Har04] for more details on this decomposition of the orthogonal subspace as a rational subspace and a totally irrational subspace.

Tackling this conjecture raises many questions, the first of which is linked to the fact that the Planar Rosa substitutions are defined by the boundary

of the metatiles. This means that these substitution are defined up-to tiling of the interior of the metatiles.

Let us remark that, for any metatyle with a given boundary any two possible tilings of this metatiles are *flip-connected*. This means that there is a series of *flips* (a flip is the action of inverting or “punching” a cube, see Figure 7.1 for an idea of what a flip is) that link one tiling to the other. This result is stated in [Ken93] but the proof is flawed, however one can deduce a valid proof from a similar result on discrete surfaces in [BFR08].

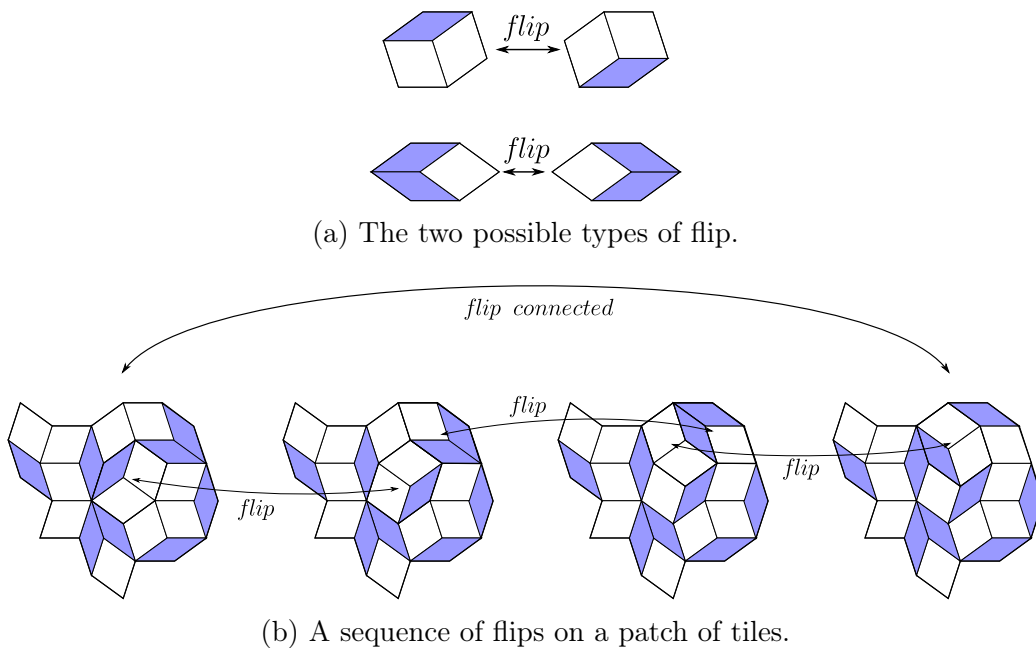


Figure 7.1: Examples of flips and flip connected patches with the Penrose rhombus tiles.

**Question 7.1.1.** *Let  $\sigma$  and  $\sigma'$  be two flip-connected substitutions with a common good seed  $S$  such that the fixpoint tiling of  $\sigma$  from seed  $S$  is cut-and-project. Is the fixpoint tiling of  $\sigma'$  from seed  $S$  also cut-and-project?*

Here flip-connected substitutions means that for any prototile  $t$ ,  $\sigma(t)$  and  $\sigma'(t)$  are flip-connected. This question comes naturally from the fact that the Planar Rosa substitutions are defined up-to flip. If Question 7.1.1 has a negative answer then Conjecture 1 will be much harder to address as there will need to be an explicit definition of the interior of the tiles.



Concerning the way we tile the interior of the Planar Rosa tiles, there is a second conjecture:

**Conjecture 2.** *The Planar Rosa substitutions can be defined in such a way that substitution preserves the symmetries of the tiles i.e. the metatiles have all the symmetries of the prototiles.*

Let us first explain this conjecture a little bit: the Penrose substitution and the Ammann-Beenker substitution do not preserve the symmetries of the tiles (see Sections 2.7 page 46 and 2.8 page 52) indeed all the prototiles are rhombuses and have reflection symmetry around both diagonals, whereas the metatiles do not have these reflection symmetries. Which means that one has to label the tiles to apply the substitution. On the other hand the Sub Rosa substitutions and the Planar Rosa substitutions for small  $n$  preserve the symmetries of the tiles (see the Sub Rosa and Planar Rosa examples in Chapter 6). However no proof of that was given for all  $n$ .

Remark that in Chapter 6 the alternative 7-fold substitution does not preserve the symmetries of the tiles, however the bigger Planar Rosa 7 substitution does preserve the symmetries of the tiles.

## 7.2 General substitution discrete planes

**Conjecture 3.** *Let  $M \in \mathcal{M}_n(\mathbb{Z})$  such that it admits a strictly expanding stable subspace  $\mathcal{E}$  of dimension 2 and is strictly contracting on the orthogonal subspace  $\mathcal{E}^\perp$ .*

*There exists a substitution discrete plane of slope  $\mathcal{E}$ .*

Let us first remark that if  $\mathcal{E}$  is the slope of a substitution discrete plane for a rhombus substitution  $\sigma$  such that its expansion  $\varphi$  is lifted to an integral linear application in  $\mathbb{R}^n$  then  $\mathcal{E}$  is a stable expanding subspace for  $\varphi$  and  $\mathcal{E}^\perp$  is stable contracting for  $\varphi$  but not necessarily strictly (see Section 3.3 page 73).

Let us remark that for  $n = 3$  this conjecture holds and it is due to a theorem which comes from the dual application of a pisot substitution on three letters. We reformulate it here to fit with the present context.

**Theorem 18** ([Fer07]). *Let  $M \in \mathcal{M}_3(\mathbb{Z})$  such that it admits a strictly expanding stable plane  $\mathcal{E}$  and is strictly contracting on the orthogonal line  $\mathcal{E}^\perp$ .*

*There exists a substitution discrete plane of slope  $\mathcal{E}$ .*

The ideas for this result comes from [AI<sup>+</sup>01] (see Section 2.10 page 57 for the relevant definitions for generalized substitutions and their dual applications), it was formalized in [Fer07] and refined in [Jol13].

Let us also remark that this conjecture is compatible with the existing results on self-affine tilings and self-similar cut-and-project sets discussed in Section 2.11 page 64. Indeed the idea in this conjecture is that the expansion  $\varphi$  is lifted to  $M$  which is an integer matrix with a two dimensional strictly expanding subspace  $\mathcal{E}$  and a  $n - 2$  dimensional strictly contracting subspace  $\mathcal{E}^\perp$ . This means that  $\varphi$  has both the properties of Theorem 10 [Kwa16] and Theorem 11 [MMP20].

In the case that  $M$  is the abelianization or 0-geometrical realization of some generalized substitution  $\sigma$  of which the 2-geometrical realization is a geometric substitution then the result follows. The thing is that given the 0-geometrical realization it is hard to find a suitable  $\sigma$  of which the 2-geometrical realization is a geometrical substitution or to prove that no such  $\sigma$  exists. Our goal is that we would be able to find a second matrix  $M'$  that has the same strictly expanding stable subspace  $\mathcal{E}$  and is also strictly contracting on the orthogonal subspace  $\mathcal{E}^\perp$ , and which would be the 0-geometrical realization of some suitable  $\sigma$ .

# List of Figures

1.1	A small fragment of the Penrose rhombus tilings without decorations. . . . .	7
1.2	Long-range order shown by diffraction patterns on tilings and quasicrystals . . . . .	8
1.3	The hierarchical structure in the Penrose rhombus tiling. . . . .	9
2.1	Examples of tiles : classical jigsaw tiles, polygons and circles are tiles. . . . .	15
2.2	The Chair tiling. . . . .	16
2.3	The Pinwheel tiling. . . . .	17
2.4	Patches and patterns of the Chair tiling. . . . .	18
2.5	Balls of the Chair tiling. . . . .	19
2.6	The 0-atlas for Penrose rhombus tiling up to translation and rotation. . . . .	21
2.7	Example of a square tile and the graphical representation of a Wang tile with integer labels or with colours. . . . .	21
2.8	The Jeandel-Rao Wang tileset [JR21]. . . . .	22
2.9	A fragment of Jeandel-Rao tiling. . . . .	22
2.10	Weak and strong periodicity. . . . .	23
2.11	Robinson tileset, classical version with square tiles cut and notches. . . . .	24
2.12	The hierarchical structure of Robinson tilings. . . . .	24
2.13	Examples of tilings with local 10-fold rotational symmetry. . . . .	25
2.14	The Penrose tilings are uniformly recurrent, here we picked a pattern and highlighted all its occurrences (up to translation). Remark that this pattern also appears in another orientation but we did not highlight these occurrences. . . . .	26
2.15	Diffraction patterns. . . . .	28
2.16	Words as tilings of the line by segments. . . . .	29

2.17	The Penrose substitution as a combinatorial substitution. . . .	31
2.18	Metatiles of the wide rhombus for the Penrose substitution. . .	32
2.19	Edge hierarchic substitution. . . . .	33
2.20	The sequences of metatiles for the Chair substitution. . . . .	34
2.21	Two slightly different fragments of regular tilings for the Chair substitution. . . . .	35
2.22	A regular seed for the chair substitution and its images. . . . .	37
2.23	A Chair fixpoint tiling. . . . .	38
2.24	Discrete surfaces and collections of squares that are not discrete surfaces in $\mathbb{R}^3$ . . . . .	40
2.25	A sketch of what $\mathcal{E} + \mathcal{H}$ looks like in dimension 4. . . . .	42
2.26	Examples of multigrids. . . . .	44
2.27	Some possible intersection points in $G_5(\gamma)$ and their dual tiles .	45
2.28	Example of a regular multigrid and its dual tiling. . . . .	46
2.29	Penrose rhombus tiles. . . . .	48
2.30	A patch with tilesets $\mathbf{T}_0$ , $\mathbf{T}_1$ and $\mathbf{T}_2$ . . . . .	49
2.31	Penrose substitutions. . . . .	50
2.32	Penrose substitution $\sigma''_{Pen}$ with rhombus tiles split in triangles.	50
2.33	The seed for $\mathcal{T}_{Pen}$ and its images by $\sigma_{Pen}$ , see that the seed appears at the center of its image by $\sigma^2_{Pen}$ . . . . .	51
2.34	The canonical Penrose rhombus tiling as a multigrid dual. . .	51
2.35	The Ammann-Beenker tiles. . . . .	53
2.36	The house condition on Ammann-Beenker tiles. . . . .	53
2.37	Ammann-Beenker substitution $\sigma_{AB}$ . . . . .	54
2.38	The seed for the Ammann-Beenker substitution $\sigma_{AB}$ , remark that it is at the centre of its image by $\sigma_{AB}$ . . . . .	55
2.39	On the left the projection of the canonical basis of $\mathbb{R}^4$ onto $P_e$ , and on the right onto $P_c$ . . . . .	60
2.40	Tiles on $P_e$ . . . . .	61
2.41	The geometrical realization $E_2(\sigma)$ on $P_e$ , the bold point represents the origin and in $E_2(\sigma)(0, 2\wedge 3)$ the dashed line represents the path from the origin to the tile. . . . .	61
2.42	Iterating $E_2(\sigma)$ from $(-e_2, 2\wedge 3)$ , the bold point represents the origin. . . . .	62
3.1	The Sub Rosa substitution of order 5 represented up to rotation, remark that there is the same sequence of rhombi on each side of each metatile. . . . .	67

3.2	Rosa patterns $R_2^1$ or $R(n)$ for $n \in \{3, 4, 5, 6, 7\}$ . . . . .	68
3.3	The decomposition $\sigma_5 = \rho_5 \circ \varphi_5$ and the edge word $\Sigma(5)$ . . . . .	69
3.4	The definition of $\sigma_5$ with the edge word $\Sigma(5)$ on each edge and a portion of $R(5)$ in each corner of the metatiles. . . . .	71
3.5	The substitution $\sigma_5$ applied to the rosa $R(5)$ , remark that $R(5)$ appears at the centre of $\sigma_5(R(5))$ . . . . .	72
3.6	In these examples $\sigma_a, \sigma_b$ and $\sigma_c$ are such that the image of two parallel edges are congruent, but $\sigma_d$ is not. . . . .	75
3.7	The metatiles of the Chair substitution decomposed as $\sigma^k(t) = \sigma \circ \sigma^{k-1}(t)$ for $k \in \{2, 3, 4\}$ . . . . .	78
3.8	Decomposition of the path $p_0 \rightarrow p_1$ as $p_0 \rightarrow p'_0 \rightarrow p'_1 \rightarrow p_1$ in $\sigma^4(t)$ with $p'_0$ and $p'_1$ being corners of the metatiles in the decomposition $\sigma^4(t) = \sigma \circ \sigma^3(t)$ . . . . .	79
3.9	Edge directions for Sub Rosa $n$ with $n = 5$ . . . . .	81
3.10	To lift $\sigma_5$ in $\mathbb{R}^5$ one only has to lift each edge direction $\vec{v}_i$ to the corresponding vector of the canonical basis $\vec{e}_i$ . . . . .	82
3.11	Edges of rhombuses along the edge of the metatiles for $n = 9$ . . . . .	84
3.12	Edge directions in Sub Rosa for even $n = 6$ . . . . .	92
3.13	Lifting $\sigma_6$ . . . . .	93
3.14	The edges and rhombuses on the edge of the metatiles for even $n$ . . . . .	95
4.1	Star $S(n)$ for $n \in \{5, 7, 9\}$ . . . . .	102
4.2	Examples of polygons defined by Sub Rosa-like metatiles for $n \in \{5, 6\}$ . . . . .	104
4.3	In shaded two chains of rhombuses. . . . .	105
4.4	A chain of rhombuses around the narrow corner of the metatiles. . . . .	109
4.5	A second chain of rhombuses around the narrow corner. . . . .	110
4.6	The two chains linking opposite sides. . . . .	112
4.7	Atlas of possible (but not necessarily valid) crossing types. . . . .	113
4.8	Ideas for the proof of Theorem 15. . . . .	123
4.9	Sketch of the metatiles with $v = \text{pref}_j(\omega)$ for some $j$ . . . . .	125
4.10	Primitivity of $\sigma_{(j)}$ for $n = 5$ and $j = 3$ . . . . .	129
4.11	Corners of metatiles. . . . .	130
4.12	The corner condition : the $\frac{\pi}{n}$ rhombus on each side in each corner of each metatiles for $n = 6$ . . . . .	135
4.13	The chains in the corner for Planar Rosa 6. . . . .	139

4.14	The narrowest metatile for Planar Rosa 6 ( <i>i.e.</i> metatile of angle $\frac{\pi}{6}$ ).	142
4.15	Corners of metatiles.	143
5.1	Central patch of the multigrid dual tiling with exactly $n$ -fold rotational symmetry for $n \in \{7, 8, 9, 10, 11, 12\}$ .	146
5.2	Intersection of three lines (in a singular multigrid).	148
5.3	A central patch of the multigrid dual tiling $P_{23}(\frac{1}{23})$ with 23-fold rotational symmetry.	156
6.1	The diffraction patterns of two fragments of different size of the same random tiling. Though there is no long-range order in this tiling, the diffraction pattern of the small fragment has bright peaks.	158
6.2	The Ammann-Beenker substitution.	159
6.3	A fragment of the (canonical) Amman-Beenker tiling.	160
6.4	The Sub Rosa substitution $\sigma_4$ .	161
6.5	A fragment of the (canonical) Sub Rosa 4 tiling.	162
6.6	A bigger fragment of the Sub Rosa 4 tiling.	162
6.7	The Planar Rosa 4 substitution $\sigma'_4$ .	163
6.8	A small central fragment of the Planar Rosa 4 tiling.	164
6.9	A bigger central fragment of the Planar Rosa 4 tiling	164
6.10	Experimental diffraction patterns from central fragments of 4-fold tilings with 20000 vertices.	165
6.11	The (canonical) Penrose tiling.	167
6.12	The Anti-Penrose tiling.	168
6.13	The Sub Rosa 5 substitution $\sigma_5$ .	169
6.14	The Sub Rosa 5 tiling.	169
6.15	A bigger fragment of the (canonical) Sub Rosa 5 tiling.	171
6.16	Experimental diffraction patterns from central fragments of 5-fold tilings with 30000 vertices.	172
6.17	$P_6(\frac{1}{2})$ .	173
6.18	The $\sigma_6$ substitution.	174
6.19	A small central fragment of the Sub Rosa 6 tiling.	174
6.20	A bigger central fragment of the Sub Rosa 6 tiling.	175
6.21	The $\sigma'_6$ substitution.	176
6.22	The Planar Rosa 6 tiling.	176

6.23	Experimental diffraction patterns computed from central fragments of 6-fold tilings with 30000 vertices. . . . .	178
6.24	$P_7(\frac{1}{7})$ . . . . .	180
6.25	$P_7(\frac{1}{2})$ . . . . .	181
6.26	The substitution $\sigma_7$ . . . . .	182
6.27	A fragment of the tiling Sub Rosa 7. . . . .	183
6.28	The substitution $\sigma'_7$ . . . . .	184
6.29	A small fragment of the tiling Planar Rosa 7. . . . .	185
6.30	A bigger fragment of the tiling Planar Rosa 7. . . . .	186
6.31	The substitution $\sigma''_7$ . . . . .	187
6.32	A smaller fragment of the fixpoint tiling of $\sigma''_7$ from the seed $S(7)$ . . . . .	188
6.33	A big fragment of the fixpoint tiling of $\sigma''_7$ from the seed $S(7)$ . . . . .	189
6.34	Experimental diffraction patterns computed from central fragments of 7-fold tilings with 30000 vertices. . . . .	191
6.35	The rosa patterns. . . . .	192
6.36	$P_{10}(\frac{1}{2})$ . . . . .	193
6.37	$P_{11}(\frac{1}{2})$ . . . . .	193
7.1	Examples of flips and flip connected patches with the Penrose rhombus tiles. . . . .	195

# List of Tables

3.1	The first values of the edge word $\Sigma(n)$ for odd $n$ . . . . .	69
3.2	The first values of the edge word $\Sigma(n)$ for even $n$ . . . . .	70
3.3	Approximate module of the eigenvalues of Sub Rosa expansions for small $n$ . . . . .	90
3.4	Approximate values of the eigenvalues of Sub Rosa expansions for small even $n$ . . . . .	100
6.1	Edgeward, approximate eigenvalues, planarity and tileability of candidates for $\sigma'_4$ . . . . .	163
6.2	Edgeward, approximate eigenvalues, planarity and tileability of candidates for $\sigma'_5$ . . . . .	170
6.3	Edgeward, approximate eigenvalues, planarity and tileability of candidates for $\sigma'_6$ . . . . .	177
6.4	Edgeward, approximate modulus of eigenvalue, planarity and tileability of candidates for $\sigma'_7$ . . . . .	184



# List of Definitions

Definition 2.1.1 (Tile, rhombus tiles, edges and vertices) . . . . .	14
Definition 2.1.2 (Tiling) . . . . .	15
Definition 2.1.3 (Subshift) . . . . .	16
Definition 2.1.4 (Prototiles and Congruence) . . . . .	16
Definition 2.1.5 (Edge-to-edge tiling) . . . . .	17
Definition 2.1.6 (Patch and Pattern) . . . . .	17
Definition 2.1.7 (Deceptions and Fragments) . . . . .	18
Definition 2.1.8 (Balls and local complexity) . . . . .	19
Definition 2.2.1 (Labelled or coloured tile) . . . . .	21
Definition 2.2.2 (Tiling valid for local rules) . . . . .	21
Definition 2.2.3 (Label simplification and sofic tilings) . . . . .	22
Definition 2.3.1 (Periodicity) . . . . .	23
Definition 2.3.2 (Aperiodic subshifts and tilesets) . . . . .	23
Definition 2.3.3 (Global and local $n$ -fold rotational symmetry) . . . . .	25
Definition 2.3.4 (Uniform recurrence) . . . . .	26
Definition 2.3.5 (Quasiperiodic) . . . . .	26
Definition 2.4.1 (Substitution on words) . . . . .	28
Definition 2.4.2 (Factors) . . . . .	28
Definition 2.4.3 (Infinite words and substitution) . . . . .	29
Definition 2.4.4 (Substitution on tiles, combinatorial substitution) . . . . .	29
Definition 2.4.5 (Metatiles) . . . . .	30
Definition 2.4.6 (Degenerate and non-degenerate substitution) . . . . .	30
Definition 2.4.7 (Edge-hierarchic substitution) . . . . .	31
Definition 2.4.8 (Vertex-hierarchic substitution) . . . . .	32
Definition 2.4.9 (Tilings regular for a substitution) . . . . .	33
Definition 2.4.10 (Primitivity) . . . . .	34
Definition 2.4.11 (Limit set of a substitution) . . . . .	36
Definition 2.4.12 (Fixpoints) . . . . .	36

Definition 2.4.13 (Seed) . . . . .	36
Definition 2.5.1 (Discrete squares and segments) . . . . .	39
Definition 2.5.2 (Discrete surface) . . . . .	39
Definition 2.5.3 (Lift) . . . . .	40
Definition 2.5.4 (Discrete plane or planar tiling) . . . . .	40
Definition 2.5.5 ( $\mathcal{V}$ -diameter, orthogonal subspace and alternate definition for discrete planes) . . . . .	41
Definition 2.5.6 (Cut-and-project tiling and window) . . . . .	41
Definition 2.5.7 (Canonical cut-and-project tiling) . . . . .	41
Definition 2.6.1 (Grid and multigrid) . . . . .	43
Definition 2.6.2 ( $n$ -fold multigrid) . . . . .	43
Definition 2.6.3 (Grid function and dual tiling) . . . . .	44
Definition 2.6.4 (Regular multigrid) . . . . .	45
Definition 2.7.1 (Penrose tilings) . . . . .	47
Definition 2.7.2 (Canonical Penrose rhombus tiling) . . . . .	49
Definition 2.8.1 (Ammann-Beenker tilings) . . . . .	52
Definition 2.8.2 (Canonical Ammann-Beenker tiling) . . . . .	54
Definition 2.9.1 (Canonical substitution tilings) . . . . .	55
Definition 2.10.1 (Generalized substitution) . . . . .	57
Definition 2.10.2 (Generalized $k$ -surfaces) . . . . .	57
Definition 2.10.3 (Geometrical realizations of $\sigma$ ) . . . . .	58
Definition 2.10.4 (Poincaré map, dual geometric realization) . . . . .	60
Definition 3.1.1 (Rosa pattern $R(n)$ ) . . . . .	68
Definition 3.1.2 (Edge word for odd $n$ ) . . . . .	69
Definition 3.1.3 (Edge word for even $n$ ) . . . . .	70
Definition 3.1.4 (Substitution $\sigma_n$ ) . . . . .	70
Definition 3.1.5 (Canonical Sub Rosa tiling $\mathcal{T}_n$ ) . . . . .	72
Definition 3.3.1 (Planar substitution) . . . . .	75
Definition 3.4.1 (Decomposition of $\mathbb{R}^n$ for odd $n$ ) . . . . .	81
Definition 3.4.2 (Abelianized edge word) . . . . .	82
Definition 3.4.3 (The eigenvalue matrix for odd $n$ ) . . . . .	84
Definition 3.5.1 (Decomposition of $\mathbb{R}^n$ for even $n$ ) . . . . .	92
Definition 3.5.2 (Abelianized edge word for even $n$ ) . . . . .	93
Definition 3.5.3 (The eigenvalue matrix for even $n$ ) . . . . .	95
Definition 4.1.1 (Star pattern $S(n)$ ) . . . . .	101
Definition 4.1.2 (Canonical Planar Rosa tilings) . . . . .	102

Definition 4.3.1 (Counting function) . . . . .	106
Definition 4.3.2 (Almost-balancedness ) . . . . .	107
Definition 4.4.1 (Decomposition of $\mathbb{R}^n$ for odd $n$ ) . . . . .	118
Definition 4.4.2 (The eigenvalue matrix for odd $n$ ) . . . . .	118
Definition 4.4.3 (Optimal rhombus frequency vector for odd $n$ ) . . .	119
Definition 4.4.4 (Definition of the sequence of edge words for odd $n$ )	120
Definition 4.4.5 (The Planar Rosa substitution for odd $n$ ) . . . . .	121
Definition 4.4.6 (Billiard line) . . . . .	122
Definition 4.5.1 (Decomposition of $\mathbb{R}^n$ for even $n$ ) . . . . .	131
Definition 4.5.2 (The eigenvalue matrix for even $n$ ) . . . . .	131
Definition 4.5.3 (Optimal rhombus frequency vector for even $n$ ) . .	132
Definition 4.5.4 (Definition of the sequence of edge words for even $n$ )	133
Definition 4.5.5 (The Planar Rosa substitution for even $n$ ) . . . . .	134
Definition 4.5.6 (Billiard line) . . . . .	134

# List of Propositions

Proposition 2.4.1 (Primitivity and uniform recurrence) . . . . .	34
Proposition 2.4.2 (Primitivity and metatiles) . . . . .	35
Proposition 2.4.3 (Fixpoint from a seed) . . . . .	36
Proposition 2.6.1 (Dual of a regular grid) . . . . .	45
Proposition 3.1.1 (KR16) . . . . .	70
Proposition 3.1.2 (KR16) . . . . .	71
Proposition 3.3.1 (Planarity of primitive substitutions) . . . . .	74
Proposition 3.3.2 (Necessary condition for planarity) . . . . .	76
Proposition 3.3.3 (Sufficient condition for non-planarity) . . . . .	76
Proposition 3.3.4 (Sufficient condition for planarity) . . . . .	77
Proposition 3.4.1 (Eigenspaces of $\varphi_n$ for odd $n$ ) . . . . .	82
Proposition 3.4.2 (Expansion matrix of $\varphi_n$ for odd $n$ ) . . . . .	83
Proposition 3.4.3 (Eigenvalues of the Sub Rosa expansion for odd $n$ )	84
Proposition 3.4.4 (Value of the eigenvalues $\lambda_j(n)$ for odd $n$ ) . . . . .	87
Proposition 3.4.5 (Planarity of Sub Rosa substitutions $\sigma_n$ for odd $n$ )	90
Proposition 3.5.1 (Eigenspaces of $\varphi_n$ for even $n$ ) . . . . .	92
Proposition 3.5.2 (Expansion matrix of $\varphi_n$ for even $n$ ) . . . . .	94
Proposition 3.5.3 (Eigenvalues of the Sub Rosa expansion for even $n$ )	95
Proposition 3.5.4 (Value of the eigenvalues $\lambda_j(n)$ for even $n$ ) . . . . .	97
Proposition 3.5.5 (Non-planarity of Sub Rosa substitutions for even $n$ ) . . . . .	99
Proposition 4.3.1 (Tileability) . . . . .	107
Proposition 4.4.1 (Expansion matrix of $\varphi$ for odd $n$ ) . . . . .	118
Proposition 4.4.2 (Eigenvalues of Sub Rosa-like expansions for odd $n$ ) . . . . .	119
Proposition 4.5.1 (Sub Rosa-like expansion matrix for even $n$ ) . . . . .	131

Proposition 4.5.2 (Eigenvalues of Sub Rosa-like expansions for even $n$ ) . . . . .	131
Proposition 5.3.1 (Regularity of multigrids and trigonometric equations) . . . . .	147

# List of Theorems

Theorem 1 (Fernique, Kari, L.2020) . . . . .	10
Theorem 2 (Kari, L. 2020) . . . . .	11
Theorem 3 ( [Lut21a]) . . . . .	11
Theorem 4 ( [Ber66]) . . . . .	24
Theorem 5 ( [Ber66]) . . . . .	25
Theorem 6 (Crystallographic restriction) . . . . .	26
Theorem 7 (Harriss2004) . . . . .	56
Theorem 8 ( [AFHI11]) . . . . .	60
Theorem 9 ( [Ei03]) . . . . .	63
Theorem 10 ( [Kwa16]) . . . . .	64
Theorem 11 ( [MMP20]) . . . . .	65
Theorem 12 (KR16) . . . . .	72
Theorem 13 (Kenyon, 93) . . . . .	105
Theorem 15 (folk.) . . . . .	123
Theorem 16 ( [Lut21a]) . . . . .	144
Theorem 17 ( [CJ76]) . . . . .	149
Theorem 18 ( [Fer07]) . . . . .	196

# Bibliography

- [AA17] S. Akiyama and P. Arnoux. *Substitution and Tiling Dynamics: Introduction to Self-inducing Structures*. Springer, 2017. doi:10.1007/978-3-030-57666-0.
- [AFHI11] P. Arnoux, M. Furukado, E. Harriss, and S. Ito. Algebraic numbers, free group automorphisms and substitutions on the plane. *Transactions of the American Mathematical Society*, 2011. doi:10.1090/S0002-9947-2011-05188-3.
- [AG86] M. Audier and P. Guyot. Al4mn quasicrystal atomic structure, diffraction data and penrose tiling. *Philosophical Magazine B*, 1986. doi:10.1080/13642818608238966.
- [AGS92] R. Ammann, B. Grünbaum, and G. C. Shephard. Aperiodic tiles. *Discrete & Computational Geometry*, 1992. doi:10.1007/BF02293033.
- [AI+01] P. Arnoux, S. Ito, et al. Pisot substitutions and rauzy fractals. *Bulletin of the Belgian Mathematical Society Simon Stevin*, 2001. doi:10.36045/bbms/1102714169.
- [AMST94] P. Arnoux, C. Mauduit, I. Shiokawa, and J. Tamura. Complexity of sequences defined by billiard in the cube. *Bulletin de la Société Mathématique de France*, 1994. doi:10.24033/bsmf.2020.
- [AP98] J. E. Anderson and I. F. Putnam. Topological invariants for substitution tilings and their associated  $c^*$ -algebras. *Ergodic Theory and Dynamical Systems*, 1998. doi:10.1017/S0143385798100457.
- [BDDG16] M. Baake and U. Damanik Davidand Grimm. What is aperiodic order?, 2016. doi:10.1090/noti1394.

- [Bee82] F. P. M. Beenker. Algebraic theory of non-periodic tilings of the plane by two simple building blocks: a square and a rhombus. 1982.
- [Ber66] R. Berger. *The undecidability of the domino problem*. American Mathematical Soc., 1966.
- [BFR08] O. Bodini, Th. Fernique, and É. Rémila. A characterization of flip-accessibility for rhombus tilings of the whole plane. *Information and Computation*, 2008. doi:10.1016/j.ic.2008.03.008.
- [BG13] M. Baake and U. Grimm. *Aperiodic Order: A Mathematical Invitation*. Cambridge University Press, 2013.
- [BGL21] Nicolas Bedaride, Franz Gähler, and Ana G. Lecuona. Cohomology groups for spaces of 12-fold tilings, 2021. arXiv:2012.00379.
- [BNRR95] D. Beauquier, M. Nivat, E. Rémila, and M. Robson. Tiling figures of the plane with two bars. *Computational Geometry*, 1995. doi:10.1016/0925-7721(94)00015-N.
- [CJ76] J. Conway and A. Jones. Trigonometric diophantine equations (on vanishing sums of roots of unity). *Acta Arithmetica*, 1976. doi:10.4064/aa-30-3-229-240.
- [Cul96] K. Culik. An aperiodic set of 13 wang tiles. *Discrete Mathematics*, 1996. doi:10.1016/S0012-365X(96)00118-5.
- [DB81] N. G. De Bruijn. Algebraic theory of penrose’s nonperiodic tilings of the plane. i and ii. *Kon. Nederl. Akad. Wetensch. Proc. Ser. A*, 1981. doi:10.1016/1385-7258(81)90016-0.
- [Ei03] H. Ei. Some properties of invertible substitutions of rank  $d$ , and higher dimensional substitutions. *Osaka Journal of Mathematics*, 2003.
- [Fer07] Th. Fernique. *Pavages, Fractions Continues et Géométrie Discrète*. PhD thesis, université Montpellier II, 2007.
- [FGH] D. Frettlöh, F. Gähler, and E. Harriss. Tilings encyclopedia. [tilings.math.uni-bielefeld.de](http://tilings.math.uni-bielefeld.de).



- [FO10] Th. Fernique and N. Ollinger. Combinatorial substitutions and sofic tilings, 2010. arXiv:1009.5167.
- [Fog02] N. Pytheas Fogg. *Substitutions in dynamics, arithmetics and combinatorics*. Lecture Notes in Mathematics. Springer, 2002.
- [GHK13] F. Gähler, J. Hunton, and J. Kellendonk. Integral cohomology of rational projection method patterns. *Algebraic & Geometric Topology*, 2013. doi:10.2140/agt.2013.13.1661.
- [GR86] F. Gähler and J. Rhyner. Equivalence of the generalised grid and projection methods for the construction of quasiperiodic tilings. *Journal of Physics A: Mathematical and General*, 1986. doi:10.1088/0305-4470/19/2/020.
- [GS87] B. Grünbaum and G. C. Shephard. *Tilings and patterns*. Courier Dover Publications, 1987.
- [GS98] C. Goodman-Strauss. Matching rules and substitution tilings. *Annals of Mathematics*, 1998. doi:10.2307/120988.
- [Har04] E. O. Harriss. *On canonical substitution tilings*. PhD thesis, University of London, 2004.
- [Har05] E. O. Harriss. Non-periodic rhomb substitution tilings that admit order  $n$  rotational symmetry. *Discrete & Computational Geometry*, 2005. doi:10.1007/s00454-005-1175-1.
- [HK03] B. Hasselblatt and A. Katok. *A first course in dynamics: with a panorama of recent developments*. Cambridge University Press, 2003.
- [Jol13] T. Jolivet. Combinatorics of pisot substitutions. *TUCS Dissertations*, 2013.
- [JR21] E. Jeandel and M. Rao. An aperiodic set of 11 wang tiles. *Advances in Combinatorics*, Jan 2021. doi:10.19086/aic.18614.
- [JV17] E. Jeandel and P. Vanier. *The Undecidability of the Domino Problem*. CIRM, chaire Jean-Morlet, 2017.

- [Kal05] P. Kalugin. Cohomology of quasiperiodic patterns and matching rules. *Journal of Physics A: Mathematical and General*, 2005. doi:10.1088/0305-4470/38/14/004.
- [Kar96] J. Kari. A small aperiodic set of wang tiles. *Discrete Mathematics*, 1996. doi:10.1016/0012-365X(95)00120-L.
- [Ken93] R. Kenyon. Tiling a polygon with parallelograms. *Algorithmica*, 1993. doi:10.1007/BF01228510.
- [KL20] J. Kari and V. H. Lutfalla. Substitution planar tilings with  $n$ -fold rotational symmetry, 2020. arXiv:2010.01879.
- [KR16] J. Kari and M. Rissanen. Sub rosa, a system of quasiperiodic rhombic substitution tilings with  $n$ -fold rotational symmetry. *Discrete & Computational Geometry*, 2016. doi:10.1007/s00454-016-9779-1.
- [Kwa16] J. Kwapisz. Inflations of self-affine tilings are integral algebraic perron. *Inventiones mathematicae*, 2016. doi:10.1007/s00222-015-0633-5.
- [Lab19] S. Labbé. Substitutive structure of jeandel–rao aperiodic tilings. *Discrete & Computational Geometry*, 2019. doi:10.1007/s00454-019-00153-3.
- [Lev86] L. A. Levin. Average case complete problems. *SIAM Journal on Computing*, 1986. doi:10.1137/0215020.
- [LM21] D. Lind and B. Marcus. *An introduction to symbolic dynamics and coding*. Cambridge university press, 2021.
- [Lut21a] V. H. Lutfalla. An Effective Construction for Cut-And-Project Rhombus Tilings with Global  $n$ -Fold Rotational Symmetry. In *AUTOMATA 2021*, 2021. doi:10.4230/OASICS.AUTOMATA.2021.9.
- [Lut21b] V. H. Lutfalla.  $n$ -fold multigrind dual tilings, 2021. Software doi:10.5281/zenodo.4698387.
- [MMP20] Z. Masáková, J. Mazáč, and E. Pelantová. On generalized self-similarities of cut-and-project sets, 2020. arXiv:1909.10753.

- [Mon] T. Monteil. Against the hierarchy. Oral presentation.
- [Moz89] S. Mozes. Tilings, substitution systems and dynamical systems generated by them. *Journal d'analyse mathématique*, 1989. doi:10.1007/BF02793412.
- [Pen74] R. Penrose. The role of aesthetics in pure and applied mathematical research. *Bull. Inst. Math. Appl.*, 1974.
- [Pen79] R. Penrose. Pentaplexity a class of non-periodic tilings of the plane. *The mathematical intelligencer*, 1979.
- [PY13] I. Pak and J. Yang. Tiling simply connected regions with rectangles. *Journal of Combinatorial Theory, Series A*, 2013. doi:10.1016/j.jcta.2013.06.008.
- [Rad94] C. Radin. The pinwheel tilings of the plane. *Annals of Mathematics*, 1994. doi:10.2307/2118575.
- [Rad97] C. Radin. Aperiodic tilings, ergodic theory, and rotations. *NATO ASI Series C Mathematical and Physical Sciences-Advanced Study Institute*, 1997.
- [Rob71] R. M. Robinson. Undecidability and nonperiodicity for tilings of the plane. *Inventiones mathematicae*, 1971. doi:10.1007/BF01418780.
- [Rob04] E. A. Robinson. Symbolic dynamics and tilings of  $\mathbb{R}^d$ . In *Proceedings of Symposia in Applied Mathematics*, 2004.
- [Sad08] Lorenzo Adlai Sadun. *Topology of tiling spaces*, volume 46. American Mathematical Soc., 2008.
- [SAI01] Y. Sano, P. Arnoux, and S. Ito. Higher dimensional extensions of substitutions and their dual maps. *Journal d'Analyse Mathématique*, 2001. doi:10.1007/BF02790261.
- [SBGC84] D. Shechtman, I. Blech, D. Gratias, and J. W. Cahn. Metallic phase with long-range orientational order and no translational symmetry. *Physical review letters*, 1984. doi:10.1103/physrevlett.53.1951.

- [Sen96] M. Senechal. *Quasicrystals and geometry*. CUP Archive, 1996.
- [ST11] J. E. S. Socolar and J. M. Taylor. An aperiodic hexagonal tile. *Journal of Combinatorial Theory, Series A*, 2011. 10.1016/j.jcta.2011.05.001.
- [Thu90] W. P. Thurston. Conway's tiling groups. *The American Mathematical Monthly*, 1990. doi:10.1080/00029890.1990.11995660.
- [Wik] Wikipedia contributors. Quasicrystals. [Online; accessed in april 2021].